A human microRNA, miR-122, promotes Hepatitis C virus RNA accumulation through three distinct mechanisms

Jasmin Chahal

Department of Microbiology and Immunology

McGill University, Montreal

December 2019

A thesis submitted to McGill University in partial fulfillment of the requirements of the degree of Doctor of Philosophy

© Jasmin Chahal, 2019

ABSTRACT

Hepatitis C virus (HCV) is a positive-sense single-stranded RNA virus. The 5' untranslated region (UTR) of the HCV genome interacts with a liver-specific microRNA, called miR-122. miR-122 binds to two sites (Site 1 and Site 2) on the 5' UTR of the viral genome and *promotes* HCV RNA accumulation, although the precise role(s) of miR-122 in the HCV life cycle have remained unclear until recently. Previous studies suggested two main mechanisms of miR-122-mediated viral RNA accumulation: 1) protection from pyrophosphatase and subsequent exoribonuclease activity; and 2) suppression of an alternative secondary structure and promotion of the HCV internal ribosomal entry site (IRES) formation.

Herein, we hypothesized that miR-122 binding to HCV genome alters the structure of 5' UTR in a manner that promotes HCV RNA accumulation. Using biophysical analyses and Selective 2' Hydroxyl Acylation analyzed by Primer Extension (SHAPE), we provided a new model of Ago:miR-122 interactions with the HCV genome that suggests that miR-122 plays three roles in the HCV life cycle. Firstly, Ago:miR-122 binds to Site 2 of HCV RNA, suppressing a more energetically favorable secondary structure, termed SLII^{alt} and promoting formation of the functional SLII structure which makes up part of the viral IRES (SLII-IV). Secondly, another Ago:miR-122 complex is recruited to Site 1, protecting the 5' terminus of the viral genome from cellular pyrophosphatase activity and subsequent exoribonuclease-mediated decay. Finally, in order to accommodate both Ago:miR-122 complexes in such close proximity, the Ago:miR-122 complex at Site 2 weakens its auxiliary base-pairing interactions, but is further stabilized by interacting with SLIIa of the HCV IRES, stabilizing the canonical SLII structure and promoting viral translation.

Recent clinical trials using miR-122 inhibitors to treat chronic HCV-infected patients revealed the selection of several resistance associated variants (RAVs) in the 5' terminus of the

HCV genome. We hypothesized that these RAVs result in changes to the secondary structure of the HCV genome that promote viral RNA accumulation, even in the absence of miR-122. We demonstrated that the RAVs could be classified into three main classes, with distinct mechanisms of action, all based on changes to the structure of the viral RNA. Specifically, Class I RAVs, including C2GC3U, U4C and G28A are 'riboswitched' and are able to form the functional SLII structure, even in the absence of miR-122. Class II RAVs, including C2GC3U, C3U and U4C result in additional base-pairing interactions at the 5' terminus of the HCV RNA that provide genome stability, independently of miR-122. Finally, the Class III RAV, C37U, alters the structure of the 3' terminus of the negative-strand intermediate, which is predicted to alter positive-strand RNA synthesis, as this region of the genome contains the positive-strand promoter.

This research has uncovered the mechanism(s) of action of miR-122 in the HCV life cycle and revealed new paradigms for miRNA function. Moreover, it has revealed three distinct mechanisms of antiviral resistance all based on modifications in RNA structure. We anticipate that this research may be applicable to other important human or veterinary pathogens and will be relevant in the design, development, and evaluation of resistance to miRNA-based therapies more broadly.

RÉSUMÉ

Le virus de l'hépatite C (VHC) est un virus à ARN simple brin à polarité positive (sens). L'extrémité 5' non-codante (UTR) du génome du VHC interagit avec un microARN spécifique du foie, appelé miR-122. Le miR-122 se lie à deux sites (Site 1 et Site 2) sur la région 5' UTR du génome viral et *favorise* l'accumulation de l'ARN du VHC. Cependant, le(s) rôle(s) précis du miR-122 dans le cycle de vie du VHC sont demeurés mal définis jusqu'à récemment. Des études ont suggéré deux mécanismes principaux pour l'accumulation de l'ARN viral médiée par le miR-122: 1) la protection contre les pyrophosphatases et une activité exonucléase subséquente; et 2) la suppression d'une structure ARN secondaire alternative et la promotion de la formation du site d'entrée interne des ribosomes (IRES) du VHC.

Ici, nous avons émis l'hypothèse que la liaison du miR-122 au génome du VHC modifie la structure de la région 5' UTR d'une manière qui favorise l'accumulation de l'ARN du VHC. À l'aide d'analyses biophysiques et de la technique d'acylation sélective d'hydroxyle en 2' analysées par extension d'amorce (SHAPE), nous avons proposé un nouveau modèle d'interactions Ago:miR-122 avec le génome du VHC qui suggère que le miR-122 joue trois rôles dans le cycle de vie du VHC. Premièrement, Ago:miR-122 se lie au site 2 de l'ARN du VHC, supprimant une structure secondaire plus favorable sur le plan énergétique, appelée SLIIalt et favorisant la formation de la structure fonctionnelle SLII qui fait partie de l'IRES viral (SLII-IV). Deuxièmement, un autre complexe Ago:miR-122 est recruté sur le site 1, protégeant l'extrémité 5' du génome viral contre l'activité de la pyrophosphatase cellulaire et la dégradation subséquente induite par les exoribonucléases. Enfin, afin d'accueillir les deux complexes Ago:miR-122 à une telle proximité, le complexe Ago:miR-122 du site 2 affaiblit ses interactions auxiliaires de

couplage de bases, mais est encore stabilisé en interagissant avec la SLIIa de l'IRES, ce qui stabilise la structure canonique SLII et favorise la traduction du génome viral.

Des essais cliniques récents utilisant des inhibiteurs de miR-122 pour traiter des patients chroniquement infectés par le VHC ont révélé la sélection de plusieurs variants associées à la résistance (RAV) à l'extrémité 5' du génome du VHC. Nous avons émis l'hypothèse que ces RAV entraînent des changements dans la structure secondaire du génome du VHC qui favorisent l'accumulation d'ARN viral, même en l'absence de miR-122. Nous avons démontré que les RAV pouvaient être classés en trois classes principales, avec des mécanismes d'action distincts, tous basés sur des changements dans la structure de l'ARN viral. Plus précisément, les RAV de classe I, y compris les C2GC3U, U4C et G28A, sont « riboswitched » et sont capables de former la structure SLII fonctionnelle, même en l'absence de miR-122. Les RAV de classe II, y compris C2GC3U, C3U et U4C, entraînent des interactions d'appariement de bases supplémentaires à l'extrémité 5' de l'ARN du VHC qui assurent la stabilité du génome, même en l'absence de miR-122. Enfin, le RAV de classe III, C37U, modifie la structure de l'extrémité 3' de l'intermédiaire à polarité négative (antisens), qui devrait modifier la synthèse d'ARN à polarité positive, car cette région du génome contient le promoteur à brin positif.

Cette étude a démontré des mécanismes d'action du miR-122 dans le cycle de vie du VHC et a révélé de nouveaux paradigmes pour la fonction des microARNs. De plus, nous avons identifié trois mécanismes distincts de résistance antivirale, tous basés sur des modifications de la structure de l'ARN. Nous prévoyons que cette recherche peut être applicable à d'autres pathogènes humains ou animaux importants et sera pertinente dans la conception, le développement et l'évaluation de la résistance aux thérapies à base de microARN.

ACKNOWLEDGEMENTS

First and foremost, I would like to thank my Ph.D. supervisor, Dr. Selena M. Sagan. Thank you for being such a great mentor and really helping me throughout my graduate studies. Your knowledge, excitement and drive are inspiring, encouraging and admirable. I appreciate the time and effort you put into making sure our weaknesses become our strengths. I hope seeing the success of your lab since 2013 makes you proud because it is the result of your leadership. Thank you for giving me the space to learn and grow as an individual and as an academic. You have been remarkable, and I am truly blessed to have you as my supervisor.

To my past and present lab mates, thank you for dealing with me. I know I complain a lot so thank you for your patience. Thank you for helping get to where I am today. I appreciate all the emotional support throughout this journey, and I would have not gotten here without all of you.

Thank you to one of my best friends and former lab mates, Annie Bernier. You are like a big sister to me. Thank you for teaching me all that you know in the lab and getting me through life. You are an amazing person and I am so honoured to call you a best friend. Thank you for teaching me everything, from managing the lab to using powerpoint. You have made the lab so enjoyable with your stories and witty jokes. I would not be here without you.

A huge thank you to my family, mom, dad, Jasraj and Simran. You have all stuck by me through these years. Thank you for listening to me rant about how tired I am and how experiments failed. Thank you, especially mom, for picking me up from the metro or even Duff after late nights in the lab. Simran, thank you for understanding that I could not always be there and had to be in the lab to finish my work. For a teenager, you have an impressive amount of patience and thank you for helping me read my papers and listening to me practice my presentations.

To my loving husband, Patrick, thank you for absolutely everything. You have given me a new ray of hope and got me through this. Thank you for helping me emotionally and talking

through experiments with me. Thank you for bringing me food during late lab nights. Thank you for all your feedback and suggestions on presentations. Thank you for being so understanding when I had to spend more time to work and was stressed. Your support has been one of the main reasons why I am here and I cannot say thank you enough. I love each and everyone of you, thank you from the bottom of my heart.

PREFACE

This thesis was written according to the McGill University's "Guidelines for Thesis Preparation". The candidate has chosen to present in a "Manuscript-based thesis" format by following these guidelines:

"As an alternative to the traditional format, a thesis may be presented as a collection of scholarly papers of which the student is the first author or co-first author. A manuscript-based doctoral thesis must include the text of a minimum of two manuscripts published, submitted or to be submitted for publication.

Manuscripts for publication in journals are frequently very concise documents. A thesis, however, is expected to consist of more detailed, scholarly work. A manuscript-based thesis will be evaluated by the examiners as a unified, logically coherent document in the same way a traditional thesis is evaluated."

The information of the published articles and manuscript in preparation are listed below. The contributions of all authors to each article are detailed in the "Contributions of authors" section.

Manuscripts presented in this thesis:

- Selena M. Sagan, Jasmin Chahal, Peter Sarnow. Cis-Acting RNA elements in the hepatitis
 C virus RNA genome. Virus Research, 2015 Jan 7; 206:90-98; doi: 10.0.3.248/j.virusres.2014.12.029.
- Jasmin Chahal, Luca F.R Gebert, Hink Hark Gan, Edna Camacho, Kristin C. Gunsalus, Ian J. MacRae, and Selena M. Sagan. miR-122 and Ago interactions with the HCV genome alter the structure of the viral 5' terminus. *Nucleic Acids Research*, 2019 April 3; 47(10): 5307-5324; doi: 10.1093/nar/gkz194.

3. **Jasmin Chahal** and Selena M. Sagan. Analysis of resistance-associated variants to a microRNA-based therapy reveals three distinct mechanisms of resistance based on alterations in RNA structure. *Manuscript in Preparation*. 2019.

CONTRIBUTIONS OF AUTHORS

Chapter 1: Introduction

Selena M. Sagan, **Jasmin Chahal**, Peter Sarnow. *Cis*-Acting RNA elements in the hepatitis C virus RNA genome. *Virus Research*, 2015 Jan 7; 206:90-98; doi: 10.1016/j.virusres.2014.12.029.

A part of this review was used in the section "1.3 Role of RNA secondary structures in the HCV life cycle" (*Chapter 1*). S.M.S., J.C. and P.S. drafted the manuscript and S.M.S., J.C. and P.S. revised and edited the final manuscript.

Chapter 2:

Jasmin Chahal, Luca F.R. Gebert, Hin Hark Gan, Edna Camacho, Kristin C. Gunsalus, Ian J. MacRae, Selena M. Sagan. miR-122 and Ago interactions with the HCV genome alter the structure of the viral 5' terminus. *Nucleic Acids Research*, 2019 April 3; 47(10): 5307-5324; doi: 10.1093/nar/gkz194.

J.C. and S.M.S. conceptualized and designed the study. J.C. generated and analyzed the data. J.C. generated and analyzed ITC with help from E.C. L.F.R.G. and I.J.M. performed hAgo2 purification and generated and analyzed hAgo2:miR-122:HCV RNA gel shift assays. H.H.G. and K.G. performed computational modeling, analysis and interpretation of the modeling results. J.C. and S.M.S. drafted the manuscript and all authors contributed to editing the manuscript.

Chapter 3:

Jasmin Chahal and Selena M. Sagan. Analysis of resistance-associated variants to a microRNA-based therapy reveals three distinct mechanisms of resistance based on alterations in RNA structure. 2019. *Manuscript in Preparation*.

J.C. and S.M.S. conceptualized and designed the study. J.C. performed the experiments and analyzed the data. J.C. and S.M.S. drafted and edited the manuscript.

TABLE OF CONTENTS

ABSTRACT	ii
RÉSUMÉ	iv
ACKNOWLEDGEMENTS	vi
PREFACE	viii
CONTRIBUTIONS OF AUTHORS	X
LIST OF FIGURES	6
LIST OF TABLES	8
LIST OF ABBREVIATIONS	9
CHAPTER 1: INTRODUCTION	11
1.1 Hepatitis C virus	11
Discovery	11
Genotypes	
HCV Transmission and Pathogenesis	14
1.2 The HCV genome and life cycle	14
HCV genome and viral proteins	14
The HCV life cycle	16
1.3 Role of RNA secondary structures in the HCV life cycle	19
RNA secondary structures in the HCV genomic RNA	19
RNA secondary structures in the negative-strand RNA intermediate	21
1.4 HCV cell culture systems	22
1.5 HCV Therapy	26
Direct-acting antivirals	26
Host-targeted antivirals	27
1.6 microRNAs	28
The microRNA pathway	28

1.7 miR-122	31
Cellular targets of miR-122	31
miR-122 interactions with the HCV genome	32
1.8 Roles of miR-122 in the HCV life cycle	34
miR-122 protects the 5' terminus of the HCV genome from cellular pyrophospho	atases and
subsequent exoribonuclease-mediated decay	34
miR-122 promotes ribosome association	35
miR-122 alters the secondary structure of the HCV 5' UTR	35
1.9 Clinical correlations of miR-122 in chronic HCV infection	37
Dysregulation of miR-122 contributes to viral pathogenesis	37
miR-122 as a target for antiviral therapy	37
1.10 Hypothesis and Specific Aims	41
1. To identify how miR-122 and Ago:miR-122 complexes alter the structure of the	he HCV 5'
UTR (Chapter 2)	41
2. To elucidate the mechanism of action of resistance-associated variants (RAV)	's) in the 5'
UTR that confer miR-122-independent HCV RNA accumulation (Chapter 3)	3) 42
1.11 References	43
CHAPTER 2: miR-122 and Ago interactions with the HCV genome alter the st	ructure of
the viral 5' terminus	57
2.1 Preface to Chapter 2	57
2.2 Abstract	57
2.3 Introduction	58
2.4 Materials and Methods	61
Viral RNA and microRNAs	61
Isothermal Titration Calorimetry (ITC)	62
Electrophoretic Mobility Shift Assay (EMSA)	62
RNA structure prediction	63
Synthesis of NAI-N ₃	63
In vitro SHAPE analysis	64
SHAPE analysis by gel electrophoresis	64

SHAPE analysis by capillary electrophoresis	65
Purification of recombinant human Ago2 loaded with miR-122	66
Electrophoretic mobility shift assays with hAgo2:miR-122	66
Computational modeling	67
2.5 Results	68
Two miR-122 molecules can bind to the HCV 5' terminus simultaneously with differen binding affinities.	
miR-122 binding alters the secondary structure of SLII of the HCV 5' UTR	73
The G28A mutation favours formation of SLII even in the absence of miR-122	77
Two hAgo2:miR-122 complexes can bind to the HCV RNA 5' UTR simultaneously	79
hAgo2:miR-122 binding alters the secondary structure of the HCV 5' UTR	81
Computational modeling of hAgo2:miR-122 and HCV RNA	84
Computational modeling of RISC-IRES-40S complex	88
2.6 Discussion	91
Two miR-122 molecules are able to bind to the HCV 5' UTR simultaneously in vitro	91
Binding of miR-122 to the HCV genome alters the structure of the 5' UTR	92
G28A favours the canonical SLII structure.	93
Two hAgo2:miR-122 complexes can bind to the 5' UTR simultaneously and their	
interactions with the 5' terminus further alter the structure of the 5' UTR	94
miR-122 has at least three roles in the HCV life cycle	98
2.7 Acknowledgements	101
2.8 Authors contributions	101
2.9 Funding	101
2.10 Conflict of Interest	102
2.11 References	103
2.12 Supplementary Figures	108
CHAPTER 3: Analysis of resistance-associated variants to a microRNA-based therap	y
reveals three distinct mechanisms of action based on alterations in RNA structure	e 115
3.1 Preface	115

3.2 Abstract	115
3.3 Introduction	116
3.4 Materials and Methods	119
Cell culture	119
Plasmids and Viral RNAs	120
MicroRNAs	121
Electroporations	121
Luciferase assays	122
In vitro SHAPE analysis and capillary electrophoresis	122
RNA structure prediction	122
In vitro Xrn-1 assay	123
3.5 Results	123
RAVs do not have a fitness advantage in the presence of miR-122 but are able to	
accumulate under conditions where miR-122 is absent or limiting	123
Several RAVs alter the structure of the 5' UTR of the positive-strand viral RNA	126
Altered base-pairing of RAVs at the 5' terminus of the genome confers viral RNA sta	ability.
	130
The C37U RAV alters the structure of the 3' end of the viral negative-strand replica	tive
intermediate	132
3.6 Discussion	134
3.8 Author Contributions	144
3.9 Funding	144
3.10 Conflict of Interest	144
The authors declare that they have no conflict of interest	144
3.11 References	145
3.12 Supplementary Material	148
Supplementary Methods	148
Supplementary Figures	149
CHAPTER 4: DISCUSSION	152

4.1 Role of miR-122 in the HCV life cycle	152
What are the substrate requirements of the cellular pyrophosphatases and do Cla	ass II RAVs
protect against pyrophosphatase activity?	152
Removing the requirement for RNA chaperone or riboswitch activity and reducin	g the
reliance on miR-122 for stability may favor miR-122-independent HCV RN.	4
accumulation	153
How does the Ago:miR-122 complex promote HCV translation?	154
How does HCV escape canonical silencing?	156
4.2 One miRNA to rule them all?	158
4.3 Other miRNA-regulated viral RNAs	160
4.3 Other miRNA-regulated viral RNAs4.4 Consequences of RAVs to miRNA-based therapies	
	161
4.4 Consequences of RAVs to miRNA-based therapies	161
4.4 Consequences of RAVs to miRNA-based therapies	
4.4 Consequences of RAVs to miRNA-based therapies Consequences of RAVs in miR-122-based therapies for chronic HCV infection Broader consequences of RAV mechanisms of action for miRNA-based therapies	
4.4 Consequences of RAVs to miRNA-based therapies	

LIST OF FIGURES

Figure 1.1 Geographic distribution of HCV genotypes.	13
Figure 1. 2. HCV genome structure and function.	15
Figure 1.3. The HCV life cycle.	18
Figure 1.4. Secondary structures across the HCV genome.	20
Figure 1.5. HCV replication systems.	24
Figure 1.6. Cell culture systems of HCV.	25
Figure 1.7. miRNA biogenesis.	29
Figure 1.8. miR122:HCV RNA interactions at the 5' terminus.	33
Figure 1.9. miR-122 protects the terminus of HCV genome from 5' decay	36
Figure 1.10. miR-122 binding to HCV RNA alters the secondary structure of SLII.	38
Figure 1.11. miR-122 inhibitor resistance-associated variants (RAVs)	40
Figure 2.1. miR-122 binds to the HCV 5' terminus with a 2:1 stoichiometry	70
Figure 2.2. miR-122 binding suppresses an alternative structure (SLIIalt) and pror	notes
functional folding of SLII.	74
Figure 2.3. The G28A mutation favours SLII formation in the absence of miR-122.	78
Figure 2.4. Two Ago2:miR-122 complexes can bind simultaneously to the 5' termin	us of the
HCV genome.	80
Figure 2.5. hAgo2:miR-122 complexes alter the secondary structure of the 5' termi	nus and
SLII of the HCV genome.	83
Figure 2.6. Model of hAgo2:miR-122:HCV RNA interactions at Sites 1 and 2	87
Figure 2.7. Model of RISC-HCV IRES-40S interactions.	90
Figure 2.8. Model for Ago2:miR-122 interactions with the HCV 5' UTR	99
Supplementary Figure S2.1. miR-124 does not interact with the HCV 5' terminus a	nd miR-
122 binds with higher affinity to Site 1 in 1-42 nt HCV RNA	108
Supplementary Figure S2. 2. miR-122 interactions with Site 1 and Site 2 of the HC	V RNA.
	109
Supplementary Figure S2.3. miR-122 interactions with Site 1 and Site 2 of the HCV	RNA.
	111
Supplementary Figure S2.4. <i>In vitro</i> SHAPE analysis of HCV RNA by gel electrop	
	112

Supplementary Figure S2. 5. miR-122 interactions with WT, S2p5,6, G28A 1-11'	7 nt and
WT 1-371 nt HCV RNA.	114
Figure 3.1. Model of miR-122 interactions with the HCV genome	118
Figure 3.2. RAV accumulation in cell culture.	125
Figure 3. 3. In vitro SHAPE analysis of viral RNAs suggests RAVs alter the stru	cture of the
viral RNA in the absence of miR-122.	129
Figure 3.4. miR-122 and Class II RAVs provide stability to the HCV genome	131
Figure 3.5. The Class III RAV (C37U) alters the structure of the positive-strand	promoter
	136
Figure 3.6. Mechanism of action of RAVs.	142
Supplementary Figure S3.1. RNA structure predictions of the 5' UTR (nucleotid	les 1-117) of
the positive-strand HCV genomic RNA	149
Supplementary Figure S3.2. Xrn-1 requires several 5' single-stranded nucleotide	es to initiate
exoribonuclease activity.	150
Supplementary Figure S3.3. RNA structure predictions of the 3' end (nucleotide	s 1-151) of
the negative-strand HCV genomic RNA.	151
Figure 4.1. Secondary structure of U3-virus 5' UTR including SLII	155
Figure 4. 2.miR-122 interactions with 5'UTR of different hepaciviruses	159

LIST OF TABLES

Table 2.1. ITC analysis of miR-122 binding to HCV RNAs.	. 71
Table 3. 1. Half-life viral RNAs in cell culture.	133

LIST OF ABBREVIATIONS

AGO Argonaute

BVDV Bovine viral diarrhea virus

CAT-1 Cationic amino acid transporter -1

CLDN1 Claudin 1

CLIP Cross-linking immunoprecipitation

CRE Cis-acting RNA elements

CSFV Classical swine fever virus

DAAs Direct-acting antivirals

ds Double-stranded

DXO Decapping exonuclease

EMCV Encephaloymyocarditis virus

EMSA Electrophoretic mobility shift assay

eIF3 Eukaryotic Initiation Factor 3

EV-71 Enterovirus-71

FDA Food and Drug Administration (USA)

GBV-B GB virus B

GW182 Glycine-tryptophan repeat-containing 182-kDa protein

HCV Hepatitis C virus

HCC Hepatocellular carcinoma

HCVcc HCV cell culture

HITS-CLIP High-Throughput Sequencing and Crosslinking Immunoprecipitation

HIV-1 Human Immunodeficiency Virus-1

IFN Interferon

IRES Internal Ribosomal Entry Site

JFH-1 Japanese Fulminant hepatitis-1

Kb Kilobase

KO Knock out

LVP Lipo-viroparticle

LNA Locked nucleic acid

miRNA microRNA

MLV Murine leukemia virus

NAI-N₃ 2-methylnicotinic acid imidazolide azide

NANBH Non-A non-B Hepatitis

NS Nonstructural

Nt Nucleotide

OCLN Occludin

ORF Open reading frame

RdRp RNA-dependent RNA polymerase

RISC RNA-induced silencing complex

RNA Ribonucleic acid

RT-PCR Reverse transcription Polymerase Chain Reaction

SHAPE Selective 2'-Hydroxyl Acylation analyzed by Primer Extension

SL Stem loop

SRB1 Scavenger Receptor Class B Member 1

ss Single-stranded

SVR Sustained Virological Response

TRBP Transactivating Response RNA-Binding Protein

UTR Untranslated region

CHAPTER 1: INTRODUCTION

1.1 Hepatitis C virus

Discovery

Hepatitis C virus (HCV), the etiologic cause of transfusion-associated or non-A, non-B hepatitis (NANBH), was discovered in 1989. Briefly, in the 1960s, many patients began to present with blood transfusion-associated hepatitis, but with no serological evidence of hepatitis A and B antigens (1). After a decade of research, it remained unclear what caused NANBH, primarily due to failed attempts to identify any specific viral antigens and/or antibodies (2). In 1989, a team led by Michael Houghton (Chiron Inc.) isolated a complementary DNA (cDNA) clone that encoded an antigen associated with NANBH infections (2). This clone was derived from single-stranded RNA (ssRNA) of around 10 000 nucleotides (nt) obtained from the plasma of experimentally infected chimpanzees and screened with sera from NANBH patients (2). The sequence of this clone shared sequence identity with viruses of the *Flaviviridae* family, and was named HCV (2).

Subsequently, an antibody assay against HCV demonstrated that it was the primary cause of parenterally-transmitted NANBH around the world (3). By 1990, blood supply screening was implemented in most Western countries. While the first-generation assay led to a significant decrease in HCV incidence following blood transfusion, the development of a more sensitive second-generation assay against several HCV antigens nearly eliminated transfusion-associated HCV transmission (4). Today, the main risk factors for HCV infection are intravenous drug use and sharing needles (5,6). Currently, there are approximately 71 million people worldwide infected with HCV, including 268 000 Canadians (5-7).

Genotypes

HCV has a large genetic diversity, mainly due to the poor fidelity of the HCV RNA-dependent RNA polymerase (RdRp) (8-10). Thus far, there are seven genotypes and more than 100 subtypes that have been characterized with distinct geographic distributions. HCV genotypes differ at the nucleotide level by 31-33% while subtypes differ by 20-25% (10-12). Genotypes 1a, 1b, 2a and 3a are distributed throughout the globe (Figure 1.1) (9.13). These are considered the "epidemic subtypes" since they were rapidly spread before the discovery of HCV through blood transfusion, injecting drug use, sexual and parental transmission (9,14-16). These genotypes also account for a large proportion of HCV infections in the high-income population. Genotype 1 is the most prevalent genotype worldwide (Figure 1.1) (9,17). Genotype 2 is primarily localized in West Africa, while genotype 3 is mainly found in Southern Asia (9,17). Genotype 4 is localized to Central Africa and the Middle East, while Genotype 5 and 6 are mainly found in Southern Africa and South East Asia, respectively (9). Finally, genotype 7 was only recently identified in 2015, and originates from the Democratic Republic of Congo (9,18). The country with the most prevalent rate of HCV infection is Egypt, with ~ 5 million infected individuals (19,20). Genotype 4 represents over 85% of all HCV infections in Egypt mainly due to schistosomiasis vaccination efforts using poorly sterilized equipment and the reuse of needles.

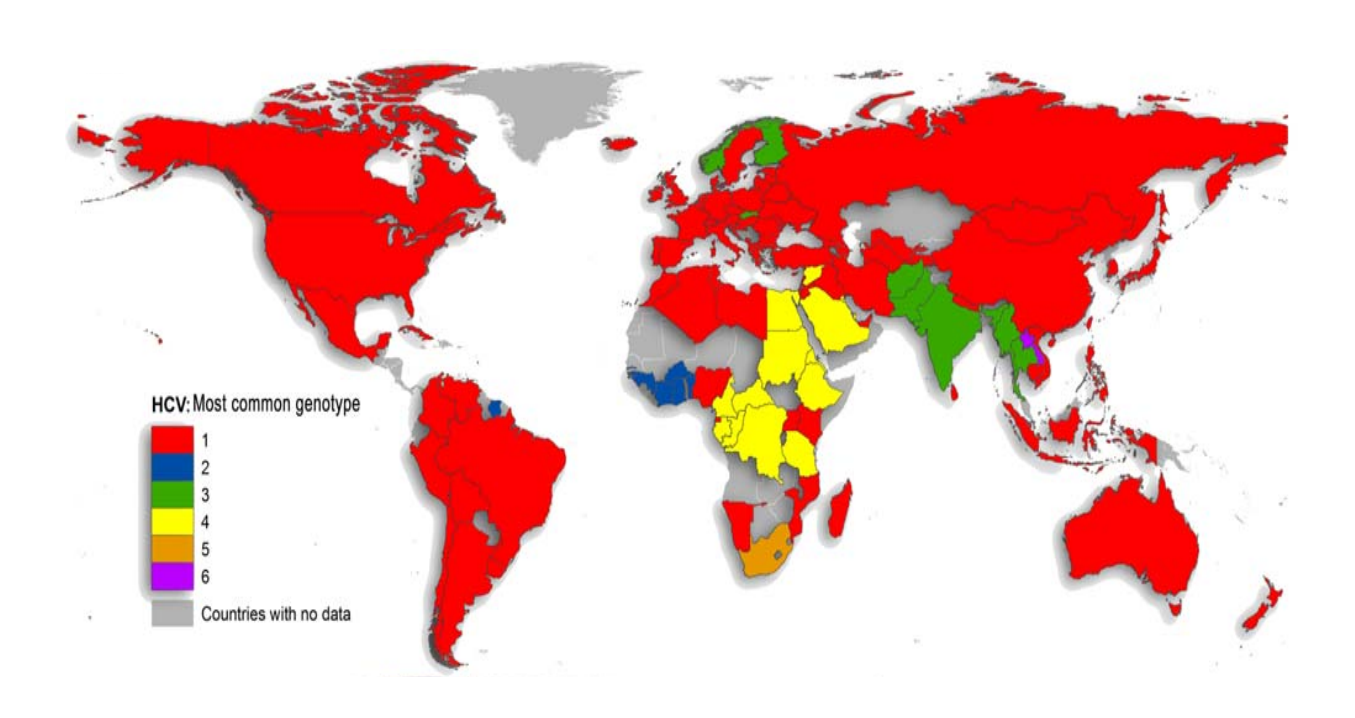


Figure 1.1 Geographic distribution of HCV genotypes. Geographic distribution of HCV genotypes 1-6. Figure from Messina, J.P. et al., *Hepatology*, 2015 (9).

HCV Transmission and Pathogenesis

HCV is a blood-borne pathogen and thus, the primarily route of transmission is through tainted blood (16,21). Prior to HCV discovery and blood screening, HCV infections were the major cause of post-transfusion hepatitis, where a study in the Netherlands showed the risk for HCV infection following transfusion of a unit of blood was greater than 90% in the 1980-1990s (22). Currently, the most common route of transmission is through injecting drug use (21,23). The first 6 months following HCV infection are referred to as the acute phase of infection, during which most patients are asymptomatic (24). Only 15-30% of patients develop mild symptoms during the acute phase and 15-25% of patients are able to clear the infection spontaneously (24,25). However, around 75% of HCV-infected individuals go on to develop a chronic infection, which can lead to chronic hepatitis, fibrosis, steatosis (fatty liver), and subsequent cirrhosis, liver failure and hepatocellular carcinoma (HCC) (26,27). Progression to cirrhosis in HCV-infected individual is slow, with 15-35% of patients progressing to cirrhosis within 20 years of infection (28,29). However, once HCV-related cirrhosis is established, HCC develops quickly with an annual rate of 1-4% (28).

1.2 The HCV genome and life cycle

HCV genome and viral proteins

The HCV genome is a ~9.6 kilobase (kb) single-stranded (ss) RNA of positive polarity. It contains a single open reading frame (ORF) that encodes a ~3000 amino acid polyprotein flanked by highly-structured 5' and 3' untranslated regions (UTRs). The viral polyprotein is processed by both host and viral proteases into 10 mature viral proteins, which include 3 structural and 7 non-structural (NS) proteins (**Figure 1.2**) (30).

The viral structural proteins include the core and envelope proteins, E1 and E2, which comprise the outer layer of the particle (**Figure 1.2**). The core protein makes direct contact with

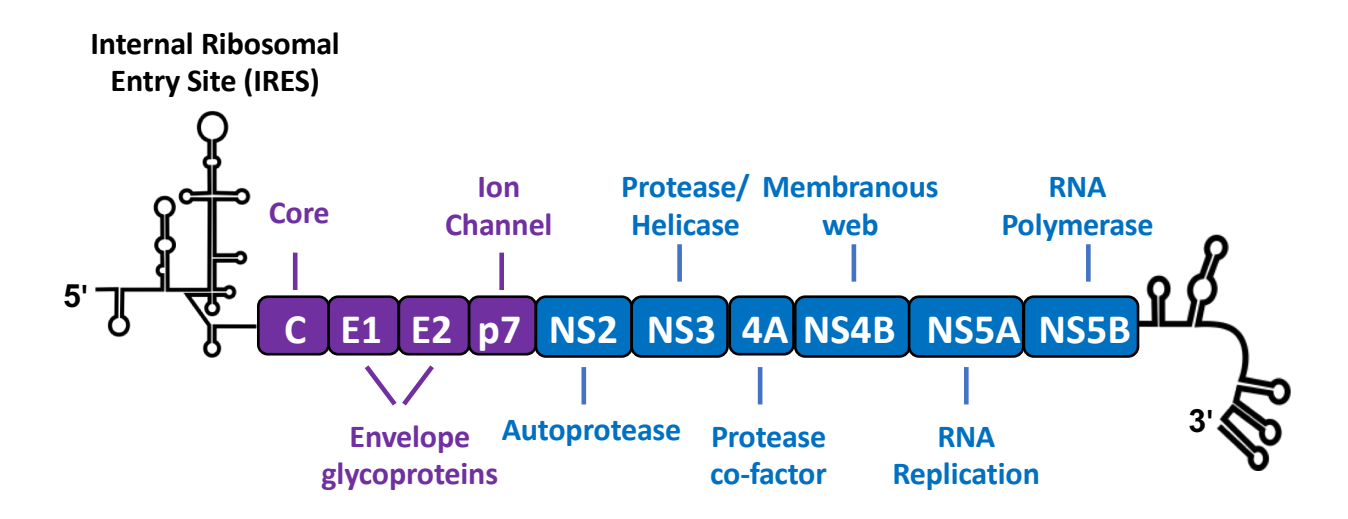


Figure 1. 2. HCV genome structure and function. The HCV genome contains a single open reading frame (ORF) encoding the viral polyprotein (subsequently cleaved into the 10 mature viral proteins). The structural (purple) and nonstructural (NS) proteins (blue) are indicated. The ORF is flanked by highly-structured 5' and 3' non-coding regions that contain cis-acting RNA elements important for translation (Internal Ribosomal Entry Site, IRES) and replication.

the viral RNA to form the nucleocapsid (31,32). The E1 and E2 proteins are glycoproteins that form the virion envelope, and these proteins take part in viral attachment and entry, mediating virion fusion with the endosomal membrane during the entry and uncoating process (reviewed in (33)).

The NS proteins include p7, NS2, NS3, NS4A, NS4B, NS5A, and NS5B (Figure 1.2). The p7 protein is an integral membrane protein and has been demonstrated to have ion channel activity, and is implicated in viral assembly and packaging (34). NS2 has protease activity that helps cleave the boundaries between the NS2-3 junction in the viral polyprotein (35). This protein has also been implicated in virion assembly (36,37). The NS3-5B proteins are essential for viral RNA synthesis and form the viral replication complex (38). The NS3 protein is a multi-functional protein that contains both serine protease and helicase/NTPase activities (33). Together with its cofactor (NS4A), the NS3/4A protein is responsible for polyprotein processing at the NS3-4A, NS4A-4B, NS4B-5A and NS5A-5B junctions (39). In addition, the NS3 helicase/NTPase activity is important for viral RNA synthesis (40). The NS4B protein is responsible for formation of the 'membranous web', which is derived from the B-layer of the endoplasmic reticulum (ER) membrane and constitutes mostly double- and multi-membraned vesicles as well as lipid droplets, which are the sites of viral replication and assembly, respectively (41). The NS5A protein does not have enzymatic activity but is known to form dimers which have RNA binding activity (42). NS5A is found in phosphorylated and hyperphosphorylated forms and is implicated in both viral RNA replication and virion assembly (42,43). Finally, the NS5B protein is the RdRp, which is responsible for viral RNA synthesis (44).

The HCV life cycle

HCV circulates as a lipoprotein-virus hydrid or lipo-viroparticle (LVP) in the bloodstream of infected individuals. This strong association with low- and very low-density lipoproteins helps

mediate the initial interactions with hepatocytes (45-47). Specifically, HCV virions interact with the low-density-lipoprotein receptor (LDLR) and glycosaminoglycans (GAGs) on heparan sulfate proteoglycans (HSPGs) to mediate attachment to hepatocytes. Several other molecules are then necessary for the HCV entry process, including CD81, scavenger receptor class B member 1 (SRB1), claudin 1 (CLDN1), and occludin (OCLN) (30,48). During entry, HCV interacts with SRB1, which induces a conformational change in the E2 protein on the surface of the virion, exposing the CD81 binding site. CD81 then directs HCV virions to the tight junction where it is able to mediate additional interactions with CLDN1 and OCLN that ultimately result in clathrin-mediated endocytosis followed by low-pH-mediated fusion with the endosome (Figure 1.3) (49,50).

Upon uncoating, the viral RNA is able to undergo cap-independent translation driven by the viral Internal Ribosomal Entry Site (IRES) element in the 5' UTR. Translation and polyprotein processing take place in ER membrane-associated ribosomes. Once enough viral proteins have accumulated, NS4B induces formation of the membranous web which is the site of viral RNA replication (51). The positive-strand genomic RNA is used as a template for the production of a full-length negative-strand RNA intermediate by the NS5B polymerase (Figure 1.3). Synthesis of negative-strands is initiated at the 3' end of the viral genome and is a rate-limiting reaction, as positive-strand RNAs are produced in an excess of 5- to 10-fold (52). Following viral translation and RNA replication, genomic RNAs are packaged into nascent HCV particles (Figure 1.3). The precise details of assembly are still unclear; however, assembly initiates on the cytosolic side of the ER membrane (37). The core and NS5A proteins coordinate the encapsidation process on the surface of lipid droplets and the nucleocapsid is thought to simultaneously acquire a lipid envelope, containing E1 and E2 heterodimers. Virions transit through the Golgi apparatus and are released via a noncanonical secretory route involving the endosomal compartment.

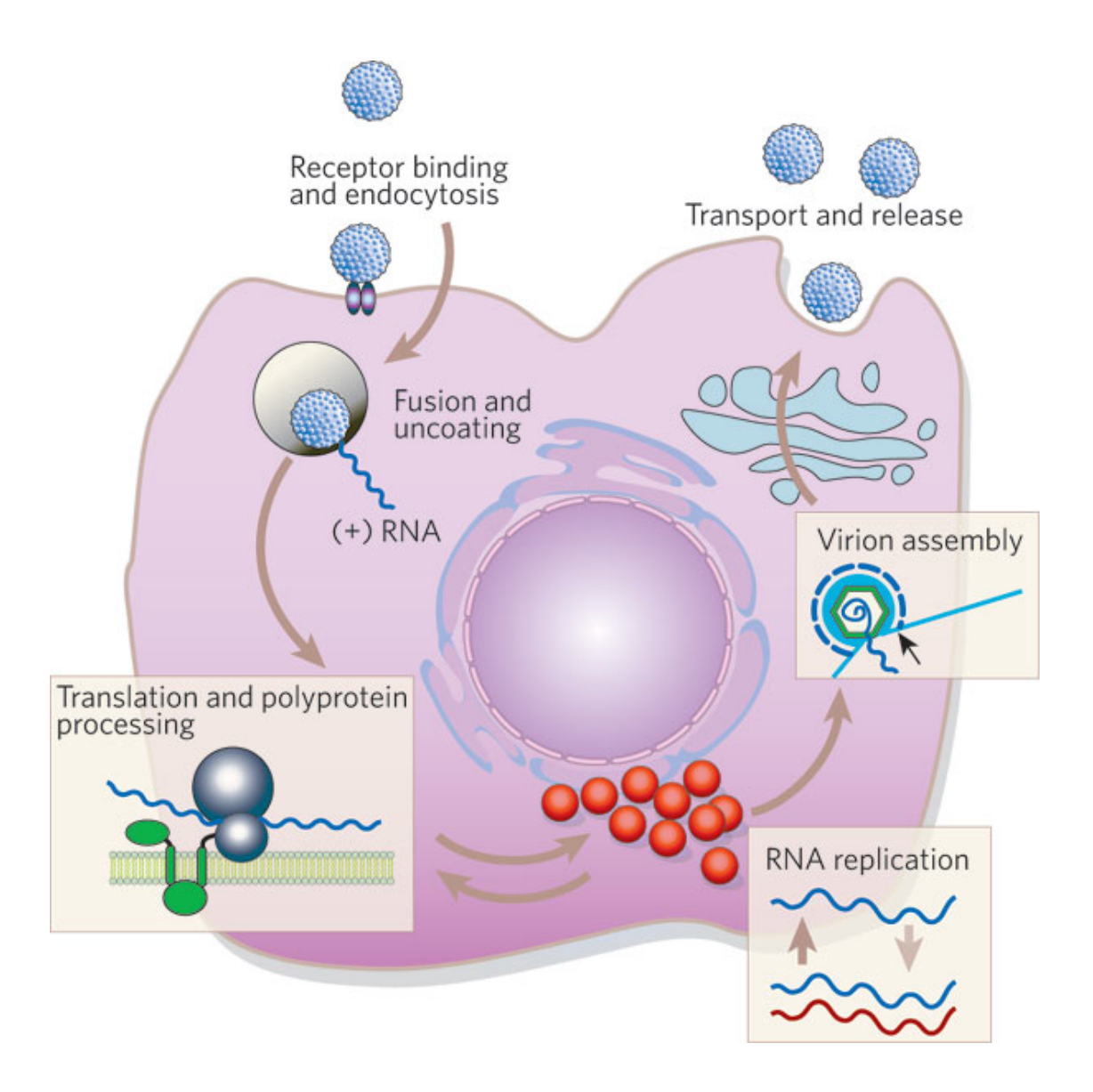


Figure 1.3. The HCV life cycle. HCV entry occurs via receptor-mediated endocytosis, after attachment (glycosaminoglycans and LDLR) and interactions with several entry receptors (SR-B1, CD81, Occludin and Claudin-1). Uncoating occurs through fusion of the viral and endosomal membranes and the viral RNA is released into the cytoplasm. Translation and polyprotein processing occur in close association with ER membranes. Replication of the viral genome takes place in the virus-induced membranous web and proceeds through a full-length negative-strand RNA intermediate which is subsequently used as a template for the synthesis of progeny positive-strand genomic RNAs. Assembly occurs in close association with the membranous web and lipid droplets and transits through the Golgi complex prior to release by a noncanonical secretory pathway involving the endosomal compartment. Figure from Lindenbach and Rice, *Nature*, 2005 (53).

1.3 Role of RNA secondary structures in the HCV life cycle

RNA secondary structures in the HCV genomic RNA

As a positive-sense RNA virus, the HCV genome itself is used as a template for translation, replication, and packaging. Therefore, the viral RNA must be a dynamic structure able to readily accommodate the unwinding, elongation and exposure of different regions of the RNA to various cellular and viral proteins for the different stages of the viral life cycle. The 5' and 3' UTRs contain *cis*-acting RNA elements (CREs), which are secondary structures that play key roles in the viral life cycle (**Figure 1.4**) (54,55).

The HCV 5' UTR contains four major stem loop (SL) structures (**Figure 1.4A-B**). SLI and SLII are important for viral RNA replication, while SLII-SLIV form the HCV IRES that mediates recruitment of the 40S ribosome for translation of the viral polyprotein. SLII-SLIV have been shown to form independently of one another (56,57). SLIIa, the apical loop of SLII, has a functional L-shaped structure that bends to direct SLIIb to the E site of the ribosome (**Figure 1.4C**) (58). SLIIa has been shown to be important in HCV translation and its deletion from the IRES inhibits the bent conformation of SLII, which is responsible for directing SLIIb to the E-site of the ribosome (59-61). SLIII has six domains, SLIIIa-f, which mediate important interactions with the 40S ribosome (**Figure 1.4C**) (56). SLIIIad interacts with the 40S ribosome surface, while the SLIIIbc junction interacts with the eukaryotic initiation factor 3 (eIF3), and SLIIIef associates with SLIV to form a pseudoknot structure that is required to position the AUG start codon into the P-site of the 40S ribosomal subunit (**Figure 1.4C**) (56,62).

SL structures in both the 5' and 3' UTRs have been implicated in viral RNA synthesis (57). Specifically, SLI and SLII of the 5' UTR are critical for HCV RNA replication (63). Studies show that the first 125 nucleotides of the viral genome are sufficient for viral RNA replication; however, replication is enhanced by the presence of the entire 5' UTR (**Figure 1.4B**) (63). The 3' UTR is also implicated in viral RNA replication, and consists of the three important domains: the variable

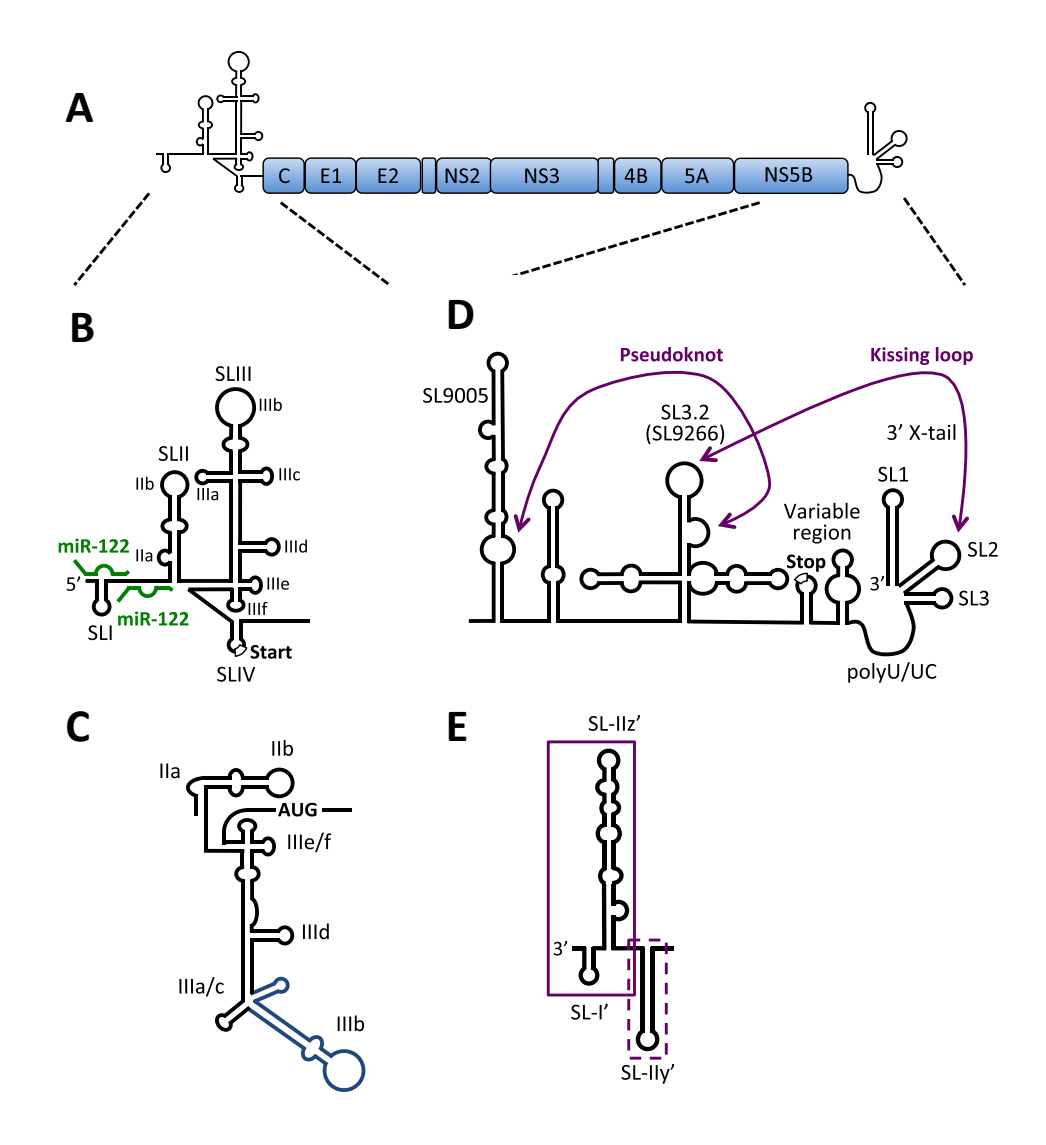


Figure 1.4. Secondary structures across the HCV genome. (A) The HCV genome contains several important RNA secondary structures in the 5' and 3' UTRs as well as NS5B coding region. (B) The 5' UTR contains four SL structures, SLI-SLIV as indicated. SLI and II are important for replication while SLII-SLIV make up the HCV IRES. The viral start codon (SLIV) as well as the interaction between the viral genome and the liver-specific microRNA-122 (miR-122, green) are indicated. (C) The orientation of SLII-IV when in complex with the 40S subunit and eIF3. This is the bent orientation which allows SLIIb to be placed in the E site of the 40S subunit. SLIIab binds to the surface of the 40S and SLIIbc (blue) binds to eIF3. SLIIIef and SLIV position the start codon in the P site of the 40S. (D) The 3' UTR contains the variable region, poly U/UC tract and 3' X-tail region (consisting of SL1-3). Several long-range interactions have been demonstrated to occur including kissing-loop interactions between 3' SL2 and SL3.2 of the NS5B region and between apical loop of NS5B pseudoknot SL3.2 and the bulge of SL9005 as shown. The nomenclature used for the SLs is based on the H77 complete genome sequence (Genbank Accession # AF011753). (E) The SLs of the 3' end of the negative-strand containing SL-I', SL-IIz', and SL-IIy'. SL-I' and SL-IIz' are required (boxed in), while SL-IIy' (dashed) contributes to the initiation of the positivestrand RNA synthesis. Adapted from Sagan S.M. et al., Virus Research, 2015 (57).

region, polyU/UC tract and the 3' X tail (**Figure 1.4D**) (57,64). The variable region contains two SL structures, the first of which overlaps with the NS5B coding region and contains the viral polyprotein stop codon. Viral replication is severely impaired in cell culture when the variable region is deleted, suggesting that it is important for efficient viral RNA accumulation (65). The polyU/UC tract consists of a stretch of 30-80 uridines interspersed by cytosine residues (64). Both the length and the composition of the polyU/UC tract is essential for HCV replication in cell culture, with 33 consecutive U residues shown to be required for viral RNA accumulation (66). The mechanism of the polyU/UC tract in HCV replication is still unclear, but this region has been shown to interact with the NS3, NS5A and NS5B proteins (67-69). Finally, the 3' X tail consists of three SL structures (SL1, SL2 and SL3) which are all essential for viral RNA replication (65). Notably, several studies have suggested that the 3' UTR also stimulates translation, at least in cell culture (70-74).

In addition to the 5' and 3' UTRs, secondary structures in the coding region, specifically in the NS5B coding region, have been implicated in modulating viral translation and replication (75-77). For example, SL3.2 (a.k.a. SL9266) of the NS5B coding region, has been shown to mediate two long-range RNA-RNA interactions: a pseudoknot interaction with the upstream SL9005 of the NS5B coding region and a kissing loop interaction with SL2 of the 3' X tail (**Figure 1.4D**) (78,79). Disruption of either of these interactions severely impairs viral replication and mutational analyses have demonstrated that these interactions are mutually exclusive, suggesting that they may play a role in the switch between translation and viral RNA replication (76,78,80,81).

RNA secondary structures in the negative-strand RNA intermediate

In addition to structures in the 5' and 3' UTRs of the positive-strand, structures in the 3' terminus of the negative-strand replicative intermediate are also implicated in viral RNA replication, as this region forms the promoter for positive-strand genomic RNA synthesis (**Figure 1.4E**) (82-85).

Computational prediction and genetic analyses suggest that the first 104 nts of the 3' terminus of the negative-strand intermediate contain three SL structures important for positive-strand RNA synthesis (Figure 1.4E) (85). Specifically, SL-I' (nt 6–20) and SL-IIz' (nt 21–104), were shown to be absolutely required for viral RNA synthesis, while SL-IIy' contributes to the efficiency of viral RNA replication (85,86). Notably, similar to the 3' terminus of the positive-strand genomic RNA, the 3' terminal nucleotide of the negative-strand intermediate is a uridine or cytosine residue in most HCV isolates, likely due to the preference for a purine (adenine or guanine) as the initiating nucleotide for the HCV NS5B RNA-dependent RNA polymerase (87). While these studies emphasized the importance of specific SL structures in directing positive-strand RNA synthesis, the distinct mechanistic roles of the structures at the 3' end of the negative-strand RNA intermediate are not yet clear and this is likely to be the focus of future studies.

1.4 HCV cell culture systems

Since the discovery of the virus in 1989, research in the HCV field has been hampered due to the difficulties in establishing a cell culture system to study the virus. Initially, cultured cell lines were infected with sera from HCV infected patients but only low levels of HCV accumulation were detected, and only exclusively from reverse transcription polymerase chain reaction (RT-PCR) (88-91). Additionally, the only animal model that could be experimentally infected with HCV were chimpanzees, as humans and chimpanzees share more than 98% of their genome (92). However, chimpanzees clear the infection at higher rates than humans, and they present challenges in terms of availability, as well as ethical and financial constraints that limited HCV research (92). Thus, efforts were made to establish HCV replication models in cell culture, and in 1999, Lohmann *et al.* demonstrated robust replication of a subgenomic HCV replicon in the human hepatoma cell line, Huh-7 (52). Subsequently, a cell line derived from Huh-7, termed Huh-7.5, proved to be even

more permissive for HCV replication due to an inactivating mutation in the pathogen recognition receptor, retinoic acid-inducible gene I (RIG-I) (93,94).

The HCV replicon model consists of a subgenomic HCV RNA where the structural region of the HCV ORF has been replaced with a reporter gene (e.g. luciferase) or a selection gene (e.g. neomycin resistance) (**Figure 1.5**). Expression of the NS proteins (NS2-5B) is driven by a heterologous encephalomyocarditis virus (EMCV) IRES element. After introduction into Huh-7 or Huh-7.5 cells, the expression of the viral replication complex proteins allows viral replication of the subgenomic replicon RNA, but due to the lack of structural proteins, no infectious viral particles are produced (52,95) (**Figure 1.6A**). This system is useful to study viral replication and polyprotein processing, but is not suitable for studies of viral entry, packaging or release of infectious viral particles.

A fully-infectious cell culture system that recapitulates the entire HCV life cycle in cell culture was developed in 2005 (99). Briefly, this system is based on the Japanese Fulminant Hepatitis-1 (JFH-1) isolate (genotype 2a), isolated from a patient with fulminant hepatitis (99-101). This viral genome, for reasons that still remain unclear, was able to undergo the complete viral life cycle in Huh-7 and Huh-7.5 cell and is termed HCV cell culture (HCVcc) (**Figure 1.6B**). This system allows the study of the entire HCV life cycle, and chimeric viruses have been developed that allow several HCV genotypes to be studied. However, to remain infectious, chimeric viruses still must be within the context of the JFH-1 (genotype 2a) NS proteins (98). In this thesis, we make use of the J6/JFH-1 chimera (a.k.a. Jc1) that has enhanced viral RNA production in Huh-7.5 cells and consists of the 5' end to the NS2 region of the J6 isolate (genotype 2a) fused to the NS3 to the 3' end of the JFH-1 isolate (genotype 2a) (97). This J6/JFH-1 virus grows to higher titers in cell culture; and we are using a *Renilla* luciferase (RLuc) reporter version, whereby RLuc is expressed as part of the viral polyprotein between the p7 and NS2 coding

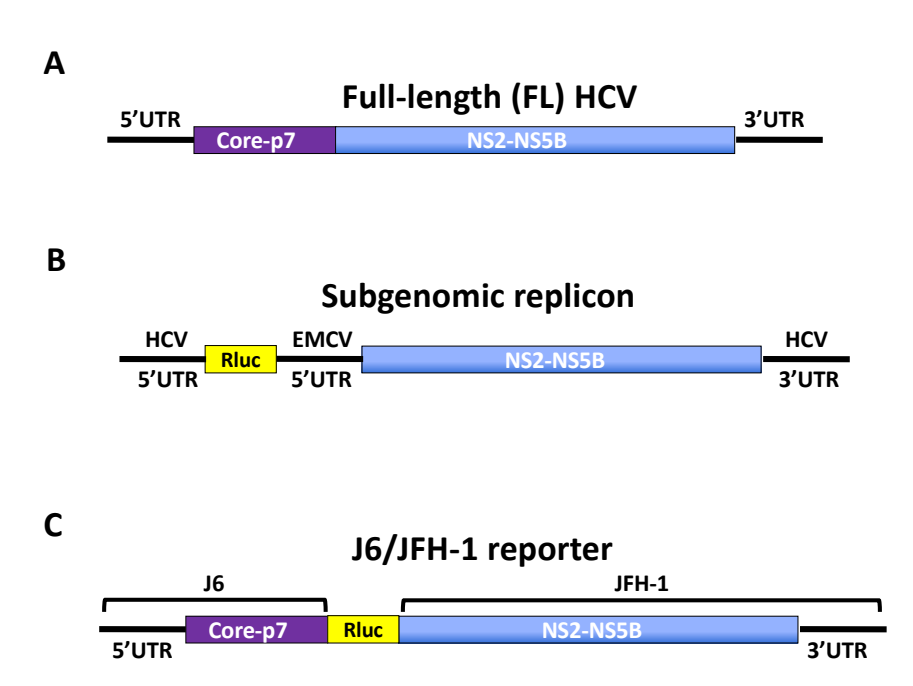


Figure 1.5. HCV replication systems. Cartoon diagrams of **(A)** the Full-Length (FL) HCV genome, **(B)** a subgenomic HCV replicon containing an Rluc reporter driven by the HCV IRES, and the HCV non-structural proteins (NS2-NS5B) driven by the EMCV IRES, **(C)** the full-length HCV J6/JFH-1 chimera containing the 5' UTR to p7 region of J6 and the NS2 to 3' UTR region of JFH-1 with the Rluc reporter gene encoded as part of the polyprotein between p7 and NS2 (36,52,96-99).

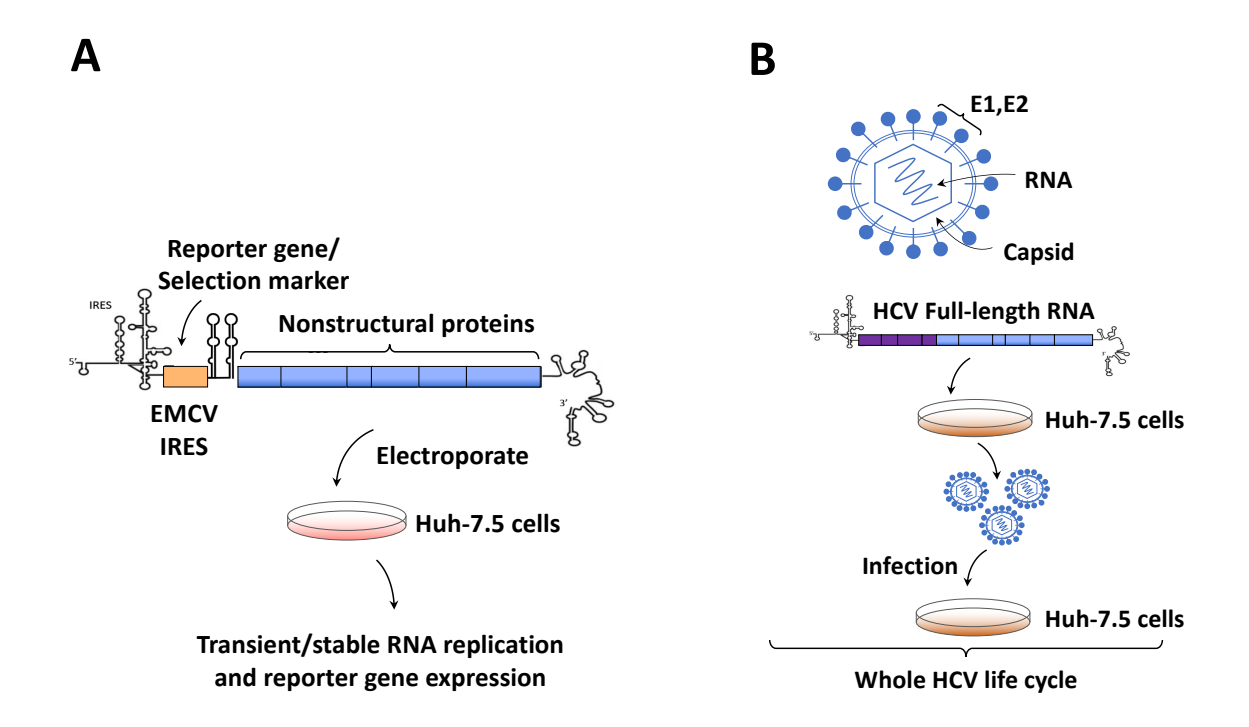


Figure 1.6. Cell culture systems of HCV. (**A**) The HCV subgenomic replicon model of viral replication consists of self-replicating HCV RNAs which include a reporter gene or selectable marker replacing the structural genes upstream of an EMCV IRES that allows translation of the viral NS proteins NS3 to NS5B. HCV replicon RNAs are transfected into Huh-7.5 cells where they are able to replicate autonomously (52). (**B**) The cell culture-derived HCV (HCVcc) model is based on the genotype 2a isolate JFH-1 (99). Full-length viral genomes are introduced into Huh-7.5 cells and this leads to translation, RNA replication and production of viral particles able to infect new target cells, thereby completing the entire HCV life cycle.

sequence which allows us to monitor viral RNA replication by luciferase assay (**Figure 1.5C**) (36,96).

1.5 HCV Therapy

As discussed previously, the majority (\sim 75%) of HCV-infected individuals will progress to chronic HCV infection, which cannot be cleared without antiviral intervention (102). Currently, there is no vaccine available, and until 2011, the only approved treatment for HCV infection was a combination of pegylated interferon-alpha (IFN- α) and ribavirin, which was poorly tolerated and ineffective in a large proportion of patients (103). A sustained virological response (SVR), defined as undetectable HCV RNA in the blood six months after the end of treatment, is tantamount to a "cure". In the context of genotype 1 infection, the combination of pegylated IFN- α and ribavirin therapy resulted in SVR rates of \sim 70% in treated patients (103,104).

Direct-acting antivirals

In 2011, the first direct-acting antivirals (DAAs) were approved for HCV treatment in Canada. In contrast to the non-specific nature of ribavirin and IFN-based therapies, DAAs target specific viral proteins to block distinct and essential steps in the viral life cycle (105). There are three classes of DAAs that target three viral proteins – the NS3/4A protease, the NS5B RdRp, and the NS5A protein (106).

The first generation DAAs were the protease inhibitors, Telaprevir and Boceprevir, which were approved in 2011 by the US Food and Drug Administration (FDA) to treat patients infected with HCV genotype 1 (106,107). This class of DAAs inhibits the serine protease activity of NS3/4A and this results in a defect in polyprotein processing (108,109). The second class of DAAs, includes nucleoside/nucleotide-analogs and the non-nucleoside inhibitors of the viral NS5B RdRp (110). The nucleoside/nucleotide analog inhibitors typically act as chain terminators when

incorporated into the RNA chain during viral RNA synthesis; whereas the non-nucleoside inhibitors bind to allosteric sites on the viral NS5B protein to inhibit the enzyme's activity (111-113). Sofosbuvir is a nucleotide analog that acts as a chain-terminator (114,115). Due to its pangenotypic activity and excellent resistance profile, Sofosbuvir is one of the most widely used DAAs in combination therapies (105,114). Finally, the third class of DAAs is the NS5A inhibitors, which include Ledipasvir and Daclatasvir (116,117). The NS5A protein is a phosphoprotein involved in RNA replication and assembly, and drugs that target this protein result in the relocalization of NS5A from the ER to lipid droplets. The precise mechanism of action of NS5A inhibitors remains unclear, but they have been demonstrated to prevent hyperphosphorylation of NS5A, and they bind into the NS5A dimer interface and may prevent RNA binding into the RNA binding channel (118-120). Currently, HCV treatment regimens typically contain a combination of two or more of these DAAs from different classes and are able to achieve SVR in over 95% of treated patients (121). For instance, a combination of Daclatasvir and Sofosbuvir in a 12-week duration gave an SVR of 98% in patients with HCV subtype 1a and 100% in patients with subtype 1b (122). Although these DAAs are highly effective, accessibility and cost remain major challenges associated with HCV elimination (123). Moreover, it is not yet clear whether alternative treatment strategies will be needed for patients with advanced disease or those that develop resistance.

Host-targeted antivirals

Host-targeted antivirals offer an alternative to DAAs and are extremely lucrative in that they may offer a high genetic barrier to resistance and pan-genotypic activity (124). For example, antibodies targeting the CD81 or SR-B1 receptors can prevent HCV infection *in vivo* (124-126). Cyclophilin A inhibitors, which inhibit an essential interaction for viral RNA replication between NS5A and Cyclophilin A, have also been used successfully to limit HCV infection (127,128). In addition,

several cholesterol and fatty acid synthesis pathways modulate HCV replication and statins, which inhibit of 3-Hydroxyl -3- Methylglutaryl-Coenzyme A reductase, a rate-limiting enzyme for cholesterol synthesis have been demonstrated to inhibit HCV replication *in vitro* (129,130). However, the *in vivo* efficacy of these drugs for chronic HCV infection remains controversial (summarized in (131)). Finally, MiravirsenTM and RG-101, two antisense inhibitors of the liver-specific microRNA, miR-122, have been used successfully to limit HCV replication in cell culture and in chronic HCV-infected patients (discussed in more detail in *section 1.8*) (132,133). Taken together, these studies suggest that targeting host factors may be an effective alternative approach to limiting HCV replication.

1.6 microRNAs

The first microRNA (miRNA) was discovered in 1993 in *Caenorhabditis elegans* (134). Since then, miRNAs have been identified in over 200 species, with over 2000 miRNAs in humans and greater than 24,000 miRNA entries in the Sanger database (135). microRNAs (miRNAs) are small (~19-25 nt), evolutionarily-conserved, non-coding RNAs that mediate post-transcriptional gene silencing (136). MiRNAs typically interact with the 3' UTR of their target genes, through base-pairing interactions primarily with the 'seed sequence' (nt 2-8) of the miRNA. Through this activity, they are predicted to regulate more than 60% of all human genes and thus are implicated in numerous diseases, including cancer, viral infections, cardiovascular and metabolic disorders (137).

The microRNA pathway

MiRNAs are mostly found in the introns of protein-coding genes and are transcribed as highly structured primary miRNA (pri-miRNA) transcripts by RNA polymerase II (138,139) (**Figure 1.7**). These pri-miRNAs are cleaved by Drosha, a nuclear RNase III enzyme, into a short (~70-nt)

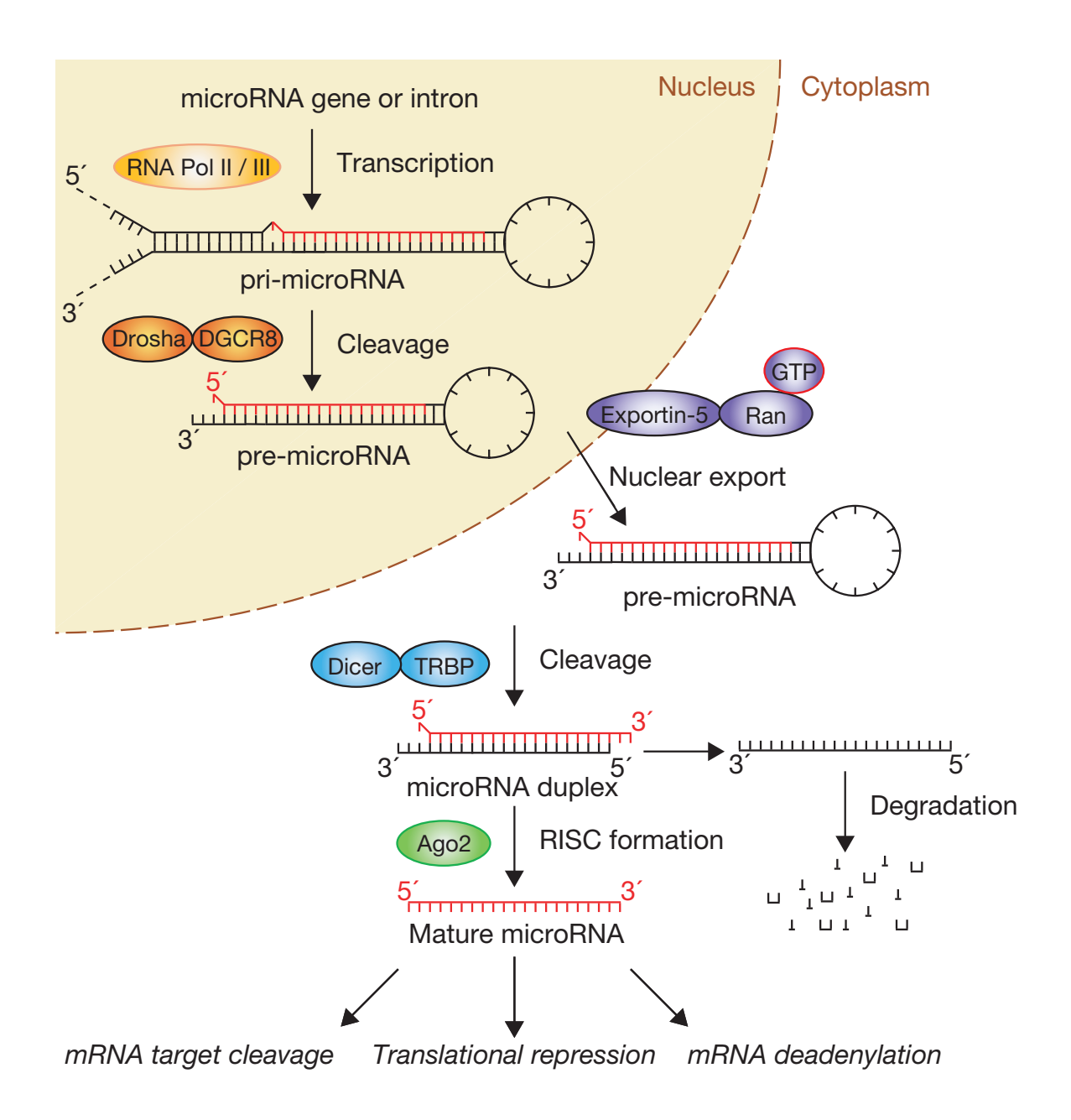


Figure 1.7. miRNA biogenesis. The pri-miRNA is transcribed by polymerase II and then cleaved by Drosha, forming the pre-miRNA. Pre-miRNA duplex is exported to the cytoplasm, which is then cleaved by Dicer. The mature miRNA is then transported to its target by Ago2 while the passenger miRNA strand is degraded. The target mRNA of miRNA would be cleaved, or translationally repressed or deadenylated. Figure from Winter et al., *Nature Cell Biology*, 2009 (155).

hairpin-shaped precursor miRNAs (pre-miRNAs). Drosha is a part of the microprocessor complex, which includes DiGeorge critical region 8 protein (DGCR8), which is suggested to help position Drosha on the pri-miRNAs (140-142). The pre-mRNAs are then transported into the cytoplasm by Exportin-5, which is a RanGTP-dependent nuclear transport protein (143).

In the cytoplasm, the pre-miRNAs are further processed by another RNase III enzyme, Dicer, into mature ~ 22 nt miRNA duplexes (144-146). Two double-stranded (ds) RNA binding proteins, transactivating response RNA-binding protein (TRBP) and protein activator of PKR (PACT), influence the strand selection and cleavage activities of Dicer (147). This protein complex also acts as a scaffold for assembly of the RNA-induced silencing complex (RISC), which contains an Argonaute (Ago) protein (148,149). The RISC couples the miRNA processing and silencing steps, and the Ago protein unwinds the miRNA duplex and uses one strand, known as the guide strand, to target complementary mRNAs (150,151). Base-pairing interactions are primarily mediated by nucleotides 2 to 8 of the miRNA, also known as the "seed sequence" (152). Binding to complementary sites in the 3' UTR of target mRNAs typically leads to direct cleavage, translational suppression of accelerated deadenylation, all of which culminate in repression of target gene expression (Figure 1.7) (153-155). One protein that is crucial for miRNA-induced repression of gene expression is the Glycine-tryptophan repeat-containing protein of 182 kDa (GW182), which is a key processing-body (p-body) protein (156-161). P-bodies are discrete cytoplasmic foci that are characterized by localization of proteins involved in mRNA decay, miRNA-mediated gene silencing, and translational repression (162). Knockdown of GW182 was shown to impair silencing of miRNA reporters, suggesting a link between miRNA-mediated gene silencing and P-bodies (163,164). GW182 is thought to be the effector protein in miRNA-induced gene silencing, and is able to recruit the decapping, deadenylation, and RNA decay machinery to targeted mRNAs.

1.7 miR-122

miR-122 is a highly abundant (~66, 000 copies per cell), liver-specific miRNA which constitutes 70% of all miRNAs in the liver (165). miR-122 is transcribed by RNA polymerase II as a highly-structured pri-miR-122 transcript from the *hcr* gene locus (165). Due to Dicer processing and 3' modifications, three major isoforms of miR-122 are present in Huh-7 and Huh-7.5 cells, which include a 21, 22 and two 23-nt isoforms (166). Specifically, the 23 nt variant includes both a templated 3' uridylated and a non-templated 3' adenylated form (166). The 22-nt isoform is the most abundant form found in both Huh-7 and Huh-7.5 cells (167,168).

Cellular targets of miR-122

The first identified target of miR-122 was cationic amino acid transporter-1 (CAT-1) (165,169). The binding of miR-122 to the 3' UTR of the CAT-1 mRNA results in translational repression (169). However, during amino acid starvation, the mRNA binding protein, HuR, binds to the 3' UTR of the CAT-1 mRNA and releases miR-122-mediated translational repression (136,169). Several other miR-122 targets were identified using antisense inhibitors of miR-122 in mice and nonhuman primates (170-172). For instance, sequestration of miR-122 in animal models results in an overall reduction in plasma cholesterol levels and an increase in fatty acid oxidation without any detectable toxicity, suggesting a role for miR-122 in regulation of cholesterol metabolism and fatty acid synthesis (170-172). MiR-122 also controls iron homeostasis through regulation of the hepcidin hormone activators: *hemochromatosis* and *hemojuvelin* (173). Moreover, miR-122-knockout mice developed steatohepatitis, fibrosis and HCC, confirming a role for miR-122 in lipid metabolism and further suggesting that it has tumour suppressor activity (174). In line with these findings, miR-122 levels are frequently reduced in HCC, while its overexpression reduces the tumorigenic properties of HCC cell lines (175,176). Thus, miR-122 is a major regulator of many

important functions in the liver, including iron homeostasis as well as cholesterol and fatty acid metabolism.

miR-122 interactions with the HCV genome

In addition to its cellular targets, miR-122 has a genetic interaction with the HCV genome and, counter to canonical miRNA interactions, miR-122 *promotes* HCV RNA accumulation in both cell culture and the livers of HCV-infected patients, independently of its effects on cholesterol and lipid metabolism (132,133,177-180). Correspondingly, HCV RNA accumulation is also dependent on the miRNA biogenesis pathway, presumably due to its reliance on miR-122, as depletion of Drosha, Dicer, DGCR8, TRBP or any of the four Ago proteins (Ago1-4) leads to a significant reduction in HCV RNA accumulation in cell culture (136,181-183).

MiR-122 binds to two tandem seed match sequences (termed Site 1 and Site 2) in the 5' UTR of the HCV genome, and had additional base-pairing interactions with nucleotides 1-3 and 29-32, creating a 3' overhang at the 5' terminus of the HCV genome (**Figure 1.8**) (178,180,184). Importantly, direct binding to the HCV genome is required and miR-122's effects on viral RNA accumulation as mutation of either Site 1 or Site 2 impairs HCV RNA accumulation, and this can only be rescued with miR-122 molecules containing compensatory mutations that restore base-pairing interactions (178-180,184,185). Moreover, mutational analyses indicates that nucleotides in the bulge and 3' tail of the miR-122 molecules are important for viral RNA accumulation (180). This suggests that these nucleotides may mediate important interactions with host and/or viral proteins or RNAs required for miR-122-mediated HCV RNA accumulation (186).

Initial investigations into the potential mechanism(s) of miR-122-mediated viral RNA accumulation suggested that miR-122 has an effect on viral IRES-mediated translation (1.4- to 2-fold), and suggested that it has no significant effect on the rate of viral RNA synthesis (at least in

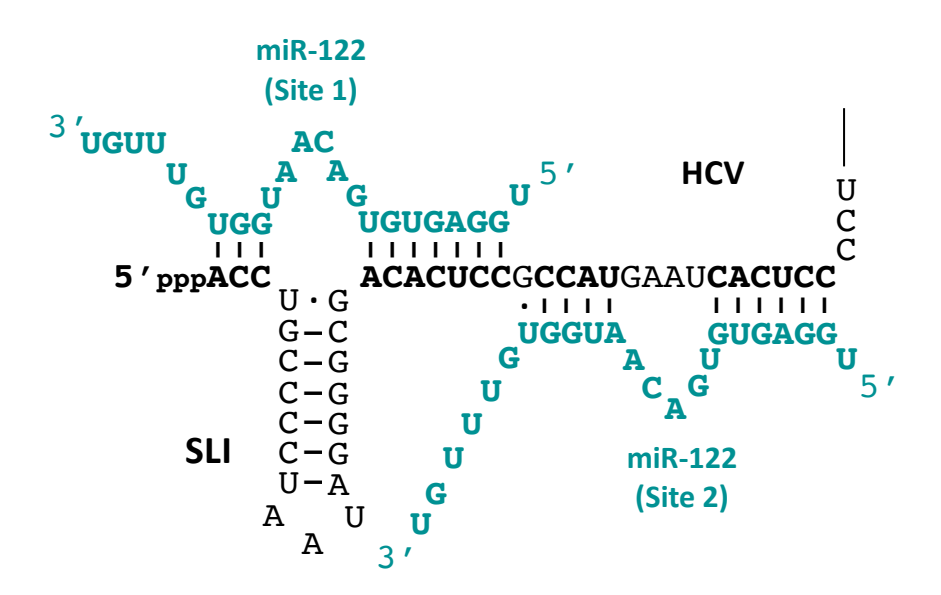


Figure 1.8. miR122:HCV RNA interactions at the 5' terminus. Model of miR-122 (green) and HCV genomic RNA (black) interactions. Nucleotides 1-42 of the HCV genome are shown (isolate JFH-1, genotype 2a).

the elongation phase) (184,185,187,188). However, recent research, including the findings described herein, have revealed three major mechanisms of miR-122-mediated viral RNA accumulation: 1) genome stability; 2) translational promotion; and 3) RNA chaperone activity (each described in more detail below). Finally, in addition to Sites 1 and 2, several other putative miR-122 binding sites have been identified across the HCV genome (184,189,190); however, beyond Sites 1 and 2 (discussed herein), these have been demonstrated to have negligible effects on HCV RNA accumulation (191).

1.8 Roles of miR-122 in the HCV life cycle

miR-122 protects the 5' terminus of the HCV genome from cellular pyrophosphatases and subsequent exoribonuclease-mediated decay

The finding that miR-122 binding to the 5' terminus of the HCV genome creates a 3' overhang suggested a role for miR-122 in protection of the HCV genome from nucleases, pyrophosphatases, and/or cellular sensors of RNA (180). Accordingly, recent research suggests that miR-122 protects the viral 5' triphosphate from recognition by two cellular pyrophosphatases, DOM3Z (a.k.a. decapping exonuclease, DXO) and dual specificity phosphatase 11 (DUSP11) (96,192). DOM3Z, is a cellular pyrophosphatase that has pyrophosphohydrolase, decapping and 5' to 3' exoribonuclease activities (193). Its normal role in the cell is in mRNA capping quality control, where it converts improperly capped mRNAs to 5' monophosphorylated mRNAs which can subsequently be degraded by 5' exoribonuclease activity (96,193,194). DUSP11 is a 5' di- and triphosphatase that regulates the levels of cellular RNA polymerase I and III transcripts (96,195,196). Recent studies suggest that although both of these pyrophosphatases are primarily nuclear, they also localize to p-Bodies (sites of RNA decay) in the cytoplasm (96,195,197,198). Interestingly, miR-122 was shown to protect or shield the HCV genome from cellular

pyrophosphatase activity; such that, in the absence of miR-122, DOM3Z and DUSP11 are able to remove the viral 5' triphosphate and make it susceptible to 5' to 3' exoribonuclease-mediated decay by the cellular exoribonucleases, Xrn-1 and 2 (96,192,199-202). Thus, miR-122 promotes HCV genome stability by protecting the 5' terminus of the viral RNA from cellular pyrophosphatases and subsequent exoribonuclease-mediated decay (**Figure 1.9**).

miR-122 promotes ribosome association

Early studies on miR-122:HCV RNA interactions focused on a role for miR-122 in viral translation, and suggested that miR-122 promotes association of the viral RNA with the ribosome by approximately 1.4 to 2-fold (187,203). Subsequent studies have suggested that an Ago protein is required for efficient miR-122-mediated HCV RNA accumulation and participates in translational promotion (182,204-207). Additionally, previous work suggests that the spacing between the miR-122 seed sequences and the IRES is important in promoting miR-122-mediated translation (206). In line with these findings, our recent study supports a role for miR-122 in promotion of HCV translation, which may be mediated by interactions between Ago2 and SLIIa of the HCV IRES (described in more detail in Chapter 2) (208).

miR-122 alters the secondary structure of the HCV 5' UTR

Recent studies have helped to further clarify the mechanism of miR-122-mediated viral RNA accumulation in the HCV life cycle. Specifically, three recent studies (including the research described herein), suggest that miR-122 interactions with the HCV genome alter the secondary structure of the viral 5' terminus (208-210). Specifically, RNA structure prediction, mutational analyses, and structure probing suggest that the first 117 nts of the HCV genome, is able to take on a more energetically stable structure, termed SLII^{alt} (**Figure 1.10**) (208-210). Moreover,

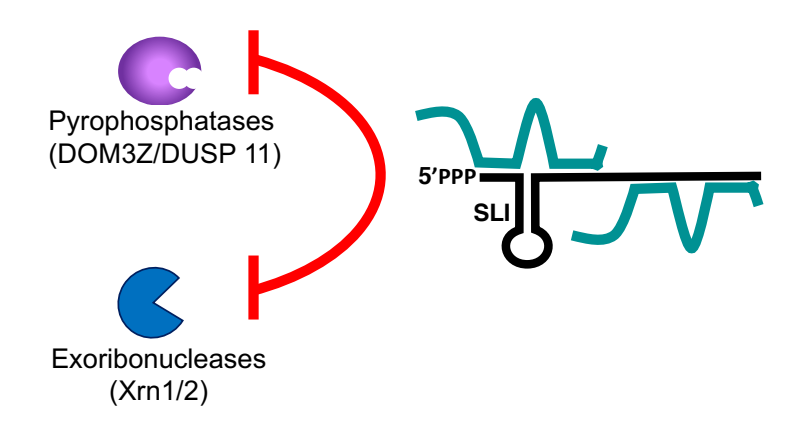


Figure 1.9. miR-122 protects the terminus of HCV genome from 5' decay. miR-122 protects the 5' triphosphate of the HCV genomic RNA from the cellular pyrophosphatases DOM3Z (a.k.a. DXO) and DUSP11, and subsequent decay by the 5' exoribonucleases, Xrn-1/2.

these studies suggest that miR-122 interactions with the HCV genome suppress SLII^{alt}, and act as an RNA chaperone, akin to a bacterial riboswitch, that re-folds the 5' terminus of the viral RNA into the SLII structure, which allows the viral IRES (SLII-IV) to form (**Figure 1.10**) (208-210). The functional SLII structure is required for efficient association with the 80S ribosome assembly, suggesting that this RNA chaperone activity is likely to promote viral translation (60).

Thus collectively, together with the research described herein, miR-122 appears to play three key roles in the viral life cycle: 1) it promotes viral genome stability; 2) it promotes HCV IRES-mediated translation; and 3) it acts as an RNA chaperone or riboswitch to suppress a more energetically favorably RNA secondary structure, allowing the viral IRES to form.

1.9 Clinical correlations of miR-122 in chronic HCV infection

Dysregulation of miR-122 contributes to viral pathogenesis

A genome-wide high-throughput sequencing and crosslinking immunoprecipitation (HITS-CLIP) analysis of human Ago revealed that the HCV genome functionally sequesters miR-122 during HCV infection (211). This "sponge" effect results in de-repression of canonical miRNA targets and dysregulation of cell proliferation and survival, collagen production, and hepatic stellate cell activation resulting in a proinflammatory response (211). Furthermore, miR-122 has been demonstrated to be a tumor suppressor, and hence sponging of miR-122 by the HCV genome may contribute to cell transformation and HCC development in chronic HCV infection (174,212,213).

miR-122 as a target for antiviral therapy

Due to the importance of miR-122 in the HCV life cycle, two antisense miR-122 inhibitors, considered the flagship miRNA-based drugs, have been developed for the treatment of chronic

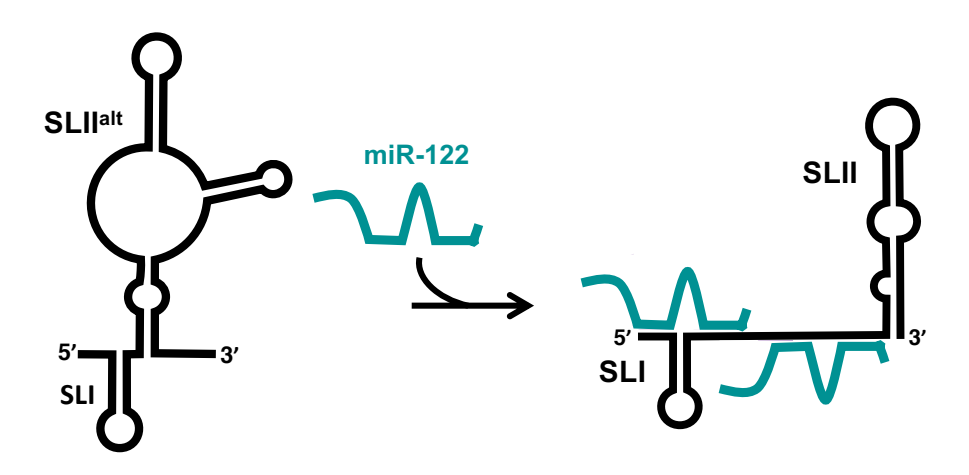


Figure 1.10. miR-122 binding to HCV RNA alters the secondary structure of SLII. SLII takes on an alternative secondary structure (SLII^{alt}), which is not favourable for translation. However, when miR-122 binds, SLII takes on a functional, open conformation, structure that is favourable for translation initiation.

HCV infection (132,133). Both MiravirsenTM (Santaris Pharma a/s) and RG-101 (Regulus Therapeutics) miR-122 inhibitors have completed Phase II or Ib clinical trials, respectively, to investigate their clinical efficacy (132,133). Excitingly, both treatments led to dose-dependent and sustained reductions in viral loads; and, in the latter study, two patients achieved a sustained virological response (at least up to 76 weeks post-treatment) after receiving a single dose of RG-101. Neither treatment was associated with significant adverse events or long-term safety issues, suggesting that antisense targeting of miR-122 may be an effective treatment that could be used in future combination therapies.

Notably, while no resistance was apparent during treatment, when viral RNA rebounded after cessation of the inhibitor, several resistance associated variants (RAVs) were identified in the viral 5' UTR (132,133). Specifically, C2GC3U, C3U and G28A were identified in patients who underwent miR-122 inhibitor-based therapies (**Figure 1.10**) (132,133,214). In addition to these RAVs, cell culture-based studies have also provided evidence of mutations in the viral 5' UTR, namely G28A, U4C and C37U, that allow HCV RNA accumulation in conditions where miR-122 is either limiting or absent (**Figure 1.11**) (215,216). However, the mechanism(s) underlying miR-122-independent viral RNA accumulation remain unclear and we will explore these RAVs and their mechanisms of action in more detail in *Chapter 3*. Understanding the emergence of RAVs and their mechanisms of action will be important to gain insight into how HCV can overcome its reliance on miR-122. More broadly, understanding the mechanisms of resistance to miRNA-based drugs is of great importance as a wave of new miRNA-based therapies enters the clinic (~3500 studies published in 2018 on miRNA-based therapeutics) (217).

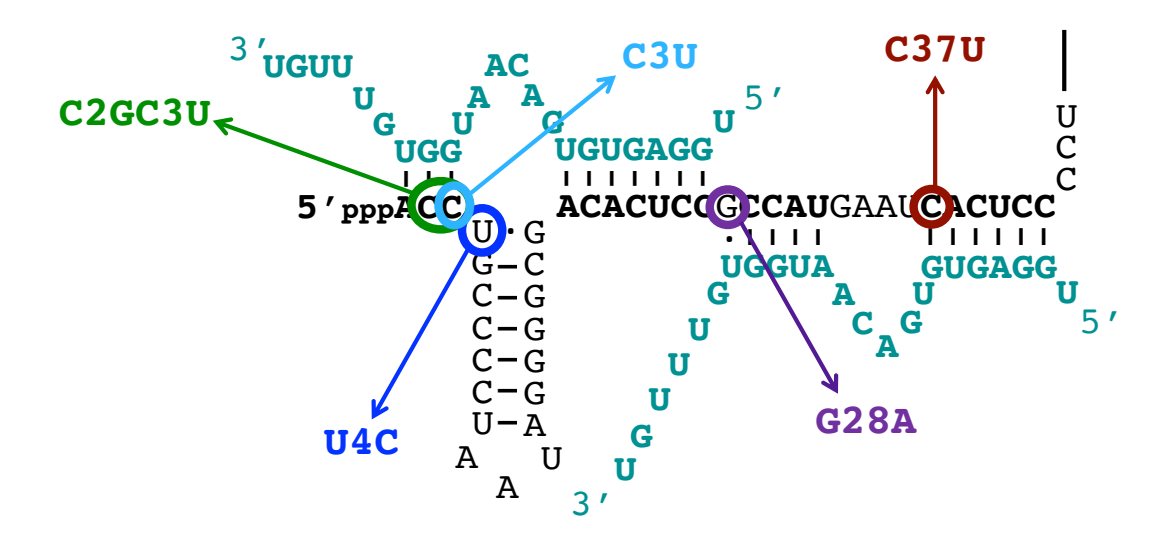


Figure 1.11. miR-122 inhibitor resistance-associated variants (RAVs). Locations of the RAVs: C2GC3U, C3U, U4C, G28A and C37U in 5' terminus of the HCV genome (nts 1-42).

1.10 Hypothesis and Specific Aims

1. To identify how miR-122 and Ago:miR-122 complexes alter the structure of the HCV 5' UTR (Chapter 2)

As discussed above, previous work suggested that miR-122 binding alters the secondary structure of the viral IRES, which may promote viral translation (210,218,219). Additionally, Ago proteins were shown to have a role in viral RNA accumulation, although their precise role in miR-122-mediated viral RNA accumulation remains unclear (182). An Ago HITS-CLIP study suggested that in addition to interactions with the two miR-122 binding sites, the Ago protein may also make contact with the HCV IRES (211). Thus, we hypothesized that miR-122 and Ago:miR-122 interactions alter the structure of the HCV 5' UTR in a manner that may promote viral RNA accumulation. We used biophysical and *in vitro* SHAPE analysis to investigate how the binding of miR-122 and the Ago2:miR-122 complex alters the structure of the HCV 5' UTR.

Overall, our findings provide a new model for Ago:miR-122 interactions with the HCV genome. Our data suggests that Ago:miR-122 complex acts as an RNA chaperone or riboswitch through its initial recruitment to Site 2, to promote the formation of the functional SLII structure. In this conformation, Site 1 becomes accessible, and recruitment of a second Ago:miR-122 complex to this site promotes viral stability by protecting the 5' terminus from pyrophosphatase and subsequent exoribonuclease-mediated decay. To accommodate the Ago:miR-122 complex at both sites, the auxiliary base-pairing interactions are weakened between the Ago:miR-122 molecule at Site 2, but this is likely further stabilized by interactions between the Ago protein and SLIIa of the HCV IRES. Furthermore, we predict that these interactions between the Ago protein and SLIIa may further stabilize the IRES, promoting viral IRES-mediated translation.

2. To elucidate the mechanism of action of resistance-associated variants (RAVs) in the 5' UTR that confer miR-122-independent HCV RNA accumulation (Chapter 3)

Our previous study suggested that miR-122 has three roles in the viral life cycle: 1) it serves as an RNA chaperone or riboswitch to suppress an alternative, more energetically favorable conformation and allows the viral IRES (SLII-IV) to form; 2) it protects the viral genome from pyrophosphatase and subsequent exoribonuclease-mediated decay; and 3) it promotes translation through contacts between the Site 2-bound Ago:miR-122 complex and SLIIa of the HCV IRES. Due to its importance in the HCV life cycle, antisense miR-122 inhibitors have been used to treat chronic HCV infection in the clinic (72,132,133,220). While the results were quite promising, several RAVs were apparent upon viral rebound in several patients. Thus, based on our previous findings, we hypothesized that RAVs alter the structure of the viral RNA in a manner that promotes HCV RNA accumulation, even in the absence of miR-122.

We explored the ability of RAVs to accumulate in cell culture and used *in vitro* SHAPE analysis to determine how RAVs alter the structure of the viral RNA. We found that RAVs can be classified into three classes, based on three distinct mechanisms of action, all based on changes in the structure of the viral RNA. More specifically, the Class I RAVs, which include C2GC3U, U4C and G28A, are riboswitched and are all able to form the functional SLII structure, even in the absence of miR-122. The Class II RAVs, including C2GC3U, C3U and U4C, have increased basepairing at the 5' terminus of the viral genome, which confers increased stability to the viral RNAs, in the absence of miR-122. Finally, the Class III RAV, C37U, alters the structure of the 3' end of the negative-strand replicative intermediate, suggesting that it may provide a stronger promoter for positive-strand synthesis (221-223).

1.11 References

- 1. Feinstone, S.M., Kapikian, A.Z., Purcell, R.H., Alter, H.J. and Holland, P.V. (1975) Transfusion-associated hepatitis not due to viral hepatitis type A or B. *N. Engl. J. Med.*, **292**, 767-770.
- 2. Qui-Lim Choo, G.K., Amy J. Weiner, Lacy R. Overby, Daniel W. Bradely, Michael Houghton. (1989) Isolation of a cDNA Clone Derived from a Blood-Borne Non-!, Non-B Viral Hepatitis Genome. *Science*, **244**, 359-362.
- 3. Kuo, G., Choo, Q.L., Alter, H.J., Gitnick, G.L., Redeker, A.G., Purcell, R.H., Miyamura, T., Dienstag, J.L., Alter, M.J., Stevens, C.E. *et al.* (1989) An assay for circulating antibodies to a major etiologic virus of human non-A, non-B hepatitis. *Science*, **244**, 362-364.
- 4. Alter, H.J. and Houghton, M. (2000) Clinical Medical Research Award. Hepatitis C virus and eliminating post-transfusion hepatitis. *Nat. Med.*, **6**, 1082-1086.
- 5. Organization, W.H. (2017), pp. 1-83.
- 6. van Buuren, N., Fradette, L., Grebely, J., King, A., Krajden, M., MacParland, S.A., Marshall, A., Saeed, S., Wilson, J., Klein, M.B. *et al.* (2016) The 5th Canadian Symposium on Hepatitis C Virus: We Are Not Done Yet-Remaining Challenges in Hepatitis C. *Can J Gastroenterol Hepatol*, **2016**, 7603526.
- 7. Dibrov, S.M., Parsons, J., Carnevali, M., Zhou, S., Rynearson, K.D., Ding, K., Garcia Sega, E., Brunn, N.D., Boerneke, M.A., Castaldi, M.P. *et al.* (2014) Hepatitis C virus translation inhibitors targeting the internal ribosomal entry site. *J. Med. Chem.*, **57**, 1694-1707.
- 8. Di Maio, V.C., Cento, V., Mirabelli, C., Artese, A., Costa, G., Alcaro, S., Perno, C.F. and Ceccherini-Silberstein, F. (2014) Hepatitis C virus genetic variability and the presence of NS5B resistance-associated mutations as natural polymorphisms in selected genotypes could affect the response to NS5B inhibitors. *Antimicrob. Agents Chemother.*, **58**, 2781-2797.
- 9. Messina, J.P., Humphreys, I., Flaxman, A., Brown, A., Cooke, G.S., Pybus, O.G. and Barnes, E. (2015) Global distribution and prevalence of hepatitis C virus genotypes. *Hepatology*, **61**, 77-87.
- 10. Nakano, T., Lau, G.M., Lau, G.M., Sugiyama, M. and Mizokami, M. (2012) An updated analysis of hepatitis C virus genotypes and subtypes based on the complete coding region. *Liver Int*, **32**, 339-345.
- 11. Simmonds, P. (2004) Genetic diversity and evolution of hepatitis C virus--15 years on. *J. Gen. Virol.*, **85**, 3173-3188.
- 12. Simmonds, P., Bukh, J., Combet, C., Deleage, G., Enomoto, N., Feinstone, S., Halfon, P., Inchauspe, G., Kuiken, C., Maertens, G. *et al.* (2005) Consensus proposals for a unified system of nomenclature of hepatitis C virus genotypes. *Hepatology*, **42**, 962-973.
- 13. Hajarizadeh, B., Grebely, J. and Dore, G.J. (2013) Epidemiology and natural history of HCV infection. *Nat. Rev. Gastroenterol. Hepatol.*, **10**, 553-562.
- 14. Magiorkinis, G., Magiorkinis, E., Paraskevis, D., Ho, S.Y., Shapiro, B., Pybus, O.G., Allain, J.P. and Hatzakis, A. (2009) The global spread of hepatitis C virus 1a and 1b: a phylodynamic and phylogeographic analysis. *PLoS Med.*, **6**, e1000198.
- 15. Smith, D.B., Pathirana, S., Davidson, F., Lawlor, E., Power, J., Yap, P.L. and Simmonds, P. (1997) The origin of hepatitis C virus genotypes. *J. Gen. Virol.*, **78** (**Pt 2**), 321-328.
- 16. Tibbs, C.J. (1995) Methods of transmission of hepatitis C. J. Viral Hepat., 2, 113-119.

- 17. Polaris Observatory, H.C.V.C. (2017) Global prevalence and genotype distribution of hepatitis C virus infection in 2015: a modelling study. *Lancet Gastroenterol Hepatol*, **2**, 161-176.
- 18. Murphy, D.G., Sablon, E., Chamberland, J., Fournier, E., Dandavino, R. and Tremblay, C.L. (2015) Hepatitis C virus genotype 7, a new genotype originating from central Africa. *J. Clin. Microbiol.*, **53**, 967-972.
- 19. Elgharably, A., Gomaa, A.I., Crossey, M.M., Norsworthy, P.J., Waked, I. and Taylor-Robinson, S.D. (2017) Hepatitis C in Egypt past, present, and future. *Int. J. Gen. Med.*, **10**, 1-6.
- 20. Khattab, M.A., Ferenci, P., Hadziyannis, S.J., Colombo, M., Manns, M.P., Almasio, P.L., Esteban, R., Abdo, A.A., Harrison, S.A., Ibrahim, N. *et al.* (2011) Management of hepatitis C virus genotype 4: recommendations of an international expert panel. *J. Hepatol.*, **54**, 1250-1262.
- 21. Henderson, D.K. (2003) Managing occupational risks for hepatitis C transmission in the health care setting. *Clin. Microbiol. Rev.*, **16**, 546-568.
- 22. Vrielink, H., van der Poel, C.L., Reesink, H.W., Zaaijer, H.L., Scholten, E., Kremer, L.C., Cuypers, H.T., Lelie, P.N. and van Oers, M.H. (1995) Look-back study of infectivity of anti-HCV ELISA-positive blood components. *Lancet*, **345**, 95-96.
- 23. Donahue, J.G., Munoz, A., Ness, P.M., Brown, D.E., Jr., Yawn, D.H., McAllister, H.A., Jr., Reitz, B.A. and Nelson, K.E. (1992) The declining risk of post-transfusion hepatitis C virus infection. *N. Engl. J. Med.*, **327**, 369-373.
- 24. Orland, J.R., Wright, T.L. and Cooper, S. (2001) Acute hepatitis C. *Hepatology*, **33**, 321-327.
- 25. Micallef, J.M., Kaldor, J.M. and Dore, G.J. (2006) Spontaneous viral clearance following acute hepatitis C infection: a systematic review of longitudinal studies. *J. Viral Hepat.*, **13**, 34-41.
- 26. Liang, T.J., Rehermann, B., Seeff, L.B. and Hoofnagle, J.H. (2000) Pathogenesis, natural history, treatment, and prevention of hepatitis C. *Ann. Intern. Med.*, **132**, 296-305.
- 27. Montoya, V., Olmstead, A.D., Janjua, N.Z., Tang, P., Grebely, J., Cook, D., Richard Harrigan, P. and Krajden, M. (2015) Differentiation of acute from chronic hepatitis C virus infection by nonstructural 5B deep sequencing: a population-level tool for incidence estimation. *Hepatology*, **61**, 1842-1850.
- 28. El-Serag, H.B. and Rudolph, K.L. (2007) Hepatocellular carcinoma: epidemiology and molecular carcinogenesis. *Gastroenterology*, **132**, 2557-2576.
- 29. Freeman, A.J., Dore, G.J., Law, M.G., Thorpe, M., Von Overbeck, J., Lloyd, A.R., Marinos, G. and Kaldor, J.M. (2001) Estimating progression to cirrhosis in chronic hepatitis C virus infection. *Hepatology*, **34**, 809-816.
- 30. Moradpour, D., Penin, F. and Rice, C.M. (2007) Replication of hepatitis C virus. *Nat. Rev. Microbiol.*, **5**, 453-463.
- 31. Barba, G., Harper, F., Harada, T., Kohara, M., Goulinet, S., Matsuura, Y., Eder, G., Schaff, Z., Chapman, M.J., Miyamura, T. *et al.* (1997) Hepatitis C virus core protein shows a cytoplasmic localization and associates to cellular lipid storage droplets. *Proc. Natl. Acad. Sci. U. S. A.*, **94**, 1200-1205.
- 32. Moriya, K., Fujie, H., Shintani, Y., Yotsuyanagi, H., Tsutsumi, T., Ishibashi, K., Matsuura, Y., Kimura, S., Miyamura, T. and Koike, K. (1998) The core protein of hepatitis C virus induces hepatocellular carcinoma in transgenic mice. *Nat. Med.*, **4**, 1065-1067.
- 33. Chevaliez, S. and Pawlotsky, J.M. (2006) In Tan, S. L. (ed.), *Hepatitis C Viruses: Genomes and Molecular Biology*, Norfolk (UK).

- 34. Gonzalez, M.E. and Carrasco, L. (2003) Viroporins. FEBS Lett., 552, 28-34.
- 35. Franck, N., Le Seyec, J., Guguen-Guillouzo, C. and Erdtmann, L. (2005) Hepatitis C virus NS2 protein is phosphorylated by the protein kinase CK2 and targeted for degradation to the proteasome. *J. Virol.*, **79**, 2700-2708.
- 36. Jones, C.T., Murray, C.L., Eastman, D.K., Tassello, J. and Rice, C.M. (2007) Hepatitis C virus p7 and NS2 proteins are essential for production of infectious virus. *J. Virol.*, **81**, 8374-8383.
- 37. Jones, D.M. and McLauchlan, J. (2010) Hepatitis C virus: assembly and release of virus particles. *J. Biol. Chem.*, **285**, 22733-22739.
- Zhang, C., Cai, Z., Kim, Y.C., Kumar, R., Yuan, F., Shi, P.Y., Kao, C. and Luo, G. (2005) Stimulation of hepatitis C virus (HCV) nonstructural protein 3 (NS3) helicase activity by the NS3 protease domain and by HCV RNA-dependent RNA polymerase. *J. Virol.*, **79**, 8687-8697.
- 39. Bartenschlager, R., Lohmann, V., Wilkinson, T. and Koch, J.O. (1995) Complex formation between the NS3 serine-type proteinase of the hepatitis C virus and NS4A and its importance for polyprotein maturation. *J. Virol.*, **69**, 7519-7528.
- 40. Tai, C.L., Chi, W.K., Chen, D.S. and Hwang, L.H. (1996) The helicase activity associated with hepatitis C virus nonstructural protein 3 (NS3). *J. Virol.*, **70**, 8477-8484.
- 41. Gretton, S.N., Taylor, A.I. and McLauchlan, J. (2005) Mobility of the hepatitis C virus NS4B protein on the endoplasmic reticulum membrane and membrane-associated foci. *J. Gen. Virol.*, **86**, 1415-1421.
- 42. Penin, F., Brass, V., Appel, N., Ramboarina, S., Montserret, R., Ficheux, D., Blum, H.E., Bartenschlager, R. and Moradpour, D. (2004) Structure and function of the membrane anchor domain of hepatitis C virus nonstructural protein 5A. *J. Biol. Chem.*, **279**, 40835-40843.
- 43. Masaki, T., Suzuki, R., Murakami, K., Aizaki, H., Ishii, K., Murayama, A., Date, T., Matsuura, Y., Miyamura, T., Wakita, T. *et al.* (2008) Interaction of hepatitis C virus nonstructural protein 5A with core protein is critical for the production of infectious virus particles. *J. Virol.*, **82**, 7964-7976.
- 44. Ago, H., Adachi, T., Yoshida, A., Yamamoto, M., Habuka, N., Yatsunami, K. and Miyano, M. (1999) Crystal structure of the RNA-dependent RNA polymerase of hepatitis C virus. *Structure*, **7**, 1417-1426.
- 45. Nielsen, S.U., Bassendine, M.F., Burt, A.D., Martin, C., Pumeechockchai, W. and Toms, G.L. (2006) Association between hepatitis C virus and very-low-density lipoprotein (VLDL)/LDL analyzed in iodixanol density gradients. *J. Virol.*, **80**, 2418-2428.
- 46. Thomssen, R., Bonk, S., Propfe, C., Heermann, K.H., Kochel, H.G. and Uy, A. (1992) Association of hepatitis C virus in human sera with beta-lipoprotein. *Med. Microbiol. Immunol.*, **181**, 293-300.
- 47. Thomssen, R., Bonk, S. and Thiele, A. (1993) Density heterogeneities of hepatitis C virus in human sera due to the binding of beta-lipoproteins and immunoglobulins. *Med. Microbiol. Immunol.*, **182**, 329-334.
- 48. Ding, Q., von Schaewen, M. and Ploss, A. (2014) The impact of hepatitis C virus entry on viral tropism. *Cell Host Microbe*, **16**, 562-568.
- 49. Blanchard, E., Belouzard, S., Goueslain, L., Wakita, T., Dubuisson, J., Wychowski, C. and Rouille, Y. (2006) Hepatitis C virus entry depends on clathrin-mediated endocytosis. *J. Virol.*, **80**, 6964-6972.
- 50. Koutsoudakis, G., Kaul, A., Steinmann, E., Kallis, S., Lohmann, V., Pietschmann, T. and Bartenschlager, R. (2006) Characterization of the early steps of hepatitis C virus infection by using luciferase reporter viruses. *J. Virol.*, **80**, 5308-5320.

- 51. Egger, D., Wolk, B., Gosert, R., Bianchi, L., Blum, H.E., Moradpour, D. and Bienz, K. (2002) Expression of hepatitis C virus proteins induces distinct membrane alterations including a candidate viral replication complex. *J. Virol.*, **76**, 5974-5984.
- 52. Lohmann, V., Korner, F., Koch, J., Herian, U., Theilmann, L. and Bartenschlager, R. (1999) Replication of subgenomic hepatitis C virus RNAs in a hepatoma cell line. *Science*, **285**, 110-113.
- 53. Lindenbach, B.D. and Rice, C.M. (2005) Unravelling hepatitis C virus replication from genome to function. *Nature*, **436**, 933-938.
- 54. Liu, Y., Wimmer, E. and Paul, A.V. (2009) Cis-acting RNA elements in human and animal plus-strand RNA viruses. *Biochimica Et Biophysica Acta (BBA)-Gene Regulatory Mechanisms*, **1789**, 495-517.
- 55. Luo, G., Xin, S. and Cai, Z. (2003) Role of the 5'-proximal stem-loop structure of the 5' untranslated region in replication and translation of hepatitis C virus RNA. *J. Virol.*, 77, 3312-3318.
- 56. Kieft, J.S., Zhou, K., Jubin, R., Murray, M.G., Lau, J.Y.N. and Doudna, J.A. (1999) The hepatitis C virus internal ribosome entry site adopts an ion-dependent tertiary fold. *J. Mol. Biol.*, **292**, 513-529.
- 57. Sagan, S.M., Chahal, J. and Sarnow, P. (2015) cis-Acting RNA elements in the hepatitis C virus RNA genome. *Virus Res.*, **206**, 90-98.
- 58. Lukavsky, P.J., Kim, I., Otto, G.A. and Puglisi, J.D. (2003) Structure of HCV IRES domain II determined by NMR. *Nat. Struct. Biol.*, **10**, 1033-1038.
- 59. Filbin, M.E., Vollmar, B.S., Shi, D., Gonen, T. and Kieft, J.S. (2013) HCV IRES manipulates the ribosome to promote the switch from translation initiation to elongation. *Nat. Struct. Mol. Biol.*, **20**, 150-158.
- 60. Locker, N., Easton, L.E. and Lukavsky, P.J. (2007) HCV and CSFV IRES domain II mediate eIF2 release during 80S ribosome assembly. *EMBO J.*, **26**, 795-805.
- 61. Parsons, J., Castaldi, M.P., Dutta, S., Dibrov, S.M., Wyles, D.L. and Hermann, T. (2009) Conformational inhibition of the hepatitis C virus internal ribosome entry site RNA. *Nat. Chem. Biol.*, **5**, 823-825.
- 62. Berry, K.E., Waghray, S., Mortimer, S.A., Bai, Y. and Doudna, J.A. (2011) Crystal structure of the HCV IRES central domain reveals strategy for start-codon positioning. *Structure*, **19**, 1456-1466.
- 63. Friebe, P., Lohmann, V., Krieger, N. and Bartenschlager, R. (2001) Sequences in the 5' nontranslated region of hepatitis C virus required for RNA replication. *J. Virol.*, **75**, 12047–12057.
- 64. Kolykhalov, A.A., Feinstone, S.M. and Rice, C.M. (1996) Identification of a highly conserved sequence element at the 3' terminus of hepatitis C virus genome RNA. *J. Virol.*, **70**, 3363-3371.
- 65. Friebe, P. and Bartenschlager, R. (2002) Genetic analysis of sequences in the 3' nontranslated region of hepatitis C virus that are important for RNA replication. *J. Virol.*, **76**, 5326-5338.
- 66. You, S. and Rice, C.M. (2008) 3' RNA elements in hepatitis C virus replication: kissing partners and long poly(U). *J. Virol.*, **82**, 184-195.
- 67. Huang, L., Hwang, J., Sharma, S.D., Hargittai, M.R., Chen, Y., Arnold, J.J., Raney, K.D. and Cameron, C.E. (2005) Hepatitis C virus nonstructural protein 5A (NS5A) is an RNA-binding protein. *J. Biol. Chem.*, **280**, 36417-36428.
- 68. Kanai, A., Tanabe, K. and Kohara, M. (1995) Poly(U) binding activity of hepatitis C virus NS3 protein, a putative RNA helicase. *FEBS Lett.*, **376**, 221-224.

- 69. Luo, G., Hamatake, R.K., Mathis, D.M., Racela, J., Rigat, K.L., Lemm, J. and Colonno, R.J. (2000) De novo initiation of RNA synthesis by the RNA-dependent RNA polymerase (NS5B) of hepatitis C virus. *J. Virol.*, **74**, 851-863.
- 70. Bai, Y., Zhou, K. and Doudna, J.A. (2013) Hepatitis C virus 3'UTR regulates viral translation through direct interactions with the host translation machinery. *Nucleic Acids Res.*, **41**, 7861-7874.
- 71. Ito, T. and Lai, M.M. (1999) An internal polypyrimidine-tract-binding protein-binding site in the hepatitis C virus RNA attenuates translation, which is relieved by the 3'-untranslated sequence. *Virology*, **254**, 288-296.
- 72. Ito, T., Tahara, S.M. and Lai, M.M. (1998) The 3'-untranslated region of hepatitis C virus RNA enhances translation from an internal ribosomal entry site. *J. Virol.*, **72**, 8789-8796.
- 73. Romero-Lopez, C., Barroso-Deljesus, A., Garcia-Sacristan, A., Briones, C. and Berzal-Herranz, A. (2012) The folding of the hepatitis C virus internal ribosome entry site depends on the 3'-end of the viral genome. *Nucleic Acids Res.*, **40**, 11697-11713.
- 74. Song, Y., Friebe, P., Tzima, E., Junemann, C., Bartenschlager, R. and Niepmann, M. (2006) The hepatitis C virus RNA 3'-untranslated region strongly enhances translation directed by the internal ribosome entry site. *J. Virol.*, **80**, 11579-11588.
- 75. Fricke, M., Dünnes, N., Zayas, M., Bartenschlager, R., Niepmann, M. and Marz, M. (2015) Conserved RNA secondary structures and long-range interactions in hepatitis C viruses. *RNA*, **21**, 1219-1232.
- 76. Tuplin, A., Evans, D.J. and Simmonds, P. (2004) Detailed mapping of RNA secondary structures in core and NS5B-encoding region sequences of hepatitis C virus by RNase cleavage and novel bioinformatic prediction methods. *J. Gen. Virol.*, **85**, 3037-3047.
- 77. Pirakitikulr, N., Kohlway, A., Lindenbach, B.D. and Pyle, A.M. (2016) The Coding Region of the HCV Genome Contains a Network of Regulatory RNA Structures. *Mol. Cell*, **62**, 111-120.
- 78. Friebe, P., Boudet, J., Simorre, J.P. and Bartenschlager, R. (2005) Kissing-loop interaction in the 3' end of the hepatitis C virus genome essential for RNA replication. *J. Virol.*, **79**, 380-392.
- 79. Palau, W., Masante, C., Ventura, M. and Di Primo, C. (2013) Direct evidence for RNA-RNA interactions at the 3' end of the Hepatitis C virus genome using surface plasmon resonance. *RNA*, **19**, 982-991.
- 80. Tuplin, A., Struthers, M., Simmonds, P. and Evans, D.J. (2012) A twist in the tail: SHAPE mapping of long-range interactions and structural rearrangements of RNA elements involved in HCV replication. *Nucleic Acids Res.*, **40**, 6908-6921.
- 81. Diviney, S., Tuplin, A., Struthers, M., Armstrong, V., Elliott, R.M., Simmonds, P. and Evans, D.J. (2008) A hepatitis C virus cis-acting replication element forms a long-range RNA-RNA interaction with upstream RNA sequences in NS5B. *J. Virol.*, **82**, 9008-9022.
- 82. Dutkiewicz, M., Swiatkowska, A., Figlerowicz, M. and Ciesiolka, J. (2008) Structural domains of the 3'-terminal sequence of the hepatitis C virus replicative strand. *Biochemistry*, **47**, 12197-12207.
- 83. Schuster, C., Isel, C., Imbert, I., Ehresmann, C., Marquet, R. and Kieny, M.P. (2002) Secondary structure of the 3' terminus of hepatitis C virus minus-strand RNA. *J. Virol.*, **76.** 8058-8068.
- 84. Smith, R.M., Walton, C.M., Wu, C.H. and Wu, G.Y. (2002) Secondary structure and hybridization accessibility of hepatitis C virus 3'-terminal sequences. *J. Virol.*, **76**, 9563-9574.

- 85. Friebe, P. and Bartenschlager, R. (2009) Role of RNA structures in genome terminal sequences of the hepatitis C virus for replication and assembly. *J. Virol.*, **83**, 11989-11995.
- 86. Mahias, K., Ahmed-El-Sayed, N., Masante, C., Bitard, J., Staedel, C., Darfeuille, F., Ventura, M. and Astier-Gin, T. (2010) Identification of a structural element of the hepatitis C virus minus strand RNA involved in the initiation of RNA synthesis. *Nucleic Acids Res.*, **38**, 4079-4091.
- 87. Cai, Z., Liang, T.J. and Luo, G. (2004) Effects of mutations of the initiation nucleotides on hepatitis C virus RNA replication in the cell. *J. Virol.*, **78**, 3633-3643.
- 88. Lohmann, V. and Bartenschlager, R. (2014) On the history of hepatitis C virus cell culture systems. *J. Med. Chem.*, **57**, 1627-1642.
- 89. Nakajima, N., Hijikata, M., Yoshikura, H. and Shimizu, Y.K. (1996) Characterization of long-term cultures of hepatitis C virus. *J. Virol.*, **70**, 3325-3329.
- 90. Seipp, S., Mueller, H.M., Pfaff, E., Stremmel, W., Theilmann, L. and Goeser, T. (1997) Establishment of persistent hepatitis C virus infection and replication in vitro. *J. Gen. Virol.*, **78** (**Pt 10**), 2467-2476.
- 91. Tagawa, M., Kato, N., Yokosuka, O., Ishikawa, T., Ohto, M. and Omata, M. (1995) Infection of human hepatocyte cell lines with hepatitis C virus in vitro. *J. Gastroenterol. Hepatol.*, **10**, 523-527.
- 92. Burm, R., Collignon, L., Mesalam, A.A. and Meuleman, P. (2018) Animal Models to Study Hepatitis C Virus Infection. *Front. Immunol.*, **9**, 1032.
- 93. Blight, K.J., McKeating, J.A. and Rice, C.M. (2002) Highly permissive cell lines for subgenomic and genomic hepatitis C virus RNA replication. *J. Virol.*, **76**, 13001-13014.
- 94. Sumpter, R., Jr., Loo, Y.M., Foy, E., Li, K., Yoneyama, M., Fujita, T., Lemon, S.M. and Gale, M., Jr. (2005) Regulating intracellular antiviral defense and permissiveness to hepatitis C virus RNA replication through a cellular RNA helicase, RIG-I. *J. Virol.*, **79**, 2689-2699.
- 95. Morrison, J.a.S.P. (2016), *Viral Pathogenesis (Third Edition)* Academic Press pp. 253-269.
- 96. Amador-Canizares, Y., Bernier, A., Wilson, J.A. and Sagan, S.M. (2018) miR-122 does not impact recognition of the HCV genome by innate sensors of RNA but rather protects the 5' end from the cellular pyrophosphatases, DOM3Z and DUSP11. *Nucleic Acids Res.*, **46**, 5139-5158.
- 97. Murayama, A., Date, T., Morikawa, K., Akazawa, D., Miyamoto, M., Kaga, M., Ishii, K., Suzuki, T., Kato, T., Mizokami, M. *et al.* (2007) The NS3 helicase and NS5B-to-3'X regions are important for efficient hepatitis C virus strain JFH-1 replication in Huh7 cells. *J. Virol.*, **81**, 8030-8040.
- 98. Pietschmann, T., Kaul, A., Koutsoudakis, G., Shavinskaya, A., Kallis, S., Steinmann, E., Abid, K., Negro, F., Dreux, M., Cosset, F.L. *et al.* (2006) Construction and characterization of infectious intragenotypic and intergenotypic hepatitis C virus chimeras. *Proc. Natl. Acad. Sci. U. S. A.*, **103**, 7408-7413.
- 99. Wakita, T., Pietschmann, T., Kato, T., Date, T., Miyamoto, M., Zhao, Z., Murthy, K., Habermann, A., Krausslich, H.G., Mizokami, M. *et al.* (2005) Production of infectious hepatitis C virus in tissue culture from a cloned viral genome. *Nat. Med.*, **11**, 791-796.
- 100. Lindenbach, B.D., Evans, M.J., Syder, A.J., Wolk, B., Tellinghuisen, T.L., Liu, C.C., Maruyama, T., Hynes, R.O., Burton, D.R., McKeating, J.A. *et al.* (2005) Complete replication of hepatitis C virus in cell culture. *Science*, **309**, 623-626.

- 101. Zhong, J., Gastaminza, P., Cheng, G., Kapadia, S., Kato, T., Burton, D.R., Wieland, S.F., Uprichard, S.L., Wakita, T. and Chisari, F.V. (2005) Robust hepatitis C virus infection in vitro. *Proc. Natl. Acad. Sci. U. S. A.*, **102**, 9294-9299.
- 102. Chen, S.L. and Morgan, T.R. (2006) The natural history of hepatitis C virus (HCV) infection. *Int. J. Med. Sci.*, **3**, 47-52.
- 103. Feld, J.J. and Hoofnagle, J.H. (2005) Mechanism of action of interferon and ribavirin in treatment of hepatitis C. *Nature*, **436**, 967-972.
- 104. Manns, M.P., Wedemeyer, H. and Cornberg, M. (2006) Treating viral hepatitis C: efficacy, side effects, and complications. *Gut*, **55**, 1350-1359.
- 105. Baumert, T.F., Berg, T., Lim, J.K. and Nelson, D.R. (2019) Status of Direct-Acting Antiviral Therapy for Hepatitis C Virus Infection and Remaining Challenges. *Gastroenterology*, **156**, 431-445.
- 106. Scheel, T.K. and Rice, C.M. (2013) Understanding the hepatitis C virus life cycle paves the way for highly effective therapies. *Nat. Med.*, **19**, 837-849.
- 107. Manns, M.P. and von Hahn, T. (2013) Novel therapies for hepatitis C one pill fits all? *Nat Rev Drug Discov*, **12**, 595-610.
- 108. Jacobson, I.M., McHutchison, J.G., Dusheiko, G., Di Bisceglie, A.M., Reddy, K.R., Bzowej, N.H., Marcellin, P., Muir, A.J., Ferenci, P., Flisiak, R. *et al.* (2011) Telaprevir for previously untreated chronic hepatitis C virus infection. *N. Engl. J. Med.*, **364**, 2405-2416.
- 109. Poordad, F., McCone, J., Jr., Bacon, B.R., Bruno, S., Manns, M.P., Sulkowski, M.S., Jacobson, I.M., Reddy, K.R., Goodman, Z.D., Boparai, N. *et al.* (2011) Boceprevir for untreated chronic HCV genotype 1 infection. *N. Engl. J. Med.*, **364**, 1195-1206.
- 110. Sofia, M.J., Chang, W., Furman, P.A., Mosley, R.T. and Ross, B.S. (2012) Nucleoside, nucleotide, and non-nucleoside inhibitors of hepatitis C virus NS5B RNA-dependent RNA-polymerase. *J. Med. Chem.*, **55**, 2481-2531.
- 111. Assis, D.N. and Lim, J.K. (2012) New pharmacotherapy for hepatitis C. *Clin. Pharmacol. Ther.*, **92**, 294-305.
- 112. Sarrazin, C., Hezode, C., Zeuzem, S. and Pawlotsky, J.M. (2012) Antiviral strategies in hepatitis C virus infection. *J. Hepatol.*, **56 Suppl 1**, S88-100.
- 113. Vermehren, J. and Sarrazin, C. (2012) The role of resistance in HCV treatment. *Best Pract. Res. Clin. Gastroenterol.*, **26**, 487-503.
- 114. Herbst, D.A., Jr. and Reddy, K.R. (2013) Sofosbuvir, a nucleotide polymerase inhibitor, for the treatment of chronic hepatitis C virus infection. *Expert Opin Investig Drugs*, **22**, 527-536.
- 115. Troke, P.J., Lewis, M., Simpson, P., Gore, K., Hammond, J., Craig, C. and Westby, M. (2012) Characterization of resistance to the nonnucleoside NS5B inhibitor filibuvir in hepatitis C virus-infected patients. *Antimicrob. Agents Chemother.*, **56**, 1331-1341.
- 116. Gitto, S., Gamal, N. and Andreone, P. (2017) NS5A inhibitors for the treatment of hepatitis C infection. *J. Viral Hepat.*, **24**, 180-186.
- 117. Morio, K., Imamura, M., Kawakami, Y., Morio, R., Kobayashi, T., Yokoyama, S., Nagaoki, Y., Kawaoka, T., Tsuge, M., Hiramatsu, A. *et al.* (2017) Real-world efficacy and safety of daclatasvir and asunaprevir therapy for hepatitis C virus-infected cirrhosis patients. *J. Gastroenterol. Hepatol.*, **32**, 645-650.
- 118. Guedj, J., Dahari, H., Rong, L., Sansone, N.D., Nettles, R.E., Cotler, S.J., Layden, T.J., Uprichard, S.L. and Perelson, A.S. (2013) Modeling shows that the NS5A inhibitor daclatasvir has two modes of action and yields a shorter estimate of the hepatitis C virus half-life. *Proc. Natl. Acad. Sci. U. S. A.*, **110**, 3991-3996.

- 119. Pawlotsky, J.M. (2013) NS5A inhibitors in the treatment of hepatitis C. *J. Hepatol.*, **59**, 375-382.
- 120. Targett-Adams, P., Graham, E.J., Middleton, J., Palmer, A., Shaw, S.M., Lavender, H., Brain, P., Tran, T.D., Jones, L.H., Wakenhut, F. *et al.* (2011) Small molecules targeting hepatitis C virus-encoded NS5A cause subcellular redistribution of their target: insights into compound modes of action. *J. Virol.*, **85**, 6353-6368.
- 121. Spengler, U. (2018) Direct antiviral agents (DAAs) A new age in the treatment of hepatitis C virus infection. *Pharmacol. Ther.*, **183**, 118-126.
- 122. Sulkowski, M.S., Gardiner, D.F., Rodriguez-Torres, M., Reddy, K.R., Hassanein, T., Jacobson, I., Lawitz, E., Lok, A.S., Hinestrosa, F., Thuluvath, P.J. *et al.* (2014) Daclatasvir plus sofosbuvir for previously treated or untreated chronic HCV infection. *N. Engl. J. Med.*, **370**, 211-221.
- 123. Hill, A., Khoo, S., Fortunak, J., Simmons, B. and Ford, N. (2014) Minimum costs for producing hepatitis C direct-acting antivirals for use in large-scale treatment access programs in developing countries. *Clin. Infect. Dis.*, **58**, 928-936.
- Baugh, J.M., Garcia-Rivera, J.A. and Gallay, P.A. (2013) Host-targeting agents in the treatment of hepatitis C: a beginning and an end? *Antiviral Res.*, **100**, 555-561.
- 125. Meuleman, P., Hesselgesser, J., Paulson, M., Vanwolleghem, T., Desombere, I., Reiser, H. and Leroux-Roels, G. (2008) Anti-CD81 antibodies can prevent a hepatitis C virus infection in vivo. *Hepatology*, **48**, 1761-1768.
- 126. Lacek, K., Vercauteren, K., Grzyb, K., Naddeo, M., Verhoye, L., Slowikowski, M.P., Fafi-Kremer, S., Patel, A.H., Baumert, T.F., Folgori, A. *et al.* (2012) Novel human SR-BI antibodies prevent infection and dissemination of HCV in vitro and in humanized mice. *J. Hepatol.*, **57**, 17-23.
- 127. Bobardt, M., Hopkins, S., Baugh, J., Chatterji, U., Hernandez, F., Hiscott, J., Sluder, A., Lin, K. and Gallay, P.A. (2013) HCV NS5A and IRF9 compete for CypA binding. *J. Hepatol.*, **58**, 16-23.
- 128. Madan, V., Paul, D., Lohmann, V. and Bartenschlager, R. (2014) Inhibition of HCV replication by cyclophilin antagonists is linked to replication fitness and occurs by inhibition of membranous web formation. *Gastroenterology*, **146**, 1361-1372 e1361-1369.
- 129. Ikeda, M., Abe, K., Yamada, M., Dansako, H., Naka, K. and Kato, N. (2006) Different anti-HCV profiles of statins and their potential for combination therapy with interferon. *Hepatology*, **44**, 117-125.
- 130. Peng, L.F., Schaefer, E.A., Maloof, N., Skaff, A., Berical, A., Belon, C.A., Heck, J.A., Lin, W., Frick, D.N., Allen, T.M. *et al.* (2011) Ceestatin, a novel small molecule inhibitor of hepatitis C virus replication, inhibits 3-hydroxy-3-methylglutaryl-coenzyme A synthase. *J. Infect. Dis.*, **204**, 609-616.
- 131. Vere, C.C., Streba, C.T., Streba, L. and Rogoveanu, I. (2012) Statins in the treatment of hepatitis C. *Hepat. Mon.*, **12**, 369-371.
- 132. Janssen, H.L.A., Reesink, H.W., Lawitz, E.J., Zeuzem, S., Rodriguez-Torres, M., Patel, K., van der Meer, A.J., Patick, A.K., Chen, A., Zhou, Y. *et al.* (2013) Treatment of HCV Infection by Targeting MicroRNA. *N. Engl. J. Med.*, **368**, 1685-1694.
- 133. van der Ree, M.H., de Vree, J.M., Stelma, F., Willemse, S., van der Valk, M., Rietdijk, S., Molenkamp, R., Schinkel, J., van Nuenen, A.C., Beuers, U. *et al.* (2017) Safety, tolerability, and antiviral effect of RG-101 in patients with chronic hepatitis C: a phase 1B, double-blind, randomised controlled trial. *Lancet*, **389**, 709-717.
- 134. Lee, R.C., Feinbaum, R.L. and Ambros, V. (1993) The C. elegans heterochronic gene lin-4 encodes small RNAs with antisense complementarity to lin-14. *Cell*, **75**, 843-854.

- 135. Kozomara, A. and Griffiths-Jones, S. (2014) miRBase: annotating high confidence microRNAs using deep sequencing data. *Nucleic Acids Res.*, **42**, D68-73.
- 136. Sarnow, P. and Sagan, S.M. (2016) Unraveling the Mysterious Interactions Between Hepatitis C Virus RNA and Liver-Specific MicroRNA-122. *Annual Review of Virology*, **3**, 309-332.
- 137. Friedman, R.C., Farh, K.K., Burge, C.B. and Bartel, D.P. (2009) Most mammalian mRNAs are conserved targets of microRNAs. *Genome Res.*, **19**, 92-105.
- 138. Lee, Y., Kim, M., Han, J., Yeom, K.H., Lee, S., Baek, S.H. and Kim, V.N. (2004) MicroRNA genes are transcribed by RNA polymerase II. *EMBO J.*, **23**, 4051-4060.
- 139. Rodriguez, A., Griffiths-Jones, S., Ashurst, J.L. and Bradley, A. (2004) Identification of mammalian microRNA host genes and transcription units. *Genome Res.*, **14**, 1902-1910.
- 140. Han, J., Lee, Y., Yeom, K.H., Kim, Y.K., Jin, H. and Kim, V.N. (2004) The Drosha-DGCR8 complex in primary microRNA processing. *Genes Dev.*, **18**, 3016-3027.
- 141. Han, J., Lee, Y., Yeom, K.H., Nam, J.W., Heo, I., Rhee, J.K., Sohn, S.Y., Cho, Y., Zhang, B.T. and Kim, V.N. (2006) Molecular basis for the recognition of primary microRNAs by the Drosha-DGCR8 complex. *Cell*, **125**, 887-901.
- 142. Lee, Y., Ahn, C., Han, J., Choi, H., Kim, J., Yim, J., Lee, J., Provost, P., Radmark, O., Kim, S. *et al.* (2003) The nuclear RNase III Drosha initiates microRNA processing. *Nature*, **425**, 415-419.
- 143. Yi, R., Qin, Y., Macara, I.G. and Cullen, B.R. (2003) Exportin-5 mediates the nuclear export of pre-microRNAs and short hairpin RNAs. *Genes Dev.*, **17**, 3011-3016.
- 144. Bernstein, E., Caudy, A.A., Hammond, S.M. and Hannon, G.J. (2001) Role for a bidentate ribonuclease in the initiation step of RNA interference. *Nature*, **409**, 363-366.
- 145. Hutvagner, G., McLachlan, J., Pasquinelli, A.E., Balint, E., Tuschl, T. and Zamore, P.D. (2001) A cellular function for the RNA-interference enzyme Dicer in the maturation of the let-7 small temporal RNA. *Science*, **293**, 834-838.
- 146. Knight, S.W. and Bass, B.L. (2001) A role for the RNase III enzyme DCR-1 in RNA interference and germ line development in Caenorhabditis elegans. *Science*, **293**, 2269-2271.
- 147. Lee, H.Y., Zhou, K., Smith, A.M., Noland, C.L. and Doudna, J.A. (2013) Differential roles of human Dicer-binding proteins TRBP and PACT in small RNA processing. *Nucleic Acids Res.*, **41**, 6568-6576.
- 148. Chendrimada, T.P., Gregory, R.I., Kumaraswamy, E., Norman, J., Cooch, N., Nishikura, K. and Shiekhattar, R. (2005) TRBP recruits the Dicer complex to Ago2 for microRNA processing and gene silencing. *Nature*, **436**, 740-744.
- 149. Liu, J., Carmell, M.A., Rivas, F.V., Marsden, C.G., Thomson, J.M., Song, J.J., Hammond, S.M., Joshua-Tor, L. and Hannon, G.J. (2004) Argonaute2 is the catalytic engine of mammalian RNAi. *Science*, **305**, 1437-1441.
- 150. Kawamata, T., Seitz, H. and Tomari, Y. (2009) Structural determinants of miRNAs for RISC loading and slicer-independent unwinding. *Nat. Struct. Mol. Biol.*, **16**, 953-960.
- 151. Rand, T.A., Petersen, S., Du, F. and Wang, X. (2005) Argonaute2 cleaves the anti-guide strand of siRNA during RISC activation. *Cell*, **123**, 621-629.
- 152. Lewis, B.P., Shih, I.H., Jones-Rhoades, M.W., Bartel, D.P. and Burge, C.B. (2003) Prediction of mammalian microRNA targets. *Cell*, **115**, 787-798.
- 153. Bartel, D.P. (2004) MicroRNAs: genomics, biogenesis, mechanism, and function. *Cell*, **116**, 281-297.
- 154. Pillai, R.S., Artus, C.G. and Filipowicz, W. (2004) Tethering of human Ago proteins to mRNA mimics the miRNA-mediated repression of protein synthesis. *RNA*, **10**, 1518-1525.

- 155. Winter, J., Jung, S., Keller, S., Gregory, R.I. and Diederichs, S. (2009) Many roads to maturity: microRNA biogenesis pathways and their regulation. *Nat. Cell Biol.*, **11**, 228-234.
- 156. Baillat, D. and Shiekhattar, R. (2009) Functional dissection of the human TNRC6 (GW182-related) family of proteins. *Mol. Cell. Biol.*, **29**, 4144-4155.
- 157. Chen, C.Y., Zheng, D., Xia, Z. and Shyu, A.B. (2009) Ago-TNRC6 triggers microRNA-mediated decay by promoting two deadenylation steps. *Nat. Struct. Mol. Biol.*, **16**, 1160-1166.
- 158. Eulalio, A., Huntzinger, E. and Izaurralde, E. (2008) GW182 interaction with Argonaute is essential for miRNA-mediated translational repression and mRNA decay. *Nat. Struct. Mol. Biol.*, **15**, 346-353.
- 159. Eulalio, A., Tritschler, F. and Izaurralde, E. (2009) The GW182 protein family in animal cells: new insights into domains required for miRNA-mediated gene silencing. *RNA*, **15**, 1433-1442.
- 160. Fabian, M.R., Sonenberg, N. and Filipowicz, W. (2010) Regulation of mRNA translation and stability by microRNAs. *Annu. Rev. Biochem.*, **79**, 351-379.
- 161. Rehwinkel, J., Behm-Ansmant, I., Gatfield, D. and Izaurralde, E. (2005) A crucial role for GW182 and the DCP1:DCP2 decapping complex in miRNA-mediated gene silencing. *RNA*, **11**, 1640-1647.
- 162. Duchaine, T.F. and Fabian, M.R. (2019) Mechanistic Insights into MicroRNA-Mediated Gene Silencing. *Cold Spring Harb. Perspect. Biol.*, **11**.
- 163. Liu, J., Valencia-Sanchez, M.A., Hannon, G.J. and Parker, R. (2005) MicroRNA-dependent localization of targeted mRNAs to mammalian P-bodies. *Nat. Cell Biol.*, 7, 719-723.
- 164. Sen, G.L. and Blau, H.M. (2005) Argonaute 2/RISC resides in sites of mammalian mRNA decay known as cytoplasmic bodies. *Nat. Cell Biol.*, 7, 633-636.
- 165. Chang, J., Nicolas, E., Marks, D., Sander, C., Lerro, A., Buendia, M.A., Xu, C., Mason, W.S., Moloshok, T., Bort, R. *et al.* (2004) miR-122, a mammalian liver-specific microRNA, is processed from hcr mRNA and may downregulate the high affinity cationic amino acid transporter CAT-1. *RNA Biol.*, **1**, 106-113.
- 166. Katoh, T., Sakaguchi, Y., Miyauchi, K., Suzuki, T., Kashiwabara, S., Baba, T. and Suzuki, T. (2009) Selective stabilization of mammalian microRNAs by 3' adenylation mediated by the cytoplasmic poly(A) polymerase GLD-2. *Genes Dev.*, **23**, 433-438.
- 167. Norman, K.L., Chen, T.C., Zeiner, G. and Sarnow, P. (2017) Precursor microRNA-122 inhibits synthesis of Insig1 isoform mRNA by modulating polyadenylation site usage. *RNA*, **23**, 1886-1893.
- 168. Yamane, D., Selitsky, S.R., Shimakami, T., Li, Y., Zhou, M., Honda, M., Sethupathy, P. and Lemon, S.M. (2017) Differential hepatitis C virus RNA target site selection and host factor activities of naturally occurring miR-122 3 variants. *Nucleic Acids Res.*, **45**, 4743-4755.
- 169. Bhattacharyya, S.N., Habermacher, R., Martine, U., Closs, E.I. and Filipowicz, W. (2006) Relief of microRNA-mediated translational repression in human cells subjected to stress. *Cell*, **125**, 1111-1124.
- 170. Elmen, J., Lindow, M., Schutz, S., Lawrence, M., Petri, A., Obad, S., Lindholm, M., Hedtjarn, M., Hansen, H.F., Berger, U. *et al.* (2008) LNA-mediated microRNA silencing in non-human primates. *Nature*, **452**, 896-899.
- 171. Elmen, J., Lindow, M., Silahtaroglu, A., Bak, M., Christensen, M., Lind-Thomsen, A., Hedtjarn, M., Hansen, J.B., Hansen, H.F., Straarup, E.M. *et al.* (2008) Antagonism of microRNA-122 in mice by systemically administered LNA-antimiR leads to up-

- regulation of a large set of predicted target mRNAs in the liver. *Nucleic Acids Res.*, **36**, 1153-1162.
- 172. Krutzfeldt, J., Rajewsky, N., Braich, R., Rajeev, K.G., Tuschl, T., Manoharan, M. and Stoffel, M. (2005) Silencing of microRNAs in vivo with 'antagomirs'. *Nature*, **438**, 685-689.
- 173. Castoldi, M., Vujic Spasic, M., Altamura, S., Elmen, J., Lindow, M., Kiss, J., Stolte, J., Sparla, R., D'Alessandro, L.A., Klingmuller, U. *et al.* (2011) The liver-specific microRNA miR-122 controls systemic iron homeostasis in mice. *J. Clin. Invest.*, **121**, 1386-1396.
- 174. Tsai, W.C., Hsu, S.D., Hsu, C.S., Lai, T.C., Chen, S.J., Shen, R., Huang, Y., Chen, H.C., Lee, C.H., Tsai, T.F. *et al.* (2012) MicroRNA-122 plays a critical role in liver homeostasis and hepatocarcinogenesis. *J. Clin. Invest.*, **122**, 2884-2897.
- 175. Coulouarn, C., Factor, V.M., Andersen, J.B., Durkin, M.E. and Thorgeirsson, S.S. (2009) Loss of miR-122 expression in liver cancer correlates with suppression of the hepatic phenotype and gain of metastatic properties. *Oncogene*, **28**, 3526-3536.
- 176. Kutay, H., Bai, S., Datta, J., Motiwala, T., Pogribny, I., Frankel, W., Jacob, S.T. and Ghoshal, K. (2006) Downregulation of miR-122 in the rodent and human hepatocellular carcinomas. *J. Cell. Biochem.*, **99**, 671-678.
- 177. Jopling, C.L., Yi, M., Lancaster, A.M., Lemon, S.M. and Sarnow, P. (2005) Modulation of hepatitis C virus RNA abundance by a liver-specific MicroRNA. *Science*, **309**, 1577-1581.
- 178. Jopling, C.L. (2008) Regulation of hepatitis C virus by microRNA-122. *Biochem. Soc. Trans.*, **36**, 1220-1223.
- 179. Norman, K.L. and Sarnow, P. (2010) Modulation of hepatitis C virus RNA abundance and the isoprenoid biosynthesis pathway by microRNA miR-122 involves distinct mechanisms. *J. Virol.*, **84**, 666-670.
- 180. Machlin, E.S., Sarnow, P. and Sagan, S.M. (2011) Masking the 5' terminal nucleotides of the hepatitis C virus genome by an unconventional microRNA-target RNA complex. *PNAS*, **108**, 3193-3198.
- 181. Randall, G., Panis, M., Cooper, J.D., Tellinghuisen, T.L., Sukhodolets, K.E., Pfeffer, S., Landthaler, M., Landgraf, P., Kan, S., Lindenbach, B.D. *et al.* (2007) Cellular cofactors affecting hepatitis C virus infection and replication. *Proc. Natl. Acad. Sci. U. S. A.*, **104**, 12884-12889.
- 182. Wilson, J.A., Zhang, C., Huys, A. and Richardson, C.D. (2011) Human Ago2 Is Required for Efficient MicroRNA 122 Regulation of Hepatitis C Virus RNA Accumulation and Translation. *J. Virol.*, **85**, 2342-2350.
- 183. Zhang, C., Huys, A., Thibault, P.A. and Wilson, J.A. (2012) Requirements for human Dicer and TRBP in microRNA-122 regulation of HCV translation and RNA abundance. *Virology*, **433**, 479-488.
- 184. Jopling, C.L., Yi, M., Lancaster, A.M., Lemon, S.M. and Sarnow, P. (2005) Modulation of Hepatitis C Virus RNA Abundance by a Liver-Specific MicroRNA. *Science*, **209**, 1577-1581.
- 185. Jangra, R.K., Yi, M. and Lemon, S.M. (2010) Regulation of hepatitis C virus translation and infectious virus production by the microRNA miR-122. *J. Virol.*, **84**, 6615-6625.
- 186. Bernier, A. and Sagan, S.M. (2018) The Diverse Roles of microRNAs at the Host(-)Virus Interface. *Viruses*, **10**.
- 187. Henke, J.I., Goergen, D., Zheng, J., Song, Y., Schüttler, C.G., Fehr, C., Jünemann, C. and Niepmann, M. (2008) microRNA-122 stimulates translation of hepatitis C virus RNA. *EMBO J.*, **27**, 3300-3310.

- 188. Villanueva, R.A., Jangra, R.K., Yi, M., Pyles, R., Bourne, N. and Lemon, S.M. (2010) miR-122 does not modulate the elongation phase of hepatitis C virus RNA synthesis in isolated replicase complexes. *Antiviral Res.*, **88**, 119-123.
- 189. Gerresheim, G.K., Dunnes, N., Nieder-Rohrmann, A., Shalamova, L.A., Fricke, M., Hofacker, I., Honer Zu Siederdissen, C., Marz, M. and Niepmann, M. (2017) microRNA-122 target sites in the hepatitis C virus RNA NS5B coding region and 3' untranslated region: function in replication and influence of RNA secondary structure. *Cell. Mol. Life Sci.*, 74, 747-760.
- 190. Nasheri, N., Singaravelu, R., Goodmurphy, M., Lyn, R.K. and Pezacki, J.P. (2011) Competing roles of microRNA-122 recognition elements in hepatitis C virus RNA. *Virology*, **410**, 336-344.
- 191. Bernier, A. and Sagan, S.M. (2019) Beyond sites 1 and 2, miR-122 target sites in the HCV genome have negligible contributions to HCV RNA accumulation in cell culture. *J. Gen. Virol.*, **100**, 217-226.
- 192. Kincaid, R.P., Lam, V.L., Chirayil, R.P., Randall, G. and Sullivan, C.S. (2018) RNA triphosphatase DUSP11 enables exonuclease XRN-mediated restriction of hepatitis C virus. *PNAS*, **115**, 8197-8202.
- 193. Jiao, X., Chang, J.H., Kilic, T., Tong, L. and Kiledjian, M. (2013) A mammalian premRNA 5' end capping quality control mechanism and an unexpected link of capping to pre-mRNA processing. *Mol. Cell*, **50**, 104-115.
- 194. Xiang, S., Cooper-Morgan, A., Jiao, X., Kiledjian, M., Manley, J.L. and Tong, L. (2009) Structure and function of the 5'-->3' exoribonuclease Rat1 and its activating partner Rai1. *Nature*, **458**, 784-788.
- 195. Burke, J.M. and Sullivan, C.S. (2017) DUSP11 An RNA phosphatase that regulates host and viral non-coding RNAs in mammalian cells. *RNA Biol.*, **14**, 1457-1465.
- 196. Deshpande, T., Takagi, T., Hao, L., Buratowski, S. and Charbonneau, H. (1999) Human PIR1 of the protein-tyrosine phosphatase superfamily has RNA 5'-triphosphatase and diphosphatase activities. *J. Biol. Chem.*, **274**, 16590-16594.
- 197. Yuan, Y., Li, D.M. and Sun, H. (1998) PIR1, a novel phosphatase that exhibits high affinity to RNA . ribonucleoprotein complexes. *J. Biol. Chem.*, **273**, 20347-20353.
- 198. Zheng, D., Chen, C.Y. and Shyu, A.B. (2011) Unraveling regulation and new components of human P-bodies through a protein interaction framework and experimental validation. *RNA*, **17**, 1619-1634.
- 199. Li, Y., Masaki, T., Yamane, D., McGivern, D.R. and Lemon, S.M. (2013) Competing and noncompeting activities of miR-122 and the 5' exonuclease Xrn1 in regulation of hepatitis C virus replication. *PNAS*, **110**, 1881-1886.
- 200. Nagarajan, V.K., Jones, C.I., Newbury, S.F. and Green, P.J. (2013) XRN 5'-->3' exoribonucleases: structure, mechanisms and functions. *Biochim. Biophys. Acta*, **1829**, 590-603.
- 201. Sedano, C.D. and Sarnow, P. (2014) Hepatitis C virus subverts liver-specific miR-122 to protect the viral genome from exoribonuclease Xrn2. *Cell host & microbe*, **16**, 257-264.
- 202. Thibault, P.A., Huys, A., Amador-Cañizares, Y., Gailius, J.E., Pinel, D.E. and Wilson, J.A. (2015) Regulation of hepatitis C virus genome replication by Xrn1 and microRNA-122 binding to individual sites in the 5' untranslated region. *J. Virol.*, **89**, 6294-6311.
- 203. Jangra, R.K., Yi, M. and Lemon, S.M. (2010) Regulation of hepatitis C virus translation and infectious virus production by the microRNA miR-122. *J. Virol.*, **84**, 6615-6625.
- 204. Berezhna, S.Y., Supekova, L., Sever, M.J., Schultz, P.G. and Deniz, A.A. (2011) Dual regulation of hepatitis C viral RNA by cellular RNAi requires partitioning of Ago2 to lipid droplets and P-bodies. *RNA*, **17**, 1831-1845.

- 205. Conrad, K.D., Giering, F., Erfurth, C., Neumann, A., Fehr, C., Meister, G. and Niepmann, M. (2013) microRNA-122 Dependent Binding of Ago2 Protein to Hepatitis C Virus RNA Is Associated with Enhanced RNA Stability and Translation Stimulation. PLoS One, 8, e56272
- 206. Roberts, A.P., Lewis, A.P. and Jopling, C.L. (2011) miR-122 activates hepatitis C virus translation by a specialized mechanism requiring particular RNA components. *Nucleic Acids Res.*, **39**, 7716-7729.
- 207. Shimakami, T., Yamane, D., Jangra, R.K., Kempf, B.J., Spaniel, C., Barton, D.J. and Lemon, S.M. (2012) Stabilization of hepatitis C virus RNA by an Ago2-miR-122 complex. *PNAS*, **109**, 941-946.
- 208. Chahal, J., Gebert, L.F.R., Gan, H.H., Camacho, E., Gunsalus, K.C., MacRae, I.J. and Sagan, S.M. (2019) miR-122 and Ago interactions with the HCV genome alter the structure of the viral 5' terminus. *Nucleic Acids Res.*, 47, 5307-5324.
- 209. Amador-Canizares, Y., Panigrahi, M., Huys, A., Kunden, R.D., Adams, H.M., Schinold, M.J. and Wilson, J.A. (2018) miR-122, small RNA annealing and sequence mutations alter the predicted structure of the Hepatitis C virus 5' UTR RNA to stabilize and promote viral RNA accumulation. *Nucleic Acids Res.*, **46**, 9776-9792.
- 210. Schult, P., Roth, H., Adams, R.L., Mas, C., Imbert, L., Orlik, C., Ruggieri, A., Pyle, A.M. and Lohmann, V. (2018) microRNA-122 amplifies hepatitis C virus translation by shaping the structure of the internal ribosomal entry site. *Nat Commun.*, **9**, 2613-2613.
- 211. Luna, J.M., Scheel, T.K.H., Danino, T., Shaw, K.S., Mele, A., Fak, J.J., Nishiuchi, E., Takacs, C.N., Catanese, M.T., De Jong, Y.P. *et al.* (2015) Hepatitis C virus RNA functionally sequesters miR-122. *Cell*, **160**, 1099-1110.
- 212. Hsu, S.H., Wang, B., Kota, J., Yu, J., Costinean, S., Kutay, H., Yu, L., Bai, S., La Perle, K., Chivukula, R.R. *et al.* (2012) Essential metabolic, anti-inflammatory, and anti-tumorigenic functions of miR-122 in liver. *J. Clin. Invest.*, **122**, 2871-2883.
- 213. Zeisel, M.B., Pfeffer, S. and Baumert, T.F. (2013) miR-122 acts as a tumor suppressor in hepatocarcinogenesis in vivo. *J. Hepatol.*, **58**, 821-823.
- 214. Ottosen, S., Parsley, T.B., Yang, L., Zeh, K., van Doorn, L.-J., van der Veer, E., Raney, A.K., Hodges, M.R. and Patick, A.K. (2015) In vitro antiviral activity and preclinical and clinical resistance profile of miravirsen, a novel anti-hepatitis C virus therapeutic targeting the human factor miR-122. *Antimicrob. Agents Chemother.*, **59**, 599-608.
- 215. Hopcraft, S.E., Azarm, K.D., Israelow, B., Leveque, N., Schwarz, M.C., Hsu, T.H., Chambers, M.T., Sourisseau, M., Semler, B.L. and Evans, M.J. (2016) Viral Determinants of miR-122 Independent Hepatitis C Virus Replication. *mSphere*, 1, 1-12.
- 216. Israelow, B., Mullokandov, G., Agudo, J., Sourisseau, M., Bashir, A., Maldonado, A.Y., Dar, A.C., Brown, B.D. and Evans, M.J. (2015) Hepatitis C virus genetics affects miR-122 requirements and response to miR-122 inhibitors. *Nat Commun.*, **5**, 1-11.
- 217. Bonneau, E., Neveu, B., Kostantin, E., Tsongalis, G.J. and De Guire, V. (2019) How close are miRNAs from clinical practice? A perspective on the diagnostic and therapeutic market. *EJIFCC*, **30**, 114-127.
- 218. Mortimer, S.A. and Doudna, J.A. (2013) Unconventional miR-122 binding stabilizes the HCV genome by forming a trimolecular RNA structure. *Nucleic Acids Res.*, **41**, 4230-4240.
- 219. Pang, P.S., Pham, E.A., Elazar, M., Patel, S.G., Eckart, M.R. and Glenn, J.S. (2012) Structural map of a microRNA-122: hepatitis C virus complex. *J. Virol.*, **86**, 1250-1254.
- 220. Lanford, R.E., Hildebrandt-Eriksen, E.S., Petri, A., Persson, R., Lindow, M., Munk, M.E., Kauppinen, S. and Ørum, H. (2010) Therapeutic silencing of microRNA-122 in primates with chronic hepatitis C virus infection. *Science*, **327**, 198-201.

- 221. Alvarez, D.E., Lodeiro, M.F., Filomatori, C.V., Fucito, S., Mondotte, J.A. and Gamarnik, A.V. (2006) Structural and functional analysis of dengue virus RNA. *Novartis Found. Symp.*, **277**, 120-132; discussion 132-125, 251-123.
- 222. Gebhard, L.G., Filomatori, C.V. and Gamarnik, A.V. (2011) Functional RNA elements in the dengue virus genome. *Viruses*, **3**, 1739-1756.
- 223. Mazeaud, C., Freppel, W. and Chatel-Chaix, L. (2018) The Multiples Fates of the Flavivirus RNA Genome During Pathogenesis. *Front Genet*, **9**, 595.

CHAPTER 2: miR-122 and Ago interactions with the HCV genome alter the structure of the viral 5' terminus

Jasmin Chahal, Luca FR Gebert, Hin Hark Gan, Edna Camacho, Kristin C. Gunsalus, Ian J. MacRae, and Selena M. Sagan

2.1 Preface to Chapter 2

As discussed in *Chapter 1*, miR-122 is important in the HCV life cycle. In previous studies, miR-122 binding was shown to alter the structure of the viral 5' UTR (1-4). Additionally, Ago2 was shown to be important in HCV accumulation as it brings miR-122 to the 5' UTR, yet its influence on the secondary structure of the 5' end of the HCV genome has not yet been elucidated (5,6). We hypothesized that binding of miR-122 as well as the Ago:miR-122 complex to the HCV genome alters the secondary structure of the 5' UTR in a manner that promotes HCV RNA accumulation. Furthermore, we investigated the secondary structure of the 5' UTR of G28A, an RAV that is able to accumulate when miR-122 is limiting (7,8). Our results suggest a new model for miR-122 and Ago:miR-122 complex interactions with the HCV genome, that suggest that miR-122 plays three roles in the viral life cycle.

This chapter was adapted from the following manuscript: miR-122 and Ago interactions with the HCV genome alter the structure of the viral 5' terminus. **Jasmin Chahal**, Luca FR Gebert, Hin Hark Gan, Edna Camacho, Kristin C. Gunsalus, Ian J. MacRae, and Selena M. Sagan. *Nucleic Acids Research*, 2019 April 3; 47(10): 5307–5324.

2.2 Abstract

Hepatitis C virus (HCV) is a positive-sense RNA virus that interacts with the liver-specific microRNA, miR-122 miR-122 binds to two sites in the 5' untranslated region (UTR) and this interaction promotes HCV RNA accumulation, although the precise role of miR-122 in the HCV

life cycle remains unclear. Using biophysical analyses and Selective 2' Hydroxyl Acylation analyzed by Primer Extension (SHAPE) we investigated miR-122 interactions with the 5' UTR. Our data suggests that miR-122 binding results in alteration of nucleotides 1–117 to suppress an alternative secondary structure and promote functional internal ribosomal entry site (IRES) formation. Furthermore, we demonstrate that two hAgo2:miR-122 complexes are able to bind to the HCV 5' terminus simultaneously and SHAPE analyses revealed further alterations to the structure of the 5' UTR to accommodate these complexes. Finally, we present a computational model of the hAgo2:miR-122:HCV RNA complex at the 5' terminus of the viral genome as well as hAgo2:miR-122 interactions with the IRES-40S complex that suggest hAgo2 is likely to form additional interactions with SLII which may further stabilize the HCV IRES. Taken together, our results support a model whereby hAgo2:miR-122 complexes alter the structure of the viral 5' terminus and promote formation of the HCV IRES.

2.3 Introduction

Hepatitis C virus (HCV) infects approximately 71 million people worldwide, with the majority of patients developing a persistent infection that can lead to chronic hepatitis, cirrhosis, and hepatocellular carcinoma (9-11). HCV is an enveloped, positive-sense RNA virus of approximately 9.6 kb that encodes a single open reading frame (12), flanked by highly structured 5' and 3' untranslated regions (UTRs) (13,14). As a positive-sense RNA virus, the HCV genome itself is used as a template for translation, replication, and packaging (14,15). Therefore, the viral RNA must be a dynamic structure able to readily accommodate unwinding, elongation, and exposure of different regions of the RNA to various cellular and viral proteins in order to mediate the different stages of the viral life cycle. The 5' and 3' UTRs contain *cis*-acting RNA elements that play key roles in the viral life cycle, including an internal ribosomal entry site (IRES) that drives translation of the viral polyprotein located in the 5' UTR. Specifically, stem loops (SL) II-

IV make up the viral IRES required for translation and stem-loop structures and sequences in both the 5' and 3' UTRs have been shown to be required for viral replication (14-19). In addition, the 5' terminus of the viral genome interacts with an abundant, liver-specific human microRNA (miRNA), called miR-122 (20-22).

miR-122 is highly expressed in the liver where it constitutes approximately 70% of liver miRNAs, with ~66,000 copies/hepatocyte (21,23). Although miRNAs typically interact with the 3' UTR of target mRNAs to downregulate gene expression, miR-122 binds to two sites in the 5' UTR of the HCV genome and this interaction *promotes* HCV RNA accumulation (**Figure 2.1A**) (21,22,24,25). While sequestration of miR-122 using antisense inhibitors results in impairment of HCV RNA accumulation in both cell culture and the livers of HCV-infected patients, the precise mechanism(s) of miR-122-mediated viral RNA accumulation remain incompletely understood (21,26). Recent studies have suggested two major mechanisms for miR-122's promotion of viral RNA accumulation: 1) protection of the 5' triphosphate moiety of the HCV genome from recognition by 5' pyrophosphatases and subsequent decay by 5'-3' exoribonucleases (2,27-29); and 2) an RNA chaperone-like mechanism whereby miR-122 binding alters the structure of the viral RNA to promote functional IRES formation (1,4).

Although miR-122 is important for HCV RNA accumulation, there is evidence of mutations in the viral 5' terminus that are less reliant on miR-122 and allow HCV to replicate to low levels in the absence of the miRNA. One of these mutants, G28A, was isolated from patients who underwent miR-122 inhibitor-based therapy after viral rebound and was subsequently demonstrated to allow low levels of viral RNA accumulation in miR-122 knock-out (KO) cells (7,30). Although the mechanism(s) underlying miR-122-independent viral RNA accumulation remain unclear, it is hypothesized that the G28A mutant can take on a conformation that favours viral RNA accumulation.

Several studies have suggested that miR-122 binding to the HCV genome can alter the structure of the HCV 5' UTR. Two previous in vitro Selective 2' Hydroxyl Acylation analyzed by Primer Extension (SHAPE) studies using HCV genotype 1b (Con1b) indicate that miR-122 binding alters the secondary structure of the HCV 5' UTR, specifically at the two miR-122 binding sites, but also in the HCV IRES region (2,3). In agreement with this finding, an Argonaute (Ago) high-throughput sequencing and crosslinking immunoprecipitation (HITS-CLIP) study suggests that Ago interacts with the HCV 5' UTR at the two miR-122 binding sites, but also with regions in the HCV IRES that do not align to known human miRNAs (25). Furthermore, computational prediction analyses suggested that the HCV 5' UTR may be able to take on an alternative conformation that could be influenced by miR-122 interactions with the viral genome (31). More recently, two studies have suggested that miR-122 binding to the HCV genome suppresses a more energetically favorable alternative secondary structure in the SLII region of the HCV 5' UTR (termed SLII^{alt}), thereby promoting the folding of a functional IRES (SLII-IV) that drives HCV translation (1,4). This is further supported by the observation that mutations in the 5' UTR are predicted to favour functional IRES formation and are able to accumulate in the absence of miR-122 (1,4). Thus, we sought to further investigate this model using biophysical analyses and provide insight into miR-122:HCV RNA interactions as well as the contribution of Ago in positioning this complex on the HCV 5' UTR.

Herein, we performed biophysical characterization of miR-122:HCV RNA interactions *in vitro* using isothermal titration calorimetry (32), electrophoretic mobility shift assays (EMSA), and structural analysis of the wild-type and G28A HCV 5' UTR in the presence and absence of miR-122. We also performed *in vitro* binding studies using hAgo2:miR-122 and we provide a computational prediction of the three-dimensional (3D) structure of the hAgo2:miR-122 complexes at the 5' terminus of the HCV genome as well as a model of the IRES-40S complex to help interpret the role Ago plays in stabilizing the bent IRES SLII conformation required for

activation of HCV translation. Taken together, our results suggests that two hAgo2:miR-122 complexes can simultaneously bind to the HCV 5' terminus and we provide a more comprehensive biophysical analysis of alterations to the 5' UTR that occur upon miR-122 and hAgo2:miR-122 binding. Our results suggest that miR-122 plays three roles in the viral life cycle, which include:

1) an RNA chaperone-like mechanism whereby hAgo2:miR-122 recruitment suppresses formation of an alternative secondary structure (SLII^{alt}) and promotes functional IRES formation; 2) protection of the 5' terminus from pyrophosphatase activity and subsequent exoribonuclease-mediated decay; and 3) direct promotion of HCV translation through contacts between hAgo2 at Site 2 and SLII of the HCV IRES.

2.4 Materials and Methods

Viral RNA and microRNAs

A plasmid containing the full-length HCV genotype 2a, JFH-1 isolate with three cell culture-adapted mutations that increase overall viral replication (JFH-1_T) was provided by Rodney Russell, Memorial University (33). A DNA template of 419 nucleotides (nts) of the 5' UTR of HCV was prepared using PCR amplification. The 419 nt PCR product was gel extracted from a 1% agarose gel, which was then used for *in vitro* transcription with the T7 RiboMAX Express kit (Promega) according the manufacturer's instructions. Full-length *in vitro* transcribed RNA was gel purified on a 6% polyacrylamide gel (29:1 acrylamide:bis-acrylamide, 1X TBE) and the RNA was eluted in 400 μL elution buffer (500 mM NH₄OAc, 10 mM EDTA and 0.1% sodium dodecylsulphate) overnight at room temperature (RT) with gentle agitation. The purified RNA was precipitated as previously described and stored at -20 °C until use. The same procedure was followed for 1-371 nt, 1-117 nt of the 5' UTR (WT and G28A) as well as 1-117 nt containing point mutations in positions 5 and 6 at Site 2 (A38U and C39G).

Wild-type (WT) HCV 1-42 (5'-ACC UGC CCC UAA UAG GGG CGA CAC UCC GCC AUG AAU CAC UCC-3'), HCV Site 2p3,4 1-42 (5'- ACC UGC CCC UAA UAG GGG CGA CAC UCC GCC AUG AAU CAC AGC -3'), and the individual sites, Site 1 (5'- ACC UGC CCC UAA UAG GGG CGA CAC UCC-3') and Site 2 (5'- GCC AUG AAU CAC UCC-3') as well as single-stranded guide strand miR-122 (5'-UGG AGU GUG ACA AUG GUG UUU GU-3') and miR-124 (5'- UAA GGC ACG CGG UGA AUG CC-3'), were synthesized by IDT. Viral RNAs were gel purified as described above.

Isothermal Titration Calorimetry (ITC)

HCV RNAs were resuspended in ITC buffer (100 mM HEPES pH 7.5, 100 mM KCl, 5 mM MgCl₂, filter-sterilized). Five-hundred microliters of 5 μM HCV RNA were heated to 65 °C for 10 min and then snap-cooled on ice for 10 min then centrifuged for 1 min at 13 000 rpm for ITC analyses. The temperature was set at 37 °C and the reference power was 3 μcal/s. A total of 20 injections of 2 μL were performed with 180 s spacing and 4 s per injection of a 100 μM stock of single-stranded guide strand miR-122 prepared in ITC buffer (2). ITC was carried out on the ITC200 and data analysis using the Origin 7 software (MicroCal), where the first injection was removed. The same procedure was performed for the individual sites (Site 1 and Site 2). The data was fitted to a two sequential binding model, except for the individual Sites 1 and 2, where the data was fitted to a one-site binding model.

Electrophoretic Mobility Shift Assay (EMSA)

2.8 μM stocks of 1-42 nt HCV,Site2p3,4 and G28A RNA were prepared by diluting in RNase-free water. The RNA was re-folded by incubating at 65 °C for 5 min and then incubated at 37 °C for 1 h. Dilutions of miR-122 or miR-124 (control) were prepared from serial dilutions from a 4:1 ratio of miRNA: HCV RNA in folding buffer (100 mM HEPES (pH 7.5), 100 mM KCl, and 5 mM

MgCl₂). The different dilutions of miR-122 were added to 2.8 μM of HCV RNA and incubated at 37 °C for 30 min (total volume of 7 μL). An equal volume of loading dye was added (30% glycerol, 0.5x TBE, 6 mM MgCl₂, 3 μL bromophenol blue and 3 μL xylene cyanol). Five microliters of the sample were separated on a 15% non-denaturing polyacrylamide gel (29:1 acrylamide:bisacrylamide, 0.5x TBE, 6 mM MgCl₂) for 2 h at 8 W at 4 °C. The band shifts were visualized with SYBR Gold (Invitrogen) staining (2).

RNA structure prediction

RNA structure predictions were carried out using the RNA prediction software RNAstructure available from the Matthews lab at https://rna.urmc.rochester.edu/index.html (34). Briefly, the RNA sequence was loaded into the RNA structure software using the "Fold RNA Single Strand" command (34). The results were saved as dot bracket files, which were used to generate the predicted structures in VARNA (35).

Synthesis of NAI-N₃

Synthesis of NAI-N₃ has been previously described (36). Briefly, Methyl 2-methylnicotinate was dissolved in anhydrous dichloromethane, followed by the addition of trichloroisocyanuric acid with overnight stirring at RT. Anhydrous N, N-dimethylformamide and sodium azide were added to the reaction. The product of this reaction (methyl 2-(azidomethyl)nicotinate) was stirred in a solution of 1:1 methanol and aqueous sodium hydroxide (NaOH). Water was added and the solution was acidified to pH 4 by the addition of HCl and extracted by ethyl acetate. This became the acid precursor of NAI-N₃, 2-(azidomethyl)nicotinic acid. Fresh carboyldiimidazole (CDI) and anhydrous DMSO were stirred until homogenous. 2-(Azidomethyl)nicotinic acid was also mixed with anhydrous DMSO until homogenous. CDI with DMSO were then added to the acid precursor

in a drop-wise manner. The reaction proceeded for 1 h at RT while stirring. This resulted in a 2 M NAI-N₃ stock that was stored at -80 °C.

In vitro SHAPE analysis

Five picomoles of the HCV 5' UTR RNA were re-folded and incubated with 10 μM of single-stranded, guide strand miR-122 or miR-124 (control) for 30 min at 37 °C in SHAPE buffer (333 mM HEPES, pH 8.0, 20 mM MgCl₂, 333 mM NaCl), followed by treatment with 0.1 M (gel electrophoresis) or 0.01 M (capillary electrophoresis) NAI-N₃ or DMSO (control) at 37 °C for 5 min. Labeled RNA was then extracted using TRIzol reagent (Thermo Fisher Scientific) according to the manufacturer's instructions. RNA was precipitated and stored at -80 °C. The same procedure was followed for G28A. For *in vitro* SHAPE with hAgo2:miR-122 complexes, 25 pmol of hAgo2 loaded with miR-122 was incubated with 5 pmol of the refolded HCV 5' UTR for 45 min at 37 °C followed by treatment with NAI-N₃ and DMSO followed by capillary electrophoresis (as described below).

SHAPE analysis by gel electrophoresis

³²P-end-labeled oligonucleotides (0.1 pmol/μL) were annealed to 500 fmol of acylated HCV 5' UTR RNA by incubating at 95 °C for 2 min, followed by step-down cool to 4 °C for 2 min. Subsequently, 1x First-Strand Buffer, 5 mM DTT, 0.5 mM dNTPs and SUPERaseIn RNase Inhibitor (Life Technologies) were added to the reaction. One millimolar ddCTP and ddTTP were used in sequencing ladder reactions. The reactions were incubated at 52 °C for 1 min, followed by the addition of SuperScript III Reverse Transcriptase (2 U/μL) followed by incubation at 52 °C for 30 min. One microliter of 2 M NaOH was then added to each reaction at 95 °C for 5 min and reactions were stopped by addition of 2 μl Formamide loading dye (95% formamide, 0.01M EDTA, bromophenol blue and xylene cyanol). The cDNA extensions were loaded and run out on

a 12% polyacrylamide gel (29:1 acrylamide:bis-acrylamide, 1X TBE). Gels were dried at 80 °C for 3 h in a gel dryer (Bio Rad, Model 583) and cDNA fragments were visualized by phosphorimager (Personal Molecular Imager, BioRad) and analyzed using SAFA software (37,38). A normalized reactivity of 1.0 was defined as the average intensity of the top 10% most reactive peaks, where the most reactive 2% of all intensities were removed from the pool. The intensities of the next 8% most reactive peaks are averaged and all reactivities are divided by this average value, as previously described (39,40).

SHAPE analysis by capillary electrophoresis

For SHAPE analysis by capillary electrophoresis, 1 pmol of 6-FAM-labeled oligonucleotide (5'-6-FAM-CGC CCG GGA ACT TAA CGT CTT-3') was annealed to 5 pmol of modified HCV RNA. The same primer extension buffers as for gel electrophoresis were used, with the addition of 2 µL DMSO per reaction sample. One picomole of NED-labeled oligonucleotide (5' NED-CGC CCG GGA ACT TAA CGT CTT-3') was used for sequencing ladders with either 0.5 mM ddGTP or 1 mM ddCTP. Capillary electrophoresis was performed at Plateforme d'Analyses Génomiques de l'Université Laval on an ABI 3100 Genetic Analyzer. Raw fluorescence data was analyzed using QuSHAPE software (41). A normalized reactivity of 1.0 was defined as the average intensity of the top 10% most reactive peaks, where the most reactive 2% of all intensities were removed from the pool. The intensities of the next 8% most reactive peaks were averaged and all reactivities are divided by this average value, as previously described (42). The Wilcoxon rank test was done between the SHAPE data of HCV RNA with hAgo2:miR-122 and that of HCV RNA alone to determine if there is a statistical difference between the SHAPE reactivities, as previously described (43). The Wilcoxon test determined there are highly significant differences in SHAPE reactivity between both groups (p < 0.0001). The baseline value for Δ SHAPE (miR-122 reactivity - miR-124 reactivity or hAgo2:miR-122 reactivity - HCV RNA reactivity) was determined by finding the average of the absolute Δ SHAPE values. Δ SHAPE values above baseline were considered significant increases and below negative baseline value were considered significant decreases in SHAPE reactivity.

Purification of recombinant human Ago2 loaded with miR-122

Human Ago2 was expressed using a baculovirus system and purified with homogeneously loaded miR-122 according to a previously published protocol (44). Briefly, Sf9 cells were infected with baculovirus encoding His-tagged hAgo2. Cells were then lysed and hAgo2 was purified by Ni-NTA affinity chromatography. The His-tag was removed using Tobacco etch virus (TEV) protease and hAgo2 was loaded with synthetic miR-122 bearing a 5'-phosphate (IDT). Homogeneously loaded hAgo2:miR-122 was captured using an antisense oligonucleotide (IDT), eluted, and purified by size exclusion chromatography using an ÄKTA FPLC (GE Healthcare Life Science). Protein concentrations in purified Ago2:miR-122 complex samples were determined by absorption at 280 using an extinction coefficient of 198370 M⁻¹ cm⁻¹ and by Bradford assay using BSA as standard.

Electrophoretic mobility shift assays with hAgo2:miR-122

Binding reactions were prepared in reaction buffer (30 mM Tris pH 8.0, 100 mM KOAc, 2 mM Mg(OAc)2, 0.5 mM TCEP, 0.005% NP-40) with a final volume of 20 μl, and a final concentration of the labeled RNAs of 0.1 nM, and of hAgo2:miR-122 ranging from 0 nM to 5 nM. Reactions were incubated for 45 min at room temperature and then run on a 15% acrylamide native gel in 0.5x TBE (45 mM Tris-borate, 1 mM EDTA, pH 8.3). The gels were used to expose a phosphorscreen overnight, which was imaged on a Typhoon scanner (GE Healthcare Life Sciences).

To calculate the K_d , equilibrium binding data of triplicate electrophoretic mobility shift assays were fit to Equation 1:

$$Y = \left(\frac{Bmax}{2*S}\right) * \left([Ago2] + S + kD \right) - \sqrt{([Ago2] + S + kD)^2 - (4*S*[Ago2])}$$

where Y is the fraction of target RNA bound, Bmax is the calculated value of maximum binding, [AGO2] is the total concentration of the AGO2:miR-122 complex, S is the concentration of RNA (0.1 nM) and K_d is the calculated dissociation constant, obtained with Prism (GraphPad Software). For the wildtype data, Bmax was normalized to 1: the total bound sites at each concentration were calculated as (2*[double shift intensity] + [single shift intensity]), and the free sites were calculated as ([single shift intensity] + 2*[unbound RNA intensity]). These numbers were then used to calculate the total signal and the bound fraction.

Computational modeling

We modeled Ago2:miR-122:HCV RNA ternary complexes, using experimentally determined secondary RNA-target duplexes and solved human Ago structures (45,46). Our model building is based on an algorithm we developed previously to construct *C. elegans* and human RISC structures (47). To construct RISC structures, we generated up to 1000 3D duplex conformations for each miRNA-target duplex using the MC-Sym algorithm (48); sampled 1000 Ago conformations using an elastic network model theory; docked each duplex conformation to each Ago conformation using a solved *T. thermophilus* RISC structure (PDB code: 3HJF); and screened for favorable RISC structures with minimal steric clashes, followed by structure refinement using energy minimization. Throughout, we used human Ago2 (4OLA) to model RISC structures. Complexes of hAgo2 bound simultaneously to adjacent recognition sites were assembled by joining two

separate RISC structures, as described previously (49). We defined a 3-base linker (CGC) in HCV RNA between the miR-122 binding sites. From experimentally solved RNA structures, we obtained 1542 CGC fragments (downloaded from RNA FRABASE 2.0). These fragments sampled many relative orientations between adjacent RISC structures. Viable RISC-RISC complexes with minimal steric clashes (<100 atomic overlaps) were then refined using energy minimization.

A similar strategy was used to the assemble RISC-RISC-IRES-40S complexes. Using the cryo-EM structure of human 40S-IRES (5A2Q) and a modeled RISC-RISC complex, we searched for complexes free of steric clashes by sampling ~2000 CC fragments (HCV RNA nucleotides 42-43) linking the duplexes in IRES SLIIa and adjacent Site 2 RISC. Since the IRES in 5A2Q structure contains nucleotides 40-42 (5°CUC) that are known to form base pairs with the seed region of miR-122 at Site 2, we removed these three nucleotides in the solved structure. Given the large size of the 40S ribosomal subunit, we simplified computational assessment of steric clashes by considering only components of IRES-40S in the vicinity of the RISC-RISC complex, which include IRES and a subset of ribosomal proteins.

2.5 Results

Two miR-122 molecules can bind to the HCV 5' terminus simultaneously with different binding affinities.

The HCV genome has two miR-122 binding sites in its 5' UTR, which are both required for optimal viral RNA accumulation (**Figure 2.1A**) (22). It was previously reported that two molecules of miR-122 can bind to the Con1b genotype of HCV RNA and alter the secondary structure of the viral terminus (2,3). As such, we first sought to confirm the stoichiometry of miR-122:HCV RNA interactions with the JFH-1 isolate (genotype 2a). To investigate miR-122 binding to the wild-type (WT) HCV 5' UTR, we performed EMSA using nts 1-42 of the HCV genome with increasing

concentrations of miR-122 (**Figure 2.1B**). With miR-122 addition, at low molar ratios, the HCV RNA began to show retarded mobility (**Figure 2.1B**), while at higher concentrations, the viral RNA was further retarded and began to become saturated at a 2:1 molar ratio of miR-122:HCV RNA, indicating that both miR-122 binding sites are able to bind simultaneously to the HCV genome (**Figure 2.1B**). Importantly, EMSAs carried out with an unrelated miRNA, miR-124, did not cause retardation of the viral RNA (**Supplementary Figure S2.1A**). This suggests that miR-122 can bind to the 5' UTR of the HCV JFH-1 isolate RNA with a 2:1 stoichiometry.

To further investigate the miR-122:HCV RNA interactions, we used isothermal titration calorimetry (32) to measure the affinity of miR-122 for the viral RNA (**Figure 2.1C**). In agreement with our EMSA results, we found that the ITC binding curve was best fit with a two-site binding model, with equilibrium dissociation constants (K_{dS}) of $K_{d1} = 20.45 \pm 11.8$ nM and $K_{d2} = 186.08 \pm 57.76$ nM (**Figure 2.1C** and **Table 2.1**). We observed no binding of miR-124 to the HCV RNA by ITC analysis (**Supplementary Figure S2.1B**). These results suggest that the two miR-122 binding sites have different binding affinities; and although they have different dissociation constants, the interactions were similar in enthalpy and entropy (**Table 2.1**). Both interactions were highly exothermic ($\Delta H_1 = -73.28$ kcal/mol and $\Delta H_2 = -57.67$ kcal/mol) with entropy changes of $\Delta S_1 = -200.67$ cal/mol/deg and $\Delta S_2 = -155.33$ cal/mol/deg and their Gibbs free energy values were calculated to be $\Delta G_1 = -11.04$ kcal/mol and $\Delta G_2 = -9.49$ kcal/mol. Thus, based on the EMSA and ITC results, two miR-122 molecules are able to interact with the HCV RNA simultaneously *in vitro*, albeit with differing binding affinities (**Table 2.1**).

To confirm whether K_d1 represents binding of miR-122 to Site 1 or Site 2, we performed EMSA and ITC analyses on an HCV RNA that contained mutations in positions 3 and 4 of the seed sequence of Site 2 (S2p3,4) (**Supplementary Figure S2.1C-E**). The results show that the

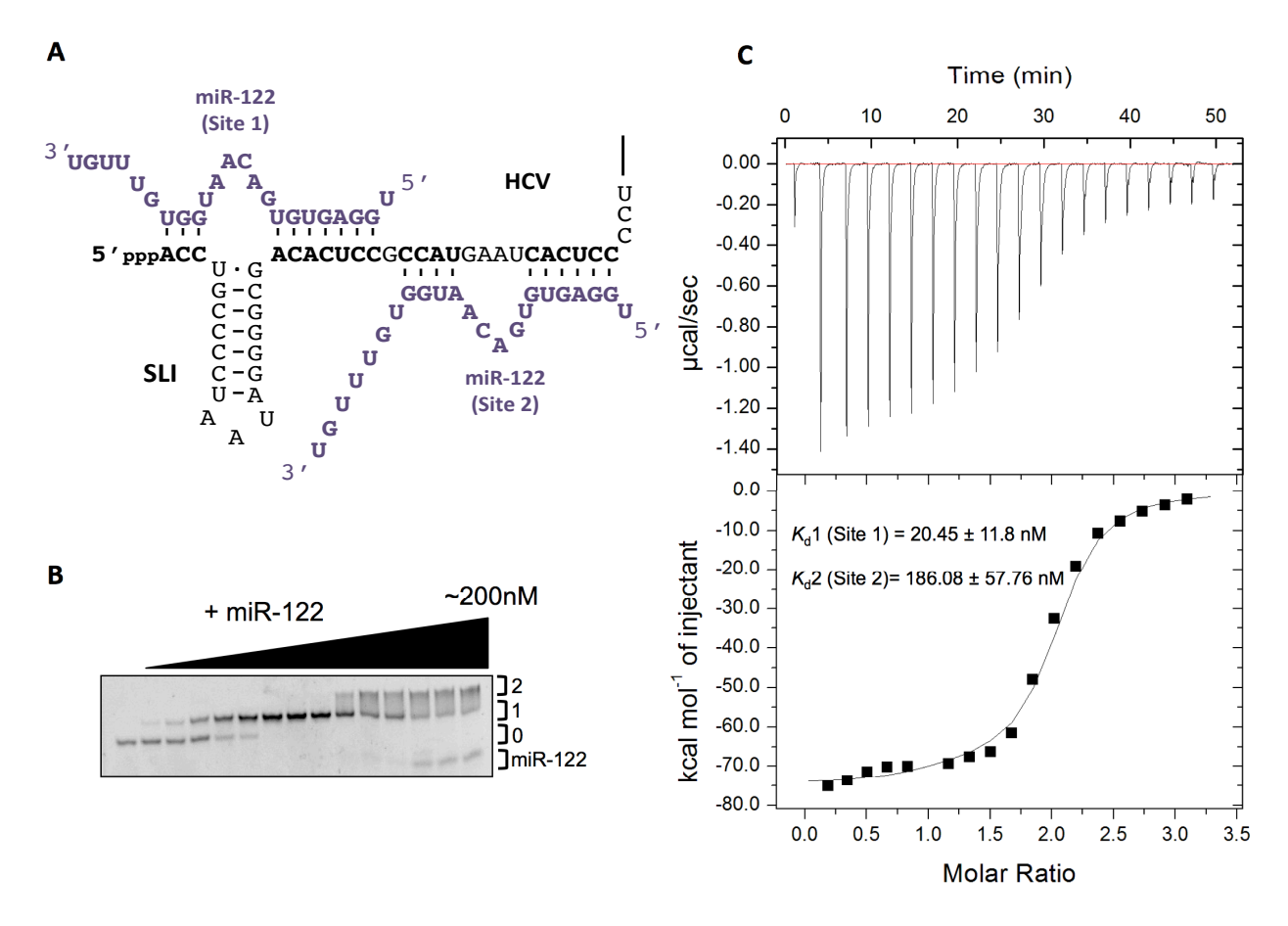


Figure 2.1. miR-122 binds to the HCV 5' terminus with a 2:1 stoichiometry. (A) Model of the interaction of miR-122 (purple) and nts 1-42 of the HCV genome (black). (B) Non-denaturing gel electrophoretic mobility shift assay (EMSA) of 1-42 nt HCV RNA and increasing amounts of miR-122. (C) Thermogram and resulting binding curve of the titration of 1-42 nt HCV RNA with miR-122. Affinities of each binding site, K_d1 (Site 1) and K_d2 (Site 2), are indicated. All data are representative of at least three independent replicates and K_d values are an average of three measurements (\pm) error propagated from individual fits.

Table 2.1. ITC analysis of miR-122 binding to HCV RNAs.

HCV RNA (nt)	ΔΗ	ΔS	K _d (nM)	
	(kcal/mol)	(cal/mol/deg)	Site 1	Site 2
HCV (1-42)	-73.28 ± 2.50	-200.67	20.45 ± 11.8	
	-57.67 ± 3.53	-155.33		186.08 ± 57.76
HCV S2p3,4 (1-42)	-75.70 ± 1.04	-209.00	25.80 ± 9.40	
	-20.30 ± 1.94	-38.53		1315.24 ± 416.06
Site 1 (1-27)	-55.53 ± 0.53	-143.67	18.80 ± 3	
Site 2 (29-42)	-128.23 ± 6.54	-372.67		228.34 ± 65.41
HCV WT (1-117)	-101.09 ± 2.51	-294.67		132.55 ± 35.43
	-20.82 ± 4.67	-44.83	13296.58 ± 7518.62	
HCV S2p5,6 (1-117)	-58.87 ± 2.26	-160		319.3 ± 86.01
	-14.33 ± 6.06	-23.93	13596.11 ± 5024.61	
G28A (1-117)	-102.18 ± 2.36	-294.33	21.24 ± 8.08	
	-39.31 ± 5.94	-101.17		2590.99 ± 863.68
HCV WT (1-371)	-104.36 ± 11.32	-308		514.27 ± 229.88
	-41.85 ± 14.72	-108.2	1426.17 ± 517.93	

^aValues reported are an average of three measurements (±) error propagated from individual fits.

first binding site had an affinity of 25.80 \pm 9.40 nM, similar to Site 1 of WT HCV (**Figure 2.1C** and **Table 2.1**), while the binding affinity of the second site was 1315.24 \pm 416.06 nM, as a result of the mutations in the seed sequence of Site 2 (**Supplementary Figure 2.1E**). This suggests that when nts 1-42 of the HCV genome are present, Site 1 is bound first *in vitro*. Additionally, the enthalpy, entropy and Gibbs free energy of the first binding site of HCV S2p3,4 had very similar to the first binding site of the WT HCV RNA (1-42 nt) (**Table 2.1**). However, the second binding site had a higher enthalpy and entropy (Δ H = -20.30 \pm 1.94 kcal/mol and Δ S = -38.53 cal/mol/deg, respectively) with Δ G = -8.35 kcal/mol, suggesting that this reaction is not as spontaneous at 37°C compared to the first binding site of WT HCV (**Table 2.1**). These results were confirmed qualitatively by performing EMSA on HCV S2p3,4 where the first binding event occurred quickly, while the second binding event did not occur until a 4:1 ratio of miR-122 to HCV S2p3,4 was reached (**Supplementary Figure S2.1D**). These results suggest that when only the two sites are present (1-42 nt HCV RNA), miR-122 binds to Site 1 with a higher affinity *in vitro*.

To investigate the specific binding sites further, we tested miR-122 binding to each individual site by ITC analysis using Site 1 (nt 1-27) or Site 2 (nt 29-42) RNAs. We found that miR-122 bound to Site 1 (K_d = 18.80 ± 3 nM) with a stronger affinity than to Site 2 (K_d = 228.34 ± 65.41 nM) (**Table 2.1** and **Supplementary Figure S2.2**). More specifically, we found that miR-122 binding to Site 1 was exothermic, with ΔH = -55.53 kcal and an entropy of ΔS = -143.67 cal/mol/deg (**Table 2.1** and **Supplementary Figure S2.2A**). These results are in good agreement with computational binding predictions, where miR-122 interactions with Site 1 are predicted to have ΔH = -69.5 kcal/mol and ΔS = -192.2 cal/mol/deg. Additionally, we found that Site 2 had a lower affinity for miR-122 with a K_d = 228.34 ± 65.41 nM; however, miR-122 binding was more exothermic, with ΔH = -128.23 kcal/mol and an entropy of ΔS = -372.67 cal/mol/deg, again in good agreement with computational binding predictions (ΔH = -109 kcal/mol and ΔS = -306.6 cal/mol/deg) (**Table 2.1** and **Supplementary Figure S2.2B**). This suggests that the individual

miR-122 binding sites, have a different rearrangement and organization compared to the 1-42 nt HCV RNA based on enthalpy and entropy. However, the K_d of the individual sites are similar to those values obtained in the context of the 1-42 nt HCV RNA. Thus, at least *in vitro*, miR-122 has a higher affinity for Site 1 than for Site 2 on the 1-42 nt HCV RNA.

miR-122 binding alters the secondary structure of SLII of the HCV 5' UTR.

To investigate structural alterations mediated by miR-122 binding to the HCV 5' UTR, we performed *in vitro* SHAPE analysis on the full HCV 5' UTR (nts 1- 371) in the presence and absence of miR-122 using both capillary (**Figure 2.2** and **Supplementary Figure S2.3**) and gel electrophoresis (**Supplementary Figure S2.4**). As recent studies and computational predictions suggest that the WT HCV 5' UTR favours a non-canonical alternative SLII structure (SLII^{alt}) in the absence of miR-122 (1,4), we used SHAPE analysis to map the reactivity of the first 117 nts (including SLI and II) of the HCV RNA in the presence or absence of miR-122 (**Figure 2.2**).

Reactivity information was obtained for almost every nucleotide in the RNA; however, we were not able to discern the SHAPE reactivity at nts 1-5 due to the high reactivity at the 5' end of the transcript and nts 14-19 due to the high background observed in this region, in line with previous studies (2,3). In the absence of miR-122, the loop of SLI (11-13 nts) and Site 2 (30-39 nts) were found to be relatively unstructured/flexible, as reported previously (**Figure 2.2A** and **Supplementary Figures S2.3-4**) (2-4). However, Site 1 (consisting of nts 20-27) had a relatively low SHAPE reactivity, suggesting that this region is constrained in the context of the 5' UTR (**Figure 2.2A**).

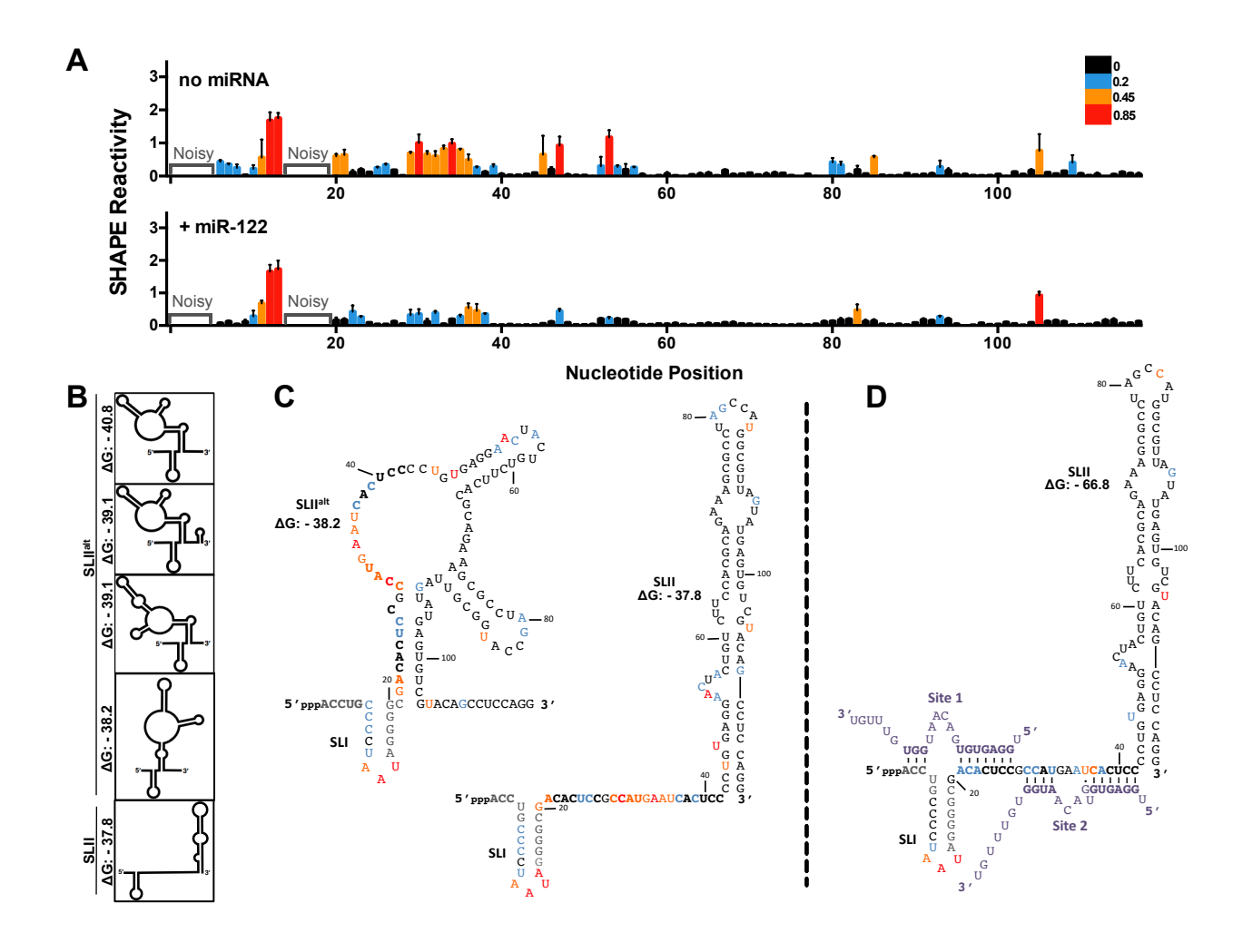


Figure 2.2. miR-122 binding suppresses an alternative structure (SLIIalt) and promotes functional folding of SLII. (A) Normalized SHAPE reactivities of HCV RNA (nts 1-117) with no miRNA (top) or in the presence of miR-122 (bottom). Nucleotides 1-5 and 14-19 were omitted due to high background reactivity. Nucleotides with high (≥ 0.85 , red), intermediate (between 0.4 and 0.85, orange), low (between 0.2 and 0.4, blue) and very low (≤ 0.2 , black) SHAPE reactivity are indicated. (B) Predictions of the lowest free energy structures formed by the first 117 nts of HCV 5' UTR and their predicted free energies (ΔG , kcal/mol). (C) SHAPE data from (A) superimposed onto two of the predicted structures of HCV RNA alone or (D) HCV RNA + miR-122, where the predicted structure and free energy values are indicated. The SHAPE data represents the results of six independent replicates and error bars indicate the standard error of the mean (SEM).

When SHAPE was performed on the HCV 5' UTR in the presence of miR-122, we observed a reproducible reduction in SHAPE reactivity, particularly in the seed region of Site 2, consistent with previous models of miR-122:HCV RNA interactions (**Figure 2.2A** and **Supplementary Figure S2.3**) (2-4). We also observed a reproducible decrease in the SHAPE reactivity in the stem region of SLI, suggesting that miR-122 binding may further stabilize this stem-loop structure (**Figure 2.2A** and **Supplementary Figure S2.3**). In addition, there was a reduction in SHAPE reactivity at positions A33, G34, and U36 on the HCV RNA (2,22). This is in agreement with previous studies and suggests that miR-122 binding may increase rigidity in this region and that the U at position 36 may be able to engage in a wobble base pair with the G at position 9 on Site 2-bound miR-122 (2-4). Moreover, we observed a lower SHAPE reactivity in SLIIa (nts 52-59) in the presence of miR-122 when compared to the HCV RNA alone (**Figure 2.2A**).

Structural predictions of nts 1-117 of the HCV genome with and without miR-122 suggest that the most energetically favourable structure(s) of the WT HCV RNA in the absence of miR-122 is an alternative non-canonical SLII structure from nts 20-104, previously termed SLII^{alt} (Figure 2.2B) (1,4). The functional SLII structure is only predicted to be the fifth most energetically favourable structure, with a ΔG of -37.8 kcal/mol, compared to the free energies of the SLII^{alt} structures, which range from -40.8 to -38.2 kcal/mol (Figure 2.2B). When we analyzed our SHAPE data with respect to the non-canonical SLII^{alt} and SLII structures, we found that the reactivity agrees well with both of these predicted structures (Figure 2.2C). Specifically, there are high overall SHAPE reactivities in nts 30-39, 53-59 and 80-85 which are all either single-stranded or in bulge regions in both structures (Figure 2.2C). However, nts 20-29 had relatively low SHAPE reactivities in the absence of miR-122, which is more consistent with the SLII^{alt} structure, since these nucleotides are base-paired versus single-stranded in the functional SLII structure (Figure 2.2C). Conversely, SHAPE analysis in the presence of miR-122 is consistent with formation of the canonical SLII structure, predicted to be the most energetically favorable structure

in the presence of miR-122 (ΔG = -66.8 kcal/mol, **Figure 2.2A and D**). Thus, although our data provides an averaged view of the equilibrium of several of the most energetically favorable structures, the quantitative SHAPE results suggest that in the absence of miR-122, the SLII^{alt} is favoured, while interactions with miR-122 promote functional SLII formation, which would support HCV IRES-mediated translation (4,50-52).

To further validate these findings, we predicted that if SLII^{alt} is the preferred conformation of the viral RNA, then in the context of nts 1-117, Site 2 should have a greater miR-122 binding affinity than Site 1, as Site 2 is in a more open (single-stranded) conformation, while Site 1 is in a closed (double-stranded) conformation (Figure 2.2C). Thus, we performed ITC analyses to measure the binding affinity of miR-122 for the 1-117 nt and 1-371 nt HCV RNA. Both binding sites had weaker affinities when compared to the 1-42 nt HCV RNA, with $K_{\rm d}1$ (Site 2) = 132.55 \pm 35.43 nM ($\Delta G = -79.2 \text{ kcal/mol}$) and K_d2 (Site 1) = 13296.58 ± 7518.62 nM ($\Delta G = -17.5 \text{ kcal/mol}$) for 1-117 nt HCV RNA, and $K_{\rm d}1$ (Site 2) = 514.27 ± 229.88 nM ($\Delta G = -81.53$ kcal/mol) and $K_{\rm d}2$ (Site 1) = 1426.17 ± 517.93 nM ($\Delta G = -33.83$ kcal/mol) for 1-371 nt HCV RNA, respectively (Table 2.1 and Supplementary Figure S2.5). This is not unexpected since the longer RNAs (1-117 and 1-371 nt) are likely able to sample more conformations than the 1-42 nt RNA. In order to discern whether K_d 1 represents binding of miR-122 to Site 1 or Site 2 on the 1-117 nt RNA, we performed ITC analyses on a Site 2 mutant (S2p5,6), whereby positions 5 and 6 of the Site 2 seed sequence were mutated to their respective Watson-Crick base (Table 2.1). These mutations are predicted to reduce binding of Site 2, without significantly altering the predicted conformation or miR-122 interactions with Site 1. As we predicted, a reduction in binding affinity was only observed for K_d1 (Site 2) = 319.3 ± 86.01 nM ($\Delta G = -47 \text{ kcal/mol}$), while K_d2 (Site 1) = 13596.11 \pm 5024.61 nM (Δ G = -12.6 kcal/mol) remained unchanged (**Table 2.1** and **Supplementary Figure S2.5**). Thus, in contrast to what we observed with nts 1-42, in the context of nts 1-117, Site 2 has a higher affinity, while Site 1 has a significantly reduced affinity for miR-122. These results are in agreement with formation of the energetically more favorable SLII^{alt}, where Site 2 is predicted to be in an open and accessible conformation, while Site 1 is predicted to be in a closed conformation.

The G28A mutation favours formation of SLII even in the absence of miR-122.

The G28A mutation was isolated from chronic HCV patients that had undergone miR-122 inhibitor-based therapy after viral rebound and was subsequently shown to be able to accumulate to low levels in miR-122 knockout (KO) cells (7,8). RNA structural predictions suggest that in contrast to WT HCV RNA, the G28A mutation is predicted to adopt only two main conformations with very similar free energies, SLII^{alt} ($\Delta G = -37.9 \text{ kcal/mol}$) and SLII ($\Delta G = -37.8 \text{ kcal/mol}$), even in the absence of miR-122 (Figure 2.3). SHAPE analysis of G28A suggests that the seed region of Site 1 (nts 20-27) has an overall higher SHAPE reactivity when compared with WT HCV RNA (Figure 2.2A versus 2.3A). Importantly, this region represents the most significant difference between the SLII^{alt} and SLII structures in that it is predicted to be base-paired in the former and single-stranded in the latter (Figure 2.3B). When we superimposed the SHAPE data onto the two G28A predictions, the data is more consistent with formation of SLII, where nts in the Site 1 seed region (nts 20-27), predicted to be single-stranded in this conformation, have a high overall SHAPE reactivity (Figure 2.3). We also observed high overall SHAPE reactivities in the loop regions of SLII (nts 52-59 and 80-85), but these are largely consistent with both structural conformations (Figure 2.3). With respect to the remaining IRES structure (i.e. SLIII-IV), the G28A mutant demonstrated similar SHAPE reactivity to the WT HCV RNA (Supplementary Figure S2.6). To further confirm these findings, we performed ITC analysis on the 1-117 nt G28A mutant (Table 2.1 and Supplementary Figure S2.6). In agreement with our SHAPE data, G28A had higher affinities for miR-122 than WT, with $K_{\rm d}1$ (Site 1) = 21.24 ± 8.08 nM ($\Delta G = -80.36$ kcal/mol) and K_d2 (Site 2) = 2590.99 ± 863.68 nM (ΔG = -31.81 kcal/mol) (**Table 2.1**).

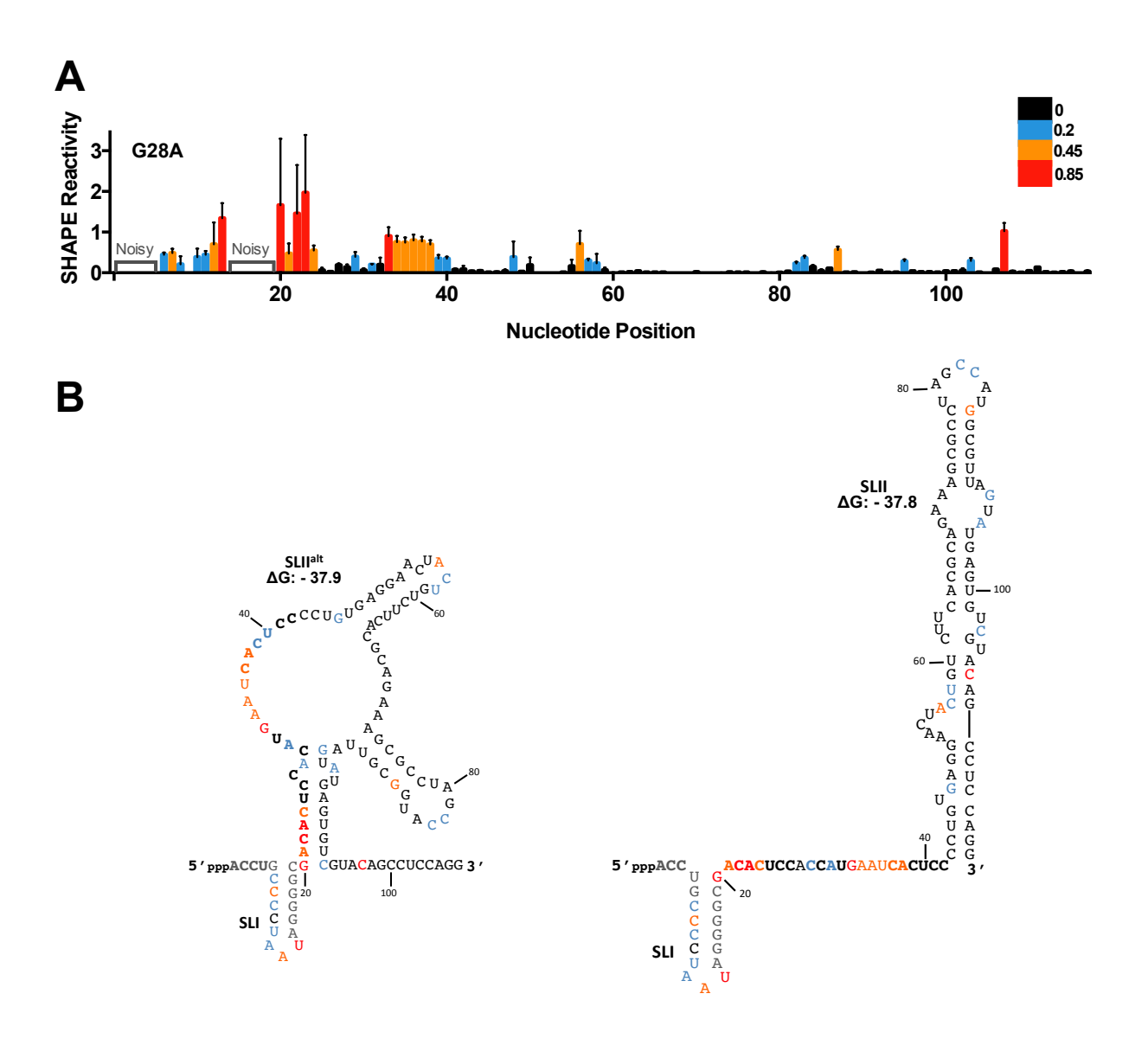


Figure 2.3. The G28A mutation favours SLII formation in the absence of miR-122. (A) Normalized SHAPE reactivities of G28A (nts 1-117). Nucleotides 1-5 and 14-19 were omitted due to high background reactivity. Nucleotides with high (\geq 0.85, red), intermediate (between 0.4 and 0.85, orange), low (between 0.2 and 0.4, blue) and very low (\leq 0.2, black) SHAPE reactivity are indicated. (B) SHAPE data from (A) superimposed on the predicted lowest free energy structures formed by the first 117 nts of the G28A 5' UTR (SLII^{alt} and SLII) and their free energy values (Δ G, kcal/mol). The SHAPE data represents the results of four independent replicates and error bars indicate the standard error of the mean (SEM).

Thus, RNA structural predictions, SHAPE, and ITC are consistent with the G28A mutation favoring formation of SLII even in the absence of miR-122, while the WT HCV RNA is more likely to adopt an alternative conformation(s) (i.e. SLII^{alt}, **Figure 2.2B-C**) in the absence of miR-122.

Two hAgo2:miR-122 complexes can bind to the HCV RNA 5' UTR simultaneously.

It is widely accepted that miR-122 interacts with the HCV genome, at least initially, in the context of a hAgo protein (5,6,22,53,54). Previous studies suggest that Ago proteins are required for miR-122 duplex unwinding, miRNA-induced silencing complex (miRISC)-loading, and recognition of the HCV RNA binding sites; however, it is unclear whether Ago remains bound to the viral RNA to participate in events leading to promotion of HCV RNA accumulation (5,6,22,53-55). Due to the close proximity of the miR-122 binding sites on the HCV genome (**Figure 2.1A**), we sought to test whether two hAgo2:miR-122 complexes are physically able to occupy the viral RNA simultaneously. To this end, we prepared purified samples of hAgo2:miR-122 in complex and performed gel shift assays with the WT (1-42 nt) and S2p3,4 HCV RNAs (**Figure 2.4A**). Using radiolabeled HCV S2p3,4 RNA, where the Site 2 sequence is mutated to disrupt pairing to the miR-122 seed region, we observed a single shift in samples containing hAgo2:miR-122, indicating a binding event occurred (**Figure 2.4A**, **left side**). Using WT HCV RNA, two shifts were observed, indicating two binding events occurred on the RNA. Importantly, the fraction of the WT HCV RNA in the supershifted band increased as hAgo2-miR-122 concentrations were increased, demonstrating a dose-dependent response (**Figure 2.4A**, **right side**).

Equilibrium binding data using a broader range of hAgo2 concentrations (**Figure 2.4B** and **Supplementary Figure S2.7**) revealed a K_d of 63 pM for the complex with HCV S2p3,4,

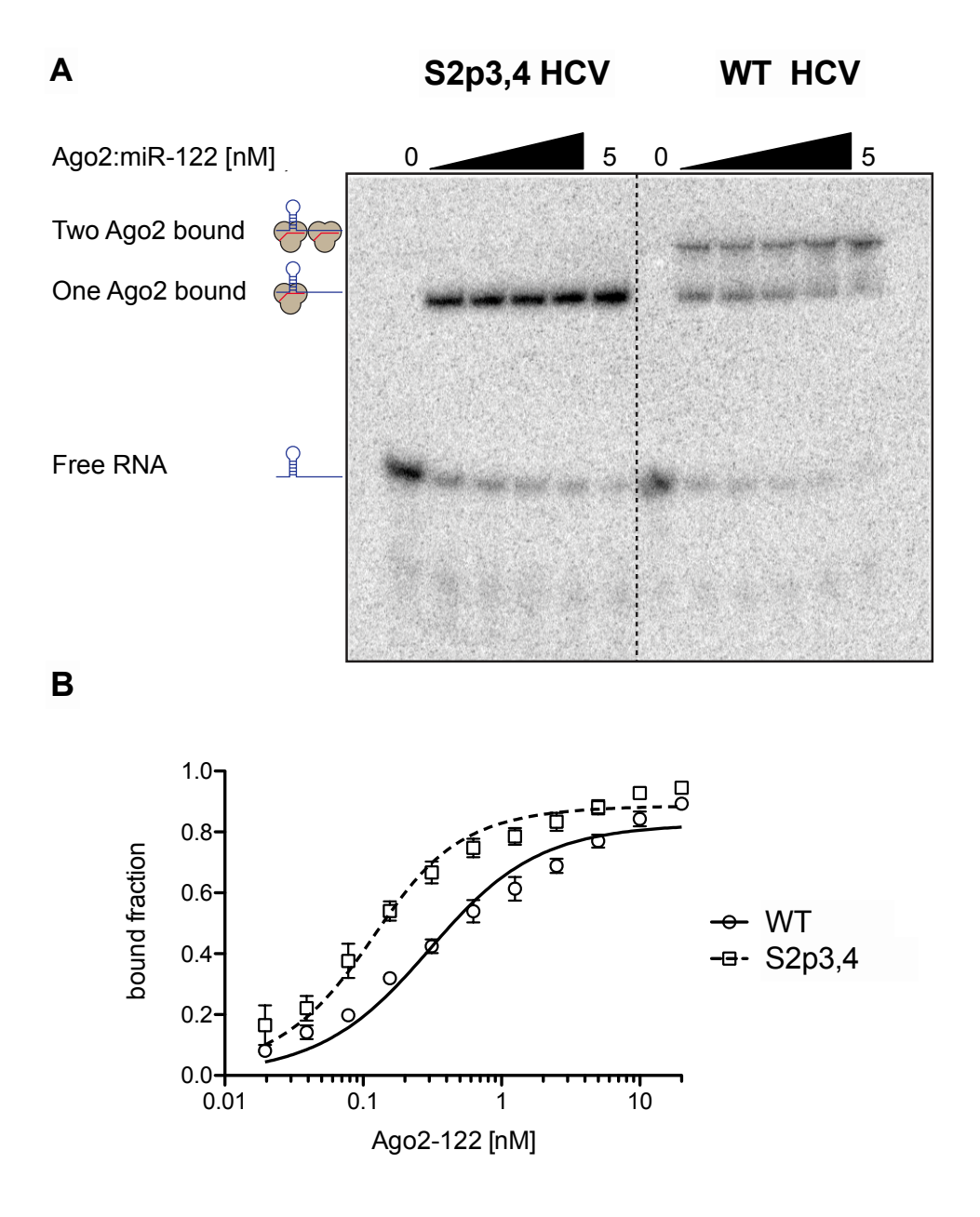
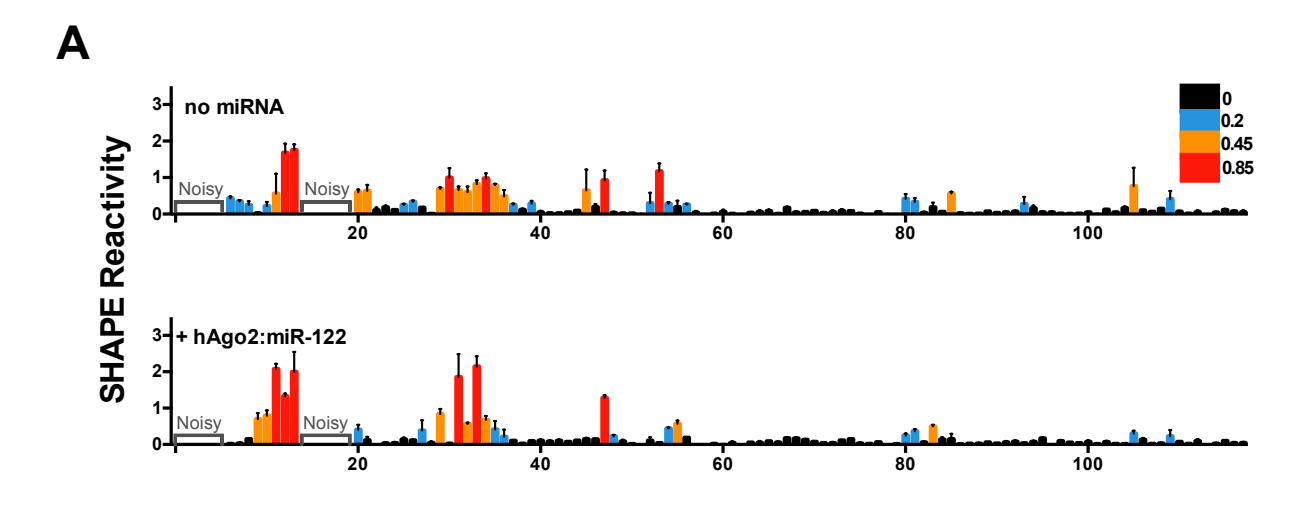


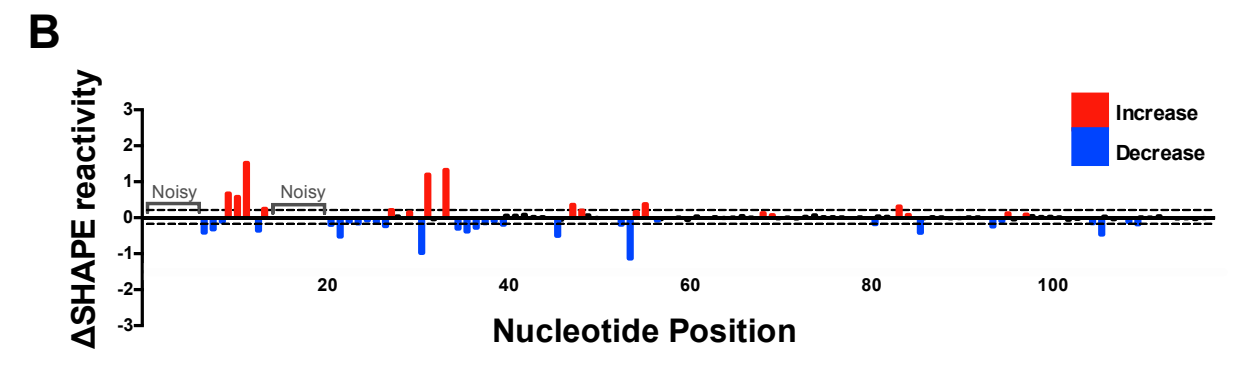
Figure 2.4. Two Ago2:miR-122 complexes can bind simultaneously to the 5' terminus of the HCV genome. (A) Recombinantly expressed hAgo2 loaded with miR-122 (final conentration: 0, 0.3125, 0.625, 1.25, 2.5, and 5 nM) was incubated with radiolabeled viral RNA comprising nts 1-42. Incubation with HCV S2p3,4 (left side) resulted in a single shift, whereas incubation with WT HCV RNA (right side) yielded an additional shift corresponding to the complex containing two hAgo2:miR-122 complexes. The depicted gel is one of five independent replicates. (B) Equilibrium binding data for Ago2:miR-122 and HCV WT and S2p3,4, based on gel shift assays (Supplementary Figure S7A). Data points are means of three replicates with standard error. The $K_d \pm$ SE for S2p3,4 is 63 \pm 10 pM, the K_d apparent for WT HCV is 250 \pm 31 pM.

and a K_d apparent of 250 pM for WT HCV. Under the assumption of independent binding, binding to Site 2 can be calculated by subtraction of the S2p3,4 data from the WT data (**Supplementary Figure S2.7B**). Fitting the calculated Site 2 data to the binding model yields a $K_d = 1.13$ nM, while previous experiments place the K_d for such a target in the low pM range for miR-122 (56). This discrepancy suggests that, although Site 1 and Site 2 can be simultaneously occupied by two Ago2:miR-122 complexes, the two binding events are negatively affected by each other in the system. This conclusion is in agreement with the increased SHAPE reactivity measured for the nucleotides spanning the 5' end of Site 1 and the 3' end of Site 2 on the HCV genome (**Supplementary Figure 2.3**).

hAgo2:miR-122 binding alters the secondary structure of the HCV 5' UTR.

To determine how hAgo2:miR-122 complex binding to the HCV 5' UTR alters the secondary structure of the viral RNA, we performed *in vitro* SHAPE analysis in the presence of purified hAgo2:miR-122 (**Figure 2.5** and **Supplementary Figures S2.3** and **S2.8**). When focusing on the 5' terminus of the HCV RNA (nts 1-42), we observed an overall increase in SHAPE reactivity at nts C27, C29, A31 and G33 in the presence of hAgo2:miR-122 (**Figure 2.5**). The increase in SHAPE reactivity at C27 was unexpected since this is the first nt of the seed region of miR-122 bound to Site 1; however, the increase in reactivity observed may be due to the close proximity of the two hAgo2:miR-122 complexes which could force this base-pair to become unpaired (particularly since the 5' end of the miR-122 molecule is anchored in the pocket of the Mid domain). The increase in SHAPE reactivity at C29 was observed with both miR-122 alone (**Figure 2.5**) and hAgo2:miR-122 (**Figure 2.5**), suggesting an alteration in the structure such that this nucleotide is more flexible, independently of the presence of hAgo2. Like C27, the significant increase in SHAPE reactivity at C31 in the presence of hAgo2:miR-122 suggests that the secondary structure of the viral RNA may be further altered in order to accommodate two





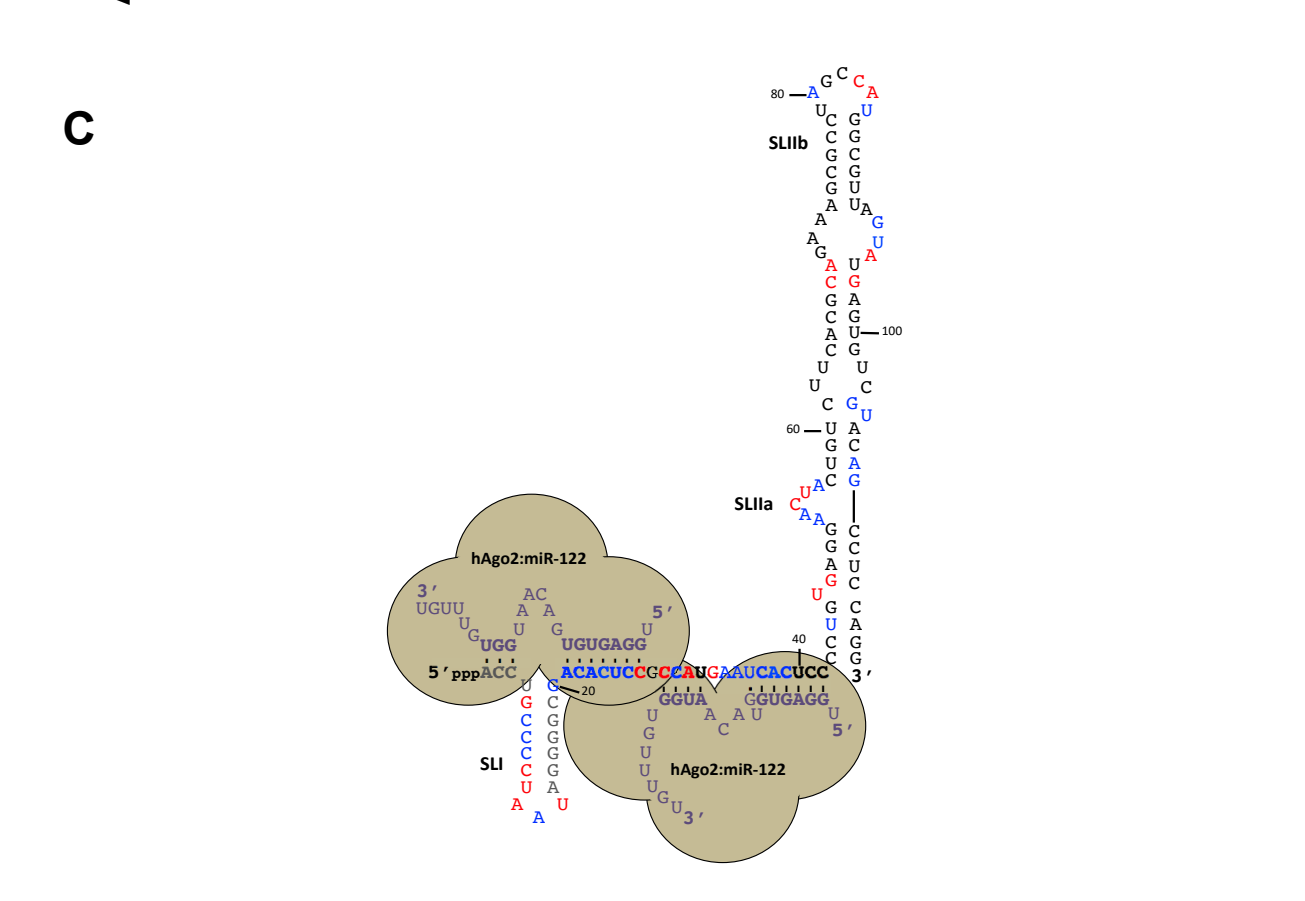


Figure 2.5. hAgo2:miR-122 complexes alter the secondary structure of the 5' terminus and SLII of the HCV genome. (A) Normalized SHAPE reactivities of 1-117 nt HCV RNA in the absence (top) or presence of hAgo2:miR-122 (bottom). Nucleotides 1-5 and 14-19 were omitted due to high background reactivity. (B) Difference plot showing changes in SHAPE reactivity upon miR-122 binding, ΔSHAPE = hAgo2:miR-122:HCV RNA reactivity – HCV RNA (no miRNA) reactivity. Significant increases in reactivity (above baseline, red) and decreases in reactivity (below baseline, blue) are indicated. (C) Changes in reactivity upon hAgo2:miR-122 binding are superimposed onto the hAgo2:miR-122:HCV RNA secondary structure model (coloured as in (B)). The data represents the results of four independent replicates and error bars represent the standard error of the mean (SEM).

hAgo2:miR-122 complexes simultaneously (**Figure 2.5**). We also observed a change in reactivity at G33 (in the bulge region of Site 2), which could suggest that it is further exposed in the presence of hAgo2:miR-122 due to lack of base pairing at this position. Similarly, we observed an increase in SHAPE reactivity in the loop region of SLI, which may be due to SLI being forced out of the hAgo2:miR-122 complex at Site 1. Beyond nts 1-42, we also observed changes in the SHAPE reactivity of SLII in the presence of hAgo2:miR-122, particularly in the bulge region of SLIIa (nts 52-58) as well as a few nucleotides on the 3' arm of SLII opposite SLIIa (104-109), which suggests further stabilization of this region (**Figure 2.5**).

To determine if hAgo2:miR-122 alters the structure of HCV RNA beyond SLII, we mapped SHAPE reactivities of the entire HCV 5' UTR (nts 1-371) in the presence of miR-122, hAgo2:miR-122, and controls (**Supplementary Figures S2.3 and S2.8**). *In vitro* SHAPE analysis of the HCV 5' UTR alone (nts 1-371) agreed well with previous models of SLIII and IV of the HCV IRES (**Supplementary Figure S2.8**) (2,3). Additionally, we found that in the presence of hAgo2:miR-122, a few nts in the apical loops SLIIIa-e displayed a modest but reproducible decrease in overall SHAPE reactivity. Moreover, we observed significant changes in SHAPE reactivity in several nts of SLIV, in close proximity to the pseudoknot and AUG start codon. Taken together, our data suggest that hAgo2:miR-122 binding results in alteration of the structure of the viral RNA at least *in vitro*, both at the 5' terminus (where the miR-122 seed and auxiliary binding sites are located), but also in the IRES region (SLII-IV), in a manner which may promote functional IRES activity.

Computational modeling of hAgo2:miR-122 and HCV RNA.

As we established that two hAgo2:miR-122 molecules were able to bind to the 5' terminus of the HCV genome (nts 1-42) simultaneously, we sought to model these interactions using the crystal structure of hAgo2. Of the $\sim 10^6$ possible complexes at each site from modeled hAgo2 and RNA

duplex conformations, we considered an increasing number of constructed complexes until sterically favorable conformations were found. Site 1 required ~150,000 complexes, whereas Site 2 needed only ~30,000 structures. The much greater number of considered complexes at Site 1 reflects the wider conformational search needed to fit a double-stranded RNA structure with a three-stem junction into a hAgo2 conformation; in contrast, the RNA structure at Site 2 has an unbranched conformation (see **Figure 2.6** displaying viable complexes at each site).

Computational modeling produced multiple RNA-induced silencing complex (RISC) structures at Site 1 and Site 2 that are free of steric clashes. Assembly of these structures generated viable RISC-RISC complexes where the 3' end duplex of miR-122 at Site 2 forms a solvent-exposed bridge between the adjacent RISC structures (Figure 2.6A). Modeling trials showed that only 3' duplexes protruding from the RNA-binding channel at Site 2 were capable of assembling into RISC-RISC complexes; straight duplex conformations generated collisions between the Mid and N-terminal domains of adjacent hAgo2 structures. This suggests that Site 2 duplex conformations are distorted in the internal loop region, resulting in the duplex protruding out of the hAgo2 RNA-binding channel (Figure 2.6A, lower panel). Alternatively, the auxiliary interactions with Site 2 of the HCV genome may become unpaired as the hAgo2:miR-122 at Site 2 adjusts to accommodate Site 1-bound hAgo2:miR-122. This latter hypothesis is further supported by our SHAPE data and the hAgo2:miR-122 gel shifts which suggest higher SHAPE reactivity in this region and a reduction in binding affinities when both Sites are occupied by hAgo2:miR-122, respectively.

Model RISC-RISC complexes exhibit conformational variability that is captured by their RNA conformations (**Figure 2.6B**). At Site 1, the SLI structure shows significant conformational flexibility. The Site 2 RNA has multiple orientations that are consistent with the RISC-RISC complex, implying that different Ago-Ago conformations are feasible. The adjacent hAgo2 structures display Mid/N-terminal and PAZ/L2 contacts. However, further

A

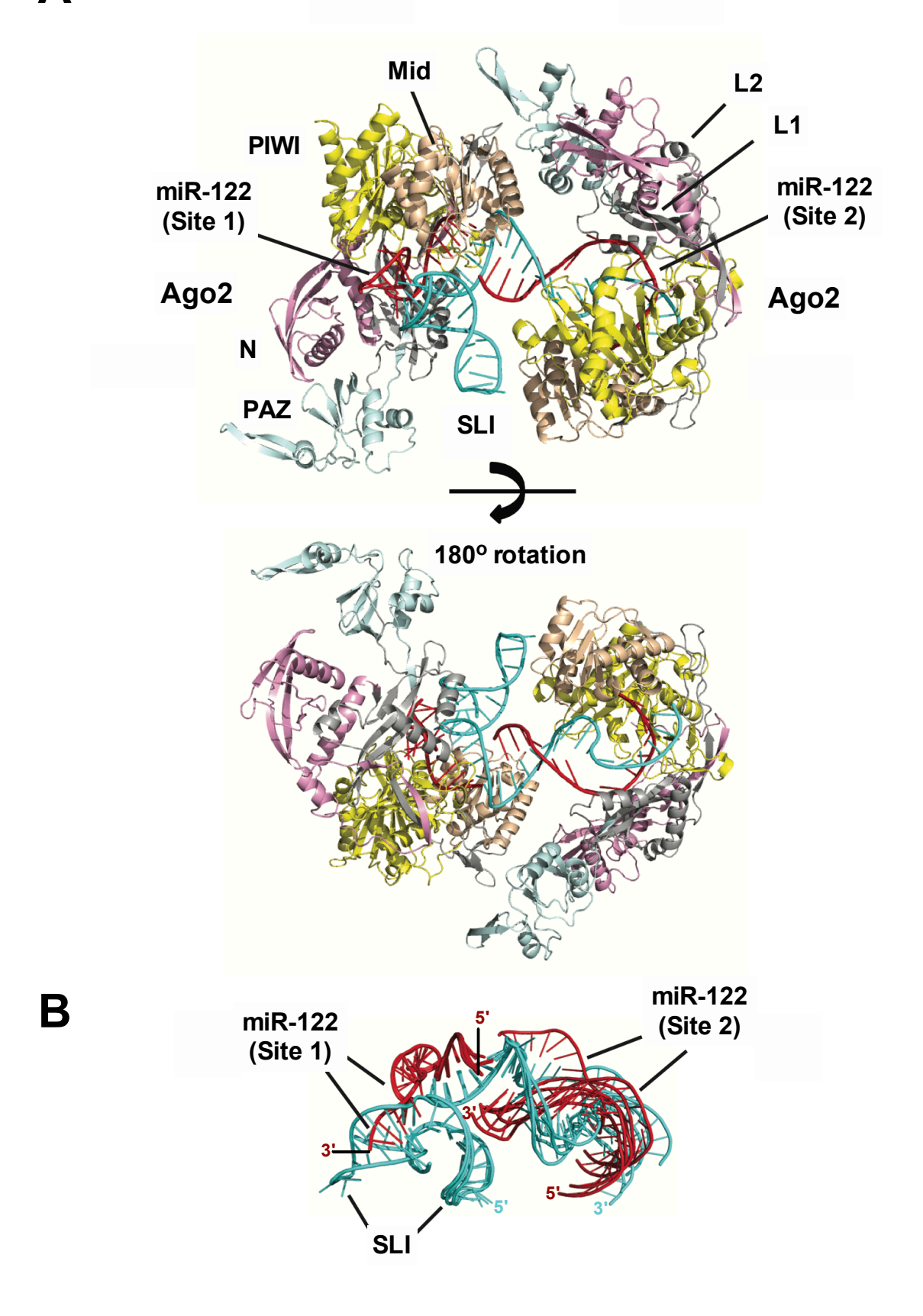


Figure 2.6. Model of hAgo2:miR-122:HCV RNA interactions at Sites 1 and 2. (A) A modeled RISC-RISC complex at Site 1 and Site 2 on the HCV genome and **(B)** miR-122:HCV RNA conformations of different complexes. **(A)** Two views of the RISC-RISC complex are shown: top structure shows the RNA-binding channel of Site 1 with the protruding SLI structure and the RNA bridge between the adjacent hAgo2 structures; bottom structure (180° rotated view) highlights the RNA conformation at Site 2 that enables simultaneous occupation of both hAgo2 binding sites. **(B)** Superimposed miR-122:HCV RNA conformations from six RISC-RISC complexes show conformational variability. In particular, SLI-3' stem structure in Site 1 has significant conformational flexibility; while the Site 2 RNA exhibits multiple orientations with respect to Site 1 RNA, indicating that the adjacent hAgo2 structures can adopt distinct conformations. The HCV RNA (cyan), miR-122 (red), and hAgo2 N terminal (pink), L1 (gray), PAZ (cyan), L2 (gray), Mid (wheat) and PIWI domain (yellow) are indicated.

computational/experimental analysis will be needed to determine whether a specific Ago-Ago conformation is favored.

To probe the RISC-RISC complex further, we examined the two RISC subunits separately. At Site 1, the shape of the predicted hAgo2 structure determined the allowed RNA conformations (Figure 2.6B). The dsRNA forms a 3-stem junction with a 7 base pair stem in the seed region (seed stem), a 7 base pair stem-loop (SLI), and a 3 base pair stem in the 3' end (3' stem). The seed stem is in an expected orientation for a recognized mRNA target. All allowed RNA structures show that the SLI-3' stem forms an L-shaped conformation, which adopts multiple orientations (Figure 2.6B) with respect to the hAgo2 structure. The source of the L-shaped structure's orientations is the miR-122's six unpaired bases (GACAAU) at the 3-stem junction. These bases also produce a sharp turn (nearly 90°) at the end of the seed stem to allow the L-shaped structure to protrude out of the RNA-binding channel; thus, avoiding steric clashes with hAgo2's PIWI and N-terminal domains. At Site 2, the assembled RISC structures show that the RNA can adopt straight and distorted duplex conformations. Duplex distortions occur at the internal loop just beyond the seed stem region, generating nonstandard RNA backbone conformations. The straight duplexes fit within the RNA-binding channel, whereas distorted duplexes protrude out of the RNA-binding channel. As noted above, only the distorted duplex conformations that protrude out of the RNA-binding channel are consistent with the overall RISC-RISC complex, which may lend support to the hypothesis that the auxiliary interactions with miR-122 at Site 2 may become unpaired when both sites are occupied by hAgo2:miR-122.

Computational modeling of RISC-IRES-40S complex.

The two RISC complexes form immediately upstream of SLII of the HCV IRES. Cryo-EM structures of IRES-40S show that SLII can adopt an active, bent conformation that maintains the 40S subunit in an open conformation to allow mRNA loading (57,58). An experimental

characterization of miR-122-HCV IRES interactions suggests that the RISC Ago proteins play a role in activation of HCV translation (5,59). To help further interpret Ago's role, we used structural modeling to characterize the RISC-IRES-40S interactions.

We assembled the RISC-IRES-40S complex by using the cryo-EM of the IRES-40S (PDB 5A2Q) and our modeled RISC-RISC structures (see Materials and Methods). We found many viable RISC-IRES-40S complexes with only slight differences in the orientation between the IRES-40S and RISC-RISC structures. The RISC-RISC structure is oriented away from the IRES-40S complex, and it only interacts with the IRES via the hAgo2 at Site 2 (Figure 2.7). Both singleand double-stranded regions of the IRES interact with Ago surfaces opposite the RNA-binding channel. The IRES-Ago interface is extremely tight fitting with a strong shape complementarity (Figure 2.7, right panels). Specifically, the Ago Mid and L2 domains interact with the backbone of the single-stranded IRES region (ACCC, nts 118-121) between SLII and III. An unstructured loop in the PIWI domain (residues 719-728, DKNERVGKSG; bold residues conserved among hAgo 1-3) interacts with the bulge nucleotides in SLIIa where SLII adopts a bent conformation. Interestingly, benzimidazole, an inhibitor of HCV IRES-driven translation initiation, binds to the same bulged IRES region to lock SLII in an extended, inactive conformation (PDB 3TZR) (60). Lastly, we found that the SLI structure does not interact with the IRES-40S complex, a result consistent with the experimental finding that deletion of SLI does not influence HCV IRESmediated translation (59).

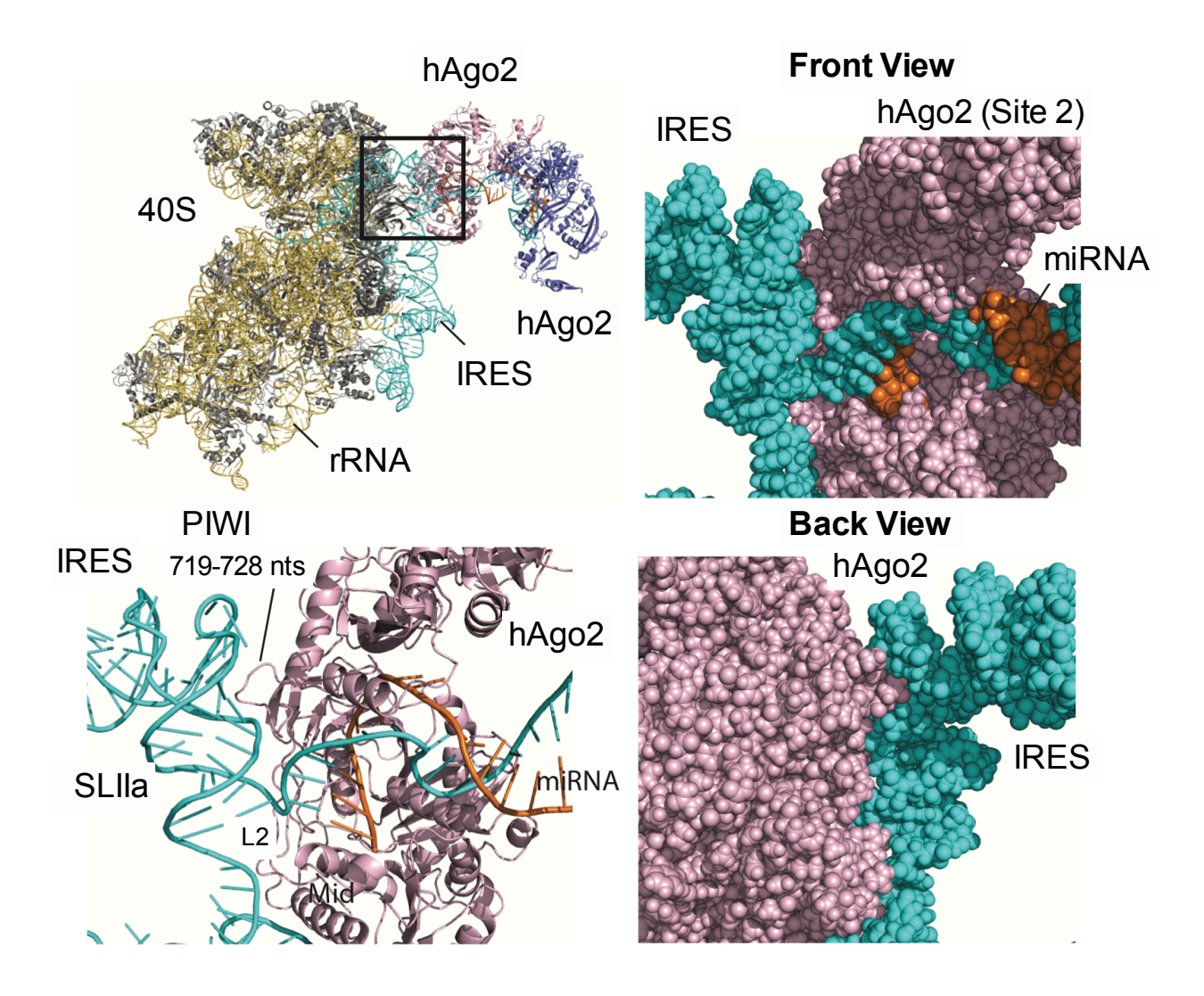


Figure 2.7. Model of RISC-HCV IRES-40S interactions. A modeled RISC-IRES-40S complex (top left panel) and detailed views of hAgo2:IRES interactions (other panels). Front and back views of the space-filling representation show a tight fit with shape complementarity between hAgo2 and IRES SLIIa (right panels). hAgo2 Mid, L2 and PIWI domains interact with single- and double-stranded regions of the HCV IRES SLIIa (bottom left). The IRES (cyan), ribosomal RNA (yellow), ribosomal proteins (gray), hAgo2s (pink and blue), and miR-122s (orange) are indicated.

2.6 Discussion

Two miR-122 molecules are able to bind to the HCV 5' UTR simultaneously in vitro.

Biophysical analysis of miR-122:HCV RNA interactions revealed a 2:1 stoichiometry in agreement with previous studies using Con1b (genotype 1b) (2). In the context of nts 1-42, we found that miR-122 binds to Site 1 with a stronger affinity than to Site 2; and miR-122 binding to Site 1 was observed to be more exothermic with a decreased entropy, when compared with Site 2. This effect could be due to different local conformational changes/rearrangements required for Site 1 to bind with miR-122, when compared with Site 2. Individual analysis of Sites 1 and 2 alone revealed that Site 1 (18.80 \pm 3.00 nM) has a higher overall binding affinity than Site 2 (228.34 \pm 65.41 nM); however, miR-122 binding to Site 2 was more exothermic and entropically favoured suggesting that in this isolated system, Site 2 binding to miR-122 brings the system to a lower energy ordered state (Table 2.1). This is in agreement with previous results with a J6/JFH-1 (genotype 2a) isolate (53); but is in contrast to studies with Con 1b (genotype 1b), where miR-122 binding to Site 2 had a stronger binding affinity than Site 1 (2). Although both ITC experiments were done similarly, it is possible that our results vary due to differences in the sequences between these two genotypes as well as the specific lengths used for binding experiments of the individual sites, since the tail of miR-122 bound to Site 2 would be predicted to have extended binding into the Site 1 seed region in the absence of Site 1-bound miR-122 (2). In contrast, when we performed ITC analyses using 1-117 nt HCV RNA, we observed that Site 2 had a much greater affinity than Site 1. This was confirmed using S2p5,6 which contains a mutation in the Site 2 seed region that resulted in a reduction in Site 2 binding but had no effect on Site 1. This is likely due to the more energetically favorable SLII^{alt} structure that the 1-117 nt HCV RNA is able to adopt. More specifically, in the SLII^{alt} conformation, Site 2 is predicted to be in a single-stranded and accessible loop region, while Site 1 is in a closed conformation. Thus, our biophysical analyses suggest that two miR-122 molecules are able to bind simultaneously to the HCV 5' terminus in vitro, with binding to Site 2 occurring with a higher affinity than Site 1 in the context of nts 1-117 of the HCV genome.

Binding of miR-122 to the HCV genome alters the structure of the 5' UTR.

In vitro SHAPE analysis in the presence of miR-122 revealed decreases in the overall SHAPE reactivity across the predicted miR-122 seed sequences, consistent with miR-122 interactions reducing the flexibility of the viral RNA in this region (2,3). Moreover, we observed an overall decrease in SHAPE reactivity at G33 and A34 of the HCV genome, which are not predicted to bind to miR-122, suggesting that miR-122 binding imparts rigidity to this region of the viral RNA. Furthermore, the decrease in SHAPE reactivity at U36 is consistent with formation of a G:U wobble pair between miR-122 and the viral RNA at this position, allowing us to further refine the model of miR-122:HCV RNA interactions at Site 2 (2-4). In addition to the seed regions, we also observed some subtle differences in the SHAPE reactivity in SLI, with an overall decrease in the stem and slight increase in the loop region. These changes in reactivity suggest that miR-122 binding may stabilize SLI. However, changes in reactivity of the loop region are not likely to have biological significance because the sequence identity of the loop is poorly conserved across HCV genotypes (22,61).

In agreement with recent studies that suggest that the HCV 5' UTR is able to adopt a more energetically favourable alternative (SLII^{alt}) structure (1,4), our SHAPE analyses support this model, whereby miR-122 binding results in a RNA chaperone-like switch in conformation to SLII, which would promote functional IRES formation by positioning the AUG start codon within the 40S ribosomal subunit for translation initiation (50,51). However, as our SHAPE data is an average of the structures that form in solution, and most of the loop regions in SLII^{alt} and SLII are overlapping, we could not definitively rule out formation of SLII and the functional IRES conformation in the absence of miR-122 for WT HCV RNA. However, this model is further

supported by our ITC analyses which suggest Site 2 has a greater binding affinity in the context of 1-117 nt WT HCV RNA. Thus, our data is consistent with formation of SLII^{alt} in the absence of miR-122, and miR-122 interactions promote functional folding of SLII at least *in vitro*.

G28A favours the canonical SLII structure.

The G28A mutation was first isolated from patients who had undergone therapy with a miR-122 antagonist and this mutation was subsequently demonstrated to reduce HCV's reliance on miR-122 in cell culture (21,26). As RNA structural predictions of the G28A mutant suggested that this mutation results in a reduced number of energetically favourable alternative structures and formation of the functional SLII structure with similar free energy to the SLIIalt structure, we sought to verify this using SHAPE analyses and ITC (1). Our SHAPE analysis indeed suggests that SLII is more preferentially formed by G28A when compared to WT HCV RNA, as reflected by higher SHAPE reactivities in the seed sequence of Site 1, which is in a more open (singlestranded) conformation in the SLII structure. Specifically, in several of the lowest free energy structures of WT HCV RNA, the G28 position is found in a G-C Watson-Crick pair and thus the G28A mutation would be predicted to disrupt formation of several of the predicted alternative structures. Moreover, nts 20-24 have a much higher SHAPE reactivity in G28A when compared with WT HCV RNA, suggesting that these nts are in a more open (single-stranded) conformation in the presence of the G28A mutation. This is further supported by our ITC analyses, which suggests a higher affinity for both sites when compared with WT HCV RNA. Taken together, this data suggests that the G28A mutation is able to more favourably form the SLII conformation, even in the absence of miR-122; but presumably, miR-122 is still required to protect the 5' terminus from pyrophosphatase activity and subsequent exonuclease-mediated decay by Xrn-1 and 2 (2,27-29). Interestingly, most HCV genotypes (1a, 1b, 3a, 4a, and 5a) already carry an A at position 28, which may indicate that these genotypes have a greater propensity to form SLII than the JFH-1

isolate used herein (14,15). This suggests that these HCV genotypes may be less reliant on miR-122 to form the SLII structure; although we cannot rule out the possibility that additional nt polymorphisms preclude formation of SLII. Notably, downstream of SLII, the WT and G28A HCV RNAs had similar SHAPE reactivities consistent with formation of SLIII-IV of the HCV IRES.

Two hAgo2:miR-122 complexes can bind to the 5' UTR simultaneously and their interactions with the 5' terminus further alter the structure of the 5' UTR.

Previous studies have suggested that HCV RNA accumulation requires miRNA biogenesis components, including Dicer, TRBP and the four Ago proteins (6,22,53-55,62,63). However, it is unclear whether Ago participates beyond miR-122 loading, as sequences in miR-122 dispensable for canonical silencing as well as downstream mediators of silencing do not appear to be required for miR-122's promotion of HCV RNA accumulation (22,64-66). Moreover, the two miR-122 sites in the 5' UTR are in very close proximity (separated by a single base) and hence, we were curious whether two hAgo2:miR-122 complexes were able to bind simultaneously to the 5' terminus of the HCV genome. To this end, we purified hAgo2 loaded with the miR-122 guide strand and performed gel shift assays. Indeed, we observed that two hAgo2:miR-122 complexes can bind to the 5' terminus of the HCV genome simultaneously, despite the close proximity of the miR-122 sites; however, the two binding events are negatively affected by one another. Previous studies have suggested that, at least for canonical RNA silencing, seed sites separated by 13-35 nt (from the seed start) may act synergistically (67). As the two miR-122 binding sites on the HCV genome are separated by 15 nt (from seed to seed), this may allow them to have a synergistic effect on HCV RNA accumulation. Alternatively, it is also possible that binding to one site (presumably Site 2) promotes changes to the conformation of the viral RNA that promote hAgo2:miR-122 interactions with the second site (Site 1). Moreover, we observed significant affinity enhancement

in the context of hAgo2:miR-122 (pM range) when compared with miR-122 alone (nM range). This is not altogether surprising since the hAgo protein holds the miRNA is a conformation that is conducive to target RNA binding. Additionally, it suggests that binding affinity predictions based solely on miRNA-RNA interactions may significantly underestimate binding affinity.

Our *in vitro* SHAPE analysis of the HCV RNA in the presence of hAgo2:miR-122 demonstrated that additional structural changes occur at the miR-122 recognition sites at the 5' terminus in the presence of hAgo2. Specifically, we observed higher overall SHAPE reactivities in the region predicted to form the Site 2 auxiliary interactions with nts 13-16 of Site 2-bound miR-122. This suggests that in order to accommodate both hAgo2:miR-122 complexes, these nts may become unpaired and are therefore available for acylation. Alternatively, since SHAPE reactivities represent an average of the HCV RNA conformations present in solution, the increase in reactivity at these sites could also be due to the contribution of viral RNA bound by hAgo2:miR-122 at one site and not the other, because of the differences in the availability and/or the affinity between the two recognition sites.

Our SHAPE analyses on the entire 5' UTR during miR-122 or hAgo2:miR-122 binding were very similar; however, we did observe some further changes in SHAPE reactivity when hAgo2:miR-122 was present. Specifically, we observed an overall decrease in SHAPE reactivity in nts 52-58 of SLIIa and nts 104-109 in the 3' arm of SLII that form base-pair interactions adjacent to SLIIa. Although this was unexpected, our computational prediction of the hAgo2:miR-122:HCV IRES complex suggest that the PIWI domain of hAgo2 at Site 2 may make contact with this region of the viral RNA, which could further stabilize this structure. This is not unprecedented as during Enterovirus 71 infection, Ago2 has been demonstrated to promote viral replication through interactions with the IRES region of the viral RNA, and hence this may point to a related mechanism during HCV infection (68). Interestingly, SLII was previously shown to fold independently of the IRES (50), and it acts as an initiator for HCV translation by taking on an L-

shaped conformation that interacts with the 40S subunit, holding the AUG start codon in the P-site of the ribosome until the translation machinery is properly assembled (4,17,51,52,69,70). Our SHAPE results support this model and suggest that hAgo2:miR-122 binding may not only promote translation through suppression of an alternative secondary structure (SLII^{alt}), but may further stabilize the SLII structure through additional contacts between hAgo2 bound to Site 2 and the viral IRES.

In addition to SLII, SLIIIa and d have been shown to make important contacts with the 40S ribosomal subunit, while SLIIIb-c makes contact with the eukaryotic translation initiation factor 3 (eIF3), to promote HCV RNA translation (17,71-73). We also observed some changes in SHAPE reactivity in the presence of hAgo2:miR-122 in SLIV at nts 337-345 and 350-371, where the 40S and 60S subunits bind (71). In further support of this finding, SHAPE analysis performed on the HCV IRES (nts 42-371) in the presence of the 40S ribosomal subunit demonstrated similar changes in reactivity to what we observed here in the presence of hAgo2:miR-122 (71). In both cases, an overall decrease in SHAPE reactivity was observed in the apical loops of SLIII, with a decrease in SHAPE reactivity directly upstream, and an increase in SHAPE reactivity at a few nts immediately downstream, of the start codon. This suggests that, beyond the 5' terminus (nts 1-42), miR-122 binding might promote a conformation of the HCV IRES that is similar to the ternary complex with eIF3 and the 40S ribosomal subunit. This is further supported by an Ago HITS-CLIP study during HCV infection which demonstrated miR-122-dependent HITS-CLIP reads in the IRES region (25). Thus, hAgo2:miR-122 interactions may alter the structure of the HCV 5' UTR that both promote formation of SLII (IRES folding) as well as additional structural changes in SLIII and IV that may promote association with the ribosome and eIF3. However, future work will be needed to confirm these findings in the context of viral replication.

Finally, we used computational prediction to model the 3D structure of the hAgo2:miR-122:HCV RNA ternary and higher-order complexes at the 5' terminus of the HCV genome.

Computational prediction of the ternary complex at Site 1 required sampling of approximately 5 times the conformations needed to model Site 2. This was expected as there is an unusually large stem-loop structure (SLI, nts 4-20) between the seed site (nts 2-8) and the 3' supplemental interactions (nts 15-17) with Site 1-bound miR-122 that can adopt numerous possible conformations. At Site 1, the dsRNA forms a 3-stem junction which is predicted to force nts 1-3 of the HCV genome into an L-shaped conformation to avoid steric clashes with hAgo2's PIWI and N terminal domains, while the seed region appears to take on an orientation expected for canonical mRNA targets. The Site 2 duplex can adopt either straight or distorted conformations, but only distorted conformations that protrude out of the RNA-binding channel, which are induced by the unpaired bases in the internal loop region, allow simultaneous hAgo2 occupation of the recognition sites. Multiple RISC-RISC structural conformations can be assembled, suggesting that the higherorder complex with adjacent hAgo2 structures likely exhibits some degree of conformational variability in addition to the flexibility of the SLI structure at Site 1. Specifically, the two hAgo2 structures are orientated differently to avoid steric clashes. Formation of the RISC-RISC complex forces adoption of a specific set of duplex conformations at Site 2, implying that hAgo2 occupation of Site 1 influences the RISC structure at Site 2. Interestingly, in this model the auxiliary interactions between the HCV RNA at Site 2 and miR-122 appears to protrude from hAgo2 (Figure 2.6A, lower panel). While this may be the case, it seems more likely that miR-122 is retained in the hAgo2-binding channel and that these auxiliary interactions with nts 13-16 of miR-122 at Site 2 become unpaired to accommodate Ago2:miR-122 binding to Site 1 (particularly since the end of the miRNA is likely to be tightly bound by the 3' nucleotide-binding pocket of the PAZ domain) (44). This is further supported by our biophysical analyses which suggest interference between the two sites, and our SHAPE data which indicates a higher SHAPE reactivity in this region in the presence of hAgo2:miR-122. Thus, it is possible that the auxiliary interactions between Site 2-bound miR-122 and nts 29-32 of the HCV genome are required for efficient initial

recruitment of hAgo2:miR-122 to the HCV genome, but that these interactions become unpaired in order to accommodate hAgo2:miR-122 interactions with Site 1.

Assembly of the larger RISC-IRES-40S complex demonstrates that the interface between the hAgo2 at Site 2 and the IRES SLIIa exhibits a tight fit with structural complementarity. Given that the RISC Ago may aid in miR-122-mediated activation of HCV translation (59,74), a plausible interpretation of our modeled complex is that Ago binding to SLIIa helps to stabilize the flexible IRES SLII in the active, bent conformation. These interactions may also help to stabilize the hAgo2:miR-122 complex at Site 2 after recruitment of Site 1, to accommodate both hAgo2:miR-122 complexes on the viral RNA. Moreover, the close proximity between Ago at Site 2 and the viral IRES may preclude interactions between Ago and the downstream RNA silencing machinery, which could help explain how the viral RNA is able to escape canonical RNA silencing. However, we note that the hAgo2 residues known to form contacts with GW182 appear to be accessible in our model (24,75). Thus, further experimental work will be needed to verify the details of these predicted RISC-RISC and RISC-IRES-40S conformations in live cells and to clarify how HCV escapes canonical RNA silencing.

miR-122 has at least three roles in the HCV life cycle.

Taken together, our biophysical, SHAPE and computational prediction analyses suggest a new model for hAgo2:miR-122 interactions with the HCV genome (**Figure 2.8**). Specifically, we predict that the HCV genome initially adopts an alternative conformation (SLII^{alt}) that allows recruitment of hAgo2:miR-122 to Site 2 of the 5' terminus. Binding to Site 2 acts in an RNA-chaperone like manner to convert the 5' terminus into SLII, allowing functional formation of the HCV IRES. This SLII conformation then allows recruitment of hAgo2:miR-122 to Site 1, which protects the 5' triphosphate moiety from pyrophosphatase activity and subsequent viral RNA decay

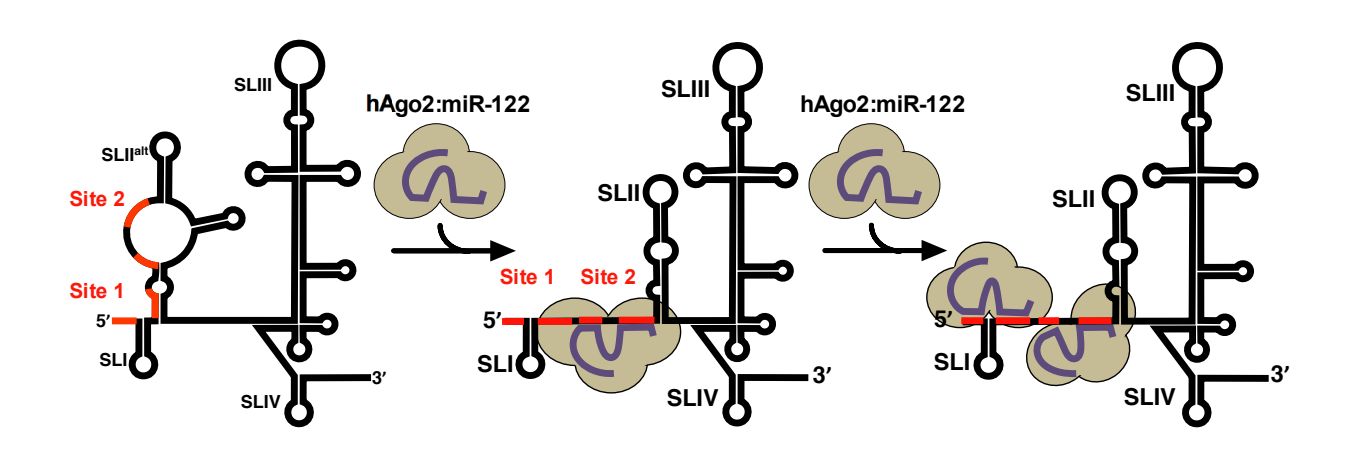


Figure 2.8. Model for Ago2:miR-122 interactions with the HCV 5' UTR. Schematic representation of Ago2:miR-122 binding to the HCV genome and the effects on the secondary structure of the viral RNA. The HCV 5' UTR initially takes on the most energetically favorable conformation (SLII^{alt}), which allows recruitment of hAgo2:miR-122 to Site 2 of the HCV genome (black). This results in a chaperone-like switch in conformation, resulting in formation of SLII, part of the HCV IRES (SLII-IV). This change in conformation allows recruitment of hAgo2:miR-122 to Site 1, which protects the 5' triphosphate moiety from pyrophosphatase activity and subsequent exonuclease-mediated decay. In order to accommodate hAgo2:miR-122 interactions at Site 1, the auxiliary interactions with Site 2-bound hAgo2:miR-122 are weakened; however, Site 2-bound hAgo2:miR-122 is further stabilized by interactions with the HCV IRES (in SLIIa and the region between SLII-III). The miR-122 seed and auxiliary binding sites on the HCV genome are indicated (red).

by Xrn-1 and 2 (2,27-29). In order to accommodate the hAgo2:miR-122 at Site 1, the auxiliary interactions between the 3' tail of the miR-122 molecule at Site 2 are likely destabilized, but the hAgo2:miR-122 complex at Site 2 is likely further stabilized by interactions with the HCV IRES. This model is consistent with our biophysical and SHAPE analyses as well as previous mutational analyses where mutation of nts 17-18 of the Site 2-bound miR-122 (predicted to reduce auxiliary interactions with the HCV genome between Sites 1 and 2) led to an approximately 1.5-fold increase in viral RNA accumulation (13). This model may also explain the sequence conservation and requirement for the auxiliary interactions with Site 2 (13), since they are likely required for the efficient initial recruitment of hAgo2:miR-122 to this site, even if they are weakened upon hAgo2:miR-122 binding to Site 1. In agreement with this, a recent study that used cooperativeimmunoprecipitation of Ago complexes in HCV-infected cells suggests that Site 1 has a higher affinity for Ago:miR-122 than Site 2 in live cells (53). Finally, the highly conserved spacing between the two miR-122 binding sites, which appears to result in interference between the two Ago proteins, is likely retained across HCV isolates because of the requirements for these sequences to form secondary structures (SL-I' and SL-IIz') in the 3' end of the negative-strand intermediate which constitutes the promoter for positive-strand viral RNA synthesis (76).

In conclusion, our results suggest that miR-122 is likely to play at least three roles in the HCV life cycle. First, the initial recruitment of hAgo2:miR-122 to Site 2 results in a chaperone-like switch in conformation which suppresses an alternative secondary structure (SLII^{alt}) and promotes SLII formation (1,4). Second, recruitment of hAgo2:miR-122 to Site 1 protects the 5' terminus from pyrophosphatase activity and subsequent exonuclease-mediated decay (22,27-29,54,77). And lastly, the hAgo2:miR-122 complex at Site 2 may further stabilize the HCV IRES through interactions between the PIWI and Mid domains of Ago and SLII of the HCV IRES to promote viral translation (59,74). This provides new insight into the role of miR-122 in the HCV

life cycle and future work will focus on clarifying this model in the context of infection and further dissecting the contribution of each of these miR-122 activities.

2.7 Acknowledgements

We would like to acknowledge Charlie Rice (University of Rockefeller) for providing Huh-7.5 cells and Rodney Russell (Memorial University) for providing JFH-1_T. We would also like to thank Julie Magnus (McGill University) for technical support, Veronique Sauvé (McGill University) for assistance with ITC analysis, Tamara Giguère and Jean-Pierre Perreault (University of Sherbrooke) for assistance with the SHAPE experiments and data analysis, and Zamboni Chem Solutions Inc. for assistance in synthesis of NAI-N₃. 3D modeling was done using High Performance Computing at NYU.

2.8 Authors contributions

JC and SMS conceptualized and designed the study. JC generated and analyzed the data with help from EC for ITC analysis. LFRG and IJM performed hAgo2 purification and generated and analyzed hAgo2:miR-122:HCV RNA gel shift assays. HHG and KG performed computational modeling, analysis and interpretation of the modeling results. JC and SMS drafted the manuscript and all authors contributed to editing the manuscript.

2.9 Funding

JC is supported by the Gerald Clavet Fellowship from McGill University. This work was supported by funds from McGill University as well as grants from the NSERC Discovery grant program [RGPIN-2014-05907] to SMS. IJM is supported by US National Institutes of Health grants R01-GM104475, R01-GM115649, and R35-GM127090. LFRG is supported by the Swiss National Science Foundation [Advanced Postdoc Mobility Fellowship P300PA_177860]. In addition, this research was undertaken, in part, thanks to funding from the Canada Research Chairs program.

2.10 Conflict of Interest

The authors declare that they have no conflict of interest.

2.11 References

- 1. Amador-Canizares, Y., Panigrahi, M., Huys, A., Kunden, R.D., Adams, H.M., Schinold, M.J. and Wilson, J.A. (2018) miR-122, small RNA annealing and sequence mutations alter the predicted structure of the Hepatitis C virus 5' UTR RNA to stabilize and promote viral RNA accumulation. *Nucleic Acids Res.*, **46**, 9776-9792.
- 2. Mortimer, S.A. and Doudna, J.A. (2013) Unconventional miR-122 binding stabilizes the HCV genome by forming a trimolecular RNA structure. *Nucleic Acids Res.*, **41**, 4230-4240.
- 3. Pang, P.S., Pham, E.A., Elazar, M., Patel, S.G., Eckart, M.R. and Glenn, J.S. (2012) Structural map of a microRNA-122: hepatitis C virus complex. *J. Virol.*, **86**, 1250-1254.
- 4. Schult, P., Roth, H., Adams, R.L., Mas, C., Imbert, L., Orlik, C., Ruggieri, A., Pyle, A.M. and Lohmann, V. (2018) microRNA-122 amplifies hepatitis C virus translation by shaping the structure of the internal ribosomal entry site. *Nat Commun.*, **9**, 2613-2613.
- 5. Conrad, K.D., Giering, F., Erfurth, C., Neumann, A., Fehr, C., Meister, G. and Niepmann, M. (2013) microRNA-122 Dependent Binding of Ago2 Protein to Hepatitis C Virus RNA Is Associated with Enhanced RNA Stability and Translation Stimulation. *PLoS One*, **8**, e56272
- 6. Wilson, J.A., Zhang, C., Huys, A. and Richardson, C.D. (2011) Human Ago2 Is Required for Efficient MicroRNA 122 Regulation of Hepatitis C Virus RNA Accumulation and Translation. *J. Virol.*, **85**, 2342-2350.
- 7. Hopcraft, S.E., Azarm, K.D., Israelow, B., Leveque, N., Schwarz, M.C., Hsu, T.H., Chambers, M.T., Sourisseau, M., Semler, B.L. and Evans, M.J. (2016) Viral Determinants of miR-122 Independent Hepatitis C Virus Replication. *mSphere*, 1, 1-12.
- 8. Israelow, B., Mullokandov, G., Agudo, J., Sourisseau, M., Bashir, A., Maldonado, A.Y., Dar, A.C., Brown, B.D. and Evans, M.J. (2015) Hepatitis C virus genetics affects miR-122 requirements and response to miR-122 inhibitors. *Nat Commun.*, **5**, 1-11.
- 9. Organization, W.H. (2017), pp. 1-83.
- 10. Hajarizadeh, B., Grebely, J. and Dore, G.J. (2013) Epidemiology and natural history of HCV infection. *Nat. Rev. Gastroenterol. Hepatol.*, **10**, 553-562.
- 11. Messina, J.P., Humphreys, I., Flaxman, A., Brown, A., Cooke, G.S., Pybus, O.G. and Barnes, E. (2015) Global distribution and prevalence of hepatitis C virus genotypes. *Hepatology*, **61**, 77-87.
- 12. Tice, J.A., Chahal, H.S. and Ollendorf, D.A. (2015) Comparative Clinical Effectiveness and Value of Novel Interferon-Free Combination Therapy for Hepatitis C Genotype 1: Summary of California Technology Assessment Forum Report. *JAMA Intern Med*, **175**, 1559-1560.
- 13. Wilson, J.A. and Sagan, S.M. (2014) Hepatitis C virus and human miR-122: Insights from the bench to the clinic. *Curr. Opin. Virol.*, 7, 11-18.
- 14. Tuplin, A., Struthers, M., Simmonds, P. and Evans, D.J. (2012) A twist in the tail: SHAPE mapping of long-range interactions and structural rearrangements of RNA elements involved in HCV replication. *Nucleic Acids Res.*, **40**, 6908-6921.
- 15. Sagan, S.M., Chahal, J. and Sarnow, P. (2015) cis-Acting RNA elements in the hepatitis C virus RNA genome. *Virus Res.*, **206**, 90-98.
- 16. Friebe, P., Lohmann, V., Krieger, N. and Bartenschlager, R. (2001) Sequences in the 5' nontranslated region of hepatitis C virus required for RNA replication. *J. Virol.*, **75**, 12047–12057.

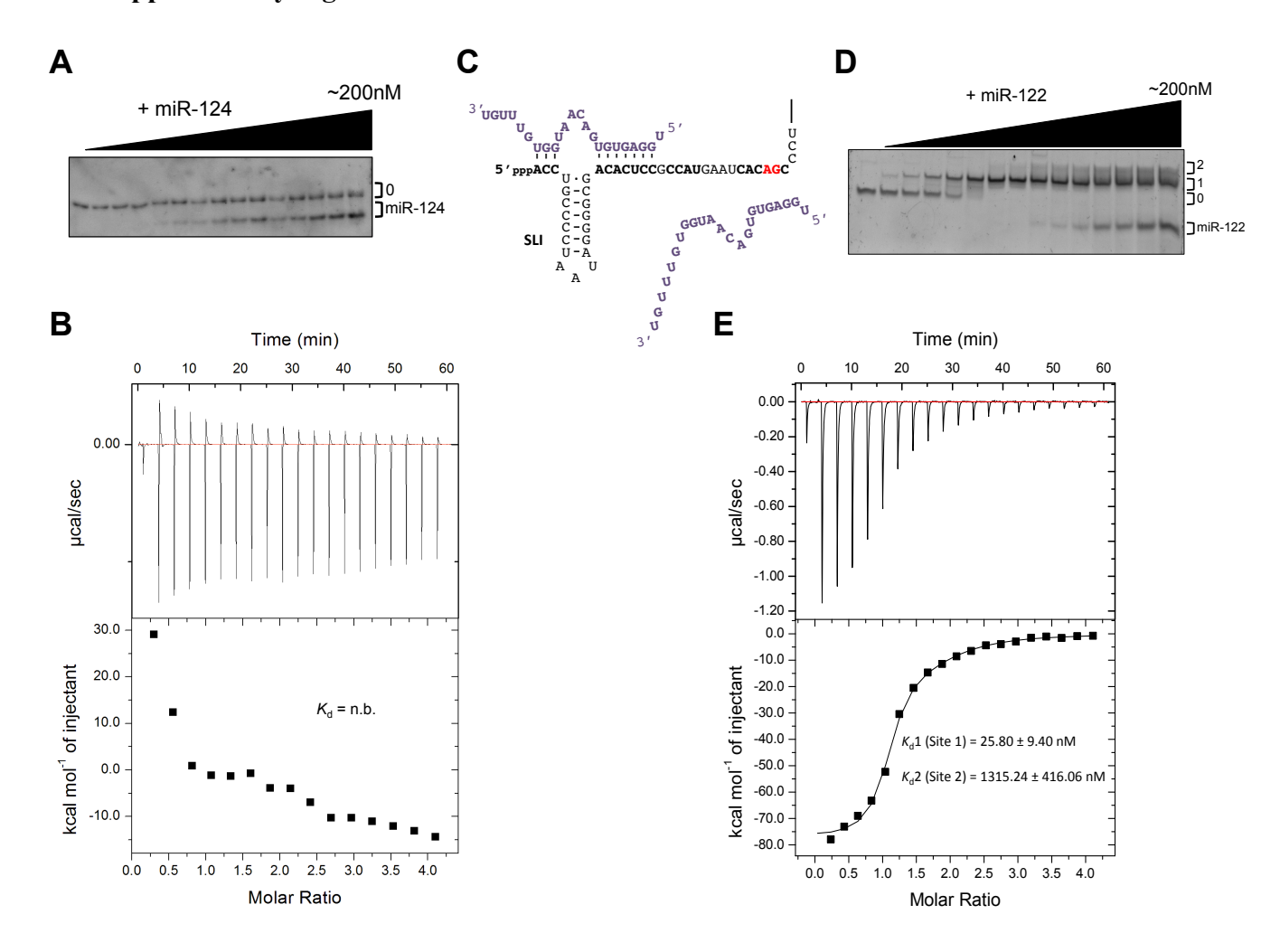
- 17. Khawaja, A., Vopalensky, V. and Pospisek, M. (2015) Understanding the potential of hepatitis C virus internal ribosome entry site domains to modulate translation initiation via their structure and function. *Wiley Interdisciplinary Reviews: RNA*, **6**, 211-224.
- 18. Tellinghuisen, T.L., Evans, M.J., von Hahn, T., You, S. and Rice, C.M. (2007) Studying Hepatitis C Virus: Making the Best of a Bad Virus. *J. Virol.*, **81**, 8853-8867.
- 19. Wang, C., Le, S.Y., Ali, N. and Siddiqui, A. (1995) An RNA pseudoknot is an essential structural element of the internal ribosome entry site located within the hepatitis C virus 5' noncoding region. *RNA*, **1**, 526-537.
- 20. Jopling, C.L. (2008) Regulation of hepatitis C virus by microRNA-122. *Biochem. Soc. Trans.*, **36**, 1220-1223.
- 21. Jopling, C.L., Yi, M., Lancaster, A.M., Lemon, S.M. and Sarnow, P. (2005) Modulation of Hepatitis C Virus RNA Abundance by a Liver-Specific MicroRNA. *Science*, **209**, 1577-1581.
- 22. Machlin, E.S., Sarnow, P. and Sagan, S.M. (2011) Masking the 5' terminal nucleotides of the hepatitis C virus genome by an unconventional microRNA-target RNA complex. *PNAS*, **108**, 3193-3198.
- 23. Chang, J., Nicolas, E., Marks, D., Sander, C., Lerro, A., Buendia, M.A., Xu, C., Mason, W.S., Moloshok, T., Bort, R. *et al.* (2004) miR-122, a mammalian liver-specific microRNA, is processed from hcr mRNA and may downregulate the high affinity cationic amino acid transporter CAT-1. *RNA Biol.*, **1**, 106-113.
- 24. Jopling, C.L., Schütz, S. and Sarnow, P. (2008) Position-Dependent Function for a Tandem MicroRNA miR-122-Binding Site Located in the Hepatitis C Virus RNA Genome. *Cell Host and Microbe*, **4**, 77-85.
- 25. Luna, J.M., Scheel, T.K.H., Danino, T., Shaw, K.S., Mele, A., Fak, J.J., Nishiuchi, E., Takacs, C.N., Catanese, M.T., De Jong, Y.P. *et al.* (2015) Hepatitis C virus RNA functionally sequesters miR-122. *Cell*, **160**, 1099-1110.
- Janssen, H.L.A., Reesink, H.W., Lawitz, E.J., Zeuzem, S., Rodriguez-Torres, M., Patel, K., van der Meer, A.J., Patick, A.K., Chen, A., Zhou, Y. et al. (2013) Treatment of HCV Infection by Targeting MicroRNA. N. Engl. J. Med., 368, 1685-1694.
- 27. Amador-Canizares, Y., Bernier, A., Wilson, J.A. and Sagan, S.M. (2018) miR-122 does not impact recognition of the HCV genome by innate sensors of RNA but rather protects the 5' end from the cellular pyrophosphatases, DOM3Z and DUSP11. *Nucleic Acids Res.*, **46**, 5139-5158.
- 28. Kincaid, R.P., Lam, V.L., Chirayil, R.P., Randall, G. and Sullivan, C.S. (2018) RNA triphosphatase DUSP11 enables exonuclease XRN-mediated restriction of hepatitis C virus. *PNAS*, **115**, 8197-8202.
- 29. Li, Y., Masaki, T., Yamane, D., McGivern, D.R. and Lemon, S.M. (2013) Competing and noncompeting activities of miR-122 and the 5' exonuclease Xrn1 in regulation of hepatitis C virus replication. *PNAS*, **110**, 1881-1886.
- 30. Ottosen, S., Parsley, T.B., Yang, L., Zeh, K., van Doorn, L.-J., van der Veer, E., Raney, A.K., Hodges, M.R. and Patick, A.K. (2015) In vitro antiviral activity and preclinical and clinical resistance profile of miravirsen, a novel anti-hepatitis C virus therapeutic targeting the human factor miR-122. *Antimicrob. Agents Chemother.*, **59**, 599-608.
- 31. Fricke, M., Dünnes, N., Zayas, M., Bartenschlager, R., Niepmann, M. and Marz, M. (2015) Conserved RNA secondary structures and long-range interactions in hepatitis C viruses. *RNA*, **21**, 1219-1232.
- 32. Jiao, X., Chang, J.H., Kilic, T., Tong, L. and Kiledjian, M. (2013) A mammalian premRNA 5' end capping quality control mechanism and an unexpected link of capping to pre-mRNA processing. *Mol. Cell*, **50**, 104-115.

- 33. Russell, R.S., Meunier, J.-C., Takikawa, S., Faulk, K., Engle, R.E., Bukh, J., Purcell, R.H. and Emerson, S.U. (2008) Advantages of a single-cycle production assay to study cell culture-adaptive mutations of hepatitis C virus. *Proc. Natl. Acad. Sci. U. S. A.*, **105**, 4370-4375.
- 34. Reuter, J.S. and Mathews, D.H. (2010) RNAstructure: software for RNA secondary structure prediction and analysis. *BMC Bioinformatics*, **11**, 129.
- 35. Darty, K., Denise, A. and Ponty, Y. (2009) VARNA: Interactive drawing and editing of the RNA secondary structure. *Bioinformatics*, **25**, 1974-1975.
- 36. Flynn, R.A., Zhang, Q.C., Spitale, R.C., Lee, B., Mumbach, M.R. and Chang, H.Y. (2016) Transcriptome-wide interrogation of RNA secondary structure in living cells with icSHAPE. *Nat. Protoc.*, **11**, 273-290.
- 37. Das, R., Laederach, A., Pearlman, S.M., Herschlag, D. and Altman, R.B. (2005) SAFA: semi-automated footprinting analysis software for high-throughput quantification of nucleic acid footprinting experiments. *RNA*, **11**, 344-354.
- 38. Laederach, A., Das, R., Vicens, Q., Pearlman, S.M., Brenowitz, M., Herschlag, D. and Altman, R.B. (2008) Semiautomated and rapid quantification of nucleic acid footprinting and structure mapping experiments. *Nat. Protoc.*, **3**, 1395-1401.
- 39. Rausch, J.W., Sztuba-Solinska, J., Lusvarghi, S. and Le Grice, S.F.J. (2016), *HIV Protocols* Vol. 1354, pp. 91-117.
- 40. Spitale, R.C., Crisalli, P., Flynn, R.A., Torre, E.A., Kool, E.T. and Chang, H.Y. (2013) RNA SHAPE analysis in living cells. *Nat. Chem. Biol.*, **9**, 18-20.
- 41. Karabiber, F., McGinnis, J.L., Favorov, O.V. and Weeks, K.M. (2013) QuShape: rapid, accurate, and best-practices quantification of nucleic acid probing information, resolved by capillary electrophoresis. *RNA*, **19**, 63-73.
- 42. Low, J.T. and Weeks, K.M. (2010) SHAPE-directed RNA secondary structure prediction. *Methods*, **52**, 150-158.
- 43. Wilkinson, K.A., Gorelick, R.J., Vasa, S.M., Guex, N., Rein, A., Mathews, D.H., Giddings, M.C. and Weeks, K.M. (2008) High-throughput SHAPE analysis reveals structures in HIV-1 genomic RNA strongly conserved across distinct biological states. *PLoS Biol.*, **6**, 883-899.
- 44. Schirle, N.T., Sheu-Gruttadauria, J. and MacRae, I.J. (2014) Structural basis for microRNA targeting. *Science*, **346**, 608-613.
- 45. Faehnle, C.R., Elkayam, E., Haase, A.D., Hannon, G.J. and Joshua-Tor, L. (2013) The making of a slicer: activation of human Argonaute-1. *Cell Rep*, **3**, 1901-1199.
- 46. Schirle, N.T. and MacRae, I.J. (2012) The crystal structure of human Argonaute2. *Science*, **336**, 1037-1040.
- 47. Gan, H.H. and Gunsalus, K.C. (2015) Assembly and analysis of eukaryotic Argonaute-RNA complexes in microRNA-target recognition. *Nucleic Acids Res.*, **43**, 9613-9625.
- 48. Parisien, M. and Major, F. (2008) The MC-Fold and MC-Sym pipeline infers RNA structure from sequence data. *Nature*, **452**, 51-55.
- 49. Flamand, M.N., Gan, H.H., Mayya, V.K., Gunsalus, K.C. and Duchaine, T.F. (2017) A non-canonical site reveals the cooperative mechanisms of microRNA-mediated silencing. *Nucleic Acids Res.*, **45**, 7212-7225.
- 50. Lukavsky, P.J., Kim, I., Otto, G.A. and Puglisi, J.D. (2003) Structure of HCV IRES domain II determined by NMR. *Nat. Struct. Biol.*, **10**, 1033-1038.
- 51. Lukavsky, P.J., Otto, G.A., Lancaster, A.M., Sarnow, P. and Puglisi, J.D. (2000) Structures of two RNA domains essential for hepatitis C virus internal ribosome entry site function. *Nat. Struct. Biol.*, 7, 1105-1110.

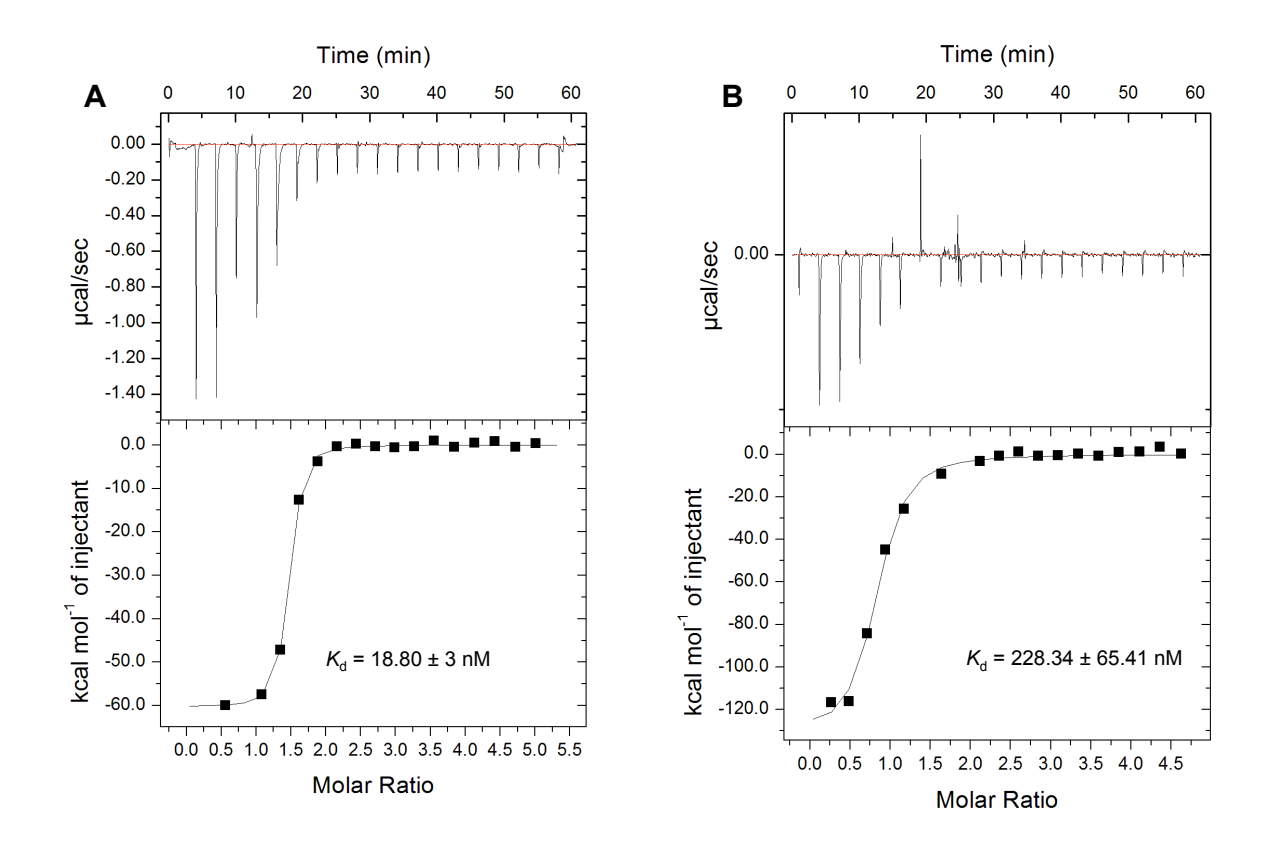
- 52. Odreman-Macchioli, F., Baralle, F.E. and Buratti, E. (2001) Mutational analysis of the different bulge regions of hepatitis C virus domain II and their influence on internal ribosome entry site translational ability. *J. Biol. Chem.*, **276**, 41648-41655.
- 53. Nieder-Röhrmann, A., Dünnes, N., Gerresheim, G.K., Shalamova, L.A., Herchenröther, A. and Niepmann, M. (2017) Cooperative enhancement of translation by two adjacent microRNA-122/argonaute 2 complexes binding to the 5' untranslated region of hepatitis C virus RNA. *J. Gen. Virol.*, **98**, 212-224.
- 54. Shimakami, T., Yamane, D., Jangra, R.K., Kempf, B.J., Spaniel, C., Barton, D.J. and Lemon, S.M. (2012) Stabilization of hepatitis C virus RNA by an Ago2-miR-122 complex. *PNAS*, **109**, 941-946.
- 55. Randall, G., Panis, M., Cooper, J.D., Tellinghuisen, T.L., Sukhodolets, K.E., Pfeffer, S., Landthaler, M., Landgraf, P., Kan, S., Lindenbach, B.D. *et al.* (2007) Cellular cofactors affecting hepatitis C virus infection and replication. *Proc. Natl. Acad. Sci. U. S. A.*, **104**, 12884-12889.
- 56. Sheu-Gruttadauria, J., Xiao, Y., Gebert, L.F.R. and MacRae, I.J. (2019) Beyond the seed: structural basis for supplementary microRNA targetting *EMBO J*.
- 57. Quade, N.B., Daniel; Leibundgut, Marc; van den Heuvel, Joop and Nenad Ban. (2015) Cryo-EM structure of Hepatitis C virus IRES bound to the human ribosome at 3.9-Å resolution. *Nat Commun.*, **6**.
- 58. Yamamoto, H., Collier, M., Loerke, J., Ismer, J., Schmidt, A., Hilal, T., Sprink, T., Yamamoto, K., Mielke, T., Burger, J. *et al.* (2015) Molecular architecture of the ribosome-bound Hepatitis C Virus internal ribosomal entry site RNA. *EMBO J.*, **34**, 3042-3058.
- 59. Roberts, A.P., Lewis, A.P. and Jopling, C.L. (2011) miR-122 activates hepatitis C virus translation by a specialized mechanism requiring particular RNA components. *Nucleic Acids Res.*, **39**, 7716-7729.
- 60. Dibrov, S.M., Parsons, J., Carnevali, M., Zhou, S., Rynearson, K.D., Ding, K., Garcia Sega, E., Brunn, N.D., Boerneke, M.A., Castaldi, M.P. *et al.* (2014) Hepatitis C virus translation inhibitors targeting the internal ribosomal entry site. *J. Med. Chem.*, **57**, 1694-1707.
- 61. Li, Y.P., Ramirez, S., Gottwein, J.M. and Bukh, J. (2011) Non-genotype-specific role of the hepatitis C virus 5' untranslated region in virus production and in inhibition by interferon. *Virology*, **421**, 222-234.
- 62. Masaki, T., Arend, K.C., Li, Y., Yamane, D., McGivern, D.R., Kato, T., Wakita, T., Moorman, N.J. and Lemon, S.M. (2015) MiR-122 stimulates hepatitis C virus RNA synthesis by altering the balance of viral RNAs engaged in replication versus translation. *Cell Host and Microbe*, 17, 217-228.
- 63. Zhang, C., Huys, A., Thibault, P.A. and Wilson, J.A. (2012) Requirements for human Dicer and TRBP in microRNA-122 regulation of HCV translation and RNA abundance. *Virology*, **433**, 479-488.
- 64. Berezhna, S.Y., Supekova, L., Sever, M.J., Schultz, P.G. and Deniz, A.A. (2011) Dual regulation of hepatitis C viral RNA by cellular RNAi requires partitioning of Ago2 to lipid droplets and P-bodies. *RNA*, **17**, 1831-1845.
- 65. Pager, C.T., Schutz, S., Abraham, T.M., Luo, G. and Sarnow, P. (2013) Modulation of hepatitis C virus RNA abundance and virus release by dispersion of processing bodies and enrichment of stress granules. *Virology*, **435**, 472-484.
- 66. Roberts, A.P., Doidge, R., Tarr, A.W. and Jopling, C.L. (2014) The P body protein LSm1 contributes to stimulation of hepatitis C virus translation, but not replication, by microRNA-122. *Nucleic Acids Res.*, **42**, 1257-1269.

- 67. Saetrom, P., Heale, B.S., Snove, O., Jr., Aagaard, L., Alluin, J. and Rossi, J.J. (2007) Distance constraints between microRNA target sites dictate efficacy and cooperativity. *Nucleic Acids Res.*, **35**, 2333-2342.
- 68. Lin, J.Y., Brewer, G. and Li, M.L. (2015) HuR and Ago2 Bind the Internal Ribosome Entry Site of Enterovirus 71 and Promote Virus Translation and Replication. *PLoS One*, **10**, e0140291.
- 69. Berry, K.E., Waghray, S., Mortimer, S.A., Bai, Y. and Doudna, J.A. (2011) Crystal structure of the HCV IRES central domain reveals strategy for start-codon positioning. *Structure*, **19**, 1456-1466.
- 70. Lyons, a.J., Lytle, J.R., Gomez, J. and Robertson, H.D. (2001) Hepatitis C virus internal ribosome entry site RNA contains a tertiary structural element in a functional domain of stem-loop II. *Nucleic Acids Res.*, **29**, 2535-2541.
- 71. Filbin, M.E. and Kieft, J.S. (2011) HCV IRES domain IIb affects the configuration of coding RNA in the 40S subunit's decoding groove. *RNA*, **17**, 1258-1273.
- 72. Kieft, J.S., Zhou, K., Grech, A., Jubin, R. and Doudna, J.A. (2002) Crystal structure of an RNA tertiary domain essential to HCV IRES-mediated translation initiation. *Nat. Struct. Biol.*, **9**, 370-374.
- 73. Kieft, J.S., Zhou, K., Jubin, R. and Doudna, J.A. (2001) Mechanism of ribosome recruitment by hepatitis C IRES RNA. *RNA*, 7, 194-206.
- 74. Henke, J.I., Goergen, D., Zheng, J., Song, Y., Schüttler, C.G., Fehr, C., Jünemann, C. and Niepmann, M. (2008) microRNA-122 stimulates translation of hepatitis C virus RNA. *EMBO J.*, **27**, 3300-3310.
- 75. Elkayam, E., Faehnle, C.R., Morales, M., Sun, J., Li, H. and Joshua-Tor, L. (2017) Multivalent Recruitment of Human Argonaute by GW182. *Mol. Cell*, **67**, 646-658 e643.
- 76. Friebe, P. and Bartenschlager, R. (2009) Role of RNA structures in genome terminal sequences of the hepatitis C virus for replication and assembly. *J. Virol.*, **83**, 11989-11995.
- 77. Thibault, P.A., Huys, A., Amador-Cañizares, Y., Gailius, J.E., Pinel, D.E. and Wilson, J.A. (2015) Regulation of hepatitis C virus genome replication by Xrn1 and microRNA-122 binding to individual sites in the 5' untranslated region. *J. Virol.*, **89**, 6294-6311.

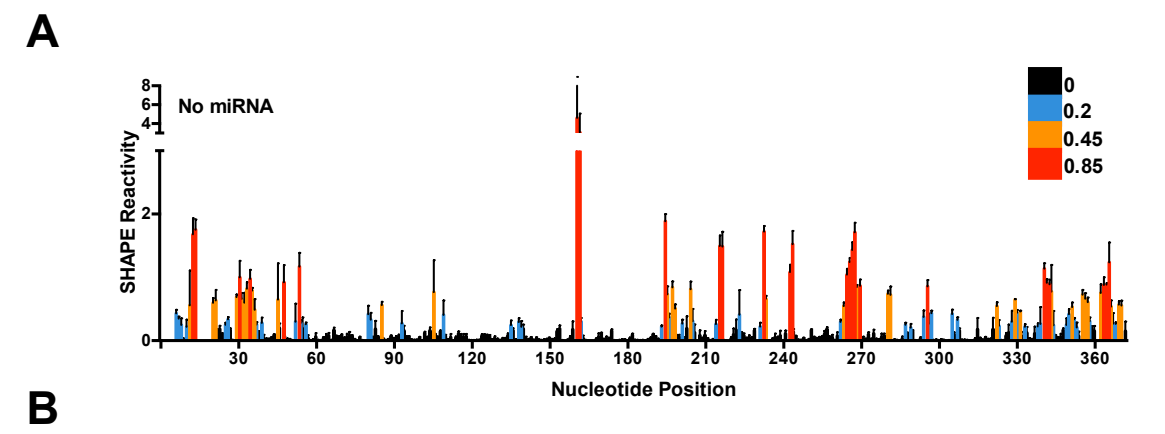
2.12 Supplementary Figures

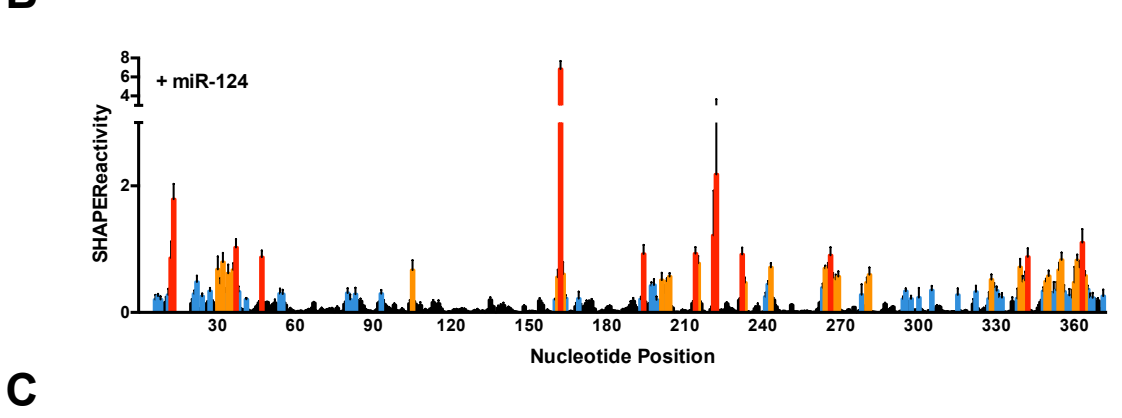


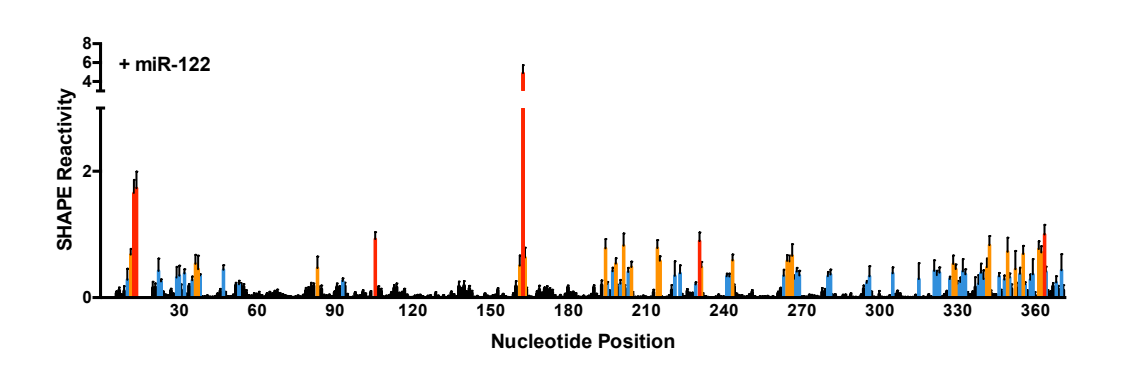
Supplementary Figure S2.1. miR-124 does not interact with the HCV 5' terminus and miR-122 binds with higher affinity to Site 1 in 1-42 nt HCV RNA. (A) Non-denaturing gel electrophoresis mobility shit assay (EMSA) of 1-42 nt HCV RNA and increasing amounts of miR-124. (B) Thermogram and resulting binding curve of the titration of 1-42 nt HCV RNA with native miR-124. n.b. = no binding. (C) Model of the interaction of miR-122 (purple) and the 1-42 nt of the HCV Site 2p3,4 mutant (black), containing mutations in positions 3 and 4 of the miR-122 seed sequence of Site 2 (red). (D) Non- denaturing gel electrophoresis mobility shit assay (EMSA) of 1-42 nt HCV Site 2p3,4 RNA and increasing amounts of miR-122. (E) Thermogram and resulting binding curve of the titration of 1-42 nt HCV Site2p3,4 with miR-122. Affinities of each binding Site (K_d 1, Site 1 and K_d 2, Site 2) are indicated. All data are representative of at least three independent replicates and K_d values are an average of three measurements (\pm) error propagated from individual fits.

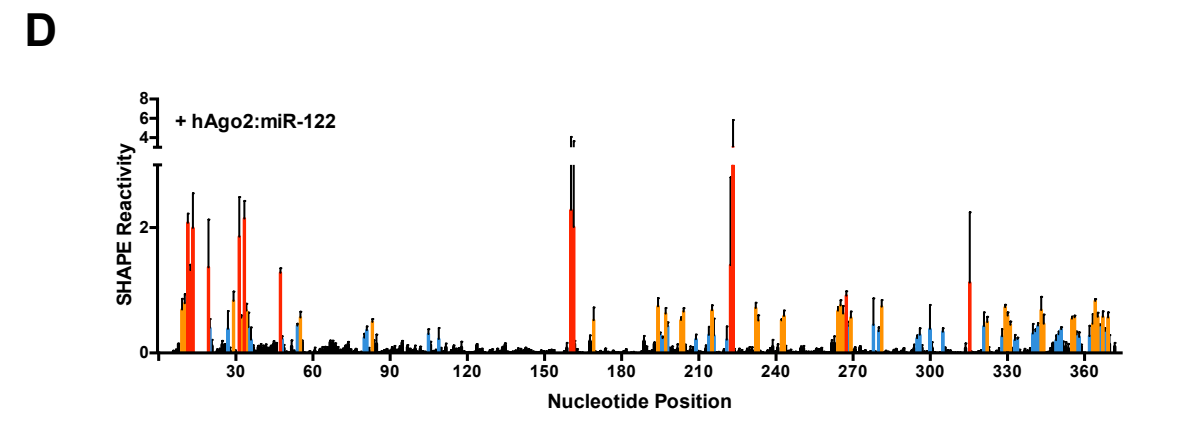


Supplementary Figure S2. 2. miR-122 interactions with Site 1 and Site 2 of the HCV RNA. Isothermal titration calorimetry (ITC) thermograms and resulting binding curve of the titration of (A) Site 1 (nts 1-27) and (B) Site 2 (nts 29-42) of the HCV RNA with miR-122. All data are representative of at least three independent replicates and K_d values are an average of three measurements (\pm) error propagated from individual fits.

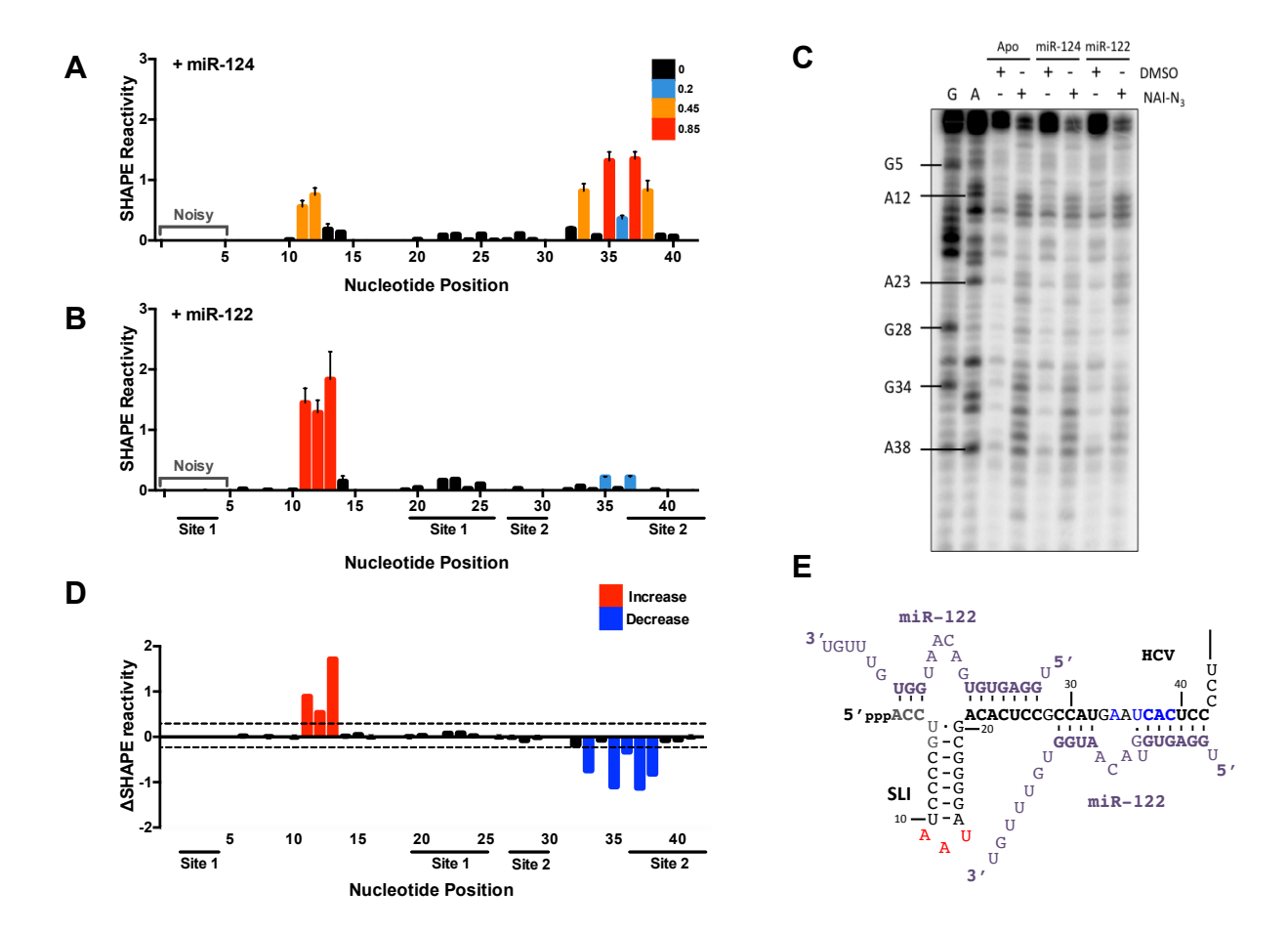




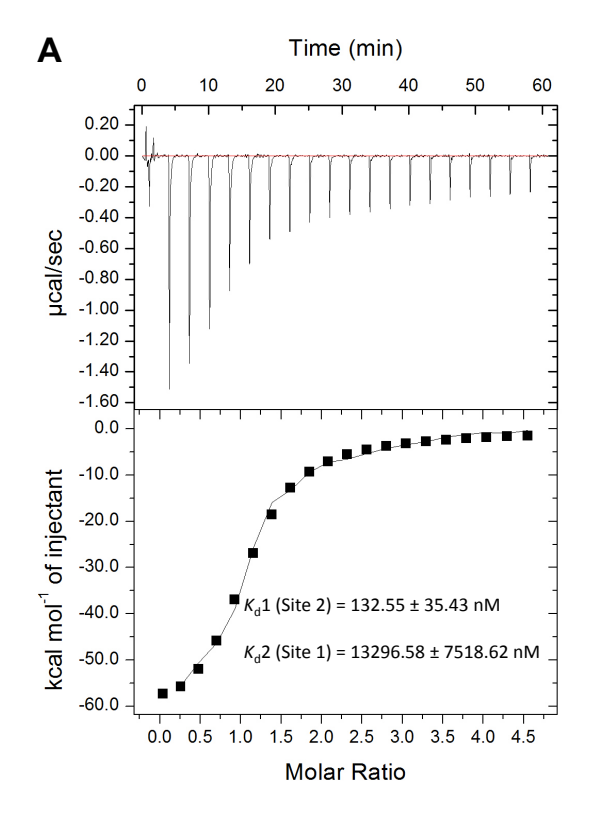


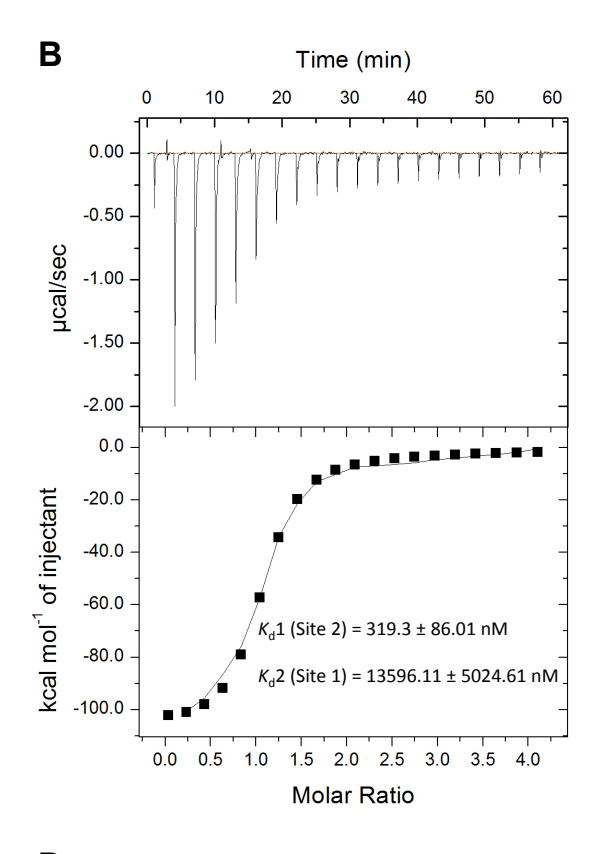


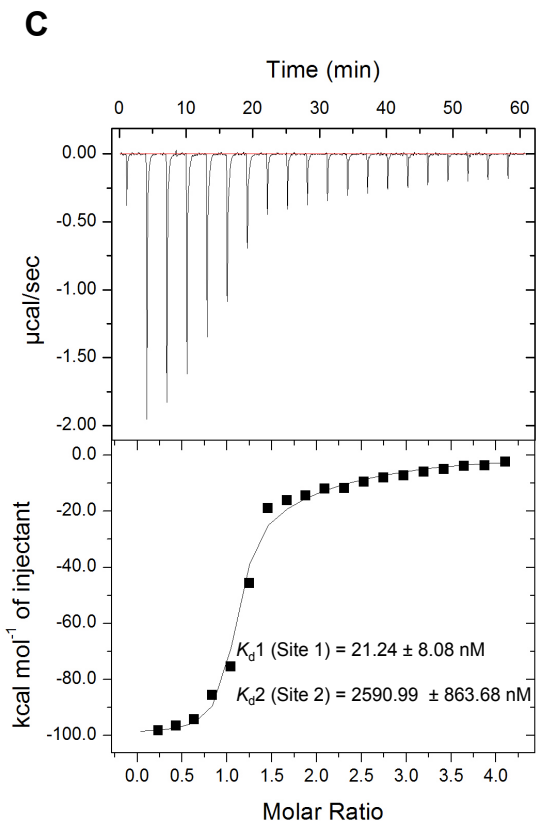
Supplementary Figure S2.3. miR-122 interactions with Site 1 and Site 2 of the HCV RNA. Normalized SHAPE reactivities of nts 1-371 of the HCV RNA with (A) no miRNA, (B) miR-124, (C) miR-122, and (D) hAgo2:miR-122. Nucleotides 1-5 and 14-19 were omitted due to high background reactivity. Nucleotides with high (≥ 0.85 , red), intermediate (between 0.4 and 0.85, orange), low (between 0.2 and 0.4, blue) and very low (≤ 0.2 , black) SHAPE reactivity are indicated. The data represents the results of at least four independent replicates and error bars represent the standard error of the mean (SEM).

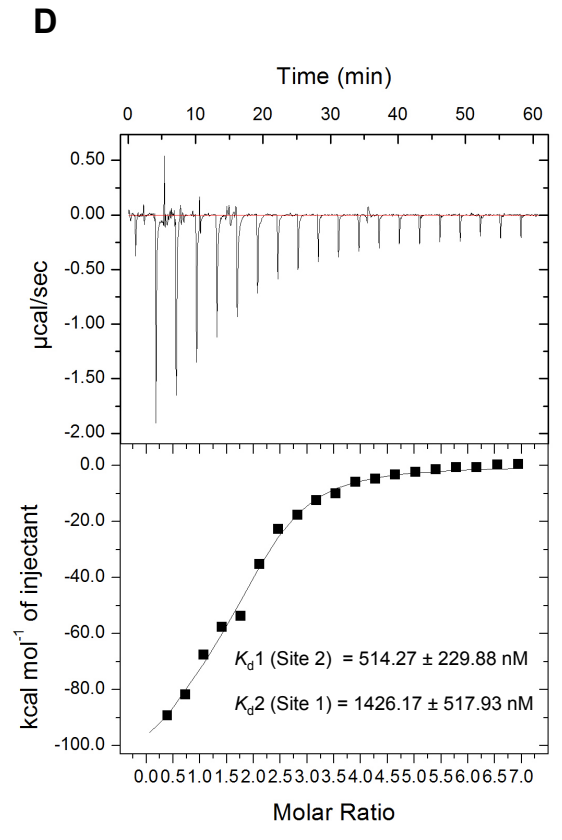


Supplementary Figure S2.4. *In vitro* SHAPE analysis of HCV RNA by gel electrophoresis. (A) Normalized SHAPE reactivity of 1-42 nt HCV RNA with miR-122 and (B) miR-124 (control). Nucleotides 1-5 were omitted due to high background reactivity. Nucleotides with high (≥ 0.85 , red), intermediate (between 0.4 and 0.85, orange), low (between 0.2 and 0.4, blue) and very low (≤ 0.2 , black) SHAPE reactivity are indicated. (C) Representative SHAPE analysis by gel electrophoresis of HCV RNA with miR-122 and miR-124 (control) (D) Graph showing the changes in SHAPE reactivity upon miR-122 binding, Δ SHAPE = miR-122 reactivity – miR-124 reactivity. Significant increases (above baseline, red) and decreases in reactivity (below baseline, blue) are indicated. (E) Changes in reactivity upon miR-122 binding are shown on the miR-122: HCV RNA secondary structure model, coloured as in (D). Data is representative of at three independent replicates and error bars represent the standard error of the mean (SEM).









Supplementary Figure S2. 5. miR-122 interactions with WT, S2p5,6, G28A 1-117 nt and WT 1-371 nt HCV RNA. Isothermal titration calorimetry (ITC) thermograms and resulting binding curve of the titration of miR-122 with 1-117 nt (A) WT, (B) Site 2 p5,6, and (C) G28A HCV RNA as well as with (D) 1-371 WT HCV RNA. All data are representative of at least three independent replicates and K_d values are an average of three measurements (\pm) error propagated from individual fits.

CHAPTER 3: Analysis of resistance-associated variants to a microRNA-based therapy reveals three distinct mechanisms of action based on alterations in RNA structure

Jasmin Chahal and Selena M. Sagan

3.1 Preface

As discussed in *Chapter 1*, two miR-122-based inhibitors have been developed and tested in chronic HCV-infected patients. Sequence analyses post-treatment have revealed a few isolated resistance-associated variants (RAVs) in both cell culture and in miR-122 inhibitor treated patients. However, the mechanism(s) of action of these RAVs is unclear. In this study, we aimed to investigate the mechanism(s) of resistance and how these mutations allow HCV to overcome its reliance on miR-122. Our results suggest three distinct mechanisms of resistance among the RAVs, all based on alterations to the structure of the viral RNA.

This chapter is adapted from the manuscript entitled: Analysis of resistance-associated variants to microRNA-based therapy reveals three distinct mechanisms of action based on alterations in RNA structure, by **Jasmin Chahal** and Selena M. Sagan, currently in preparation for publication.

3.2 Abstract

Hepatitis C virus (HCV) is a positive-sense RNA virus that interacts with the liver-specific microRNA, miR-122. MiR-122, in complex with an Argonaute (Ago) protein, binds to two sites in the 5' untranslated region (UTR) of the HCV genome and this interaction plays three important roles in the HCV life cycle. Firstly, the Ago:miR-122 complex acts as an RNA chaperone or riboswitch to suppress a more energetically favorable secondary structure that allows the viral internal ribosomal entry site (IRES) to form. Secondly, the Ago:miR-122 interactions at Site 1 promote genome stability by base-pairing with the 5' terminus and protecting the genome from cellular pyrophosphatases and subsequent exoribonuclease activity. And finally, through

translation. Due to the reliance of HCV on miR-122 for efficient viral RNA accumulation, antisense miR-122 inhibitors were developed for the treatment of chronic HCV infection. However, both in cell culture and in human patients, miR-122 resistance-associated variants (RAV) arose that allowed viral RNA accumulation when miR-122 was limiting. We hypothesized that these RAVs take on alternative RNA secondary structures that can negate the requirement for one of more of miR-122's activities. Herein, we compared viral RNA accumulation of RAVs in cell culture and performed *in vitro* Selective-2' Hydroxyl Acylation analyzed by Primer Extension (SHAPE) analysis to determine the mechanisms of action of the RAVs. We demonstrate that RAVs to miR-122-based therapies have three distinct mechanisms of action, all based on changes to the structure of the viral RNA. Furthermore, our data suggests that these RAVs allow viral RNA accumulation when miR-122 is limiting, by fulfilling one or more of miR-122's roles in the HCV life cycle. These findings provide insight into novel mechanisms of resistance to antiviral therapy, but also provide insight into potential mechanisms of resistance to miRNA-based therapies more broadly as this new class of therapeutics increasingly enters into the clinic.

3.3 Introduction

Hepatitis C virus (HCV) virus infects approximately 71 million people worldwide, with the majority of patients developing a persistent infection, which can lead to chronic hepatitis, cirrhosis, and hepatocellular carcinoma (1-3). HCV is a positive-sense single-stranded RNA virus of ~9.6 kb that encodes a single open reading frame, flanked by highly structured 5' and 3' untranslated regions (UTRs) (3,4). As a positive-sense RNA virus, the viral genome itself serves as a template for translation, replication, and packaging (4). Both the 5' and 3' UTRs contain *cis*-acting RNA elements that play key roles in the viral life cycle, including an internal ribosomal entry site (IRES) that drives translation in the 5' UTR (4-6). More specifically, stem loops (SL) II-IV make up the

viral IRES required for viral translation, while SL structures in both the 5' and 3' UTRs are required for viral RNA synthesis (4,7-10). In addition, the 5' terminus of the viral genome interacts with an abundant, liver-specific human microRNA (miRNA), called miR-122 (11-14).

miR-122 is highly expressed in the liver where it constitutes ~70% of liver miRNAs with ~66,000 copies per hepatocyte (11,15). Although miRNAs typically interact with the 3' UTRs of their target mRNAs to downregulate gene expression, miR-122 binds to two sites on the 5' UTR (Site 1 and Site 2) of the HCV genome and this interaction *promotes* viral RNA accumulation (11,12,14). Recent studies have provided a new model for miR-122:HCV RNA interactions that suggest that miR-122 plays at least three roles in the HCV life cycle (Figure 3.1) (16-19). Firstly, the HCV 5' UTR is thought to adopt the most energetically favorable conformation (termed SLII^{alt}), which results in the initial recruitment of an Ago:miR-122 complex to Site 2 of the HCV genome. This results in an RNA chaperone-like switch in conformation, akin to a bacterial riboswitch, resulting in formation of SLII, and allowing the viral IRES (SLI-IV) to form (17-19). Secondly, this change in conformation allows recruitment of Ago:miR-122 to Site 1, which protects the 5' terminus from pyrophosphatase activity and subsequent exoribonuclease-mediated decay (14,16,20-22). Finally, the Ago protein bound to Site 2 makes direct contact with the viral IRES, promoting HCV IRES-mediated translation (18).

Due to the importance of miR-122 in the HCV life cycle, two miR-122 inhibitors (antisense oligonucleotides), considered the flagship miRNA-based drugs, have been developed and used to treat chronic HCV infection in the clinic (23,24). Both MiravirsenTM (Santaris Pharma, a/s) and RG-101 (Regulus Therapeutics) miR-122 inhibitors have completed Phase II or Ib clinical trials, respectively, to investigate their clinical efficacy in chronic HCV infection (23,24). Excitingly, both treatments led to dose-dependent and sustained reductions in viral loads; and, in the latter study, two patients achieved sustained virological response (at least up to 76 weeks post-treatment)

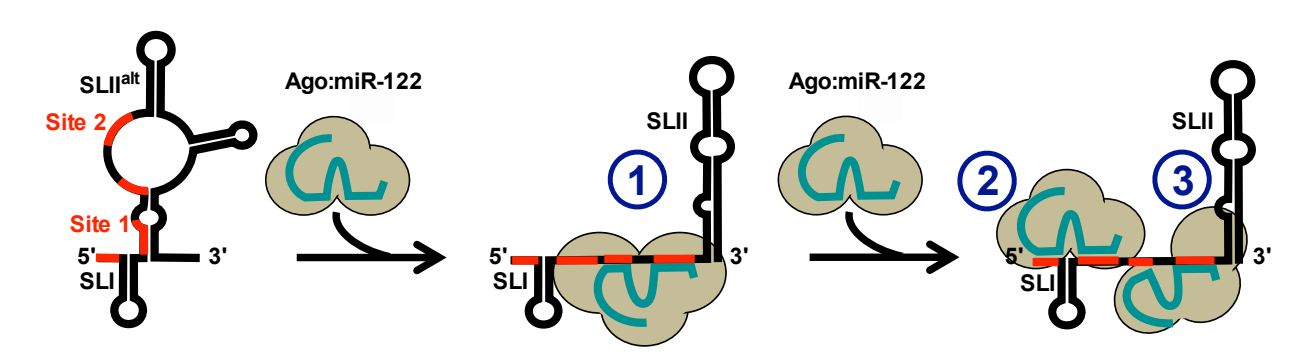


Figure 3.1. Model of miR-122 interactions with the HCV genome. The HCV genomic RNA is thought to enter the cell in an energetically stable conformation termed SLII^{alt}. Recruitment of the first Ago:miR-122 molecule serves as an RNA chaperone to re-fold the RNA into the functional, SLII conformation, which allows the viral IRES (SLII-LV) to form (1). Subsequent recruitment of a second Ago:miR-122 molecule to Site 1 promotes genome stability by protecting the 5' terminus from cellular pyrophosphatases and exoribonuclease-mediated decay (2). In order to accommodate the Ago:miR-122 complex at Site 1, the Ago:miR-122 complex at Site 2 releases its auxiliary interactions, but is likely stabilized by interactions between the Ago protein and SLII of the HCV IRES (3). Collectively, these interactions promote HCV IRES-mediated translation.

after receiving a single-dose of RG-101 (24). Neither treatment was associated with significant adverse events or long-term safety issues, suggesting that antisense targeting of miR-122 may be an effective treatment that could be used in future combination therapies. Interestingly, while no resistance was apparent during treatment, when viral RNA rebounded after the cessation of the inhibitor, several resistance associated variants (RAVs) were identified in the 5' UTR of the HCV genome (24). Together with recent cell culture-based studies, several miR-122 RAVs have been identified, including C2GC3U, C3U, U4C, G28A and C37U (Figure 3.2A) (24-26). Previous work suggests that the G28A mutation is 'riboswitched' and promotes formation of the functional SLII structure even in the absence of miR-122 (18,19). Similar to G28A, we hypothesized that the other RAVs also alter the structure of the viral RNA in a manner that negates the requirement for one or more miR-122 activities. Thus, we sought to provide insight into the mechanism(s) of action of the RAVs using RNA structure analysis and assays for viral RNA accumulation and decay. Our analyses suggest that each of the RAVs alter the structure of the viral RNA and that they can be categorized into three distinct classes based on three unique mechanisms of action.

3.4 Materials and Methods

Cell culture

The cell line Huh-7.5 (27) was kindly provided by C. M. Rice and miR-122 knockout (KO) Huh-7.5 cells were kindly provided by M. Evans (25). Both Huh-7.5 and miR-122 KO cells were maintained in Dulbecco's minimal essential medium (DMEM) supplemented with 10% fetal bovine serum (FBS), 1% nonessential amino acids, and 200 µM L-glutamate (Wisent Inc, Montreal, Canada).

Plasmids and Viral RNAs

The plasmid containing the full-length JFH-1_T isolate (Japanese Fulminant Hepatitis-1 isolate, genotype 2a), with three cell-culture adapted mutations, was provided by Rodney Russell, Memorial University (28). Plasmids pJ6/JFH-1 FL Rluc WT and GNN bear full-length HCV sequences that consist of structural proteins from the J6 isolate and the non-structural proteins from JFH-1 isolate, and a *Renilla* luciferase (RLuc) reporter (29). The 'GNN' mutant contains the indicated inactivating mutations in the viral polymerase GDD motif. The S1:p3 (C26A), S2:p3 (C41A), as well as the RAVs (C2GC3U, C3U, U4C, G28A and C37U) were generated by overlapping PCR, and subcloned using the *EcoR1* and *Kpn1* restriction sites on the pJ6/JFH-1 WT and GNN plasmids.

To make full-length viral RNAs, all plasmid templates were linearized and *in vitro* transcribed as previously described (16). To generate capped Firefly luciferase (30) mRNA, the Luciferase T7 Control DNA plasmid (Promega) was linearized using *XmnI* and *in vitro* transcribed using the mMessage mMachine T7 Kit (Life Technologies) according to the manufacturer's instructions.

For *in vitro* SHAPE analyses, the 5' UTR (nucleotides 1-371) of the HCV genome was *in vitro* transcribed using the T7 RiboMAX Express kit (Promega), followed by gel purification as previously described (18). For negative-strand RNA analysis, we synthesized a geneblock (IDT) containing a T7 promoter, nucleotides 1-151 of the 3' terminus of the WT JFH-1 negative-strand HCV RNA (5' to 3'), immediately followed by a 67 nucleotide deletion variant of the hepatitis delta virus ribozyme (HDVr) (31), all flanked by *EcoRI* and *BamHI* restriction sites. This geneblock was subcloned into pUC18 using *EcoRI* and *BamHI*, and the RAVs were generated using the QuikChange II XL Site-Directed Mutagenesis Kit (Agilent Technologies) according to the manufacturer's instructions. After linearization with *BamHI*, *in vitro* transcription reactions were carried out as described above. Negative-strand RNA transcripts were generated after self-

cleavage by the HDVr concurrently with the transcription reaction (31), and subsequently negative-strand RNAs with precise 3' termini (151 nucleotides in length) were gel purified.

For Xrn-1 exoribonuclease activity assays, nucleotides 1-42 of the WT HCV RNA (5'-ACC UGC CCC UAA UAG GGG CGA CAC UCC GCC AUG AAU CAC UCC-3') as well as each of the RAVs (C2GC3U: 5'-AGU UGC CCC UAA UAG GGG CGA CAC UCC GCC AUG AAU CAC UCC-3'; C3U: 5'-ACU UGC CCC UAA UAG GGG CGA CAC UCC GCC AUG AAU CAC UCC-3'; U4C: 5'-ACC CGC CCC UAA UAG GGG CGA CAC UCC GCC AUG AAU CAC UCC-3'; G28A: 5'-ACC UGC CCC UAA UAG GGG CGA CAC UCC ACC AUG AAU CAC UCC-3'; and C37U: 5'-ACC UGC CCC UAA UAG GGG CGA CAC UCC GCC AUG AAU UAC UCC-3'; were synthesized by IDT.

MicroRNAs

WT miR-122 (guide strand): 5'-UGG AGU GUG ACA AUG GUG UUU GU-3', miR-122* (passenger strand): 5'-AAA CGC CAU UAU CAC ACU AAA UA-3', miR-122 p3U: 5'-UGU AGU GUG ACA AUG GUG UUU GU-3', miR-122 p3U*: 5'-AAA CGC CAU UAU CAC ACU CAA UA-3', and miR-124 (guide strand): 5'- UAA GGC ACG CGG UGA AUG CC-3'), were all synthesized by IDT.

Electroporations

Electroporations were carried out as previously described (16,32). Briefly, 1.5 x 10^7 cells in 400 μ L of cold sterile PBS (Wisent) were co-electroporated with 10 μ g of WT, GNN and RAV full-length HCV RLuc RNAs, 2 μ g of capped FLuc mRNA, and in some cases, 60 pmol of duplexed miR-122 p3U. Cells were electroporated using 4 mm cuvettes at infinite resistance, 270 V and 950 μ F, optimized for the BioRad GenePulser XCell (BioRad; Mississauga, ON, Canada). Cells were

resuspended in 4.5 mL of media and 500 µL per timepoint were plated in 12-well or 6-well plates for luciferase assays at 2 h to 7 days post-electroporation.

Luciferase assays

Cells were washed with cold sterile PBS (Wisent) and harvested in 100 µL 1X Passive Lysis buffer (Promega). The Dual Luciferase Assay Reporter Kit (Promega) was used for all samples analyzed for both *Renilla* and Firefly luciferase activity according to the manufacturer's protocol. Firefly luciferase was used to ensure similar electroporation efficiency across samples.

In vitro SHAPE analysis and capillary electrophoresis

In vitro SHAPE analysis was performed as previously described (18). For positive-strand RNA analysis, 1 pmol of 6-FAM- or NED-labeled oligonucleotides (5'-6-FAM/NED-CGC CCG GGA ACT TAA CGT CTT-3') were used for the SHAPE samples and the sequencing ladders, respectively. For negative-strand RNA intermediate analysis, 1 pmol of 6-FAM- or NED-labeled oligonucleotides (5'-6-FAM/NED-ACC TGC CCC TAA TAG GGG CGA C -3') were used for the SHAPE samples and the sequencing ladders, respectively. Capillary electrophoresis was performed at Plateforme d'Analyses Génomiques de l'Univeristé Laval on an ABI 3100 Genetic Analyzer. Raw fluorescence data was analyzed using the QuSHAPE software as previously described (18,33).

RNA structure prediction

RNA structure predictions were carried out using the RNAstructure software, available from the Matthews Lab at https://rna.urmc.rochester.edu/index.html (34). Briefly, the RNA sequence was

loaded into the RNA structure software using the "Fold RNA Single Strand" command as previously described (18,34).

In vitro Xrn-1 assay

One hundred picomoles of monophosphorylated 1-42 nucleotide WT and RAV HCV RNAs were end-labeled using T4 RNA ligase and [γ-³²P] ATP and purified using an RNA Clean & Concentrator-5 spin column (Zymo Research). Two pmol of end-labeled RNA was refolded by denaturing at 95°C for 3 min followed by incubation at 37°C for 10 min. For experiments with miRNAs, 4 pmol of miR-122 or miR-124 (control) were added and the RNAs were incubated for an additional 20 min at 37°C following the refolding step. Xrn-1 assays were carried out using 1 unit of Terminator 5'-Phosphate-Dependent Exonuclease in 1X Terminator Reaction Buffer A (Lucigen) and 1 unit of Ribolock (Life Technologies). The reactions were incubated at 30°C and were quenched with 1 μL of 100 mM EDTA after incubation for 1 – 60 min. At the indicated time points, 10 μL of Gel Loading dye (Life Technologies) was added to each sample and 5 μL of each sample was resolved on a 15% denaturing polyacrylamide gel (29:1 acrylamide:bis-acrylamide, 1X TBE), dried at 80°C for 1.5 h (BioRad Gel dryer, Model 583), and visualized by phosphorimager (Storm, GE Life Sciences). Image analysis was performed using the ImageJ software.

3.5 Results

RAVs do not have a fitness advantage in the presence of miR-122 but are able to accumulate under conditions where miR-122 is absent or limiting.

Each of the HCV RAVs were isolated under conditions where miR-122 was absent and/or limiting in cell culture or in miR-122 inhibitor-treated patients (24-26,35). Thus, we first sought to assess

their ability to accumulate in cell culture in comparison to wild-type (WT) HCV RNA (Figure 3.2). First, we assessed viral RNA accumulation in miR-122 replete conditions in wild-type Huh-7.5 cells (Figure 3.2B). Our results suggest that in the presence of miR-122, WT HCV RNA has a fitness advantage and accumulates to the greatest extent, while GNN (the replication-defective viral RNA) is quickly decayed. WT was closely followed by the C3U and U4C, with the G28A and C37U RAVs accumulating to a lesser extent, with approximately 37.2- and 13.8-fold reductions in viral RNA accumulation at Day 2 post-electroporation compared to WT (Figure 3.2B). The C2GC3U RAV accumulated to a lesser extent, with a 1166.5-fold reduction in luciferase activity, although this was still significantly above background. Thus, under miR-122 replete conditions, WT HCV RNA has a fitness advantage compared with the RAVs.

Next, we asked whether we could detect viral RNA accumulation of any of the RAVs in the absence of miR-122, using miR-122 KO Huh-7.5 cells (Figure 3.2C). In this case, both WT and the majority of the RAVs were quickly degraded and were below the limit of detection, similar to GNN, with the exception of the U4C RAV (Figure 3.2C). Interestingly, U4C was the only RAV able to accumulate in miR-122 KO cells, albeit at levels approximately 1000-fold lower than WT HCV RNA in Huh-7.5 cells (Figure 3.2C). However, it is possible that the other RAVs are able to accumulate, but to levels that are below the level of detection in this assay. Nonetheless, these results suggest that only U4C has a distinct fitness advantage in viral RNA accumulation in the absence of miR-122.

As the RAVs identified in both cell culture and miR-122 inhibitor-treated patients were selected under conditions where miR-122 was limiting, but not necessarily completely absent, we decided to investigate HCV RNA accumulation under conditions where miR-122 was limiting (24-26,35). To do so, we introduced point mutations into the viral RNAs at either Site 1 (C26A, **Figure 3.2D**) or Site 2 (C41A, **Figure 3.2E**), and co-electroporated the viral RNAs with miR-122

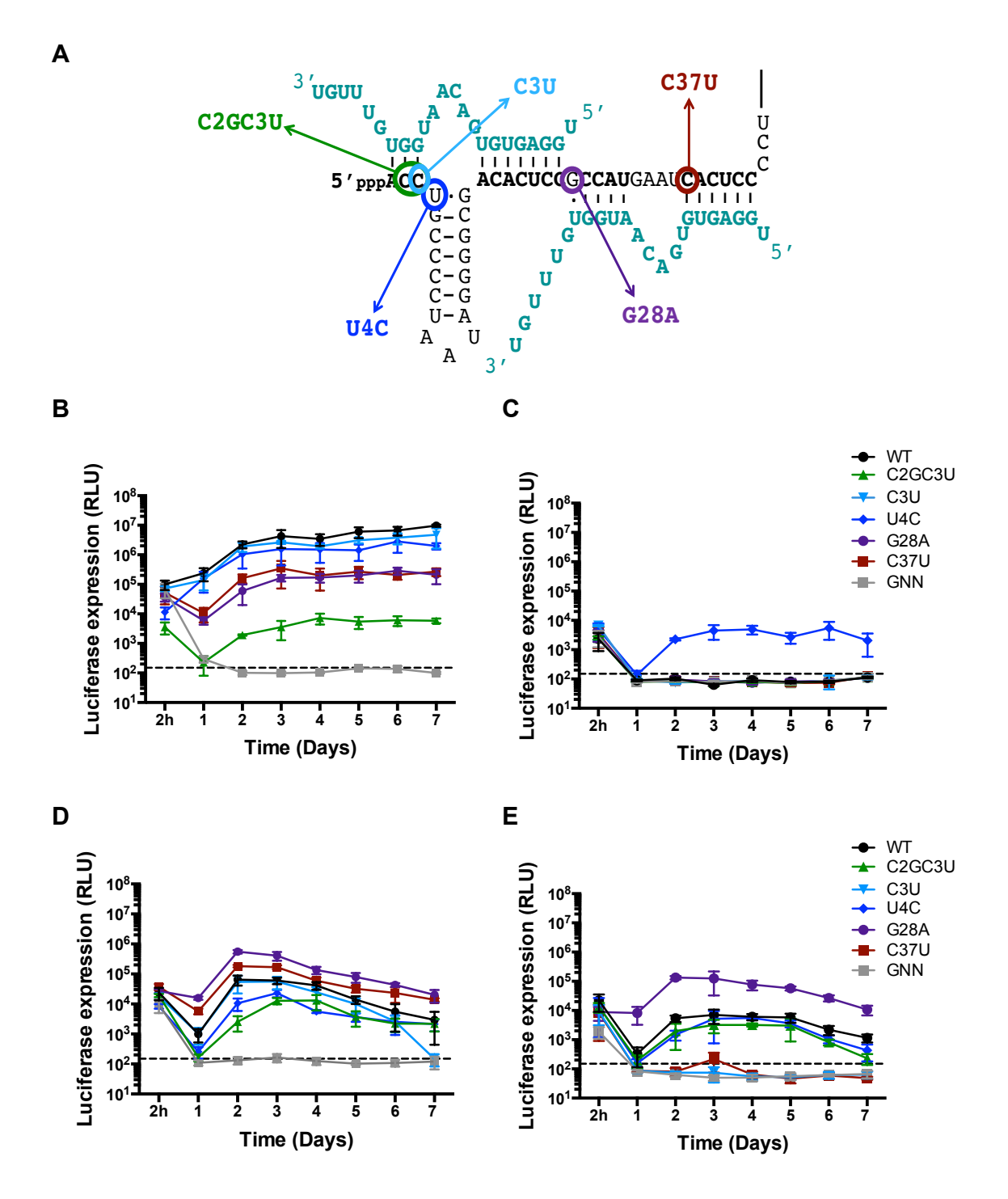


Figure 3.2. RAV accumulation in cell culture. (A) The positions of the RAVs on the 5' UTR of the HCV RNA. Full-length Renilla Luciferase (RLuc) HCV genomic reporter RNAs (WT and RAVs) were co-electroporated with a capped Firefly Luciferase (FLuc) mRNA into (B) Huh-7.5 or (C) miR-122 KO cells. Full-length RLuc HCV genomic reporter RNAs containing mutations at (D) Site 1 (S1:p3A) or (E) Site 2 (S2:p3A) were co-electroporated with a capped FLuc mRNA and a miR-122p3U into miR-122 KO cells. Luciferase activity was measured at the indicated time points post-electroporation. The limit of detection is indicated and all data are representative of three independent replicates. Error bars represent the standard deviation of the mean.

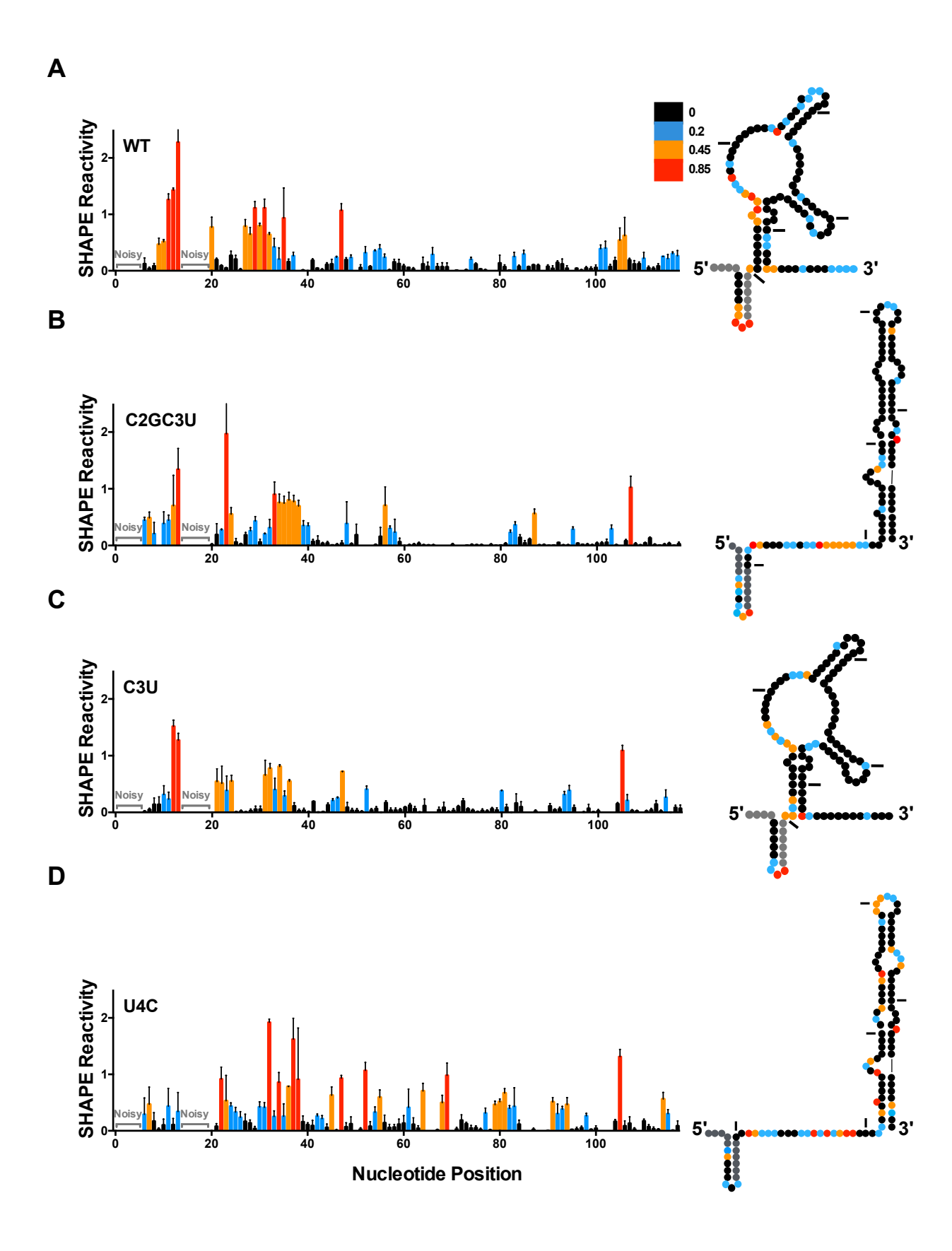
molecules containing compensatory point mutations at position 3 (miR-122p3:U) into miR-122 KO cells. Note that these specific mutations were identified because they do not result in any predicted change to the conformation of the viral RNA (based on RNA structure prediction analyses), and previous studies suggest that mutations in the seed sequence are sufficient to abolish miR-122 interactions (14,18). Interestingly, when miR-122p3U was provided to Site 1, all RAVs and WT were able to accumulate to some extent in miR-122 KO cells (Figure 3.2D). The G28A and C37U RAVs were able to accumulate to a greater extent than WT; while the C3U, U4C, and C2GC3U RAVs accumulated to a lesser extent. In contrast, complementation at Site 2 allowed for the greatest accumulation of G28A, followed by similar levels of accumulation of the WT, C2GC3U and U4C RAVs, while C3U and C37U were substantially impaired under these conditions (Figure 3.2E). Taken together, these results suggest that the U4C RAV is the most fit in the absence of miR-122, while the remaining RAVs can compensate for the loss of miR-122 at least at one of the two miR-122-binding sites. Moreover, the differential ability of the RAVs to accumulate either in the absence of miR-122 or when complemented specifically at Site 1 or Site 2, suggested that they may have unique mechanism(s) of resistance.

Several RAVs alter the structure of the 5' UTR of the positive-strand viral RNA.

In contrast to WT HCV RNA, several recent studies have suggested that the G28A RAV is able to more favorably form the functional SLII structure, even in the absence of miR-122 (18,19). Thus, we performed RNA structure prediction and *in vitro* SHAPE analysis to determine whether the RAVs alter the secondary structure of the viral 5' UTR (Figure 3.3 and Supplementary Figure S3.1). We performed *in vitro* SHAPE analysis followed by capillary electrophoresis on the 5' UTR (nucleotides 1-371) of the WT HCV RNA as well as each of the RAVs and the results for nucleotides 1-117 (which includes SLI and SLII) are presented in Figure 3.3. As previously shown, in the absence of miR-122, the WT HCV RNA adopts an alternative, more energetically

favorable structure, termed SLII^{alt} (**Figure 3.3A and Supplementary Figure S3.1**) (17-19). In agreement with RNA structure predictions, several of the RAVs, including C2GC3U, U4C and G28A are essentially 'riboswitched' and adopt the functional SLII structure, even in the absence of miR-122 (**Figure 3.3B-F**). Like WT, the C3U and C37U RAVs favored the alternative (SLII^{alt}) structure (**Figure 3.3C and F**). However, although the most energetically favorable predicted structure of C3U and G28A is the alternative (SLII^{alt}) structure, there is a close equilibrium between the two structures, which is reflected in our *in vitro* SHAPE analysis, particularly at nucleotides 20-23 and 30-37 (**Figure 3.3C and Supplementary Figure S3.1**). Since SHAPE reactivity reflects an average of the structures that form in solution, the difference in reactivity at these nucleotides, when compared with WT, suggest that the C3U and G28A RAVs are likely to exist in a close equilibrium between the alternative and functional structures. Additionally, SHAPE analysis of C37U agreed with the RNA structure prediction and suggests that the C37U mutant takes on the alternative structure (SLII^{alt}) similar to WT HCV RNA (**Figure 3.3F and Supplementary Figure S3.1**).

In addition to the 'riboswitched' conformation, we also noticed other subtle changes in RNA structure that might have functional consequences for the RAVs. Specifically, we noted that the C2GC3U, C3U and U4C RAVs had additional base-pairing interactions at the 5' terminus that reduce the number of single-stranded nucleotides at the 5' end of the genome (**Figure 3.3A-D**). Thus, our results suggest that the RAVs can be generally categorized into three main classes based on changes to the structure of the viral RNA. Class I RAVs include C2GC3U, U4C, and G28A, which are functionally 'riboswitched', even in the absence of miR-122. The Class II RAVs, which include C2GC3U, C3U, and U4C, have additional base-pairing interactions at the 5' terminus of the HCV genome. And finally, the Class III RAV, C37U, does not appear to alter the structure of the 5' UTR of the positive-strand viral RNA when compared with WT.



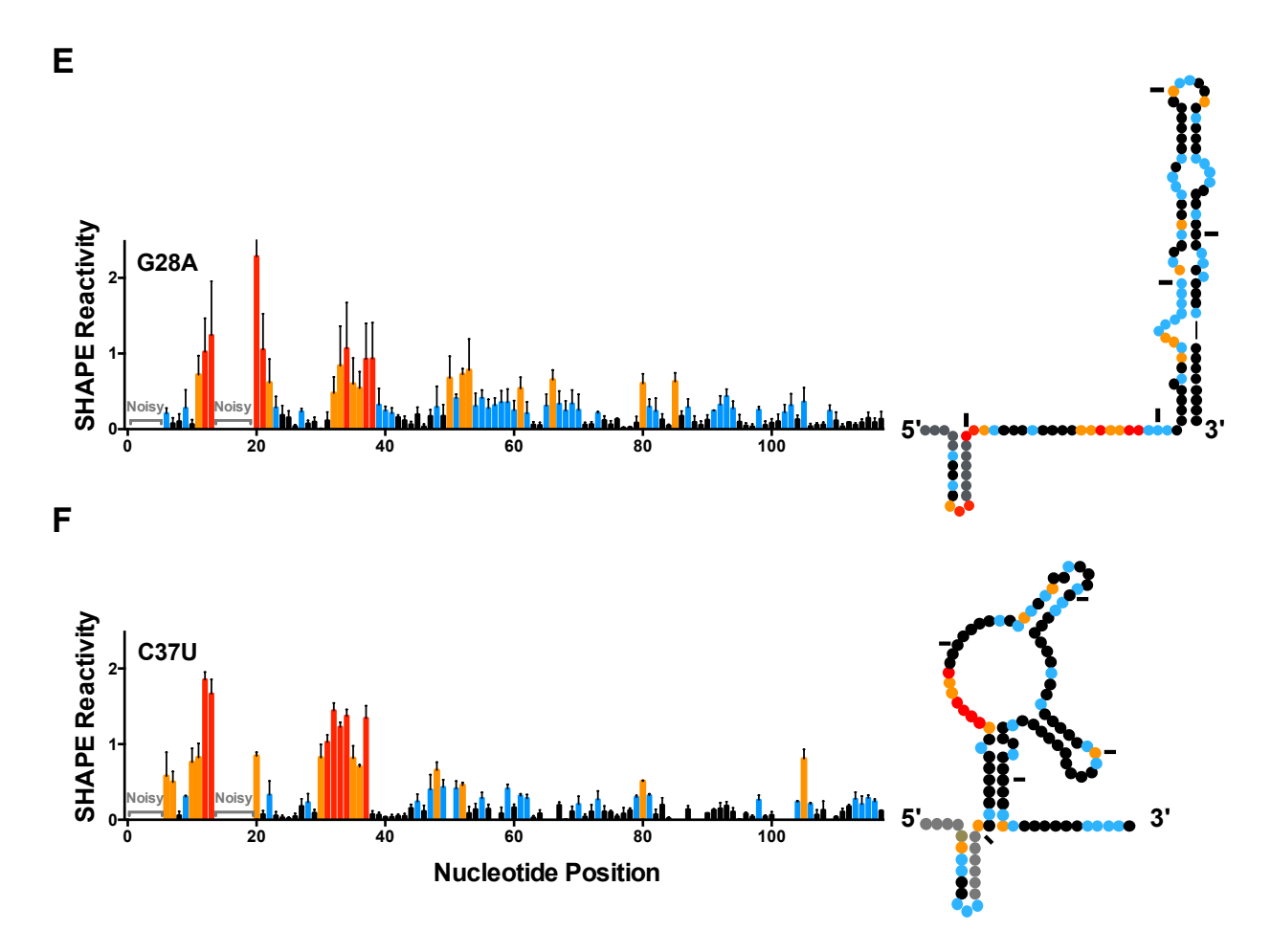


Figure 3. 3. In vitro SHAPE analysis of viral RNAs suggests RAVs alter the structure of the viral RNA in the absence of miR-122. Normalized SHAPE reactivities of nucleotides 1-117 of (A) WT, (B) C2GC3U, (C) C3U, (D) U4C, (E) G28A, and (F) C37U HCV RNAs. Nucleotides 1-5 and 14-19 were omitted due to high background reactivity. Nucleotides with high (\geq 0.85, red), intermediate (between 0.4 and 0.85, orange), low (between 0.2 and 0.4, blue) and very low (\leq 0.2, black) SHAPE reactivity are indicated. The SHAPE reactivity data is superimposed on dot plots representative of the structural prediction that best fits the SHAPE reactivity of nucleotides 1-117 of the viral RNAs (right). Tick marks represent 20 nucleotide intervals. The data is representative of three or more independent replicates and error bars represent the standard error of the mean.

Altered base-pairing of RAVs at the 5' terminus of the genome confers viral RNA stability.

Recent studies suggest that miR-122 protects the HCV genome from two cellular pyrophosphatases, decapping exoribonuclease (DXO, also known as DOM3Z) and Dual Specificity Phosphatase 11 (DUSP11), and subsequent exoribonuclease-mediated decay by Xrn-1 and 2 (16,20-22,36,37). We therefore hypothesized that base-pairing interactions between miR-122 and the 5' terminus of the HCV genome could shield the 5' terminus from pyrophosphatase and/or exoribonuclease activities. To explore this further, we performed *in vitro* exoribonuclease assays using Xrn-1 and nucleotides 1-42 of the HCV genomic RNA in the presence or absence of miR-122 or negative control miRNA (miR-124) (**Figure 3.4A-B**). Our results suggest that in the absence of miR-122, the viral RNA is quickly degraded, but that miR-122 base-paring interactions provide stability to the viral RNA from Xrn-1-mediated decay.

Based on our RNA structure predictions and the *in vitro* SHAPE analysis (**Figure 3.3**), the Class II RAVs (C2GC3U, C3U and U4C) have additional base-pairing interactions at the 5' terminus of the HCV genome. Thus, we hypothesized that this additional base-pairing could provide stability to the viral RNAs, even in the absence of miR-122. Thus, we performed *in vitro* exoribonuclease assays with each of the RAVs (**Figure 3.4C-D**). Interestingly, the C2GC3U RAV, which reduces the number of single-stranded nucleotides at the 5' terminus of the HCV genome to one, substantially stabilizes the viral RNA (**Figure 3.3B**). While U4C, which converts a G-U wobble base-pair to a C-G Watson-Crick pair at the base of SLI (**Figure 3.3D**), also slightly stabilized the viral RNA (**Figure 3.4C-D**). The C3U mutation, which is predicted to provide only one additional base-pair interaction (**Figure 3.3C**), as well as the G28A and C37U RAVs, that do not alter base-pairing at the 5' terminus, had a similar stability to WT HCV RNA (**Figure 3.4C-D**). These results are not altogether surprising, as we observed that a two-nucleotide single-stranded 5' overhang was required for Xrn-1 to initiate exoribonuclease activity, and that the

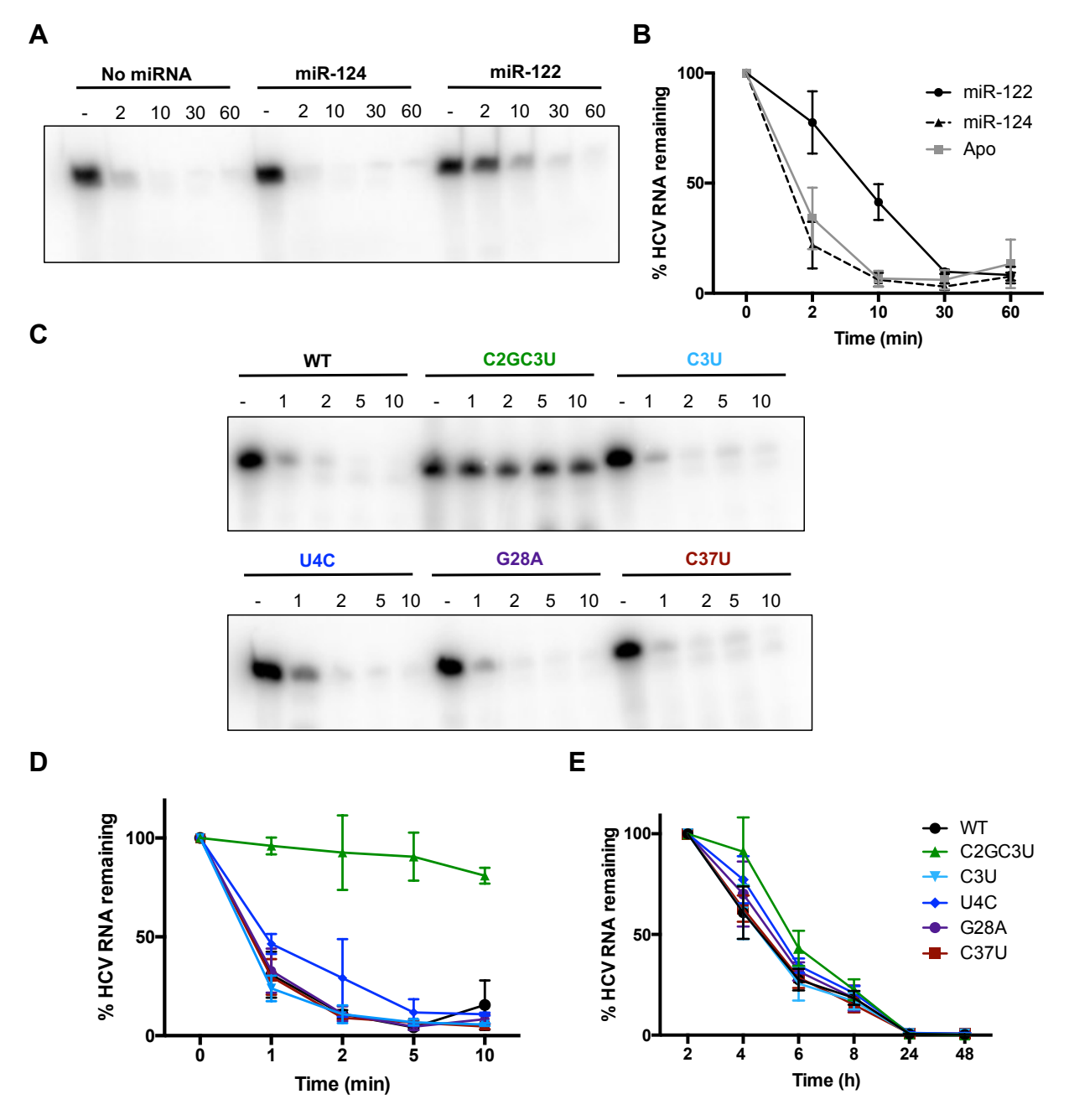


Figure 3.4. miR-122 and Class II RAVs provide stability to the HCV genome. (A) Xrn-1 assay with ³²P-end-labeled monophosphorylated WT HCV RNA (nucleotides 1-42) incubated with no microRNA, or the guide strand of miR-124 (negative control) or miR-122 incubated for 2 – 60 min (as indicated). (B) Quantification of the results in (A) graphed as % HCV RNA remaining over time. (C) Xrn-1 assay with ³²P-end-labeled monophosphorylated WT and RAV HCV RNAs (nucleotides 1-42) incubated for 1 – 10 min (as indicated). (D) Quantification of the results in (C) graphed as % HCV RNA remaining over time. (E) miR-122 KO cells were co-electroporated with full-length RLuc S2:p3 GNN (replication defective) HCV RNAs, a capped FLuc mRNA, and compensatory miR-122p3U. Luciferase activity was measured at the indicated time points post-electroporation. Viral RNA decay is represented as % HCV RNA remaining based on the luciferase activity at the 2 h time point. All data are representative of three independent replicates and error bars represent the standard deviation of the mean.

activity was more efficient as we increased the length of the single-stranded 5' overhang (**Supplementary Figure S3.2**). This is in agreement with a previous study that suggests Xrn-1 requires a single-stranded 5' overhang that is sufficiently long to reach the active site of the enzyme (38).

To further demonstrate whether this increase in base-pairing at the 5' terminus of the HCV genome results in increased stability of the viral RNA in cell culture, we performed viral RNA stability assays in miR-122 KO cells (**Figure 3.4E and Table 3.1**). Specifically, we coelectroporated full-length RLuc S2:p3 GNN (replication defective) versions of WT and each of the RAVs with miR-122p3U, and followed viral RNA decay by luciferase assay. This experimental set up allows us to compensate for both the riboswitch and translational promotion activities provided by the Site 2-bound miR-122 and thus assess viral RNA stability in the absence of Site 1-bound miR-122. In agreement with our results *in vitro*, the C2GC3U and U4C RAVs had increased half-lives ($t_{1/2} = 3.5$ and 2.9 h, respectively), when compared to WT HCV RNA ($t_{1/2} = 2.4$ h) in miR-122 KO cells (**Figure 3.4E and Table 3.1**). The remaining RAVs, including C3U and C37U had similar half-lives to WT; however, the G28A RAV demonstrated a slight increase in stability over WT HCV RNA ($t_{1/2} = 2.7$ vs. 2.4 h, respectively). Taken together, our findings suggest that the increase in base-pairing at the 5' terminus of the HCV genome provided by the Class II RAVs provides HCV genome stability, even in the absence of Site 1-bound miR-122.

The C37U RAV alters the structure of the 3' end of the viral negative-strand replicative intermediate.

Our RNA prediction and SHAPE analyses suggested that the C37U RAV did not alter the secondary structure of the viral 5' UTR; thus, we hypothesized that this RAV might alter base-pairing of the 3' terminus of the negative-strand replicative intermediate, which adopts several stem-loop structures that are required for positive-strand RNA synthesis (7). Specifically, the 3'

Table 3. 1. Half-life viral RNAs in cell culture.

HCV	Half-life (h) ^a	95% Confidence Intervals
WT	2.394	2.15 to 2.741
C2GC3U	3.519	2.828 to 4.658
C3U	2.308	2.016 to 2.701
U4C	2.946	2.541 to 3.503
G28A	2.679	2.296 to 3.215
C37U	2.383	2.173 to 2.637

^a Values reported are an average of three independent measurements.

terminus of the negative-strand adopts three stem-loop structures, termed SL-I', SL-IIz' and SL-IIy' (**Figure 3.5A**). While SL-I' and SL-IIz' were previously demonstrated to be absolutely required for positive-strand RNA synthesis, SL-IIy' was shown to improve the efficiency of positive-strand RNA synthesis (7). When we performed RNA structure prediction analyses, all the Class I and II RAVs were predicated to adopt a WT-like conformation; however, the C37U RAV was predicted to adopt an alternative conformation, which we confirmed in solution using *in vitro* SHAPE analysis (**Supplementary Figure 3.3 and Figure 3.5B**). These results suggest that that the Class III RAV, C37U, alters the structure of the 3' terminus of the negative-strand replicative intermediate, which represents the promoter for viral positive-strand (genomic) RNA synthesis.

3.6 Discussion

Taken together, our analysis of miR-122 inhibitor RAVs have revealed three distinct mechanisms of action, all based on alterations to the structure of the viral RNA. More specifically, the Class I RAVs, which include C2GC3U, U4C and G28A, are riboswitched, even in the absence of miR-122. The Class II RAVs, which include C2GC3U, C3U and U4C, have increased base-pairing interactions at the 5' terminus of the HCV genome that provide stability to the viral RNA in the absence of miR-122 interactions. Finally, the Class III RAV, C37U, alters the structure of the 3' terminus of the negative-strand RNA intermediate, which is predicted to promote positive-strand RNA synthesis.

Previous studies suggested that the G28A mutation results in a riboswitched conformation of the viral RNA, whereby the functional SLII structure, which makes up part of the viral IRES (SLII-IV), is favored over the alternative more energetically favorable conformation (SLII^{alt}) formed by WT HCV RNA in the absence of miR-122 (17-19). This finding prompted us to explore

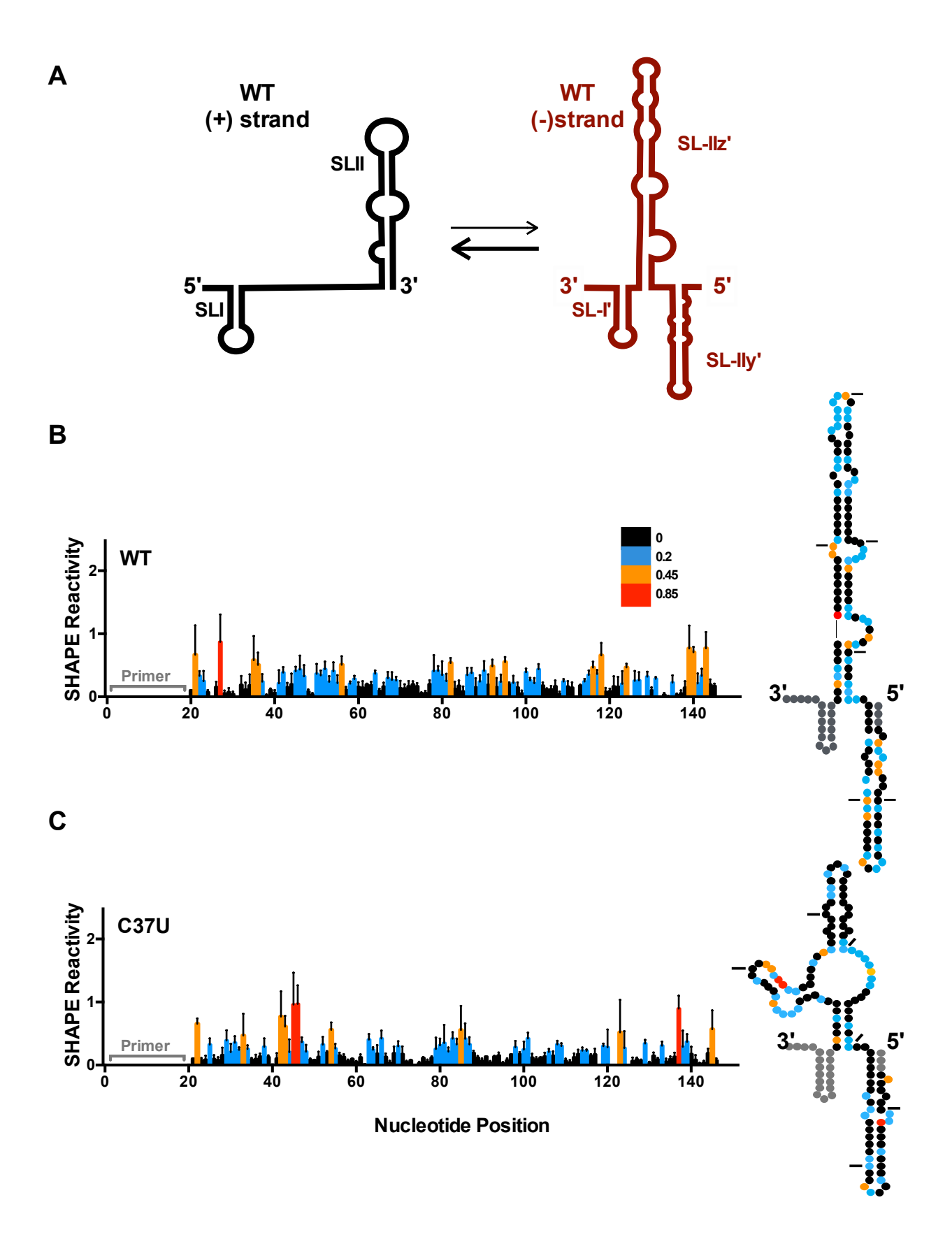


Figure 3.5. The Class III RAV (C37U) alters the structure of the positive-strand promoter. (A) A model of the 5' terminus of the positive-strand genomic RNA and the complementary 3' terminus of the negative-strand RNA intermediate. Normalized SHAPE reactivities of nucleotides 1-151 of the 3' terminus of the negative-strand RNA intermediate of (B) WT and (C) C37U, numbered from the 3' end. Nucleotides 1-19 and 149-151 were omitted as the former corresponds to the primer binding site and the latter demonstrated high SHAPE reactivity at the end of the transcript. Nucleotides with high (\geq 0.85, red), intermediate (between 0.4 and 0.85, orange), low (between 0.2 and 0.4, blue) and very low (\leq 0.2, black) SHAPE reactivity are indicated. The SHAPE reactivity data is superimposed on dot plots representative of the structural prediction that best fits the SHAPE reactivity of nucleotides 1-151 of the 3' terminus of the negative-strand RNA intermediate (right). Tick marks represent 20 nucleotide intervals. The data is representative of three or more independent replicates and error bars represent the standard error of the mean.

whether other RAVs also altered the conformation of the viral RNA, and we found that both the C2GC3U and U4C RAVs also fell into this category of riboswitched viral RNAs. This more favorable conformation helps to explain the viral RNA accumulation profiles of these viral RNAs in cell culture.

Previous studies had suggested that the G28A mutation is better able to compete for endogenous miR-122 than WT HCV RNA (26), as this mutation is predicted to increase the affinity of the viral RNA for miR-122. However, under miR-122 replete conditions, we observed that the G28A mutation was not as fit as WT HCV RNA and accumulated to levels that were reduced by approximately 37.2-fold compared with WT in Huh-7.5 cells. While we were initially puzzled by this result, we realized that the increased binding of miR-122 to the HCV genome could in fact interfere with recruitment of the second miR-122 molecule. Specifically, our previous findings and model for miR-122:HCV RNA interactions (Figure 3.1) suggest that under WT conditions, the first miR-122 molecule is recruited to Site 2 of the HCV genome, which changes the conformation of the viral RNA to allow recruitment of the second miR-122 molecule to Site 1. Due to the close proximity of the miR-122 sites, in order to accommodate the miR-122 molecule at Site 1, the miR-122 molecule at Site 2 relaxes 3' auxiliary base-pairing interactions with the HCV genome. Since the G28A mutation converts a potential G-U wobble base pair to a A-U Watson-Crick base pair at this position, we predict that this provides an advantage in terms of recruiting miR-122 to Site 2 (based on an increase in binding affinity), but could result in a reduction in recruitment of a second Ago:miR-122 complex to Site 1. In addition, a recent study suggests that human Ago2 possesses a solvated surface pocket that specifically binds adenine nucleobases in the 1 position (t1) of target RNAs that can help anchor Ago2 to t1A-containing targets (39-41). This finding suggests that in addition to an increased affinity of miR-122 to Site 2, the G28A mutation is also likely to increase the overall affinity of the Ago2:miR-122 complex to Site 1 of the HCV genome. This increase in affinity to both Site 1 and Site 2 explains our

findings under miR-122 replete conditions, since the initial recruitment to either Site 1 or Site 2 (since G28A is riboswitched) would preclude interactions with the second Ago2:miR-122 complex. However, this also explains the results we obtained under miR-122 limiting conditions at both sites, since G28A would be better able to recruit miR-122 to either site, when compared with WT HCV RNA. Moreover, this could also explain the slight increase in half-life of the G28A RAV observed when Site 2 was complemented (**Table 3.1 and Figure 3.4E**), as the more efficient recruitment to Site 2 of the miR-122p3U molecule may enhance ribosome association, thereby stabilizing the viral RNA.

In addition to G28A, both the C2GC3U and U4C RAVs were also found to be Class I RAVs which are riboswitched. Interestingly, both of these RAVs are also classified as Class II RAVs, which have increased base-pairing at the 5' terminus of the HCV genome. The U4C mutation, like G28A, is predicted to convert a U-G wobble base pair (this time in SLI of the HCV genome) to a strong C-G Watson-Crick base pair. While this mutation is not predicted to alter miR-122 base-pairing interactions with the HCV genome, this mutation favors formation of the functional SLII structure and also stabilizes SLI, which may interfere with recruitment of miR-122 to Site 1 by constraining the distance between miR-122 seed and auxiliary interactions. Under miR-122 replete conditions, this RAV accumulated to a similar extent as WT HCV RNA at Day 2 post-electroporation (2.0-fold less than WT) but to a slightly lesser extent by Day 7 postelectroporation (4.8-fold reduction compared to WT). Remarkably, U4C was the only RAV able to accumulate in the absence of miR-122. This is likely due to the fact that it is both riboswitched and has reduced base-pairing at the 5' terminus of the HCV genome, which based on in vitro exoribonuclease activity assays and viral RNA decay in cell culture results in stabilization of the viral RNA. This also explains the accumulation under conditions where miR-122 was limiting at Site 1 and Site 2, since U4C accumulated to a slightly lesser extent than WT when miR-122 was complemented at Site 1 (2.6-fold reduction compared to WT), while it accumulated to a similar or

slightly lesser extent as WT when Site 2 was complemented. Alternatively, the slight impairment compared with WT HCV RNA may be a result of stabilizing SLI, which could impair melting of SLI during viral RNA replication (42).

The C2GC3U RAV was also demonstrated to be both a Class I and Class II RAV, having both a riboswitched conformation and increased base-pairing at the 5' terminus of the viral genome. This RAV is predicted to create two new Watson-Crick base pairs at the 5' terminus of the HCV genome, effectively lengthening SLI and reducing the number of single-stranded base pairs at the 5' terminus. This reduction in 5' single-stranded bases results in a substantial increase in viral RNA stability, both *in vitro* and in cell culture (**Figure 3.4**). However, this did not translate into a fitness advantage under miR-122 replete or KO conditions. While C2GC3U was able to accumulate in Huh-7.5 cells, it was significantly impaired in viral RNA accumulation, which could be due to the increased stability of SLI or destabilization and/or impairment of miR-122 recruitment. Either way, the stabilizing effect of this increase in base-pairing does not appear to provide as much stability as recruitment of an Ago2:miR-122 complex to Site 1 of the viral genome.

While we classified the C3U RAV into Class II, RNA structure prediction and SHAPE analyses suggest that although it favors the alternative structure (SLII^{alt}), like G28A, it likely exists in a close equilibrium between the alternative and functional structures (**Figure 3.3 and Supplementary Figure S3.1**). In the functional conformation, the C3U mutant is predicted to form one additional U-A Watson-Crick base-pair with nucleotide 21 of the HCV genome, effectively lengthening SLI and reducing the number of 5' single-stranded nucleotides at the terminus of the viral genome to two nucleotides. However, in line with a previous study, this did not result in significant stabilization of the genome in either *in vitro* exoribonuclease activity assays or viral RNA decay in cell culture (**Figure 3.4**) (42). This helps to explain the viral RNA accumulation pattern in cell culture, as the C3U mutation would be predicted to slightly decrease the affinity for Site 1-bound miR-122 in both the miR-122 replete condition as well as when miR-122 is directed

to Site 1 specifically; and, like WT, C3U is unable to accumulate in miR-122 KO cells (**Figure 3.2B-C**). However, we are puzzled by the finding that C3U is unable to accumulate when miR-122 is provided to Site 2 only (**Figure 3.2E**). It is possible that the additional Watson-Crick base pair created is not sufficient to stabilize the viral RNA (like C2GC3U or U4C mutations), but that the identity of this specific nucleotide changes the requirements for cellular RNA binding proteins for efficient viral RNA accumulation. This is in line with a recent study which suggests a differential set of RNA binding protein interactions between WT and C3U mutant viral RNAs in cell culture (42).

Finally, we were initially quite perplexed by the Class III RAV, C37U, which did not result in alteration of the structure of the viral 5' UTR (Figure 3.3). Moreover, the C37U mutation falls within the seed sequence of Site 2, which converts a C-G Watson-Crick base pair to a less stable U-G wobble base pair. Since this means that C37U can still base pair with miR-122, albeit through a wobble base pair, this explains the pattern of viral RNA accumulation in miR-122 replete conditions, as C37U accumulation was reduced by 13.8-fold when compared with WT HCV RNA. However, we were surprised by the result that C37U was able to accumulate to a greater extent than WT when miR-122 was specifically directed to Site 1 (2.8-fold increase compared to WT at Day 2 post-electroporation). However, previous studies demonstrated that the 3' terminus of the negative-strand RNA replicative intermediate (complementary to the 5' UTR of the genomic positive-strand RNA), forms several RNA secondary structures (termed SL-I', SL-IIz' and SL-IIy', **Figure 3.5**) important for viral positive-strand synthesis (7,43,44). We hypothesized that the C37U mutation could therefore alter the structure of the positive-strand promoter. This was confirmed by both RNA structure predictions and SHAPE analyses, which suggested that the C37U mutation results in a more energetically favorable, Y-shaped alternative conformation (Supplementary figure 3.3 and Figure 3.5). Interestingly, this Y-shaped structure resembles the conformation of SLA of the related flaviviruses, a Y-shaped structure at the 5' terminus of the viral genome known

to interact with the viral RNA-dependent RNA polymerase (45-48). Thus, it is possible that the C37U mutation causes a conformational change in the positive-strand promoter region that enhances recruitment of the HCV NS5B RNA-dependent RNA polymerase, thereby providing a fitness advantage. This could explain the increase in viral RNA accumulation when compared to WT when miR-122 was provided to Site 1, as the stabilization provided by miR-122 at Site 1 could allow C37U to be stable for long enough to establish replication complexes. However, when miR-122 was only provided to Site 2, we did not see significant viral RNA accumulation from C37U, except for a small increase at Day 3. We suspect that this is due to the lack of stability provided to Site 1, and that a small amount of C37U was able to establish replication complexes but diminishing levels of Site 2 complemented miR-122p3U at this point failed to allow further viral RNA accumulation. Alternatively, the reduced affinity for miR-122 at Site 2 may have resulted in an impaired ability to promote the riboswitch and translation activities to sufficient levels to establish replication complexes. Thus, in future we plan to continually complement Site 2 to examine whether C37U levels might rebound under these conditions. In addition, we plan to assess whether the C37U mutation affects the promoter for positive-strand viral RNA synthesis mediated by the HCV NS5B RNA-dependent RNA polymerase. Nonetheless, our data supports the hypothesis that the C37U RAV changes to the structure of the 3' terminus of the negative-strand RNA intermediate, and we believe that this provides a fitness advantage by modulating the promoter for positive-strand viral RNA synthesis.

In summary, we have identified three distinct classes of RAVs to miR-122 inhibitor-based therapies that all alter the structure of the viral RNA but have unique mechanisms of action (**Figure 3.6**). The Class I RAVs (G28A, C2GC3U and U4C) are riboswitched *a priori* and are thus able to form the HCV IRES, even in the absence of miR-122. The Class II RAVs (C2GC3U, C3U and U4C) increase base-pairing at the 5' terminus of the HCV genome, thereby protecting the viral RNA from exoribonuclease activity, even in the absence of miR-122. While we did not explore it

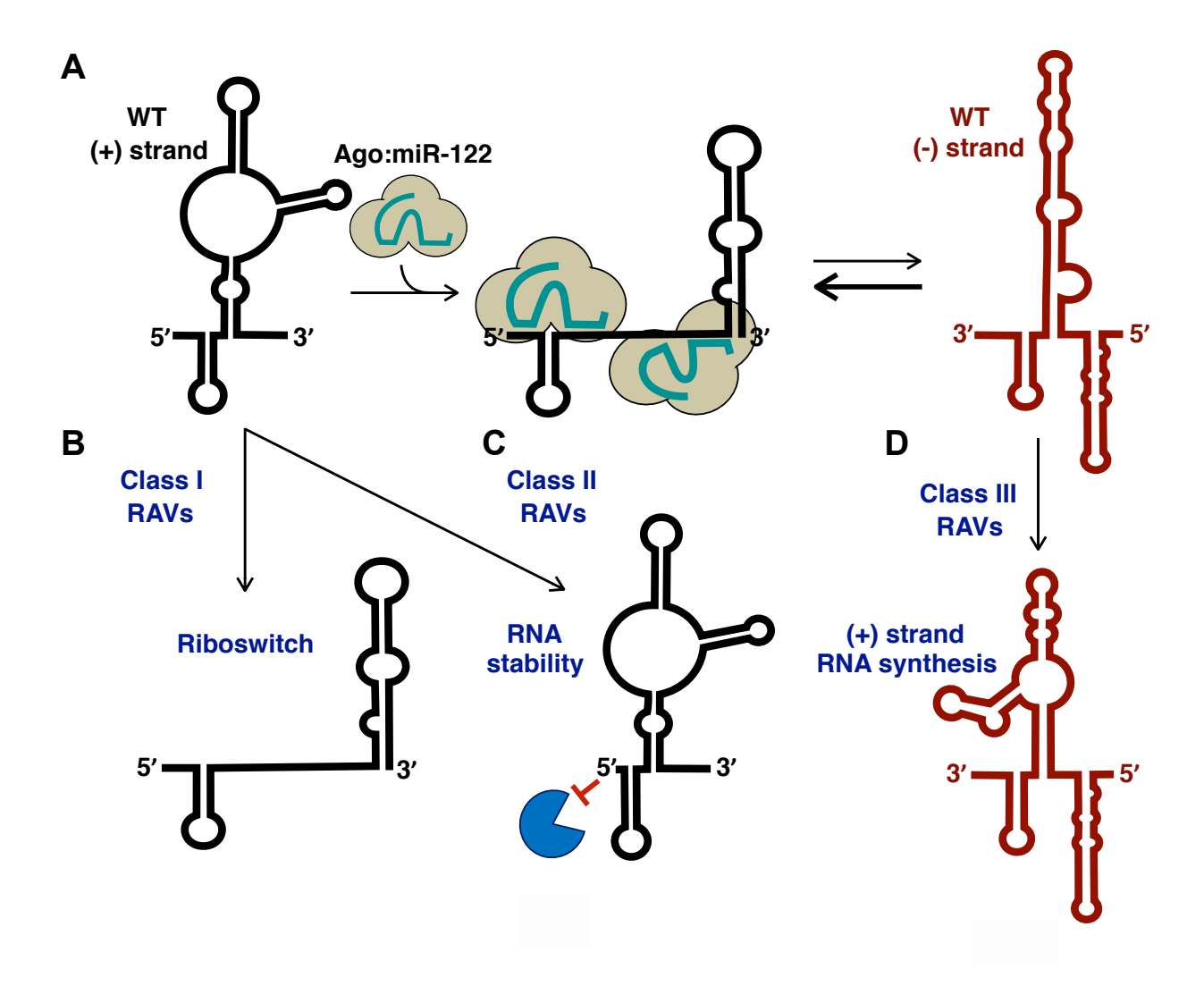


Figure 3.6. Mechanism of action of RAVs. (A) miR-122 promotes riboswitch, RNA stability and translation of the WT positive-sense HCV RNA genome. **(B)** Class I RAVs (C2GC3U, U4C and G28A) are riboswitched a priori, even in the absence of miR-122. **(C)** Alterations in base-pairing at the 5' terminus of the Class II RAVs (C2GC3U, C3U and U4C) help to stabilize the viral RNA even in the absence of miR-122. **(D)** The Class III RAV (C37U) alters the structure of the negative-strand RNA intermediate which may result in more efficient positive-strand RNA synthesis.

directly herein, it is possible that this reduction in 5' single-stranded nucleotides also protects the genome from cellular pyrophosphatase (DXO and DUSP11) activity (16,20,49). Finally, the Class III RAV (C37U) alters the structure of the 3' terminus of the negative-strand replicative intermediate, which is predicted to promote positive-strand RNA synthesis.

Importantly, our analysis herein was based on a genotype 2a (JFH-1 isolate), and while the U4C, G28A and C37U mutations were isolated from genotype 2, the C2GC3U and C3U mutations were isolated from genotype 3/4 and genotype 1 patients, respectively (24,50). Interestingly, the C3U RAV was often isolated in genotype 1 and is predicted to adopt several additional alternative structures in this context which may contribute to its resistance to miR-122 inhibitors (50). In contrast, the C2GC3U RAV was isolated from genotype 3/4 and RNA structure predictions in this context suggest that it adopts the same structure as genotype 2a used herein. Thus, although both miR-122 binding sites are 100% conserved across HCV isolates, and the remainder of the 5' terminus is very highly conserved (14), subtle nucleotide substitutions between genotypes may account for some of the nuance observed with these mutants. Nonetheless, our findings provide the first in-depth analysis of resistance to miR-122-based therapy and has revealed three unique mechanisms of resistance, all based on changes to the structure of the viral RNA. Importantly, since the miR-122 inhibitors are the flagship miRNA-based inhibitors, understanding resistance will be increasingly important as more miRNA-based therapeutics enter into the clinic targeted against a wide variety of ailments.

3.7 Acknowledgements

We would like to acknowledge Charlie Rice (University of Rockefeller) for providing Huh-7.5 cells and the J6/JFH-1 virus, Matthew Evans for providing miR-122 KO cells, and Rodney Russell (Memorial University) for providing JFH-1_T. We would also like to thank Julie Magnus (McGill University) for technical support, Rachel Hayes (McGill University) for constructing the HCV

negative-strand plasmid templates, Tamara Giguère (University of Sherbrooke) for assistance with the SHAPE experiments and data analysis, and Zamboni Chem Solutions Inc. for assistance in synthesis of NAI-N₃.

3.8 Author Contributions

JC and SMS conceptualized and designed the study. JC generated and analyzed the data. JC and SMS drafted the manuscript and contributed to editing the manuscript.

3.9 Funding

JC is supported by the Gerald Clavet Fellowship from McGill University. This work was supported by funds from McGill University as well as grants from the NSERC Discovery grant [RGPIN-2014-05907], CIHR Operating grant [MOP-136915], and Canadian Foundation for Innovation [32590] programs to SMS. In addition, this research was undertaken, in part, thanks to funding from the Canada Research Chairs program.

3.10 Conflict of Interest

The authors declare that they have no conflict of interest.

3.11 References

- 1. Organization, W.H. (2017), pp. 1-83.
- 2. Hajarizadeh, B., Grebely, J. and Dore, G.J. (2013) Epidemiology and natural history of HCV infection. *Nat. Rev. Gastroenterol. Hepatol.*, **10**, 553-562.
- 3. Messina, J.P., Humphreys, I., Flaxman, A., Brown, A., Cooke, G.S., Pybus, O.G. and Barnes, E. (2015) Global distribution and prevalence of hepatitis C virus genotypes. *Hepatology*, **61**, 77-87.
- 4. Sagan, S.M., Chahal, J. and Sarnow, P. (2015) cis-Acting RNA elements in the hepatitis C virus RNA genome. *Virus Res.*, **206**, 90-98.
- 5. Tuplin, A., Evans, D.J. and Simmonds, P. (2004) Detailed mapping of RNA secondary structures in core and NS5B-encoding region sequences of hepatitis C virus by RNase cleavage and novel bioinformatic prediction methods. *J. Gen. Virol.*, **85**, 3037-3047.
- 6. Wilson, J.A. and Sagan, S.M. (2014) Hepatitis C virus and human miR-122: Insights from the bench to the clinic. *Curr. Opin. Virol.*, 7, 11-18.
- 7. Friebe, P. and Bartenschlager, R. (2009) Role of RNA structures in genome terminal sequences of the hepatitis C virus for replication and assembly. *J. Virol.*, **83**, 11989-11995.
- 8. Friebe, P., Lohmann, V., Krieger, N. and Bartenschlager, R. (2001) Sequences in the 5' nontranslated region of hepatitis C virus required for RNA replication. *J. Virol.*, **75**, 12047–12057.
- 9. Tuplin, A., Struthers, M., Simmonds, P. and Evans, D.J. (2012) A twist in the tail: SHAPE mapping of long-range interactions and structural rearrangements of RNA elements involved in HCV replication. *Nucleic Acids Res.*, **40**, 6908-6921.
- 10. Wang, C., Le, S.Y., Ali, N. and Siddiqui, A. (1995) An RNA pseudoknot is an essential structural element of the internal ribosome entry site located within the hepatitis C virus 5' noncoding region. *RNA*, **1**, 526-537.
- 11. Jopling, C.L., Yi, M., Lancaster, A.M., Lemon, S.M. and Sarnow, P. (2005) Modulation of Hepatitis C Virus RNA Abundance by a Liver-Specific MicroRNA. *Science*, **209**, 1577-1581.
- 12. Jopling, C.L. (2008) Regulation of hepatitis C virus by microRNA-122. *Biochem. Soc. Trans.*, **36**, 1220-1223.
- 13. Luna, J.M., Scheel, T.K.H., Danino, T., Shaw, K.S., Mele, A., Fak, J.J., Nishiuchi, E., Takacs, C.N., Catanese, M.T., De Jong, Y.P. *et al.* (2015) Hepatitis C virus RNA functionally sequesters miR-122. *Cell*, **160**, 1099-1110.
- 14. Machlin, E.S., Sarnow, P. and Sagan, S.M. (2011) Masking the 5' terminal nucleotides of the hepatitis C virus genome by an unconventional microRNA-target RNA complex. *PNAS*, **108**, 3193-3198.
- 15. Chang, J., Nicolas, E., Marks, D., Sander, C., Lerro, A., Buendia, M.A., Xu, C., Mason, W.S., Moloshok, T., Bort, R. *et al.* (2004) miR-122, a mammalian liver-specific microRNA, is processed from hcr mRNA and may downregulate the high affinity cationic amino acid transporter CAT-1. *RNA Biol.*, **1**, 106-113.
- 16. Amador-Canizares, Y., Bernier, A., Wilson, J.A. and Sagan, S.M. (2018) miR-122 does not impact recognition of the HCV genome by innate sensors of RNA but rather protects the 5' end from the cellular pyrophosphatases, DOM3Z and DUSP11. *Nucleic Acids Res.*, 46, 5139-5158.
- 17. Amador-Canizares, Y., Panigrahi, M., Huys, A., Kunden, R.D., Adams, H.M., Schinold, M.J. and Wilson, J.A. (2018) miR-122, small RNA annealing and sequence mutations

- alter the predicted structure of the Hepatitis C virus 5' UTR RNA to stabilize and promote viral RNA accumulation. *Nucleic Acids Res.*, **46**, 9776-9792.
- 18. Chahal, J., Gebert, L.F.R., Gan, H.H., Camacho, E., Gunsalus, K.C., MacRae, I.J. and Sagan, S.M. (2019) miR-122 and Ago interactions with the HCV genome alter the structure of the viral 5' terminus. *Nucleic Acids Res.*, 47, 5307-5324.
- 19. Schult, P., Roth, H., Adams, R.L., Mas, C., Imbert, L., Orlik, C., Ruggieri, A., Pyle, A.M. and Lohmann, V. (2018) microRNA-122 amplifies hepatitis C virus translation by shaping the structure of the internal ribosomal entry site. *Nat Commun.*, **9**, 2613-2613.
- 20. Kincaid, R.P., Lam, V.L., Chirayil, R.P., Randall, G. and Sullivan, C.S. (2018) RNA triphosphatase DUSP11 enables exonuclease XRN-mediated restriction of hepatitis C virus. *PNAS*, **115**, 8197-8202.
- 21. Li, Y., Yamane, D. and Lemon, S.M. (2015) Dissecting the roles of the 5' exoribonucleases Xrn1 and Xrn2 in restricting hepatitis C virus replication. *J. Virol.*, **89**, 4857-4865.
- 22. Sedano, C.D. and Sarnow, P. (2014) Hepatitis C virus subverts liver-specific miR-122 to protect the viral genome from exoribonuclease Xrn2. *Cell host & microbe*, **16**, 257-264.
- Janssen, H.L.A., Reesink, H.W., Lawitz, E.J., Zeuzem, S., Rodriguez-Torres, M., Patel, K., van der Meer, A.J., Patick, A.K., Chen, A., Zhou, Y. et al. (2013) Treatment of HCV Infection by Targeting MicroRNA. N. Engl. J. Med., 368, 1685-1694.
- 24. van der Ree, M.H., de Vree, J.M., Stelma, F., Willemse, S., van der Valk, M., Rietdijk, S., Molenkamp, R., Schinkel, J., van Nuenen, A.C., Beuers, U. *et al.* (2017) Safety, tolerability, and antiviral effect of RG-101 in patients with chronic hepatitis C: a phase 1B, double-blind, randomised controlled trial. *Lancet*, **389**, 709-717.
- 25. Hopcraft, S.E., Azarm, K.D., Israelow, B., Leveque, N., Schwarz, M.C., Hsu, T.H., Chambers, M.T., Sourisseau, M., Semler, B.L. and Evans, M.J. (2016) Viral Determinants of miR-122 Independent Hepatitis C Virus Replication. *mSphere*, 1, 1-12.
- 26. Israelow, B., Mullokandov, G., Agudo, J., Sourisseau, M., Bashir, A., Maldonado, A.Y., Dar, A.C., Brown, B.D. and Evans, M.J. (2015) Hepatitis C virus genetics affects miR-122 requirements and response to miR-122 inhibitors. *Nat Commun.*, **5**, 1-11.
- 27. Blight, K.J., McKeating, J.A. and Rice, C.M. (2002) Highly permissive cell lines for subgenomic and genomic hepatitis C virus RNA replication. *J. Virol.*, **76**, 13001-13014.
- 28. Russell, R.S., Meunier, J.-C., Takikawa, S., Faulk, K., Engle, R.E., Bukh, J., Purcell, R.H. and Emerson, S.U. (2008) Advantages of a single-cycle production assay to study cell culture-adaptive mutations of hepatitis C virus. *Proc. Natl. Acad. Sci. U. S. A.*, **105**, 4370-4375.
- 29. Jones, C.T., Murray, C.L., Eastman, D.K., Tassello, J. and Rice, C.M. (2007) Hepatitis C virus p7 and NS2 proteins are essential for production of infectious virus. *J. Virol.*, **81**, 8374-8383.
- 30. Genin, E.C., Madji Hounoum, B., Bannwarth, S., Fragaki, K., Lacas-Gervais, S., Mauri-Crouzet, A., Lespinasse, F., Neveu, J., Ropert, B., Auge, G. *et al.* (2019) Mitochondrial defect in muscle precedes neuromuscular junction degeneration and motor neuron death in CHCHD10(S59L/+) mouse. *Acta Neuropathol.*, **138**, 123-145.
- 31. Schurer, H., Lang, K., Schuster, J. and Morl, M. (2002) A universal method to produce in vitro transcripts with homogeneous 3' ends. *Nucleic Acids Res.*, **30**, e56.
- 32. Wilson, J.A., Zhang, C., Huys, A. and Richardson, C.D. (2011) Human Ago2 Is Required for Efficient MicroRNA 122 Regulation of Hepatitis C Virus RNA Accumulation and Translation. *J. Virol.*, **85**, 2342-2350.

- 33. Karabiber, F., McGinnis, J.L., Favorov, O.V. and Weeks, K.M. (2013) QuShape: rapid, accurate, and best-practices quantification of nucleic acid probing information, resolved by capillary electrophoresis. *RNA*, **19**, 63-73.
- 34. Reuter, J.S. and Mathews, D.H. (2010) RNAstructure: software for RNA secondary structure prediction and analysis. *BMC Bioinformatics*, **11**, 129.
- 35. Ottosen, S., Parsley, T.B., Yang, L., Zeh, K., van Doorn, L.-J., van der Veer, E., Raney, A.K., Hodges, M.R. and Patick, A.K. (2015) In vitro antiviral activity and preclinical and clinical resistance profile of miravirsen, a novel anti-hepatitis C virus therapeutic targeting the human factor miR-122. *Antimicrob. Agents Chemother.*, **59**, 599-608.
- 36. Li, Y., Masaki, T., Yamane, D., McGivern, D.R. and Lemon, S.M. (2013) Competing and noncompeting activities of miR-122 and the 5' exonuclease Xrn1 in regulation of hepatitis C virus replication. *PNAS*, **110**, 1881-1886.
- 37. Thibault, P.A., Huys, A., Amador-Cañizares, Y., Gailius, J.E., Pinel, D.E. and Wilson, J.A. (2015) Regulation of hepatitis C virus genome replication by Xrn1 and microRNA-122 binding to individual sites in the 5' untranslated region. *J. Virol.*, **89**, 6294-6311.
- 38. Jinek, M., Coyle, S.M. and Doudna, J.A. (2011) Coupled 5' nucleotide recognition and processivity in Xrn1-mediated mRNA decay. *Mol. Cell*, **41**, 600-608.
- 39. Schirle, N.T. and MacRae, I.J. (2012) The crystal structure of human Argonaute2. *Science*, **336**, 1037-1040.
- 40. Schirle, N.T., Sheu-Gruttadauria, J. and MacRae, I.J. (2014) Structural basis for microRNA targeting. *Science*, **346**, 608-613.
- 41. Sheu-Gruttadauria, J., Xiao, Y., Gebert, L.F.R. and MacRae, I.J. (2019) Beyond the seed: structural basis for supplementary microRNA targetting *EMBO J*.
- 42. Mata, M., Neben, S., Majzoub, K., Carette, J., Ramanathan, M., Khavari, P.A. and Sarnow, P. (2019) Impact of a patient-derived hepatitis C viral RNA genome with a mutated microRNA binding site. *PLoS Pathog.*, **15**, e1007467.
- 43. Schult, P., Nattermann, M., Lauber, C., Seitz, S. and Lohmann, V. (2019) Evidence for Internal Initiation of RNA Synthesis by the Hepatitis C Virus RNA-Dependent RNA Polymerase NS5B In Cellulo. *J. Virol.*, **93**.
- 44. Smith, R.M., Walton, C.M., Wu, C.H. and Wu, G.Y. (2002) Secondary structure and hybridization accessibility of hepatitis C virus 3'-terminal sequences. *J. Virol.*, **76**, 9563-9574.
- 45. Alvarez, D.E., Lodeiro, M.F., Filomatori, C.V., Fucito, S., Mondotte, J.A. and Gamarnik, A.V. (2006) Structural and functional analysis of dengue virus RNA. *Novartis Found. Symp.*, **277**, 120-132; discussion 132-125, 251-123.
- 46. Gebhard, L.G., Filomatori, C.V. and Gamarnik, A.V. (2011) Functional RNA elements in the dengue virus genome. *Viruses*, **3**, 1739-1756.
- 47. Lodeiro, M.F., Filomatori, C.V. and Gamarnik, A.V. (2009) Structural and functional studies of the promoter element for dengue virus RNA replication. *J. Virol.*, **83**, 993-1008.
- 48. Mazeaud, C., Freppel, W. and Chatel-Chaix, L. (2018) The Multiples Fates of the Flavivirus RNA Genome During Pathogenesis. *Front Genet*, **9**, 595.
- 49. Burke, J.M. and Sullivan, C.S. (2017) DUSP11 An RNA phosphatase that regulates host and viral non-coding RNAs in mammalian cells. *RNA Biol.*, **14**, 1457-1465.
- 50. Ono, C., Fukuhara, T., Motooka, D., Nakamura, S., Okuzaki, D., Yamamoto, S., Tamura, T., Mori, H., Sato, A., Uemura, K. *et al.* (2017) Characterization of miR-122-independent propagation of HCV. *PLoS Pathog.*, **13**, e1006374.

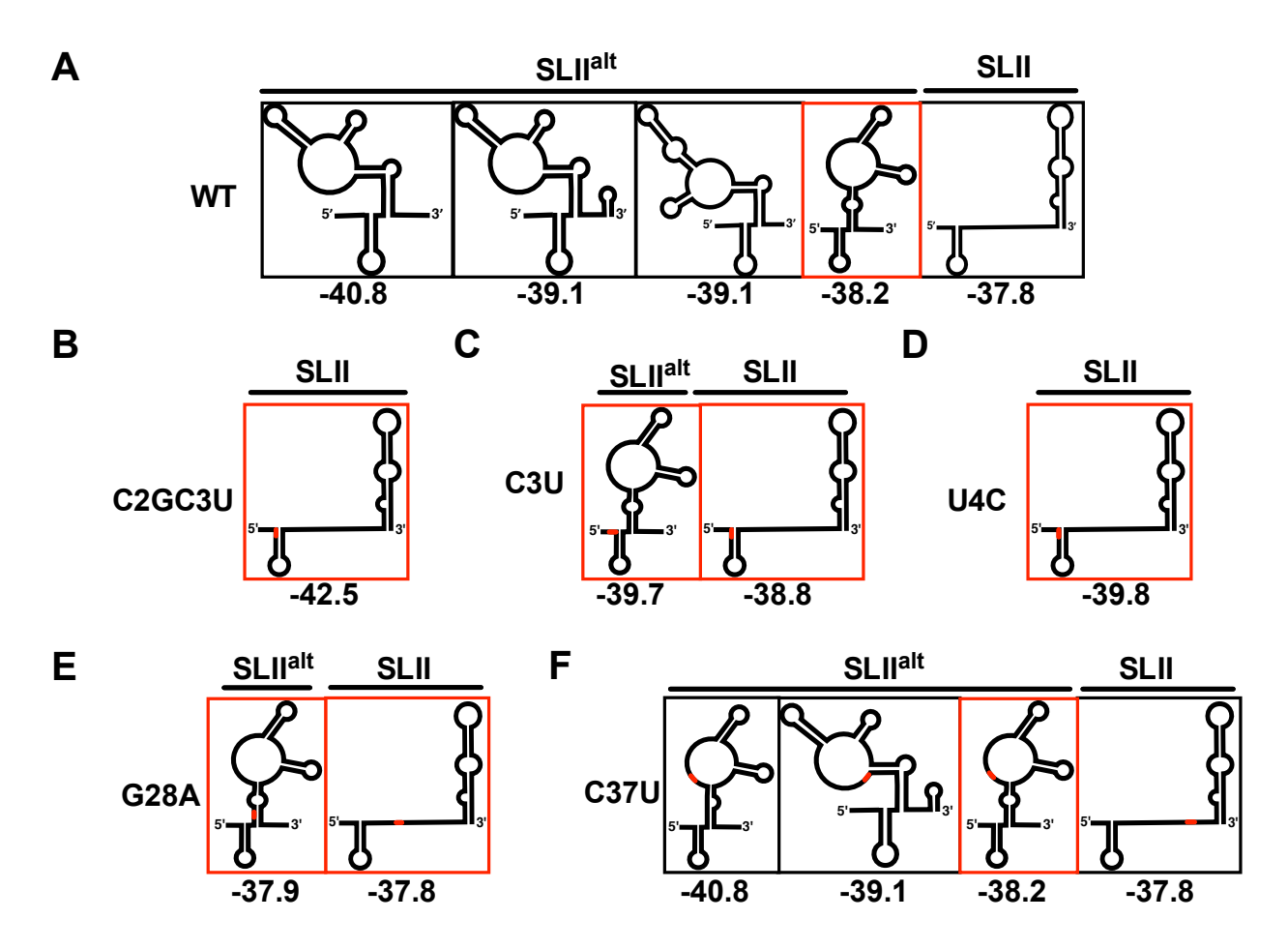
3.12 Supplementary Material

Supplementary Methods

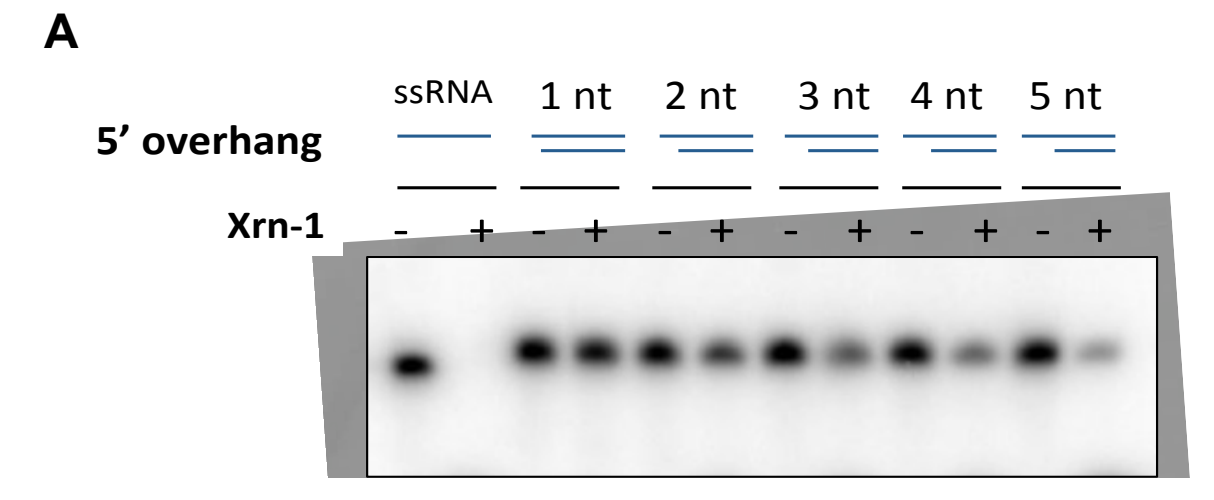
In vitro Xrn-1 assay using duplex substrates

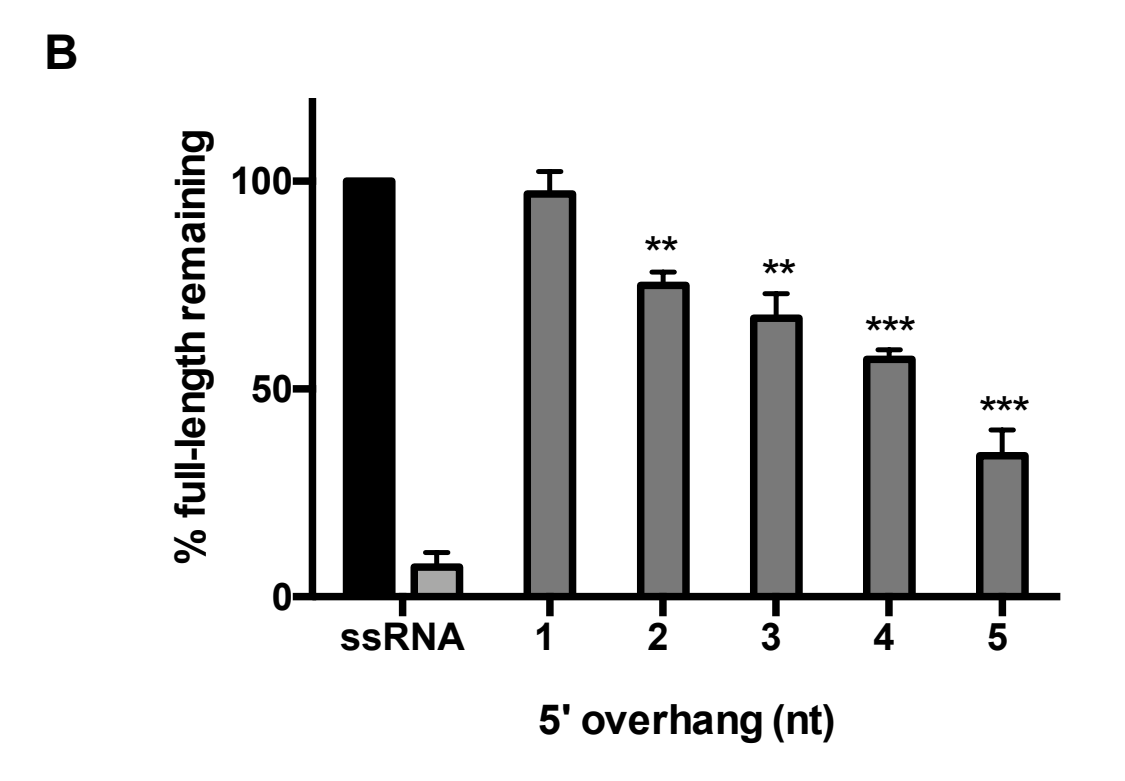
For Xrn-1 assays using duplex substrates, the following oligonucleotides were used: 25-nt substrate RNA (5'-AAA AAA AAC CCC ACC ACC ACC ACC U- 3') and 20 – 24 nt complementary DNA strands (25-nt: 5'-dAdAdG dTdGdA dTdGdG dTdGdG dTdGdG dGdGdT dTdTdT dTdTdT- 3'; 24-nt: 5'-dAdAdG dTdGdA dTdGdG dTdGdG dTdGdG dGdGdT dTdTdT dTdT- 3'; 23-nt: 5'-dAdAdG dTdGdA dTdGdG dTdGdG dGdGdT dTdTdT dT- 3'; 22-nt: 5'-dAdAdG dTdGdG dTdGdG dTdGdG dGdGdT dTdTdT- 3'; 21-nt: 5'-dAdAdG dTdGdG d

One hundred picomoles of the monophosphorylated single-stranded 25-nt RNA oligonucleotide was end-labeled using T4 RNA ligase and [γ -32P] ATP and purified using an RNA Clean & Concentrator-5 spin column (Zymo Research). The 20-24-nt complementary DNA oligonucleotides were added to the end-labeled RNA (in a 2.5-fold molar excess of DNA to RNA), followed by denaturation at 65°C for 3 min and cooled to room temperature. Xrn-1 assays were carried out as described using one unit of Terminator 5'-Phosphate-Dependent Exonuclease in 1X Terminator Reaction Buffer A (Lucigen), and 1 unit of Ribolock (Life Technologies). The reactions were incubated at 30°C and quenched with 1 μ L of 100 mM EDTA after incubation for 5 min. Ten microliters of Gel Loading dye (Life Technologies) was added to each sample and 5 μ L of each sample was resolved on a 15% denaturing polyacrylamide gel (29:1 acrylamide:bisacrylamide, 1X TBE), dried at 80°C for 1.5 h (BioRad Gel dryer, Model 583), and visualized by phosphorimager (Storm, GE Life Sciences). Image analysis was performed using the ImageJ software.

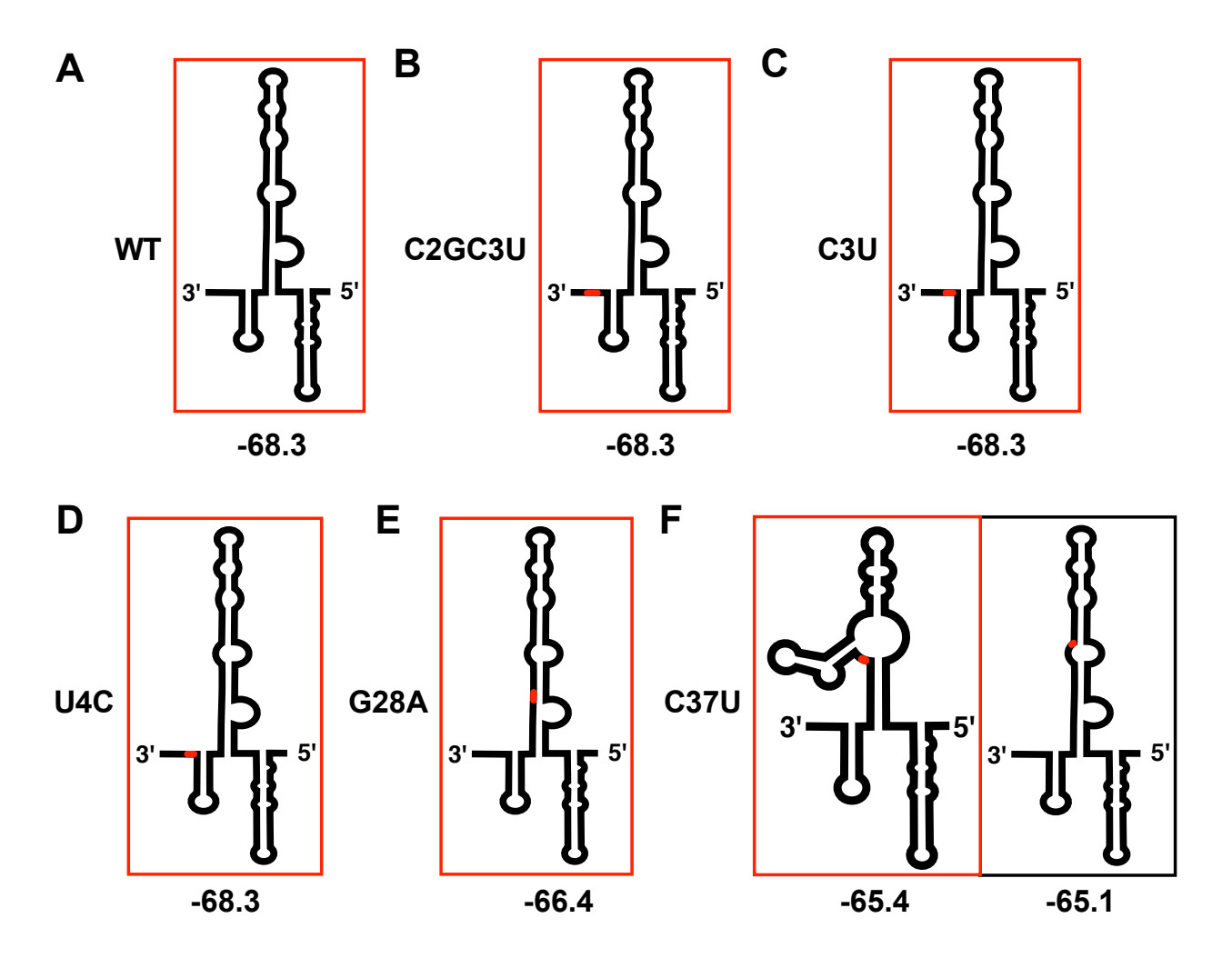


Supplementary Figure S3.1. RNA structure predictions of the 5' UTR (nucleotides 1-117) of the positive-strand HCV genomic RNA. Alternative structural predictions and the predicted free energies (ΔG, kcal/mol) are indicated. (A) WT, (B) C2GC3U, (C) C3U, (D) U4C, (E) G28A and (F) C37U. The mutations in the HCV RNAs are shown in red. The structure best aligned with SHAPE analysis is highlighted in red.





Supplementary Figure S3.2. Xrn-1 requires several 5' single-stranded nucleotides to initiate exoribonuclease activity. (A) Xrn-1 assay with 32 P-end-labeled monophosphorylated single-stranded RNA oligos were hybridized to various length complementary DNA oligos, resulting in 5' overhangs of 1-5 nucleotides. (B) Quantification of the results in (A) graphed as % full-length RNA remaining. All data are representative of three independent replicates and error bars represent the standard deviation of the mean. Statistical significance was determined by unpaired t-test, ** $p \le 0.005$, *** $p \le 0.0005$.



Supplementary Figure S3.3. RNA structure predictions of the 3' end (nucleotides 1-151) of the negative-strand HCV genomic RNA. Alternative structural predictions and the predicted free energies (ΔG, kcal/mol) are indicated. (A) WT, (B) C2GC3U, (C) C3U, (D) U4C, (E) G28A and (F) C37U. The mutations in the HCV RNAs are shown in red. The most favourable structure based on RNA structure analysis (B through E) or with *in vitro* SHAPE analysis (A and F) is highlighted in red.

CHAPTER 4: DISCUSSION

4.1 Role of miR-122 in the HCV life cycle

As outlined herein, miR-122 interactions with HCV RNA are important for viral RNA accumulation; however, the precise role(s) of miR-122 in the viral life cycle remained elusive until recently. Though early studies demonstrated that miR-122 had a small effect on HCV translation and viral RNA stability; together with several recent studies, our analysis herein elucidates the three roles of miR-122 in the viral life cycle: 1) RNA chaperone or riboswitch activity; 2) protection from pyrophosphatases and subsequent decay by exoribonucleases; 3) translational promotion (1-8).

What are the substrate requirements of the cellular pyrophosphatases and do Class II RAVs protect against pyrophosphatase activity?

Eukaryotic mRNAs contain a 7-methylguanosine (m⁷G) cap structure at the 5' terminus (9). The cap provides stability of the RNA by ensuring protection against 5' exoribonucleases (10). Many viruses cap their mRNAs or viral genomic RNAs, by taking advantage of the cellular capping machinery, using 'cap-snatching' strategies, or by carrying their own capping machinery that helps provide viral RNA stability (11). However, the 5' terminus of the HCV genome contains a triphosphate moiety (3). Previous studies demonstrated that miR-122 can protect the 5' triphosphate of the HCV genome from pyrophosphatases (DOM3Z and DUSP11) as well as subsequent degradation from the exoribonucleases, Xrn-1 and 2 (1,3-5,12). However, these mechanisms were shown indirectly in cell culture using knockdown or knockout experiments. We demonstrated herein that miR-122 base-pairing interactions as well as increasing intramolecular base-pairing at the 5' terminus of the viral genome resulted in stabilization of the viral RNA *in vitro* as well as *in vivo* (*Chapter 3*). This is due to the fact that Xrn-1 is a 5' to 3' exoribonuclease

that requires several single-stranded nucleotides in order to bind to substrates and initiate activity. Since Xrn-2 has very high homology to Xrn-1, we would predict that this enzyme has similar substrate requirements (13-16). In future, it will be interesting to explore the substrate requirements for the cellular pyrophosphatases (DOM3Z and DUSP11) using a similar approach *in vitro*. Specifically, γ^{32} P-labeled substrate RNAs could be used with increasing 5' overhangs to explore enzymatic activity using purified DOM3Z and DUSP11. Preliminary findings using a similar approach have suggested that DOM3Z can accommodate four 5' single-stranded nucleotides, while DUSP11 was shown to be active on trinucleotide substrates containing a 5' triphosphate moiety (17,18). However, further clarification of the substrate requirements of these cellular pyrophosphatases, as well as exploration of whether additional base-pairing interactions [i.e. mediated by miR-122 and/or the Class II RAVs (C2GC3U, C3U and U4C)] can protect the viral RNA from pyrophosphatase activity will help further clarify the mechanism of action of both miR-122 and the RAVs.

Removing the requirement for RNA chaperone or riboswitch activity and reducing the reliance on miR-122 for stability may favor miR-122-independent HCV RNA accumulation.

Our research suggests that miR-122 promotes both RNA chaperone/riboswitch activity as well as viral RNA stability (*Chapter 2*). Moreover, RAVs that promote one or both of these activities (Class I and II RAVs) allow HCV RNA accumulation under conditions where miR-122 is absent (U4C) or limiting (C2GC3U, C3U, U4C, G28A) (*Chapter 3*). In addition to these, a previous study selected chimeric viruses that can promote miR-122-independent viral RNA accumulation (6,19). In this study, Li *et al.* passaged wild-type HCV in the presence of a miR-122 inhibitor and selected for viruses which were able to accumulate under these conditions. The resultant viruses that they selected were chimeric viruses which had incorporated the human U3 snoRNA, U6 small nuclear RNA or a fragment of the 5' UTR of ATPase family AAA domain containing 1 (ATAD1) mRNA

in place of SLI on the HCV genome (19). Interestingly, the U3-virus is resistant to miR-122 antagonism, despite having an intact miR-122 Site 2 seed sequence (**Figure 4.1**). Our results herein provide insight into the mechanism of action of viral RNA accumulation of this U3-virus (*Chapters 2 and 3*). Firstly, the U3-virus contains only two single-stranded nucleotides at the 5' terminus, which would be predicted to promote viral RNA stability by preventing access of the viral 5' terminus of Xrn-1 (and presumably the cellular pyrophosphatases and Xrn-2). Secondly, the U3-virus is predicted to significantly favour the functional SLII structure ($\Delta G = -51.6 \text{ kcal/mol}$) even in the absence of miR-122, meaning it is functionally riboswitched, like the Class I RAVs (C2GC3U, U4C and G28A). Thus, this suggests a mechanism whereby U3-virus is able to confer miR-122-independent viral RNA accumulation. Moreover, this suggests that the RNA chaperone/riboswitch and viral RNA stability effects are dominant over the translational promotion activity since the U3-virus is not significantly affected by miR-122 antagonism in Huh-7.5 cells.

How does the Ago:miR-122 complex promote HCV translation?

Previous studies suggested that miR-122 promotes association of the viral RNA with the ribosome, but it is unclear if this is simply due to the RNA chaperone activity of the Ago:miR-122 complex or if this complex also actively promotes HCV IRES-dependent translation (20-24). Our SHAPE analysis and computational modeling (*Chapter 2*) suggests that the latter may be true as the PIWI domain of the Ago2 bound to Site 2 appears to make direct contact with the HCV IRES at SLIIa, which we predict may further stabilize the viral IRES as SLIIa was shown to be important for the formation of the L-shaped conformation of SLII which is 'ribosome-ready' (25-28). Interestingly, this unstructured domain of the PIWI protein is conserved across human Ago1-3, but not in Ago4 (7). Moreover, a study which explored silencing of the RNAi machinery suggested that knockdown of hAgo4 has the most potent effect on HCV RNA accumulation (i.e. ~80% vs. ~50% reductions

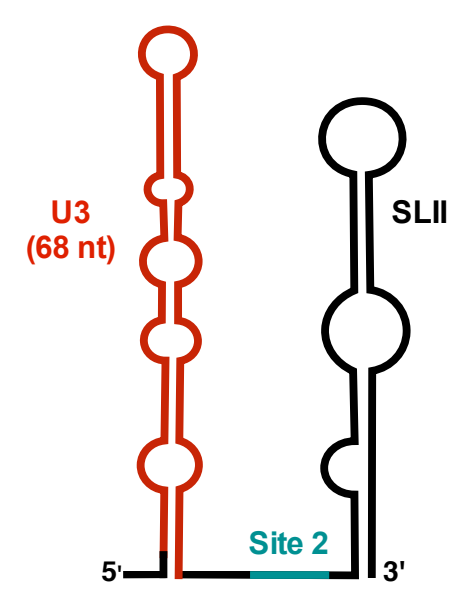


Figure 4.1. Secondary structure of U3-virus 5' UTR including SLII. Cartoon diagram of chimeric U3-virus containing the U3 snoRNA sequences (68-nt, red) inserted between nucleotides 3 and 32 of the HCV 5' UTR (black). The Site 2 miR-122 binding remained intact and is highlighted (teal). RNAstructure software prediction analysis predicts a free energy of $\Delta G = -51.6$ kcal/mol.

in viral RNA accumulation with knockdown of Ago4 vs. Ago1-3); despite the fact that Ago1-2 are the most abundant in Huh-7.5 cells (23). Clearly, further research will be needed to clarify whether Ago proteins have a role in promotion of HCV IRES-mediated translation, beyond RNA chaperone activity, and the importance of the unstructured PIWI domain of the Ago proteins.

In addition to interactions with SLII of the HCV genome, Ago2 was also shown to bind to SLII of a picornavirus, Enterovirus-71 (EV-71) and enhance viral IRES-mediated translation (29). During EV-71 infection, the viral RNA can serve as a template for Dicer processing, which results in the production of several viral RNA-derived small RNAs (29). One of these small RNAs, termed vsRNA1 is derived from SLII of the viral IRES and can direct Ago2 binding to this region of the genome. However, previous investigations transfected single-stranded vsRNA1, which would not be accessible for uptake into the RISC complex, and hence the results are unclear (30). Future work should therefore use duplexed vsRNA1 mimics which can be efficiently incorporated into an Ago protein. Nonetheless, the promotion of EV-71 IRES activity by Ago2 (potentially in complex with vsRNA1) could suggest a conserved mechanism of Ago:miRNA complex-mediated translational promotion across diverse RNA virus families.

How does HCV escape canonical silencing?

As discussed in *Chapter 1*, the canonical role of miRNAs is to downregulate gene expression of target mRNAs through translational repression, accelerated deadenylation and decay. The RISC recruits the downstream effector protein, GW182 which mediates important interactions with the deadenylation, decapping, and RNA decay machinery (31-38). Recent work suggests that GW182 (specifically the paralogs TNRC6B and C) is associated with the Ago:miR-122 complex at the 5' terminus of the HCV genome (39). However, there have been conflicting reports as to the importance of GW182 in the HCV life cycle (32,35,36,39). Thus, it is unclear how HCV is able to escape canonical RNA silencing and what downstream proteins are recruited to this complex.

Interestingly, several studies have sought to explore proteins that interact with the 5' terminus of the HCV genome and/or p-body proteins that localize to viral RNA replication sites during HCV infection (31,32,34,37). More specifically, depletion of the DDX6 RNA helicase was shown to decrease HCV RNA accumulation and interact with the 5' terminus of the HCV genome, but its effects appear to be independent of miR-122 activity (31,33,34). Additionally, LSm1, a 5' to 3' decapping protein located in p-bodies, was also shown to contribute to miR-122-mediated HCV translational promotion; however, this was in the context of reporter RNAs, rather than viral infection (36). Thus, future research will be needed to clarify the role of these proteins in HCV RNA accumulation, reveal the proteins that participate in the miR-122 enhancing complex at the 5' terminus of the HCV genome, and to clarify how HCV is able to escape canonical RNA silencing.

Considering HCV has a 5' triphosphate and is not polyadenylated, it is interesting that there is evidence of GW182 and LSm1 association with the 5' end of the viral RNA. Notably, these factors associate with the decapping and deadenylation machinery; however, HCV does not have a 5' cap or poly(A) tail (40,41). Thus, these proteins might be recruited to the HCV genome, but it is unclear how this might affect HCV RNA accumulation. Interestingly, recent work has suggested that Ago2 and a specific paralog of GW182 (TNRC6B) can drive a phase-separation which can accelerate deadenylation and subsequent degradation of target mRNAs by condensing the RISC-target RNA complex (42). Thus, since TNRC6B is recruited to the HCV genome, it is possible that this condensation reaction may help mediate the switch from active translation to viral RNA replication. Additionally, LSm1 was also demonstrated to have binding sites in both the 5' and 3' UTRs of the HCV genome; specifically, in SLIII of the 5' UTR, which might alter the secondary structure or contribute to this potential condensation reaction (37). Thus, the importance of these interactions, as well as the identification of additional host and viral factors that participate in this

complex, is likely to help clarify the precise mechanism of miRNA-mediated viral RNA accumulation and how HCV is able to escape canonical silencing.

4.2 One miRNA to rule them all?

In addition to HCV, other viruses in the *hepacivirus* genus have also been shown to rely on miR-122. For example, GB virus B (GBV-B), which was isolated from laboratory tamarins injected with serum from a human subject that had hepatitis, has two miR-122 binding sites in its 5' terminus and miR-122 has been shown to promote GBV-B viral RNA accumulation (43). Interestingly, a deletion mutant of GBV-B that lacks both miR-122 binding sites (Δ 4-29 nts), is still able to accumulate in cell culture, suggesting that GBV-B can overcome its reliance on miR-122 (44). Based on our data, the Δ 4-29 mutant removes the two miR-122 binding sites from the GBV-B genome resulting in a three-nucleotide single-stranded overhang at the 5' end, thereby providing stability to the viral RNA (**Figure 4.2**). Moreover, this deletion might also allow for the functional formation of the SLII structure, even in the absence of miR-122, as seen in our Class I RAVs (C2GC3U, U4C and G28A).

Moreover, recent viral discovery efforts have identified several novel *hepaciviruses* in a variety of species, including: equine hepacivirus, initially found in domesticated dogs and subsequently in horses; rodent hepaciviruses, found in mice and rats; bat hepaciviruses; bovine hepaciviruses; *Guerza* hepacivirus in an Old World monkey; Wenling shark hepacivirus, and *Sifaka hepacivirus* of lemurs (45-55). Of these viruses, except for the ones where the complete 5' UTR sequences are not yet available, have at least one miR-122 binding site in their 5' UTR (45-52). While it is still unknown if many of these hepaciviruses are responsive to miR-122, recent studies suggest that miR-122 sequestration inhibits equine hepacivirus accumulation, at least in cell culture (50).

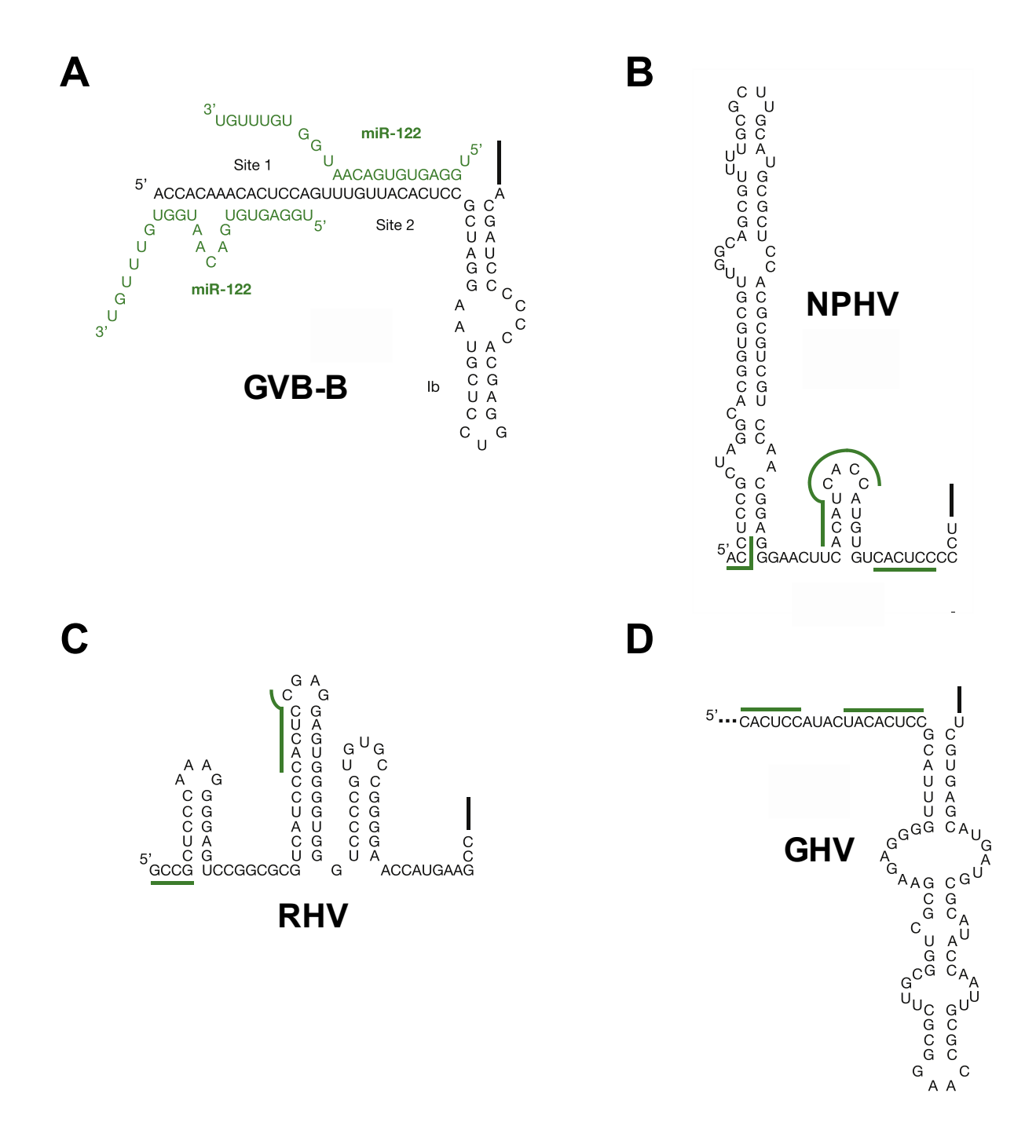


Figure 4.2.miR-122 interactions with 5'UTR of different hepaciviruses. MiR-122 (green) interactions on **(A)** GB virus B (GBV-B), **(B)** non-primate hepacivirus (NPHV), **(C)** rodent hepacivirus (RHV) and **(D)** guereza hepacivirus. Adapted from Sagan S.M. et al., *Virus Research*, 2015 (56).

The presence of conserved miR-122 binding sites across hepaciviruses of diverse species suggests a conserved mechanism of viral accumulation which may allow them to collectively exploit the liver microenvironment. Additionally, the presence of miR-122 seed sequences suggests that although they infect different hosts, they are likely to have evolved from a common hepatotropic ancestor (56). Additionally, it is possible that these viruses have evolved common strategies for miR-122-mediated viral RNA accumulation, since the location of at least one of the miR-122 binding sites is just upstream of SLII, and in some cases (e.g. equine hepacivirus) has been shown to enhance translation (49,57). Like in chronic HCV infection, it is possible that this interaction could be exploited for antiviral therapies for these veterinary pathogens, particularly in horses, where as much as 22% of the population may be infected with equine hepacivirus (45,58,59). Taken together, it is clear that binding to miR-122 may be a common strategy to promote viral RNA accumulation across distinct hepaciviruses and further study will be needed to clarify whether these viruses employ distinct or common strategies for miR-122-mediated viral RNA accumulation.

4.3 Other miRNA-regulated viral RNAs

In addition to miR-122-mediated viral RNA accumulation of *hepaciviruses*, several other viruses have been shown to be regulated by miRNAs. For example, several of the related *pestiviruses*, including bovine viral diarrhea virus (BVDV) and classical swine fever virus (CSFV) have been shown to bind to cellular miRNAs that are important for viral RNA accumulation, at least in cell culture (60). More specifically, these viruses interact with miR-17 and let-7 at the 3' UTR of the viral genome (60). Sequestration of miR-17 or let-7 during BVDV infection significantly impairs viral RNA accumulation; while only sequestration of miR-17 significantly impairs CSFV RNA accumulation in cell culture (60). Interestingly, the seed binding sites for let-7 and miR-17 are highly conserved across *pestiviruses*, suggesting that these viruses may have also evolved to use

abundant cellular miRNAs to accumulate in their hosts. Although the miRNA binding sites are in the 3' UTR, like miR-122, miR-17 has been shown to stabilize BVDV and enhance its translation, suggesting that it may have a similar mechanism to miR-122 interactions with the HCV genome (60). Although future research is needed, these results suggest that miRNA-virus interactions that promote viral RNA accumulation are not unique to hepaciviruses and it is likely that this may also occur on host transcripts which suggests additional, hitherto unrecognized mechanisms of action for miRNAs in regulation of gene expression.

In contrast to miRNA-mediated viral RNA accumulation, there are also several other noncanonical interactions between viruses and cellular miRNAs. The most notable example is in Herpesvirus saimiri (HVS), a virus of New World primates that infects T cells and causes leukemia (61). Interestingly, HVS encodes a non-coding RNA that selectively degrades a T cell miRNA, miR-27 (62). miR-27 functions as a key regulator in T cell differentiation and function and has multiple roles in mediating T cell immunity (63,64). The virus has evolved a mechanism to selectively degrade miR-27; although it is still unclear how the down-regulation of miR-27 benefits HVS accumulation (62). This suggests that host miRNAs can both limit and promote viral RNA accumulation in different contexts, highlighting that we are just beginning to understand the complex nature of host miRNA-virus interactions and their consequences for viral infection and host antiviral responses.

4.4 Consequences of RAVs to miRNA-based therapies

Consequences of RAVs in miR-122-based therapies for chronic HCV infection.

As discussed in *Chapter 3*, several RAVs have been isolated in cell culture or chronic HCV-infected patients who underwent miR-122 inhibitor-based therapies that are able to accumulate when miR-122 is limiting or absent (65-68). We identified three classes of RAVs, with three distinct mechanisms of action: Class I RAVs, including C2GC3U, U4C and G28A are

riboswitched, even in the absence of miR-122; Class II RAVs, including C2GC3U, C3U and U4C have additional base-pairing at the 5' terminus that protects the genome from degradation; and the Class III RAV, C37U, which alters the structure of the negative-strand intermediate and is predicted to promote positive-strand RNA synthesis. For the Class III RAV, there is still some research to be done to clarify whether this C37U mutation alters the activity of the positive-strand promoter. In future, we plan to determine the positive-to-negative strand ratio compared with WT HCV RNA in cell culture using qRT-PCR, as a more efficient positive-strand promoter would be predicted to increase the number of positive-strands. Moreover, we plan to perform *in vitro* analysis of NS5B polymerase binding affinities for WT and C37U negative-strand 3' termini as well as *de novo* initiation assays to demonstrate whether this RAV confers increased binding and/or initiation of RNA synthesis from the negative-strand intermediate.

Additionally, it would be interesting to investigate whether combinations of RAVs would be able to confer complete miR-122-independent HCV RNA accumulation. This is not unprecedented as Hopcraft *et al.* previously demonstrated that the combination of U4C, G28A and C37U resulted in a significant level of viral RNA accumulation in miR-122 KO cells (65). Based on our data, this mutant would be predicted to be riboswitched (G28A), stable (U4C), and have a more efficient positive-strand promoter (C37U). This virus or other confirmations might be useful as a tool to better understand the miR-122 enhancing complex through identification of RNA-binding proteins or miRNA effector proteins involved in this complex by comparison of viral RNA pulldowns from miR-122-dependent and miR-122-independent viral RNAs.

Broader consequences of RAV mechanisms of action for miRNA-based therapies

miRNA-based therapies are gaining attention in the biomedical field and are making their way into clinical trials. In 2011, 18,226 miRNAs have been recorded in animals, plants and viruses and of these, 1,921 miRNAs are predicted to be encoded in the human genome (69). As miRNAs are

predicted to regulate as much as 60% of all human genes, it is not surprising that they are implicated in many human diseases, including metabolic disorders, cardiovascular disease, cancer, and infectious disease. In 2017, approximately 20 clinical trials were initiated using miRNA or siRNA-based therapies (70). Moreover, miRNA-based therapies are being developed for several viral infections, and the miR-122 inhibitors, MiravirsenTM and RG-101 were the flagship miRNA-based drugs and first to enter the clinic (71,72). Interestingly, the majority of RAVs to miR-122-based therapies were outside of the miRNA's seed binding sequence on the HCV genome. Moreover, each of the RAVs altered the structure of the viral RNA in some way, suggesting that future analysis of RAVs to miRNA-based therapies should involve RNA structure analysis and go beyond sequencing of the miRNA binding sites on the target gene(s). Importantly, viral pathogens as well as cancerous cells accumulate mutations at a faster rate and may therefore reveal novel strategies to evade miRNA-based therapies. Thus, it will be important to understand the potential mechanisms of resistance that may arise, and this study may provide insight into the potential mechanisms of action of RAVs to miRNA-based therapies more broadly.

4.5 Concluding remarks

In summary, we have shown that Ago:miR-122 complex plays three critical roles in the HCV life cycle. The HCV genome is predicted to enter the cell in an alternative, more favorable conformation (termed SLII^{alt}) and recruitment of Ago:miR-122 to Site 2 promotes the functional SLII structure and acts as an RNA chaperone or riboswitch to allow the viral IRES (SLII-IV) to form. This provides access to Site 1, and a second Ago:miR-122 complex is then recruited to this site, where it directly protects the 5' terminus from cellular pyrophosphatases and exoribonuclease-mediated decay. Additionally, due to the close proximity of the two Ago:miR-122 complexes, the auxiliary interactions at Site 2 are weakened to accommodate Ago:miR-122 complex binding to Site 1. To further stabilize the Ago:miR-122 complex at Site 2, the Ago protein at this site interacts

with SLIIa, which is predicted to stabilizes the functional SLII structure and thus promote translation.

Using our understanding of the mechanism(s) of action of miR-122, we investigated how RAVs isolated in cell culture or in patients who underwent miR-122 inhibitor-based therapies were able to accumulate when miR-122 is absent or limiting. We determined that the RAVs promote alternative RNA conformations of the viral RNA that support RNA accumulation under conditions where miR-122 is limiting or absent. Specifically, the Class I RAVs, including C2GC3U, U4C, and G28A, are 'riboswitched' and are able to form the canonical SLII structure, even in the absence of miR-122. The Class II RAVs, including C2GC3U, C3U, and U4C, are able to form additional base-pairing interactions at the 5' terminus the HCV genome, which provides stability against exoribonucleases, and presumably the pyrophosphatases. The Class III RAV, C37U, alters the structure of the 3' terminus of the negative-strand replicative intermediate, which we propose creates a more efficient promoter for positive-strand genomic RNA synthesis. Taken together, this research reveals new paradigms for miRNA function, novel mechanisms of antiviral resistance based on changes to RNA structure and reveals insight into the mechanism of an important hostvirus interaction that may be applicable to other important human and veterinary pathogens. Moreover, this research showcases how important RNA secondary structures are in the context of the HCV life cycle and how even single nucleotide mutations can significantly alter both RNA structure and function.

4.6 References

- 1. Amador-Canizares, Y., Bernier, A., Wilson, J.A. and Sagan, S.M. (2018) miR-122 does not impact recognition of the HCV genome by innate sensors of RNA but rather protects the 5' end from the cellular pyrophosphatases, DOM3Z and DUSP11. *Nucleic Acids Res.*, **46**, 5139-5158.
- 2. Henke, J.I., Goergen, D., Zheng, J., Song, Y., Schüttler, C.G., Fehr, C., Jünemann, C. and Niepmann, M. (2008) microRNA-122 stimulates translation of hepatitis C virus RNA. *EMBO J.*, **27**, 3300-3310.
- 3. Li, Y., Masaki, T., Yamane, D., McGivern, D.R. and Lemon, S.M. (2013) Competing and noncompeting activities of miR-122 and the 5' exonuclease Xrn1 in regulation of hepatitis C virus replication. *PNAS*, **110**, 1881-1886.
- 4. Li, Y., Yamane, D. and Lemon, S.M. (2015) Dissecting the roles of the 5' exoribonucleases Xrn1 and Xrn2 in restricting hepatitis C virus replication. *J. Virol.*, **89**, 4857-4865.
- 5. Sedano, C.D. and Sarnow, P. (2014) Hepatitis C virus subverts liver-specific miR-122 to protect the viral genome from exoribonuclease Xrn2. *Cell host & microbe*, **16**, 257-264.
- 6. Amador-Canizares, Y., Panigrahi, M., Huys, A., Kunden, R.D., Adams, H.M., Schinold, M.J. and Wilson, J.A. (2018) miR-122, small RNA annealing and sequence mutations alter the predicted structure of the Hepatitis C virus 5' UTR RNA to stabilize and promote viral RNA accumulation. *Nucleic Acids Res.*, **46**, 9776-9792.
- 7. Chahal, J., Gebert, L.F.R., Gan, H.H., Camacho, E., Gunsalus, K.C., MacRae, I.J. and Sagan, S.M. (2019) miR-122 and Ago interactions with the HCV genome alter the structure of the viral 5' terminus. *Nucleic Acids Res.*, **47**, 5307-5324.
- 8. Schult, P., Roth, H., Adams, R.L., Mas, C., Imbert, L., Orlik, C., Ruggieri, A., Pyle, A.M. and Lohmann, V. (2018) microRNA-122 amplifies hepatitis C virus translation by shaping the structure of the internal ribosomal entry site. *Nat Commun.*, **9**, 2613-2613.
- 9. Shatkin, A.J. (1976) Capping of eucaryotic mRNAs. *Cell*, **9**, 645-653.
- 10. Darnell, J.E., Jr. (1979) Transcription units for mRNA production in eukaryotic cells and their DNA viruses. *Prog. Nucleic Acid Res. Mol. Biol.*, **22**, 327-353.
- 11. Decroly, E., Ferron, F., Lescar, J. and Canard, B. (2011) Conventional and unconventional mechanisms for capping viral mRNA. *Nat. Rev. Microbiol.*, **10**, 51-65.
- 12. Kincaid, R.P., Lam, V.L., Chirayil, R.P., Randall, G. and Sullivan, C.S. (2018) RNA triphosphatase DUSP11 enables exonuclease XRN-mediated restriction of hepatitis C virus. *PNAS*, **115**, 8197-8202.
- 13. Amberg, D.C., Goldstein, A.L. and Cole, C.N. (1992) Isolation and characterization of RAT1: an essential gene of Saccharomyces cerevisiae required for the efficient nucleocytoplasmic trafficking of mRNA. *Genes Dev.*, **6**, 1173-1189.
- 14. Chang, J.H.X., Song; Tong, Liang. (2011) *Chapter 7: 5'-3' Exoribonucleases*. Springer-Verlag Berlin Heidelberg.
- 15. Krzyszton, M., Zakrzewska-Placzek, M., Koper, M. and Kufel, J. (2012) Rat1 and Xrn2: The Diverse Functions of the Nuclear Rat1/Xrn2 Exonuclease. *Enzymes*, **31**, 131-163.
- 16. Nagarajan, V.K., Jones, C.I., Newbury, S.F. and Green, P.J. (2013) XRN 5'-->3' exoribonucleases: structure, mechanisms and functions. *Biochim. Biophys. Acta*, **1829**, 590-603.
- 17. Chang, J.H., Jiao, X., Chiba, K., Oh, C., Martin, C.E., Kiledjian, M. and Tong, L. (2012) Dxo1 is a new type of eukaryotic enzyme with both decapping and 5'-3' exoribonuclease activity. *Nat. Struct. Mol. Biol.*, **19**, 1011-1017.

- 18. Jiao, X., Chang, J.H., Kilic, T., Tong, L. and Kiledjian, M. (2013) A mammalian premRNA 5' end capping quality control mechanism and an unexpected link of capping to pre-mRNA processing. *Mol. Cell*, **50**, 104-115.
- 19. Li, Y.P., Gottwein, J.M., Scheel, T.K., Jensen, T.B. and Bukh, J. (2011) MicroRNA-122 antagonism against hepatitis C virus genotypes 1-6 and reduced efficacy by host RNA insertion or mutations in the HCV 5' UTR. *Proc. Natl. Acad. Sci. U. S. A.*, **108**, 4991-4996.
- 20. Conrad, K.D., Giering, F., Erfurth, C., Neumann, A., Fehr, C., Meister, G. and Niepmann, M. (2013) microRNA-122 Dependent Binding of Ago2 Protein to Hepatitis C Virus RNA Is Associated with Enhanced RNA Stability and Translation Stimulation. *PLoS One*, **8**, e56272
- 21. Machlin, E.S., Sarnow, P. and Sagan, S.M. (2011) Masking the 5' terminal nucleotides of the hepatitis C virus genome by an unconventional microRNA-target RNA complex. *PNAS*, **108**, 3193-3198.
- 22. Nieder-Röhrmann, A., Dünnes, N., Gerresheim, G.K., Shalamova, L.A., Herchenröther, A. and Niepmann, M. (2017) Cooperative enhancement of translation by two adjacent microRNA-122/argonaute 2 complexes binding to the 5' untranslated region of hepatitis C virus RNA. *J. Gen. Virol.*, **98**, 212-224.
- 23. Randall, G., Panis, M., Cooper, J.D., Tellinghuisen, T.L., Sukhodolets, K.E., Pfeffer, S., Landthaler, M., Landgraf, P., Kan, S., Lindenbach, B.D. *et al.* (2007) Cellular cofactors affecting hepatitis C virus infection and replication. *Proc. Natl. Acad. Sci. U. S. A.*, **104**, 12884-12889.
- 24. Shimakami, T., Yamane, D., Jangra, R.K., Kempf, B.J., Spaniel, C., Barton, D.J. and Lemon, S.M. (2012) Stabilization of hepatitis C virus RNA by an Ago2-miR-122 complex. *PNAS*, **109**, 941-946.
- 25. Dibrov, S.M., Johnston-Cox, H., Weng, Y.H. and Hermann, T. (2007) Functional architecture of HCV IRES domain II stabilized by divalent metal ions in the crystal and in solution. *Angew. Chem. Int. Ed. Engl.*, **46**, 226-229.
- 26. Dibrov, S.M., Parsons, J., Carnevali, M., Zhou, S., Rynearson, K.D., Ding, K., Garcia Sega, E., Brunn, N.D., Boerneke, M.A., Castaldi, M.P. *et al.* (2014) Hepatitis C virus translation inhibitors targeting the internal ribosomal entry site. *J. Med. Chem.*, **57**, 1694-1707.
- 27. Lukavsky, P.J., Otto, G.A., Lancaster, A.M., Sarnow, P. and Puglisi, J.D. (2000) Structures of two RNA domains essential for hepatitis C virus internal ribosome entry site function. *Nat. Struct. Biol.*, 7, 1105-1110.
- 28. Zhao, Q., Han, Q., Kissinger, C.R., Hermann, T. and Thompson, P.A. (2008) Structure of hepatitis C virus IRES subdomain IIa. *Acta Crystallogr. D Biol. Crystallogr.*, **64**, 436-443
- 29. Lin, J.Y., Brewer, G. and Li, M.L. (2015) HuR and Ago2 Bind the Internal Ribosome Entry Site of Enterovirus 71 and Promote Virus Translation and Replication. *PLoS One*, **10**, e0140291.
- 30. Weng, K.F., Hung, C.T., Hsieh, P.T., Li, M.L., Chen, G.W., Kung, Y.A., Huang, P.N., Kuo, R.L., Chen, L.L., Lin, J.Y. *et al.* (2014) A cytoplasmic RNA virus generates functional viral small RNAs and regulates viral IRES activity in mammalian cells. *Nucleic Acids Res.*, **42**, 12789-12805.
- 31. Ariumi, Y., Kuroki, M., Kushima, Y., Osugi, K., Hijikata, M., Maki, M., Ikeda, M. and Kato, N. (2011) Hepatitis C virus hijacks P-body and stress granule components around lipid droplets. *J. Virol.*, **85**, 6882-6892.

- 32. Berezhna, S.Y., Supekova, L., Sever, M.J., Schultz, P.G. and Deniz, A.A. (2011) Dual regulation of hepatitis C viral RNA by cellular RNAi requires partitioning of Ago2 to lipid droplets and P-bodies. *RNA*, **17**, 1831-1845.
- 33. Huys, A., Thibault, P.A. and Wilson, J.A. (2013) Modulation of hepatitis C virus RNA accumulation and translation by DDX6 and miR-122 are mediated by separate mechanisms. *PLoS One*, **8**, e67437.
- 34. Jangra, R.K., Yi, M. and Lemon, S.M. (2010) DDX6 (Rck/p54) is required for efficient hepatitis C virus replication but not for internal ribosome entry site-directed translation. *J. Virol.*, **84**, 6810-6824.
- 35. Pager, C.T., Schutz, S., Abraham, T.M., Luo, G. and Sarnow, P. (2013) Modulation of hepatitis C virus RNA abundance and virus release by dispersion of processing bodies and enrichment of stress granules. *Virology*, **435**, 472-484.
- 36. Roberts, A.P., Doidge, R., Tarr, A.W. and Jopling, C.L. (2014) The P body protein LSm1 contributes to stimulation of hepatitis C virus translation, but not replication, by microRNA-122. *Nucleic Acids Res.*, **42**, 1257-1269.
- 37. Scheller, N., Mina, L.B., Galao, R.P., Chari, A., Gimenez-Barcons, M., Noueiry, A., Fischer, U., Meyerhans, A. and Diez, J. (2009) Translation and replication of hepatitis C virus genomic RNA depends on ancient cellular proteins that control mRNA fates. *Proc. Natl. Acad. Sci. U. S. A.*, **106**, 13517-13522.
- 38. Eulalio, A., Behm-Ansmant, I. and Izaurralde, E. (2007) P bodies: at the crossroads of post-transcriptional pathways. *Nat. Rev. Mol. Cell Biol.*, **8**, 9-22.
- 39. Li, Y., Wang, L., Rivera-Serrano, E.E., Chen, X. and Lemon, S.M. (2019) TNRC6 proteins modulate hepatitis C virus replication by spatially regulating the binding of miR-122/Ago2 complexes to viral RNA. *Nucleic Acids Res.*, **47**, 6411-6424.
- 40. Kolykhalov, A.A., Feinstone, S.M. and Rice, C.M. (1996) Identification of a highly conserved sequence element at the 3' terminus of hepatitis C virus genome RNA. *J. Virol.*, **70**, 3363-3371.
- 41. Lytle, J.R., Wu, L. and Robertson, H.D. (2002) Domains on the hepatitis C virus internal ribosome entry site for 40s subunit binding. *RNA*, **8**, 1045-1055.
- 42. Sheu-Gruttadauria, J. and MacRae, I.J. (2018) Phase Transitions in the Assembly and Function of Human miRISC. *Cell*, **173**, 946-957 e916.
- 43. Stapleton, J.T., Foung, S., Muerhoff, A.S., Bukh, J. and Simmonds, P. (2011) The GB viruses: a review and proposed classification of GBV-A, GBV-C (HGV), and GBV-D in genus Pegivirus within the family Flaviviridae. *J. Gen. Virol.*, **92**, 233-246.
- 44. Sagan, S.M., Sarnow, P. and Wilson, J.A. (2013) Modulation of GB virus B RNA abundance by microRNA-122: dependence on and escape from microRNA-122 restriction. *J. Virol.*, **87**, 7338-7347.
- 45. Burbelo, P.D., Dubovi, E.J., Simmonds, P., Medina, J.L., Henriquez, J.A., Mishra, N., Wagner, J., Tokarz, R., Cullen, J.M., Iadarola, M.J. *et al.* (2012) Serology-enabled discovery of genetically diverse hepaciviruses in a new host. *J. Virol.*, **86**, 6171-6178.
- 46. Drexler, J.F., Corman, V.M., Muller, M.A., Lukashev, A.N., Gmyl, A., Coutard, B., Adam, A., Ritz, D., Leijten, L.M., van Riel, D. *et al.* (2013) Evidence for novel hepaciviruses in rodents. *PLoS Pathog.*, **9**, e1003438.
- 47. Kapoor, A., Simmonds, P., Gerold, G., Qaisar, N., Jain, K., Henriquez, J.A., Firth, C., Hirschberg, D.L., Rice, C.M., Shields, S. *et al.* (2011) Characterization of a canine homolog of hepatitis C virus. *Proc. Natl. Acad. Sci. U. S. A.*, **108**, 11608-11613.
- 48. Kapoor, A., Simmonds, P., Scheel, T.K., Hjelle, B., Cullen, J.M., Burbelo, P.D., Chauhan, L.V., Duraisamy, R., Sanchez Leon, M., Jain, K. *et al.* (2013) Identification of rodent homologs of hepatitis C virus and pegiviruses. *MBio*, 4, e00216-00213.

- 49. Lattimer, J., Stewart, H., Locker, N., Tuplin, A., Stonehouse, N.J. and Harris, M. (2019) Structure-function analysis of the equine hepacivirus 5' untranslated region highlights the conservation of translational mechanisms across the hepaciviruses. *J. Gen. Virol.*, **100**, 1501-1514.
- 50. Lauck, M., Sibley, S.D., Lara, J., Purdy, M.A., Khudyakov, Y., Hyeroba, D., Tumukunde, A., Weny, G., Switzer, W.M., Chapman, C.A. *et al.* (2013) A novel hepacivirus with an unusually long and intrinsically disordered NS5A protein in a wild Old World primate. *J. Virol.*, **87**, 8971-8981.
- 51. Quan, P.L., Firth, C., Conte, J.M., Williams, S.H., Zambrana-Torrelio, C.M., Anthony, S.J., Ellison, J.A., Gilbert, A.T., Kuzmin, I.V., Niezgoda, M. *et al.* (2013) Bats are a major natural reservoir for hepaciviruses and pegiviruses. *Proc. Natl. Acad. Sci. U. S. A.*, 110, 8194-8199.
- 52. Scheel, T.K., Kapoor, A., Nishiuchi, E., Brock, K.V., Yu, Y., Andrus, L., Gu, M., Renshaw, R.W., Dubovi, E.J., McDonough, S.P. *et al.* (2015) Characterization of nonprimate hepacivirus and construction of a functional molecular clone. *Proc. Natl. Acad. Sci. U. S. A.*, **112**, 2192-2197.
- 53. Canuti, M., Williams, C.V., Sagan, S.M., Oude Munnink, B.B., Gadi, S., Verhoeven, J.T.P., Kellam, P., Cotten, M., Lang, A.S., Junge, R.E. *et al.* (2019) Virus discovery reveals frequent infection by diverse novel members of the Flaviviridae in wild lemurs. *Arch. Virol.*, **164**, 509-522.
- 54. Corman, V.M., Grundhoff, A., Baechlein, C., Fischer, N., Gmyl, A., Wollny, R., Dei, D., Ritz, D., Binger, T., Adankwah, E. *et al.* (2015) Highly divergent hepaciviruses from African cattle. *J. Virol.*, **89**, 5876-5882.
- 55. Shi, M., Lin, X.D., Vasilakis, N., Tian, J.H., Li, C.X., Chen, L.J., Eastwood, G., Diao, X.N., Chen, M.H., Chen, X. *et al.* (2016) Divergent Viruses Discovered in Arthropods and Vertebrates Revise the Evolutionary History of the Flaviviridae and Related Viruses. *J. Virol.*, **90**, 659-669.
- 56. Sagan, S.M., Chahal, J. and Sarnow, P. (2015) cis-Acting RNA elements in the hepatitis C virus RNA genome. *Virus Res.*, **206**, 90-98.
- 57. Baron, A.L., Schoeniger, A., Becher, P. and Baechlein, C. (2018) Mutational Analysis of the Bovine Hepacivirus Internal Ribosome Entry Site. *J. Virol.*, **92**.
- 58. Badenhorst, M., Tegtmeyer, B., Todt, D., Guthrie, A., Feige, K., Campe, A., Steinmann, E. and Cavalleri, J.M.V. (2018) First detection and frequent occurrence of Equine Hepacivirus in horses on the African continent. *Vet. Microbiol.*, **223**, 51-58.
- 59. Tang, W., Zhu, N., Wang, H., Gao, Y., Wan, Z., Cai, Q., Yu, S. and Tang, S. (2018) Identification and genetic characterization of equine Pegivirus in China. *J. Gen. Virol.*, **99**, 768-776.
- 60. Scheel, T.K., Luna, J.M., Liniger, M., Nishiuchi, E., Rozen-Gagnon, K., Shlomai, A., Auray, G., Gerber, M., Fak, J., Keller, I. *et al.* (2016) A Broad RNA Virus Survey Reveals Both miRNA Dependence and Functional Sequestration. *Cell Host Microbe*, **19**, 409-423.
- 61. Ensser, A. and Fleckenstein, B. (2005) T-cell transformation and oncogenesis by gamma2-herpesviruses. *Adv. Cancer Res.*, **93**, 91-128.
- 62. Cazalla, D., Yario, T. and Steitz, J.A. (2010) Down-regulation of a host microRNA by a Herpesvirus saimiri noncoding RNA. *Science*, **328**, 1563-1566.
- 63. Cho, S., Wu, C.J., Yasuda, T., Cruz, L.O., Khan, A.A., Lin, L.L., Nguyen, D.T., Miller, M., Lee, H.M., Kuo, M.L. *et al.* (2016) miR-23 approximately 27 approximately 24 clusters control effector T cell differentiation and function. *J. Exp. Med.*, **213**, 235-249.

- 64. Cruz, L.O., Hashemifar, S.S., Wu, C.J., Cho, S., Nguyen, D.T., Lin, L.L., Khan, A.A. and Lu, L.F. (2017) Excessive expression of miR-27 impairs Treg-mediated immunological tolerance. *J. Clin. Invest.*, **127**, 530-542.
- 65. Hopcraft, S.E., Azarm, K.D., Israelow, B., Leveque, N., Schwarz, M.C., Hsu, T.H., Chambers, M.T., Sourisseau, M., Semler, B.L. and Evans, M.J. (2016) Viral Determinants of miR-122 Independent Hepatitis C Virus Replication. *mSphere*, 1, 1-12.
- 66. Israelow, B., Mullokandov, G., Agudo, J., Sourisseau, M., Bashir, A., Maldonado, A.Y., Dar, A.C., Brown, B.D. and Evans, M.J. (2015) Hepatitis C virus genetics affects miR-122 requirements and response to miR-122 inhibitors. *Nat Commun.*, **5**, 1-11.
- 67. Ottosen, S., Parsley, T.B., Yang, L., Zeh, K., van Doorn, L.-J., van der Veer, E., Raney, A.K., Hodges, M.R. and Patick, A.K. (2015) In vitro antiviral activity and preclinical and clinical resistance profile of miravirsen, a novel anti-hepatitis C virus therapeutic targeting the human factor miR-122. *Antimicrob. Agents Chemother.*, **59**, 599-608.
- 68. van der Ree, M.H., de Vree, J.M., Stelma, F., Willemse, S., van der Valk, M., Rietdijk, S., Molenkamp, R., Schinkel, J., van Nuenen, A.C., Beuers, U. *et al.* (2017) Safety, tolerability, and antiviral effect of RG-101 in patients with chronic hepatitis C: a phase 1B, double-blind, randomised controlled trial. *Lancet*, **389**, 709-717.
- 69. Kozomara, A. and Griffiths-Jones, S. (2014) miRBase: annotating high confidence microRNAs using deep sequencing data. *Nucleic Acids Res.*, **42**, D68-73.
- 70. Chakraborty, C., Sharma, A.R., Sharma, G., Doss, C.G.P. and Lee, S.S. (2017) Therapeutic miRNA and siRNA: Moving from Bench to Clinic as Next Generation Medicine. *Mol Ther Nucleic Acids*, **8**, 132-143.
- 71. Baumann, V. and Winkler, J. (2014) miRNA-based therapies: strategies and delivery platforms for oligonucleotide and non-oligonucleotide agents. *Future Med. Chem.*, **6**, 1967-1984.
- 72. Deng, J., Xiao, J., Ma, P., Gao, B., Gong, F., Lv, L., Zhang, Y. and Xu, J. (2017) Manipulation of Viral MicroRNAs as a Potential Antiviral Strategy for the Treatment of Cytomegalovirus Infection. *Viruses*, **9**.

APPENDIX

Permissions to use copyright material

Chapter 1: Introduction and Chapter 5: Discussion: Sections and Figures from Selena M. Sagan, Jasmin Chahal, Peter Sarnow. *Cis*-Acting RNA elements in the hepatitis C virus RNA genome. *Virus Research*, 2015 Jan 7; 206:90-98; doi: 10.1016/j.virusres.2014.12.029. As an author of this Elsevier article, we retain the right to include it in a thesis or dissertation, provided it is not published commercially. According to Rights and Conditions and Copyright Clearance Center of Elsevier, we do not require additional permission as long as the original work is properly cited. All co-authors agreed to the inclusion of parts of this manuscript to the present thesis.

Chapter 2: miR-122 and Ago interactions with the HCV genome alter the structure of the viral 5' terminus. From Jasmin Chahal, Luca F.R Gebert, Hink Hark Gan, Edna Camacho, Kristin C. Gunsalus, Ian J. MacRae, and Selena M. Sagan. *Nucleic Acids Research*, 2019 April 3; 47(10): 5307-5324; doi: 10.1093/nar/gkz194. This is an open access article under the terms of the Creative Commons License (Attribution-Non-commercial), allowing non-commercial/educational purposes, provided the original work is properly cited. All co-authors agreed to the inclusion of parts of this manuscript to the present thesis.

Figure 1.12 Geographic distribution of HCV genotypes. From Messina, J.P. et al. Global distribution and prevalence of hepatitis C virus genotypes. *Hepatology*, 2015, 61, 77-87. This is an open access article under the terms of the Creative Commons License (Attribution-Noncommercial), allowing non-commercial/educational purposes, provided the original work is properly cited.

Figure 1.13. The HCV life cycle. From Lindenbach B.D. and Rice C.M. Unravelling hepatitis C virus replication from genome to function. *Nature*, 2005, 436, 933-938. This article is under the terms of the Creative Commons License (Attribution-Non-commercial), allowing non-commercial/educational purposes, provided the original work is properly cited.

Figure 1.14. miRNA biogenesis. Figure from Winter et al. Many roads to maturity: microRNA biogenesis pathways and their regulation. *Nature Cell Biology*, 2009, 11 (3): 228-34. Permission was granted by Springer Nature and Copyright Clearance Center for Thesis/Dissertation, provided the original work is properly cited.